A Geological and Geophysical Synthesis of the Svartliden Project, Sweden and its application in defining gold exploration targets.

by

Yannic (Ian) F. Laurent

A thesis submitted in
partial fulfilment of the requirements
for the degree of
Master of Economic Geology

CODES SRC
Centre for Ore Deposit Research

University of Tasmania

March 2001

Authority of Access

This thesis is not to be made available for loan for a period of XX years following the date this statement was signed. Following that time it may be made available for loan and limited copying in accordance with the *Copyright Act of 1968*.

Signed 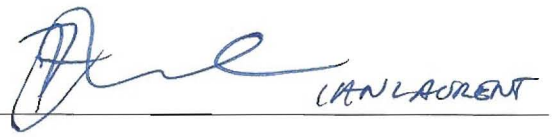 IAN LAURENT

'Qu'est-ce après tout que l'intelligence? L'étymologie définit ce terme comme étant simplement la capacité générale de comprendre.'

Jacques-Yves Cousteau, 1989

'*translation*:- What is intelligence, after all? Etymology defines this term as simply being the general ability to understand'

ACKNOWLEDGEMENTS

The undertaking of this thesis would not have been possible without the assistance and support of many people. I would like to extend my thanks to:

VIKING GOLD CORPORATION

Ken Phillips (Director) for authorising this research on the Svartliden Project, and for giving moral and financial support over the last 4 years. Scott Marsh (former Exploration Manager and former CODES Masters graduate) for giving me encouragement to undertake this research project. Greta and Pereric Stenvall for allowing their shed to be used as a temporary core farm, for feeding me on those cold Scandinavian winter nights, and for shuffling snow to allow access to site and the core farm.

DRAGON MINING NL (owner of Viking Gold since December 1999)

James Searle and Neale Edwards for providing further geological information obtained after completion of their due diligence study in 1999, and encouragement in the completion of this thesis.

CODES SRC (Centre for Ore Deposit Research)

Dr Michael Roach for help in organising and executing the project, as well as his geophysical input. Dr Robert Scott for providing assistance with petrology and structural geology. Dr J.Bruce Gemmell for organising and co-ordinating the CODES Masters course. Marilyn Feast for her assistance in all administrative matters and for providing the much-needed coffee required, to keep us going during our 2 week courses in Hobart. Simon Stephens for the preparation of thin sections and polished mounts.

Most Importantly, I would like to thank my wife, Céline, for her continual encouragement, love and support throughout the last 2 years, regardless of how irritable I became. MERCI BEAUCOUP!!

ABSTRACT

The Svartliden Project is located in north central Sweden, 75km west-northwest of the town of the Lycksele. The geology comprises of a Palaeoproterozoic package of intercalated turbiditic sedimentary rocks and extrusive coherent and non-coherent basaltic rocks.

Gold mineralisation is associated with diopside +green amphibole +silica +arsenopyrite. Alteration is best developed along the intersection lineation between bedding and the primary cleavage. Mineralisation is concentrated in areas of low shear strain formed by the pressure shadow effect from the regional rotating syn-orogenic granitoids.

Pyrrhotite is the most pervasive sulphide and is found as a primary mineral in carbonaceous sediments and as a late-stage sulphide in the "Mineralised Zone". Pyrrhotite is responsible for the conductivity, chargeability and, along with magnetite, the magnetic susceptibility found in the Svartliden shear zone.

Ground magnetic and electromagnetic surveys were carried out over the project area. The ground magnetics does not differentiate the magnetite-bearing volcanics from the pyrrhotite-bearing carbonaceous sediments and the "Mineralised Zone". The ground electromagnetic survey defines high conductive zones, generated by the pyrrhotite-bearing sediments and the "Mineralised Zone", within resistive granitoids and volcanics.

Downhole apparent resistivity, IP and magnetic susceptibility were conducted on three drillholes along 1700mE. The magnetic susceptibility, as with the ground magnetics, is unable to differentiate magnetite-bearing volcanic rocks from the pyrrhotite-bearing units. Apparent resistivity has an inverse correlation with chargeability.

Log transformation of the ground in-phase EM data delineates first- and second-order conductive anomalies. First-order anomalies represent the pyrrhotite-bearing carbonaceous sedimentary unit. Second-order anomalies represent the pyrrhotite-bearing "Mineralised Zone". Second-order anomalies, calculated from in-phase EM data, can be used to target areas for gold exploration at both a project and regional scale.

TABLE OF CONTENTS

LIST OF FIGURES

Figure

LIST OF TABLES

Tables

1. INTRODUCTION

The Svartliden Gold Project is located in the Västerbotten County, North Central Sweden, and is approximately 200km south of the Arctic Circle. The Svartliden Project consists of three exploration permits totaling 729 ha. The three permits overlie a prospective stratigraphy beyond the southwest margin of the mineral-rich Skellefteå district.

In 1996, Viking Gold Corporation entered into a joint venture as operator and manager of the recently discovered Svartliden Project and has been actively exploring the project, working towards completion of a feasibility study. Viking Gold has drilled over 7,000m of core and chemically analysed over 4,000 samples for 31 elements.

The overall objective of this project is to define further mineral exploration targets within the Svartliden Project based on the synthesis of the existing geophysical and geological information.

The research plan consists of three main components:

a) To competently process, model and interpret geophysical data,
b) To correlate the geophysical interpretations with the geological model, and
c) Define further mineral exploration targets within the Svartliden concession.

The outcome of the project is to provide fundamental information on:

- The geophysical signatures of the main lithologies and alteration zones;
- The geophysical signatures of the brittle and ductile structures; and,
- The geophysical signatures, if any, that represent the gold mineralisation.

2. REGIONAL SETTING

2.1 LOCATION AND ACCESS

The Svartliden Gold Project is located in north central Sweden at Longitude 17°41'E and Latitude 64°44'N (Figure 2.1). The property straddles the boundary of the Lycksele and Storuman communes, Västerbotten County.

Svartliden is reached by following the sealed Highway 360 from Lycksele towards Vilhelmina for 59km before turning off to the village of Pauträsk. An all-weather gravel road runs through the property joining Lycksele, Pauträsk and Storuman. The road crosses the Svartliden mineralisation normal to the strike, some 6km north of the Highway junction and 8km south of Pauträsk. This gravel road continues 28km north from Pauträsk, where it joins the sealed Highway 46 from Vilhelmina to Storuman at Skärvsjöby, 15km from Storuman (Figure 2.2).

2.2 PHYSIOGRAPHY AND GEOMORPHOLOGY

The topography of the area is dominated by two hills, a)'Svartliden' (Black Hill), elevation of 525 mASL, southeast of the project area; and, b)'Ekorrliden' (Squirrel Hill), elevation of 490 mASL, in the western part of Ekorrliden EP. The region between the two hills is flat to gently undulating and is dissected by 'Svartlidbäcken' (Black Hill Creek) draining south-southeast to north-northwest, flowing into 'Pauträsket' (Pauträsk Lake). The Svartliden deposit underlies a relatively flat area (465 mASL) on the eastern side of Ekorrliden hill, which ascends eastwards for approximately two kilometres at a slope of 1° to 2°. The prospect area is forested, mostly cut pine and some uncut pine in the west.

Figure 2.1 Location map of the Svartliden Project in Scandinavia. The project lies in the North-central Sweden.

The Svartliden Project is situated in the centre of Swedish Map Sheet 22H-NO.

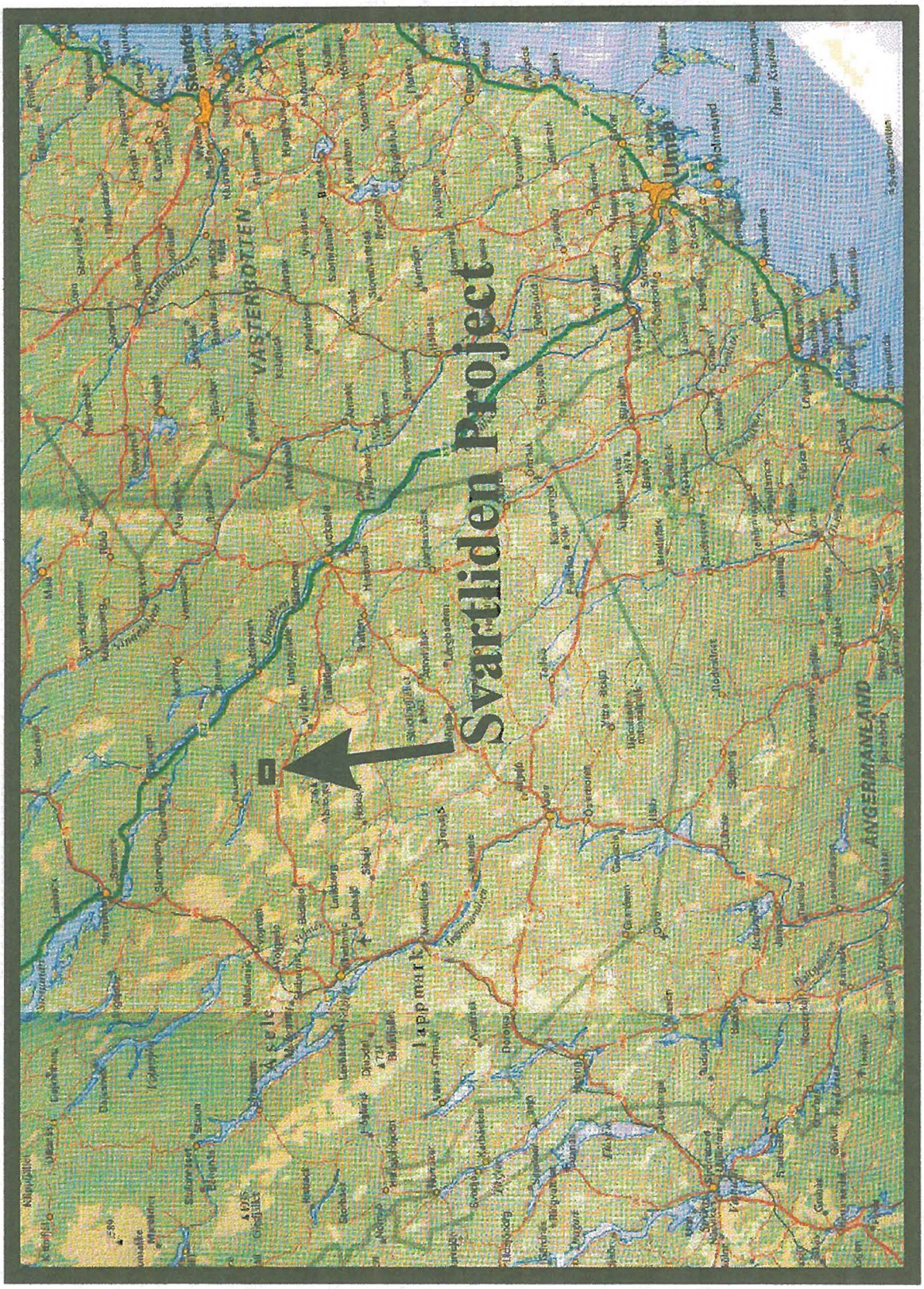

Figure 2.2 Location map of the Svartliden Project in North-central Sweden. The Project lies 8km south of the town of Pauträsk, 175km northwest of Umeå.

2.3 CLIMATE

During the winter months temperatures vary between 0°C and -30°C. Snow up to 2 m thick covers the whole area between late November and April/May. The thaw usually occurs in late April/early May and the summer months of July and August have average temperatures of between +10° and +25° C. The prospect area becomes boggy post the thaw and during summer.

2.4 MINING HISTORY

Active gold exploration in Sweden has increased markedly since the early 1990's when the Swedish Government altered the Minerals Act to encourage foreign investment and exploitation of its natural resources.

The three major historical mining centres in Sweden are the Bergslagen, Skellefteå and Norrbotten districts. These districts have been mined for centuries for precious and base metals, iron ore and more recently for diamonds.

Of the three major historical mining centres in Sweden, the Skellefteå district has provided most success for gold explorers and miners. In 1996 alone, five new gold deposits or prospects were discovered in the Skellefteå district, namely Åkulla (0.15 Mt @ 2.2 g/t Au, 15 g/t Ag) and Åkerberg (0.35 Mt @ 5.0 g/t Au) on the NE side, and Barsele, Storsjärnhobben and Svartliden on the SW side. The largest known single gold deposit in the district is Björkdal (13.9 Mt @ 2.2 g/t Au; originally +20 Mt @ +3g/t Au) which is located in the eastern part of the region, NW of Skellefteå. (Weihed, J.B., Bergström, U., Billström, K. & Weihed, P., 1996)

The Skellefteå district is 50 km wide, 150 km long, and trends NW-SE from Malå to Skellefteå on the Baltic Sea coast. Over 100 base and precious metal deposits have been discovered in the district since the 1920's with gold recently becoming a more significant commodity.

The majority of base metal occurrences are volcanogenic-hosted massive sulphide deposits with significant precious metal credits, such as Boliden and Kristineberg (Table 2.1). Gold mineralisation is also hosted by hydrothermal quartz veins in granodiorite and gabbro, such as at Björkdal (discovered 1986) and Åkerberg (Weihed, J.B., Bergström, U., Billström, K. & Weihed, P., 1996). Location of these deposits is shown in figure 3.3.

Svartliden lies on the southwestern margin of the Skellefteå district and represents a new style of mineralisation for the area - gold in hydrothermally altered shear zones.

Table 2.1 Tonnage and grade estimates of known deposits in the Skellefteå district. (data sourced from Weihed, J.B., Bergström, U., Billström, K. & Weihed, P., 1996)

Deposit	Tonnes Millions	Cu %	Pb %	Zn %	Au g/t	Ag g/t
Boliden	8.4	1.4	0.3	0.9	15.5	50
Kristineberg	20.1	1.0	0.5	3.7	1.0	35
Björkdal	13.9				2.2	
Åkerberg	0.35				5.0	

2.5 EXPLORATION HISTORY

Svartliden is located approximately 100km south of the Barsele and 60km south-east of the Storsjärnshobben gold prospects, in a region which previously had attracted little exploration attention for gold. Svartliden is a 'greenfields' discovery in a region now considered to be highly prospective for hydrothermal gold deposits.

The Swedish Geological Survey (SGU) conducted regional mapping, till sampling, gravimetrics and aeromagnetics throughout northern Sweden. The Svartliden Project is located on Map sheet 22H-NO (Northeast).

Lappland Guld AB first discovered the Svartliden deposit, in October 1994, after conducting a boulder-tracing (prospecting) expedition and trench-sampling programme.

In 1995, they carried out a trenching and preliminary magnetic and geophysical survey. This was followed by a four-hole diamond drill programme, which resulted in discovery of the main gold-bearing structure at Svartliden.

By June 1998, Viking Gold completed an exploration drilling program of 45 diamond drill core holes for a total of 7,647 meters distributed over a strike length of 1800 metres, in conjunction with some trenching and ground geophysical surveying. Check assay programs indicate no major bias or systematic errors in sampling, preparation or assaying. All exploration has been conducted using standard industry practices.

2.6 PROJECT RESOURCE

A preliminary Resource Calculation on the Svartliden Project was conducted by Computer Aided Geoscience (CAG), in April 1998.

The specific aims of the study were:-

a) Audit and validate the exploration databases;
b) Prepare a 3 dimensional interpretation and computer model of gold mineralisation geometry;
c) Investigate mineralisation statistics and geostatistics to identify homogenous assay populations;
d) Create a 3 dimensional grade model of the mineralisation;
e) Summarise the Geologic Resource by area and resource category

The following resource for the Svartliden Project was calculated for a 1.0g/t Au cutoff. At the time of writing, the total geological resource was 2.5 million tonnes @ 5.4g/t Au. This equates to contained 435,000 ounces gold.

3. REGIONAL GEOLOGY

3.1 GEOLOGY OF THE FENNOSCANDIAN (BALTIC) SHIELD

The Fennoscandian (Baltic) Shield occupies the northern part of Europe. Areas of Precambrian rocks are exposed in Norway, Sweden, Finland and Russia. The Caledonian orogenic belt to the west borders the craton (Freden, 1994) (Figure 3.1).

The Fennoscandian Shield is composed of Archaen to Neoproterozoic rocks. The term 'Svecokarelian' refers to the orogeny, which occurred between 1.9Ga and 1.8Ga (emphasising deformation and metamorphism). The term 'Svecofennian' refers to the supracrustal rocks that were emplaced during c. 1.95Ga to 1.85Ga (Weihed & Maki, 1997)

Archaen and Palaeoproterozoic complexes make up the pre-Svecokarelian crustal growth. These complexes consist of greenstone belts and TTG-terranes, while crustal growth during the Palaeoproterozoic involved rifting of the Archaen basement with the formation of rift-fill sequences of sedimentary and igneous rocks. (Weihed & Maki, 1997)

3.1.1 Pre-Svecokarelian Crustal Growth

The Archaen complexes consist of tonalitic gneisses and migmatites of ages between 3.20Ga-2.70Ga. Greenstone belts were emplaced during the magmatic and metamorphic event around 2.84Ga. The greenstone belts were subsequently deformed and intruded by younger granitoids of age between 2.75Ga and 2.69Ga.These greenstone belts form a prominent part of the Finnish and Russian bedrock, but are only minor components in Sweden. (Weihed & Maki, 1997)

3.1.2 Palaeoproterozoic Complexes

The post-Archaen crustal growth of the Karelian craton (see Karelian Province on figure 3.1) consisted of several episodes of sedimentation, rifting and magmatism between 2.50Ga-1.90Ga. The Lapland Greenstone Belt, situated in northern Sweden and Finland, is composed mainly of mafic volcanics intercalated with sedimentary rocks, deposited unconformably on the Archaen basement between 2.50Ga and 2.00Ga. After this stage, juvenile volcanic arcs formed at the margin of the Karelian craton. Rocks formed by this process are referred to as 'Svecofennian' rocks. (Weihed & Maki,1997).

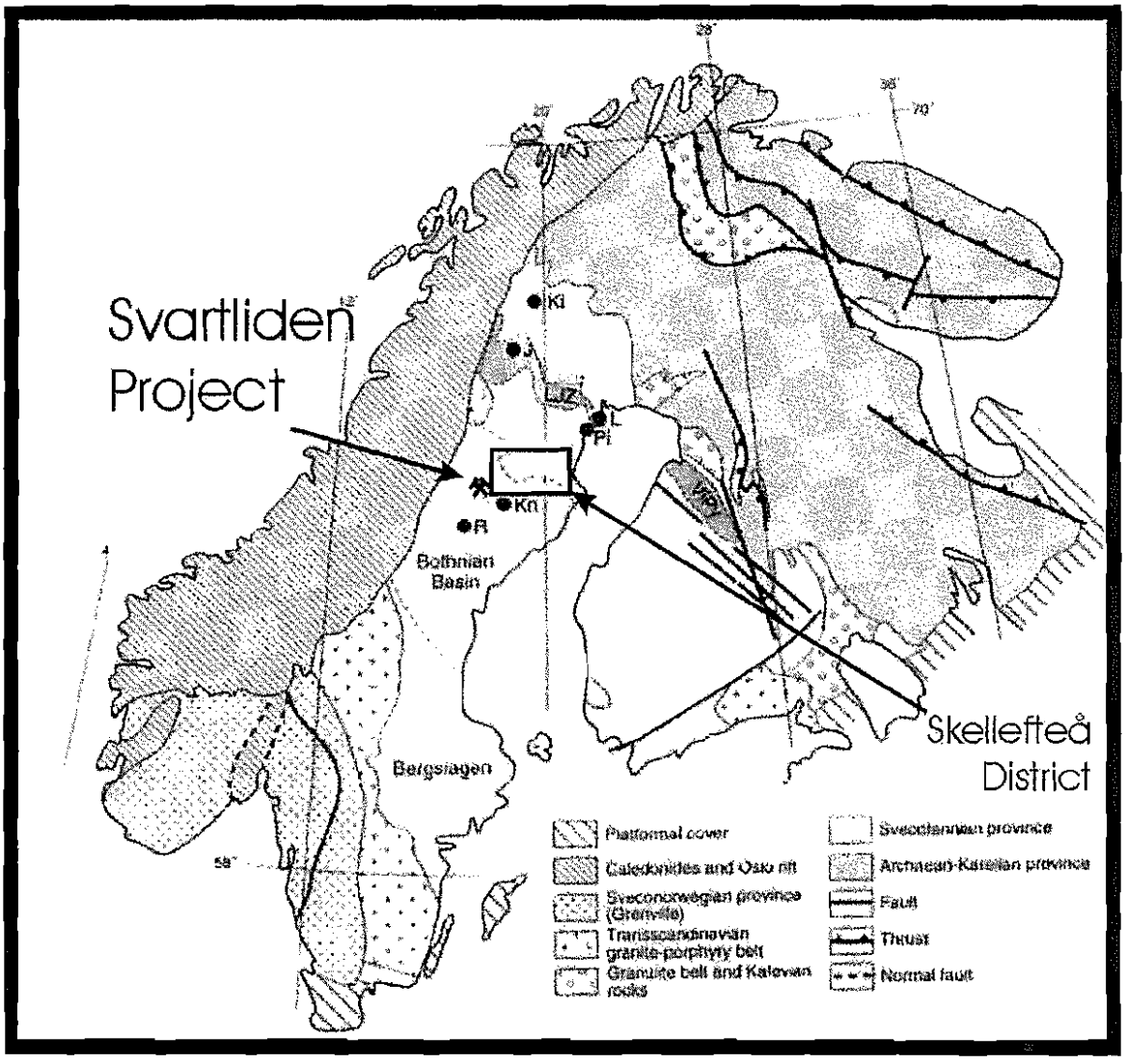

Figure 3.1 Generalised Geology Map of Scandinavia and the location of the Skellefteå District and Svartliden Project (after Billström & Weihed, 1996). J = Jokkmokk, Ki = Kiruna, Kn = Knaften, L = Los, LJZ = Luleå-Jokkmokk zone, Lu = Luleå, Pi = Piteå, R = Rockliden, ViPy = Vihanti-Pyhälsami area. LJZ is marked in grey shading. The box outline to the east of the Svartliden Project corresponds to the location of the Skellefteå District in Figure 3.3.

3.1.3 Svecokarelian Orogeny and Svecofennian Crustal Growth

The Svecofennian rock suite consist of 3 groups:-

a) The supracrustal rocks deposited between c. 1.95Ga and 1.85Ga;

b) Late orogenic S-Type granites emplaced around 1.83Ga and 1.80Ga; and,

c) Late to post-Svecokarelian (c. 1.80Ga), A- to I-Type alkaline granitoids.

In Sweden, from the Skellefteå district southwards, the peak metamorphism is between 1.84Ga and 1.80Ga (Billström & Weihed, 1996).

Several palaeoproterozoic provinces, including the Bergslagen and Skellefteå districts in Sweden, border the Karelian Craton. These are probably remnants of volcanic arc systems that were accreted to the Karelian continent shortly after emplacement. All these areas are extensively mineralised and the different character of the metallogeny reflects variations in the tectonic setting (Figure 3.2).

3.2 GEOLOGY OF THE SKELLEFTEÅ DISTRICT

The Skellefteå District is a loosely defined area containing ore bearing, mainly submarine felsic volcanic units, between Kristineberg in the west and Boliden in the east. (Weihed et al, 1996)

The Svartliden Project lies beyond the western margin of the Skellefteå district in northern Sweden, 54km southwest of Kristineberg. The district forms part of the Svecofennian supracrustal sequence and associated intrusive rocks (c.1.90Ga – 1.85Ga). A thick pile of felsic volcanic rocks dominates the area, which host over 85 pyritic, base metal deposits. (Weihed *et al*, 1996)

The Skellefteå district is bordered to the north by low-grade, shallow water to subaerial volcanic rocks (Arvidsjaur Volcanics) and to the south by high-grade gneisses and migmatites of the Bothnian Basin. The general stratigraphy consists of volcanic rocks (Skellefteå Group) overlain by turbiditic sedimentary rocks and coarser clastic rocks, as well as younger, volcanic rocks (Vargsfors Group) (Weihed *et al*, 1996) (Figure 3.3).

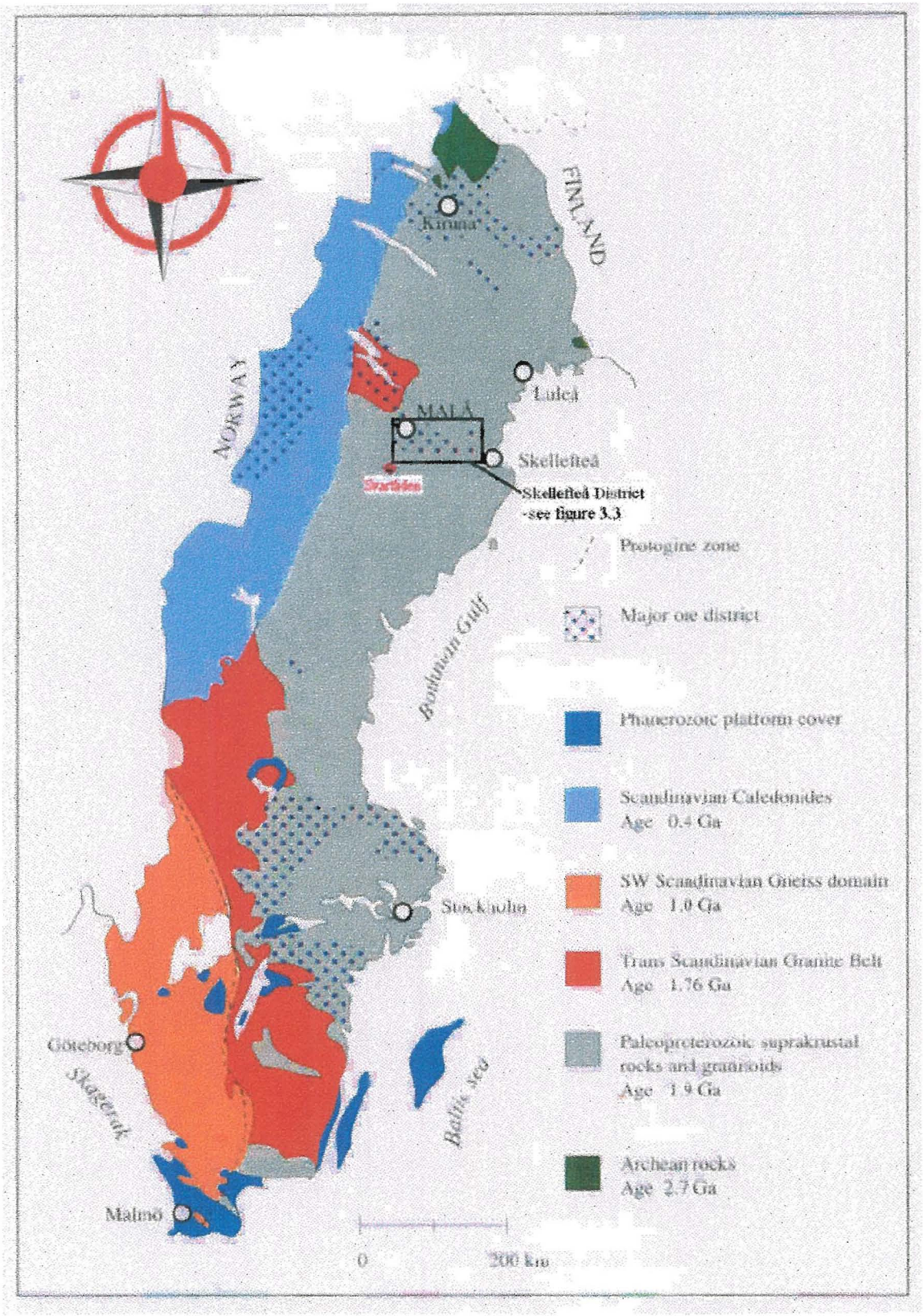

Figure 3.2 Simplified Geology Map of Sweden showing the major geological units and ages. The principal mining districts are shown with a dotted pattern. The main regions are from the north: Norrbotten, Skellefteå and Bergslagen (Freden, 1994).

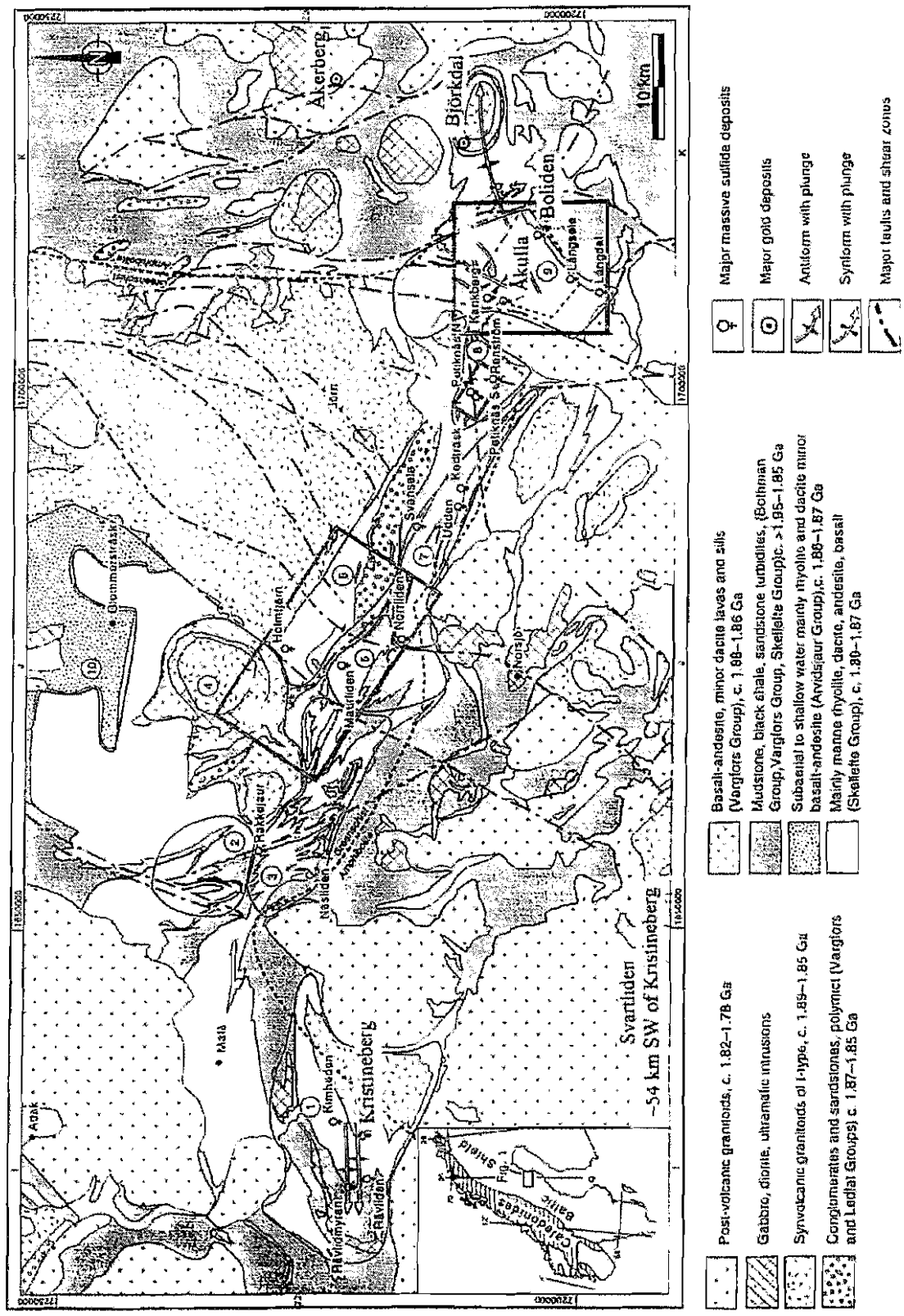

Figure 3.3. Simplified geological map of the Skellefteå district, with the location of ten geologic domains (Allen *et al*, 1996). 1=Kristineberg, 2=Hälträsk, 3=Näsliden-Mensträsk, 4=Gallejaur, 5=Maurliden, 6=Petikträsk, 7=Udden, 8=Renström, 9=Boliden, 10=Arvidsjaur. Locations of the major Skellefteå ore deposits, and the metamorphic boundary between greenschist and amphibolite facies.

4. PROJECT GEOLOGY

The Svartliden Project is situated on the southwestern edge of the Skellefteå District amongst a volcano-sedimentary 'greenstone' sequence within the Bottnian Basin.

Svartliden is located in the centre of Swedish Map Sheet 22H-NO (Northeast). A geological map for map sheet 22H-NO was compiled by the Swedish Geological Survey (SGU) using the regional aeromagnetics.

The Svartliden Project is centred on a 'lozenge' of volcano-sedimentary rocks wrapped around a syn-deformational granitoid (red) and trending in an east northeast-west southwest direction (Figure 4.1).

The geology of the Svartliden Project area, compiled from +7,000m of drill core, comprises of a Palaeoproterozoic package of intercalated turbiditic sedimentary rocks and extrusive coherent and non-coherent basaltic lava flows within a broad ductile shear zone. The whole sequence has been intruded by pre- and syn-deformational granitoid dykes and sills, and is metamorphosed to upper amphibolite grade facies (Figure 4.2).

Hydrothermal Alteration has taken place during the main deformational event and is synchronous with the granitoid intrusions. Gold mineralisation has focussed within favourable structural and lithological traps within the broad ductile shear zone.

4.1 CAINOZOIC GEOLOGY

During the Cainozoic, several glacial events deposited layers of glacial till over the Baltic Shield. The ice-sheet movement over Sweden is understood to be to the southeast. (Freden, 1986)

Svartliden hill and Ekorrliden hill are residual topographic highs. The remainder of the project area is covered by glacial till of a thickness between 1 and 14 meters. (Marsh & Laurent, 1998).

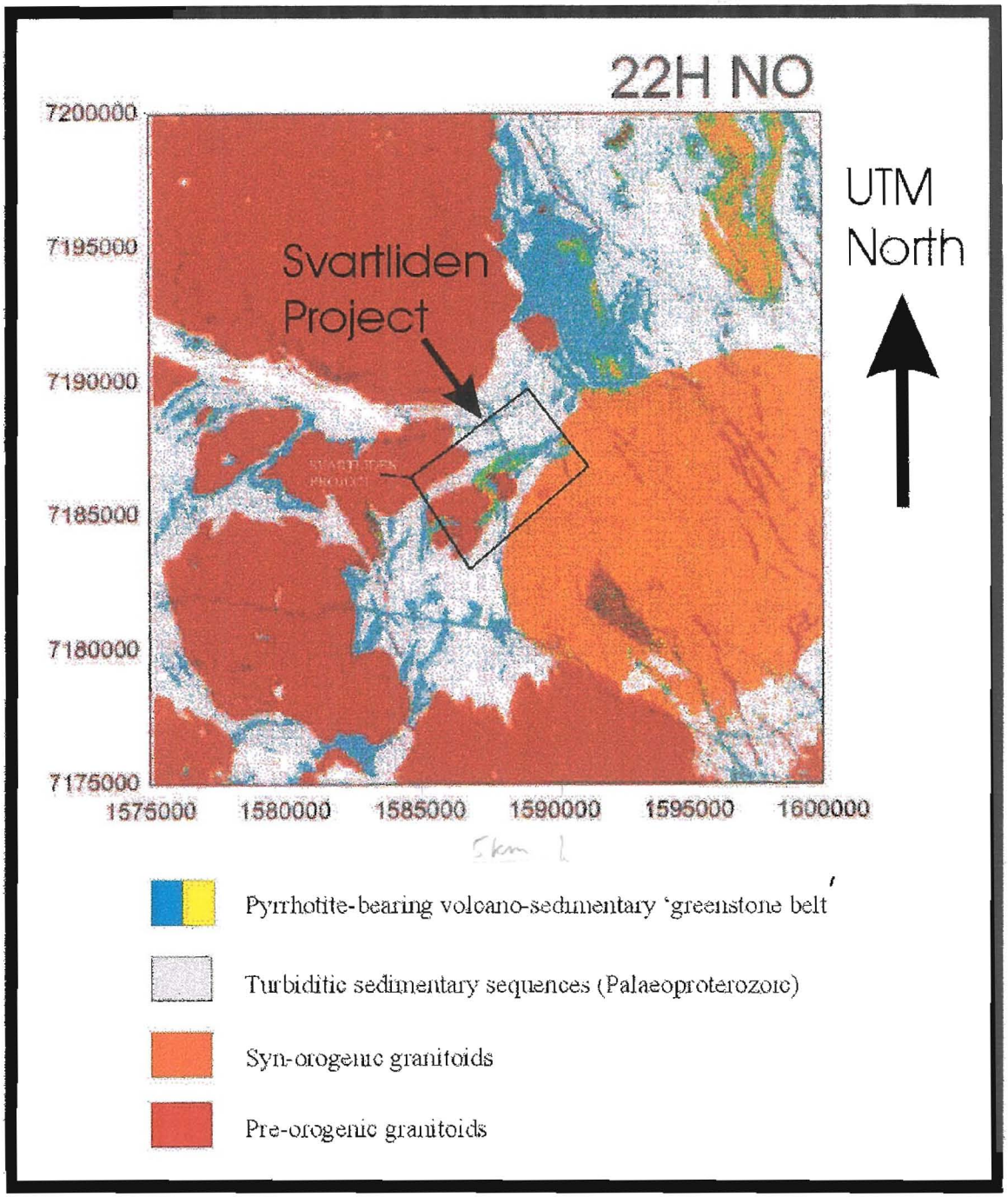

Figure 4.1 Interpreted Geology from aeromagnetics (modified from Freden 1994). Map Sheet 22H-NO.

The greenstone belts have, in general, a north-northeast trend with local fluctuations caused by the granitoid intrusions. The greenstone sequence on the Svartliden Project has a distinct east-northeast trend and has flexed in the shape of an 'S' as a result of the intrusion of the syn-deformational granitoid.

The 'cyan' syn-deformational granitoid to the east of the Svartliden Project is a granite dome, which peaks at Svartliden Hill, some 1.5km southeast of the project boundary. The main 'red' pre-deformational granitoid covering the northeastern part of the map is Pauträsk Hill and peaks behind the town of Pauträsk (approx. 7km from project boundary).

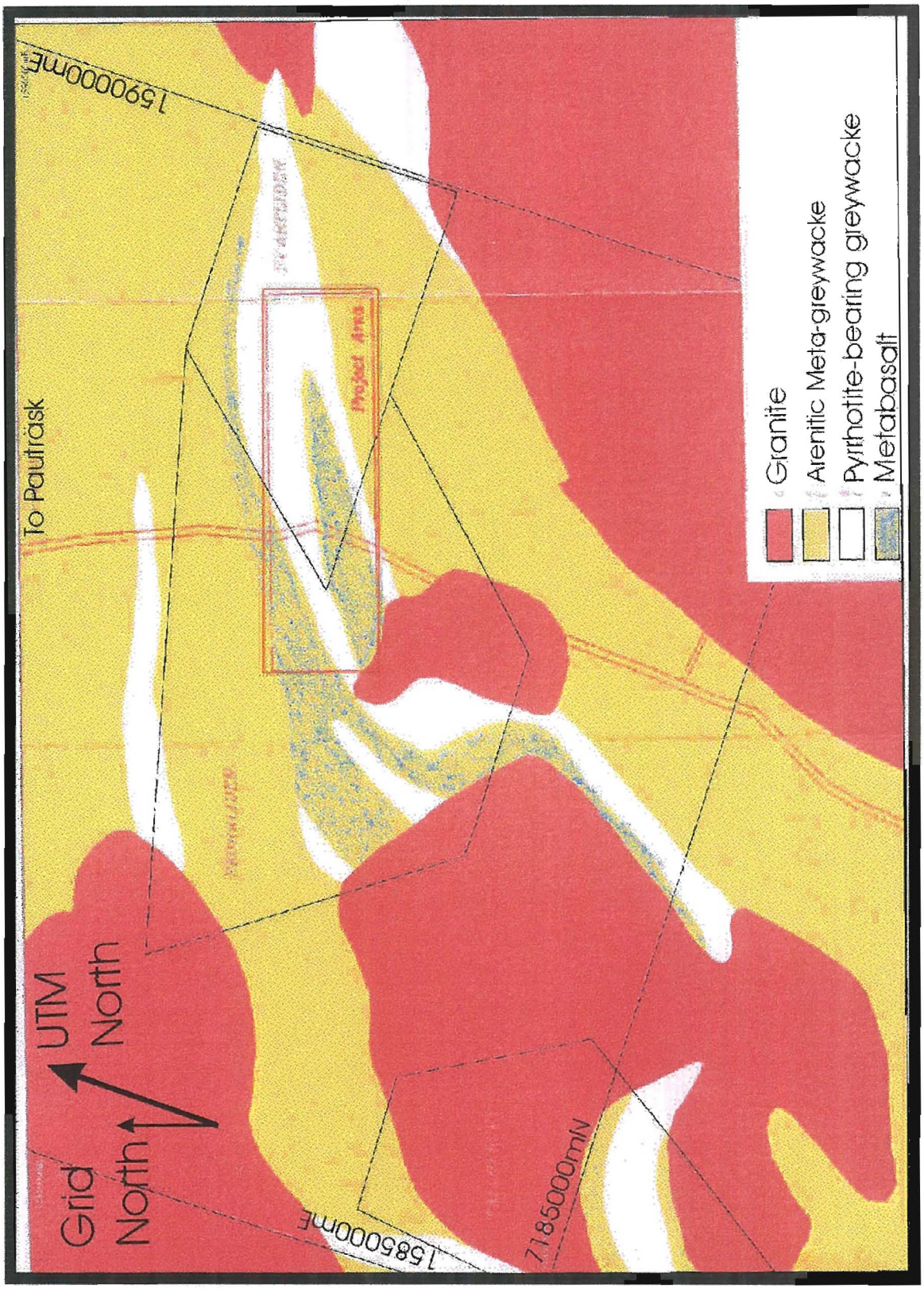

Figure 4.2 Interpreted Geology Map of the Svartliden Project. The geology is based on a combination of a) the drilling conducted within the project area (red outline), and b) interpretation of the regional aeromagnetics. This map is oriented grid north (341.4°magnetic).

4.2 LITHOLOGIES

4.2.1 Sedimentary Rocks

The suite of sedimentary rocks consists of intercalated and interbedded carbonaceous ± pyrrhotite rich shales, siltstones and sandstones. This sedimentary package is typical of a turbiditic sequence. Individual sedimentary units vary from sub-cm to >20m thick within sedimentary packages over 30m thick. Primary sedimentary textures are difficult to discern due to the high degree of metamorphism and internal deformation. However coarse upward fining sequences have been recognized within sandstone and siltstone units.

The carbonaceous ± pyrrhotite-rich, shale units are black, often strongly silicified and display strong internal deformation features. Pyrrhotite concentrations vary between <1% to 30% over widths of 1m to 20m and occur in thin lenses parallel to cleavage and wrapping around folded quartz veins, and as 'saddle-reef' type aggregates within fold closures (Figure 4.3).

Siltstone units are commonly brown or grey and display a high degree of internal textural and compositional variation. This variation represents primary lithological variations such as bedding and facies changes. Pyrrhotite does occur in siltstone units along cleavage planes and/or remobilised into fractures and veins. Deformation textures such as folded beds, folded quartz veins and 'kinked' cleavage are common. Silica and metamorphic biotite are common macroscopic minerals associated with this rock type (Figure 4.4).

Sandstone units make up approximately 10% of the sedimentary package and display similar internal variations and textures to those in the siltstone units. However there is a higher proportion of siliciclastic material in the sandstones than in the siltstones.

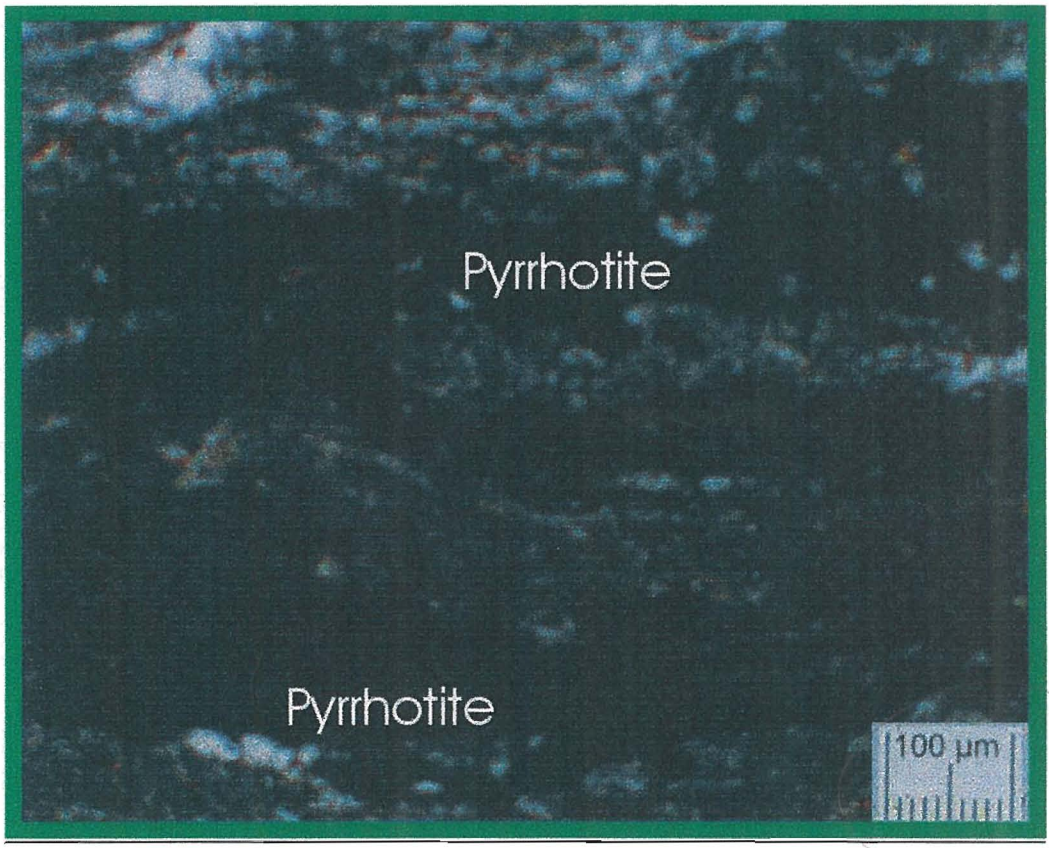

Figure 4.3 Photomicrograph of Pyrrhotitic siltstone. Note the concentration of pyrrhotite in bands and aggregates (anisotropic) developed along the penetrative fabric amongst a groundmass of biotite + quartz + K-felspar. Sample 9718a ; Plane-polars ; FOV = 1.935mm

Figure 4.4 Core sample of foliated carbonaceous±pyrrhotitic sediment. Note the granite dyke cross cutting the fabric, but also ductilely deformed, as shown by the 'pressure shadow' around the granite intrusion. Core sample = drill hole SV9712. Core length is ~20cm (from 57m drillhole depth).

4.2.2 Volcanic Rocks

Basalt units vary from <1m to more than 50m thick but they are commonly 10m to 20m thick. Primary depositional textures such as vesicles near pillow margins, hyaloclastite, peperite and autobreccia have been logged throughout the sequence (Figure 4.5).

A unit of coarse-grained basalt exhibits gabbroic textures. Initially it was believed that this unit was a gabbro dyke intruding the existing basalt layer. A gradational facies change rather than chilled contacts suggest that this gabbroic unit is the product of a slower cooling core of a large basaltic flow.

Within the ductile shear zone the basalts exhibit strongly foliated to mylonitic textures (Figure 4.6 & 4.7). Outside the shear zone, the basalts are generally homogenous and weakly foliated. Brown biotite is the main metamorphic mineral, whereas green amphibole (tremolite?) and clinopyroxene (diopside) are the common hydrothermal alteration minerals (Figure 4.8). A moderate to strong cleavage depicted by alignment of biotite is prevalent throughout most units.

4.2.3 Granitoid Rocks

The granitoid units (granites and/or) granodiorites are leucocratic, having undergone regional metamorphism and hydrothermal alteration within the ductile shear zone. There are textural varieties of granites ranging from coarse-grained pegmatite, through equigranular granite to aplite dykes (Figure 4.9 & 4.10). Despite this textural range, only one compositional type of granite was observed (McCuaig, 2000). The dominant minerals are quartz, feldspar (sericite and/or albite), muscovite, garnets and rare late-stage hornblende laths overprinting all previous textures (McCuaig, 2000).

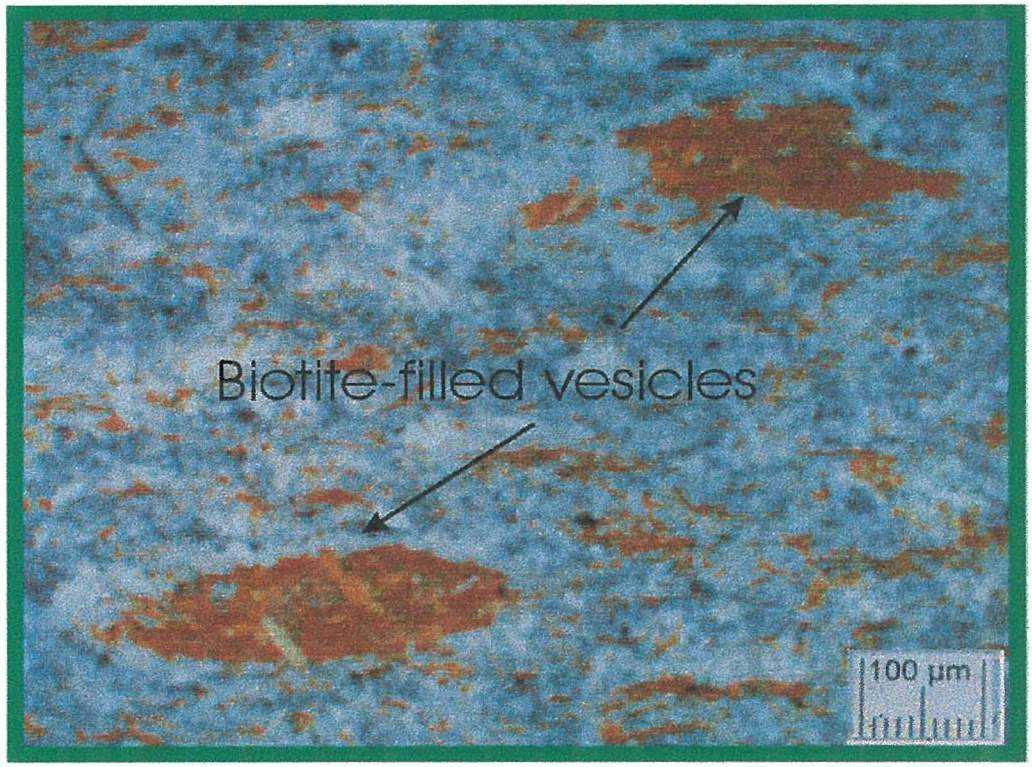

Figure 4.5 Photomicrograph of foliated vesicular basalt. The vesicles have been devitrified and replaced by biotite. The vesicles have been 'squashed' during the primary deformation event and are aligned along the penetrative fabric. Sample 9841 (174.00m-174.05m) ; plane polars ; FOV = 1.935mm

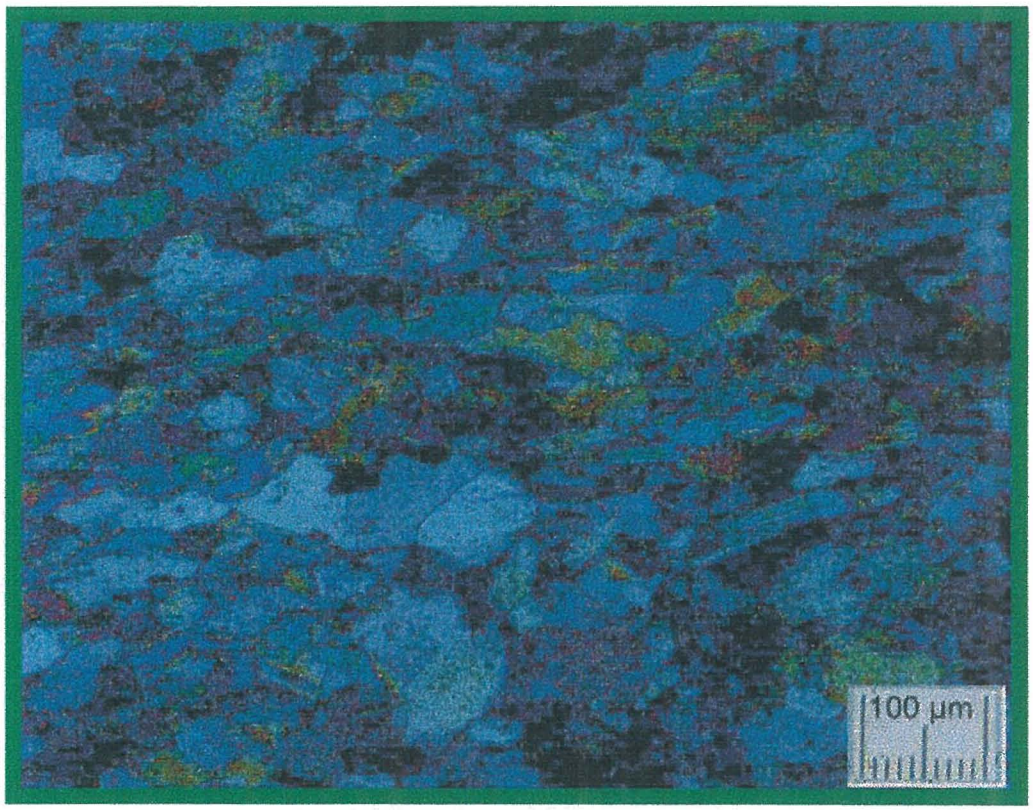

Figure 4.6 Photomicrograph of altered foliated basalt. The stubby, pleochroic mineral is hornblende. The high-temperature recrystallised quartz has undulose extinction. Foliation trends from left to right. Sample SV9836 (167.20m-167.25m) ; cross-polars ; FOV = 1.935mm

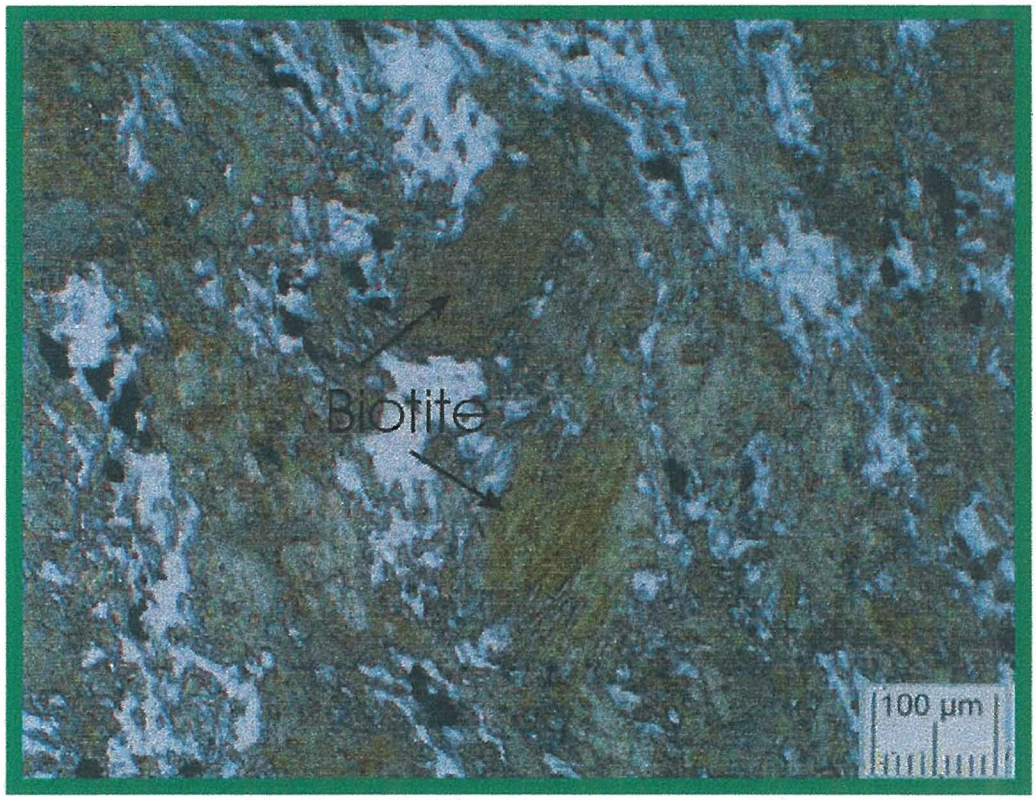

Figure 4.7 Photomicrograph of amphibole-rich foliated basalt. Penetrative fabric trends from top left to bottom right. There is amphibole (actinolite?) development across the fabric. The opaques are pyrrhotite blebs. Sample SV9724 (130.00m-130.10m) ; plane-polars ; FOV = 1.935mm

Figure 4.8 Core sample of altered volcanic rock from drillhole SV9712. The top of sample at bottom right (5.4m) has the alteration assemblage (clinopyroxene-amphibole-arsenopyrite-quartz). The bottom of sample at the top left (11m) has the outer biotite alteration zone.

The granitoids occur as 45° south-dipping dykes that have been warped and altered within the shear zone. The granitoid intrusions crosscut the pervasive fabric at high angles. Contacts with surrounding rocks are often sheared but with a penetrative cleavage that crosscuts the margins. These textures suggest that the granite dykes intruded late in the ductile deformation event (McCuaig, 2000) as they both cut the fabric and are deformed by the pervasive fabric.

Down-hole intersections vary between <1 m and 64 m wide, giving true widths of up to 30 m, trending upto 80 m in length. Measured contact angles and internal open-spaced cleavage textures are orientated parallel to the main cleavage. Due to refraction within the ductile shear zone, the granitic unit has flattened. This flattening affect has created interference patterns sub-parallel to the pervasive fabric (Figure 4.11).

4.3 METAMORPHISM

Peak metamorphic grade is mid- to upper-amphibolite facies based on the presence of metastable biotite, albite and quartz in non-hydrothermally altered rocks. This is consistent with the greenschist-amphibolite boundary drawn by Allen et al. (1996) in Figure 3.3. Based on detailed chronological studies Billström & Weihed (1996) interpreted peak metamorphism to have occurred between 1.84 & 1.82Ga. The main deformation event is considered synchronous with peak metamorphism due to the presence of biotite and albite within the most deformed zones. (Marsh & Laurent, 1998)

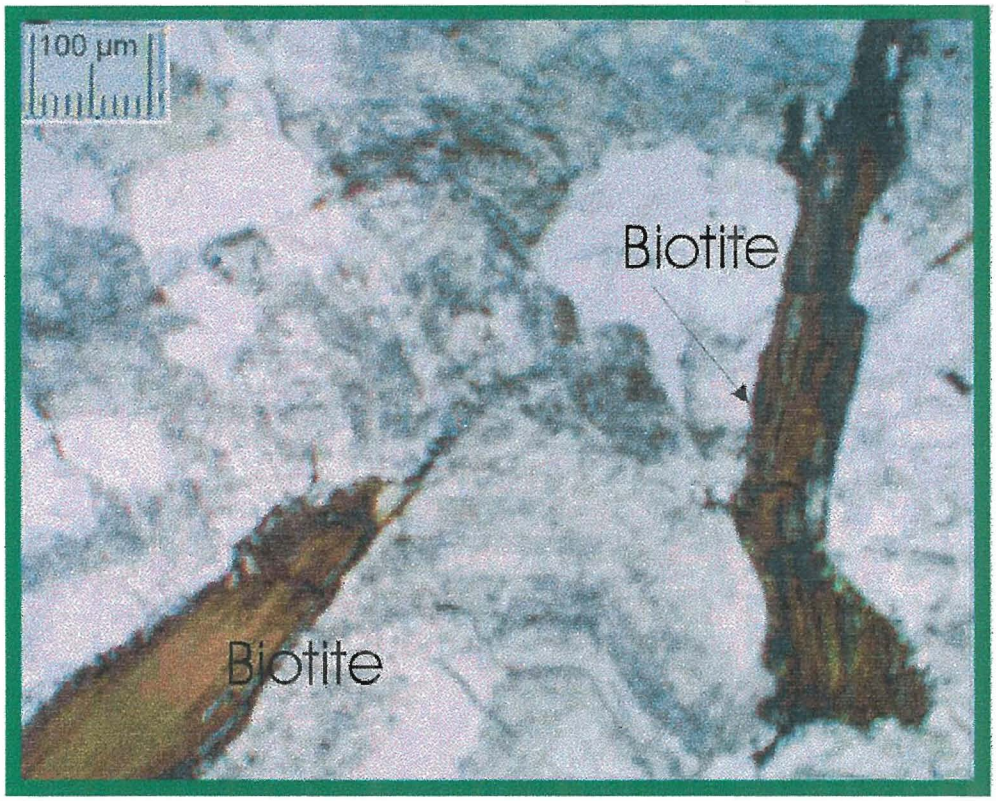

Figure 4.9 Photomicrograph of syn-deformational granite.
As a result of the deformation event, the biotite is strained and there is sericite alteration of the K-feldspar.
Sample SV9839 (35.40m – 35.45m) ; plane-polars ; FOV = 1.935mm

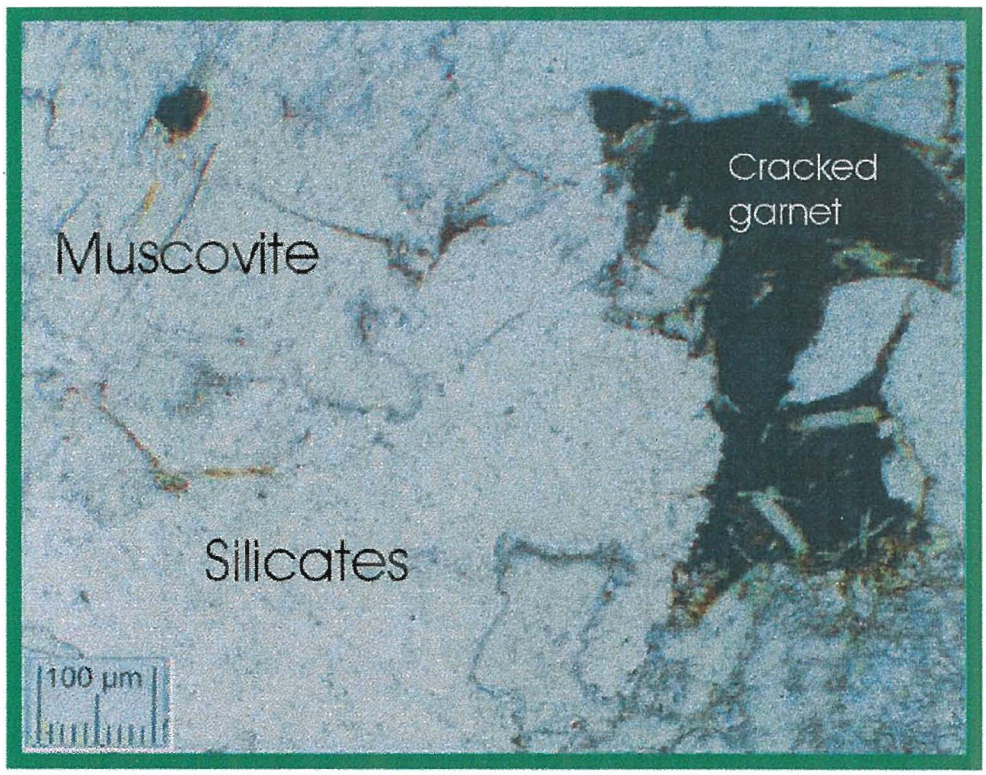

Figure 4.10 Photomicrograph of a coarse-grained granite. Coarse-grained muscovite in the top left.
The opaque mineral is a group of rotated and cracked garnets.
Sample SV9831 (33.50m – 33.55m); plane-polars ; FOV = 1.935mm

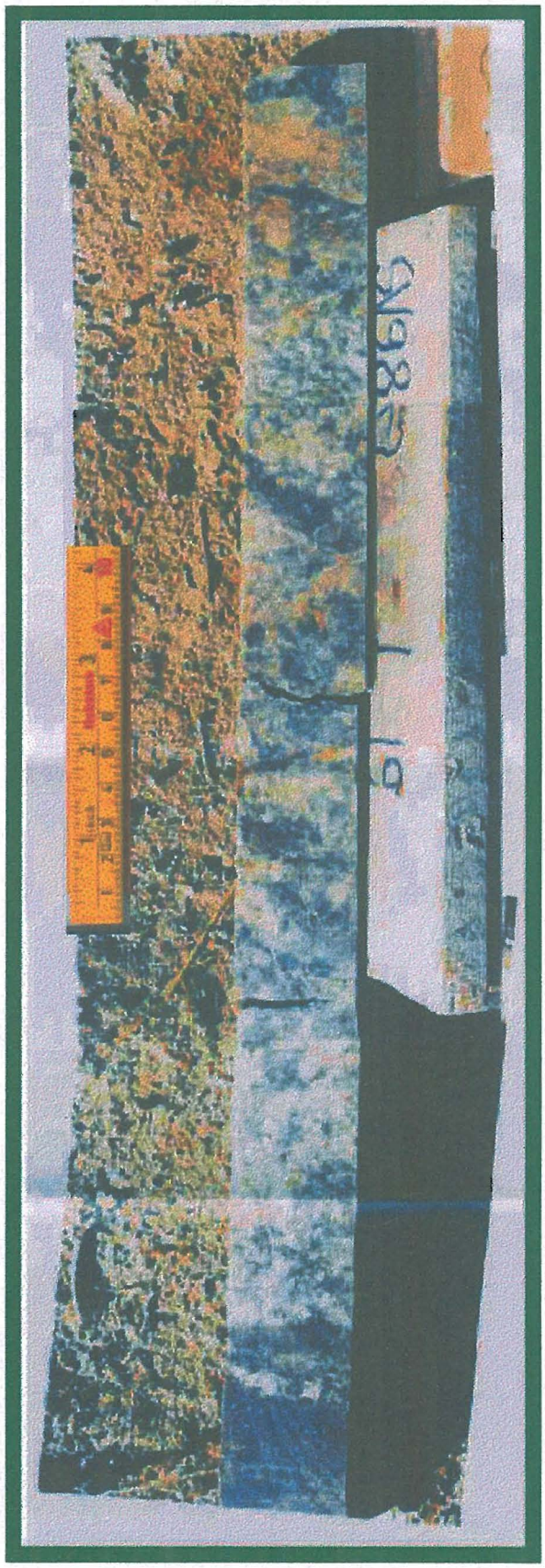

Figure 4.11 Core sample of altered granite from drillhole SV9723 (71.8m-72.2m). BOH to bottom of page. The granite has significant textural variation, the likely result of deformation.

4.4 STRUCTURAL GEOLOGY

4.4.1 Folding

The major deformation event (1.84Ga- 1.82Ga) created a broad ductile shear zone, which induced strain partitioning and subsequent folding synchronous with peak metamorphism. During the folding event, the less competent sedimentary rocks underwent foliation development and tended to become shear compartments. This created a high degree of internal distortion in these units. The more competent granitic (and to a lesser extent volcanic) rocks experience less shear and, hence, become shortening compartments.

Common structural textures include:

1) Tight to isoclinal ptigmatic folds. These folds have axial planes parallel to the regional cleavage. The fold axes mirror the plunge and plunge-direction of L^0_1 lineations seen on fracture surfaces and in outcrop, which plunge between 6°-18° to the ENE and WSW.
2) Folded quartz veins. These folds have the same textures and orientations as the ptigmatic folds. The presence of folded quartz veins also suggests there was an early phase of hydrothermal activity that deposited the veins.
3) Subparallel bedding/cleavage relationships. The predominant cleavage orientation strikes ENE with a subvertical or steep southerly dip (~80°). Local variations from this trend do occur with some cleavage planes having a steep northerly dip (~80°) in the eastern part of the deposit.

These observations and interpretation of the ground magnetic and EM data, suggest that the structural setting at Svartliden is an isoclinal anticline, which strikes east-northeast with a fold axis plunging 6°-18° to the east and west of 1500mE. The axial plane cleavage data indicates the presence of a slightly overturned fold axis to the south with local internal variation to the north.

4.4.2 Axial plane Shearing

Shear zones have been logged in drill core across the length of the entire deposit. The stratigraphy south of the main Svartliden Shear Zone is discordant to the shear zone. The shear zones are characterised as zones that are either intensely foliated, contain quartz ± albite-rich mylonite zones, or are intensely silicified. The shear zones vary between <1m to more than 50 m wide. The shear zones lie parallel to the axial plane cleavage and control the location of the hydrothermal gold mineralisation.

The shear zone has undergone reverse movement (S-block up) based on the presence of:-

a) S-C fabrics;
b) tension gashes (figure 4.12) ;
c) quartz/clinopyroxene boudins with asymmetric pressure shadows; and,
d) Subhorizontal intersection lineations.

4.4.3 Late-stage Faulting

Late-stage faulting and fracture zones are characterised by carbonate±quartz±pyrite veins and fracture-fill within narrow fault/shear zones that crosscut all other features. A late-stage fault based on a core fracture angle, strikes between NW and NE and dips sub-vertically; it is believed to be essentially a strike-slip fault.

Figure 4.12 Example of a rotated tensional gash cutting the alteration band at high angle. Core from SV9723 (from 57.55m); BOH to right.

4.5 HYDROTHERMAL ALTERATION

Hydrothermal fluids migrated along the penetrative S^1 fabric during the later stages of the broad ductile deformation event at Svartliden. A zonation of alteration has developed, consisting of a transition from intensely silicified and deformed host rocks with quartz-diopside-green amphibole-graphite-calcite veins and selvages (ore zone), to 'least-altered' host rocks, through biotite-altered host rocks (distal zone). The 'ore-zone' has the greatest concentration of gold and/or silver mineralisation.

4.5.1 Wallrock alteration

The outer limits of this hydrothermal alteration (or distal zone), was dominated by alteration of existing mineralogical assemblages with little or no deposition of metals within tensional quartz veins. The dominant alteration mineralogy of sedimentary and volcanic rocks in the distal zone is biotite±quartz±pyrrhotite (Figure 4.13). The granitoids that have undergone distal hydrothermal alteration have resilicified and have had sericite alteration of the feldspars.

Biotite is a meta-stable mineral in the wallrock (dominantly basalts and siltstones). Hydrothermal alteration of the wallrock has altered the medium-grained red-brown biotite crystals to fine-grained brown-green crystals (Figure 4.14). Hydrothermal fluids have introduced more silica into the wallrock and have resulted in recrystallisation of existing quartz crystals and 'crack-sealed' tensional gashes and veins. Pyrrhotite is a primary mineral in the carbonaceous shale unit and appears to have been remobilised into the shear zone during the hydrothermal event. This is supported by the presence of:-

a) Pyrrhotite along micro-fold hinges in the sheared sediments;
b) Pyrrhotite bands within the foliated sediments; and,
c) Trace pyrrhotite aggregates within altered granites (usually near contacts).

Gold mineralisation in this distal zone ranges from 0.50g/t to below detection. Some small ore zone selvages (~20cm) within the distal alteration zone have gold grades of upto 2g/t.

4.5.2 Ore Zone

Ore zones occur in dilational sites formed in shallow south-dipping flexures of the steeply south-dipping shear zone. These dilational sites or 'pressure shadows' have developed in flexures around more competent granitoid and basalt (amphibolite) blocks and dykes. The best dilational sites are developed subparallel to the shallow-plunging[1] intersection lineation, giving the ore zone a subhorizontal cigar shape.

The original rock fabric in the ore zone has often been obliterated. Hydrothermal-related silica and arsenopyrite aggregates overprint metamorphic textures. These dilational sites allowed the growth of calc-silicates such as diopsides and tremolite in the sheared meta-volcanics and graphite in the sheared meta-sediments.

The principal mineralogy within the ore zone is clinopyroxene (diopside) + green amphibole (tremolite) + quartz + carbonate (± calcite) + pyrrhotite + arsenopyrite ± chalcopyrite ± graphite ± GOLD±SILVER (silver tends to crystallise on the margins of the entire shear zone or hydrothermal cell) (Figure 4.14 & 4.15).

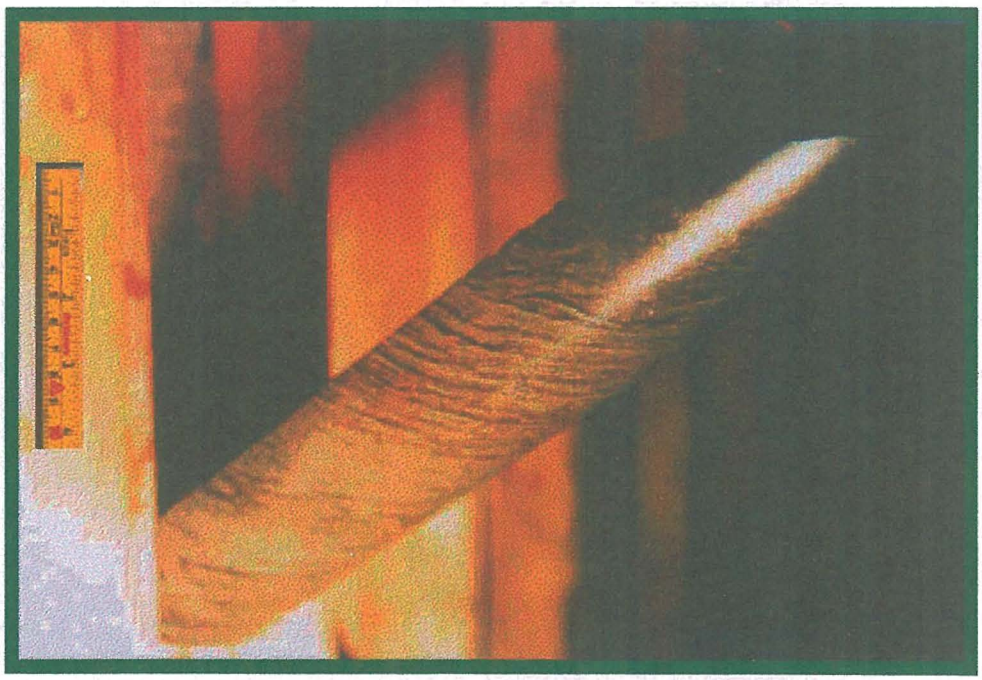

Figure 4.13 Core sample of Shear Zone from drillhole SV9712. Biotite/Pyrrhotite alteration

[1] Measured intersection lineations at Svartliden have plunges between 6° and 18° to, both, grid east and to grid west of the 1500mE.

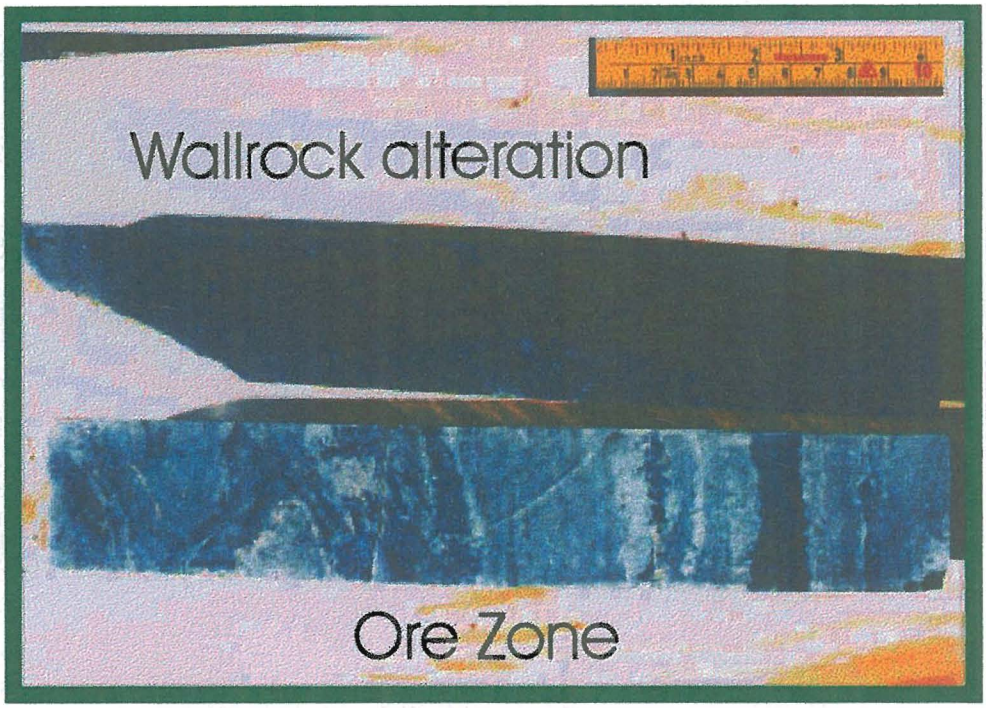

Figure 4.14 Core sample of alteration zone. Top = 52.9m. Top of ore zone. Biotite ± pyrrhotite alteration (distal zone). C-Fabric is shallow to core axis. Bottom = 54.8m. Upper ore zone. Clinopyroxene (stubby light green mineral) + amphibole (fibrous dark green mineral) + sulphides (arsenopyrite/pyrrhotite) + quartz veins.

Figure 4.15 Core sample of ore zone from SV9712. Alteration bands cut by the pervasive ductile foliation, defined by Clinopyroxene (stubby light green mineral) + amphibole (fibrous dark green mineral) + sulphides (arsenopyrite/pyrrhotite) + quartz veins. The alteration and deformation are synchronous.

4.6 MINERALISATION

4.6.1 Gold

Gold has a variable distribution and size range within the ore zone. Visible gold was encountered in the core. All gold grains examined microscopically are argentian. Gold can be associated with the hydrothermal minerals identified in the ore zone.

Refractory gold in coarse arsenopyrite and loellingite crystals is common. Gold grains usually appear as very angular inclusions within the arsenopyrite. The size range is between <2 to 50 microns. Coarser visible gold is present in very coarse-grained arsenopyrite (Figure 4.16).

Gold grains have grown within the calc-silicates. Aggregates of sub-angular gold particles ranging in size from 5 to 130 microns can be set within the clinopyroxene (diopside and clinozoisite) and amphiboles (tremolite and hornblende). Although the silicates are often surrounded by quartz, no gold has grown beyond the calc-silicate grain boundaries (Figure 4.17). In some cases, gold grains between 2 and 20 microns, are attached to narrow pyrrhotite veins, which crosscut the pyroxenes.

Clusters of gold 'fines' can, also, be found associated with graphite. Graphite has an average grain size of 70 microns hosting gold fines between <1 and 10 microns (Figure 4.18).

4.6.2 Silver

There is a silver zone at the eastern edge of the Svartliden deposit. It has a similar alteration assemblage to that developed in the gold bearing 'ore-zone' but with locally developed cataclasite, which is generally absent from the main shear zone. The dominant silver sulphide is argentite. It appears as a corona around the coarser grained gold (>100 microns) in the ore zone, and as a thin grey laminae within silicified zones at the eastern edge of the Svartliden deposit.

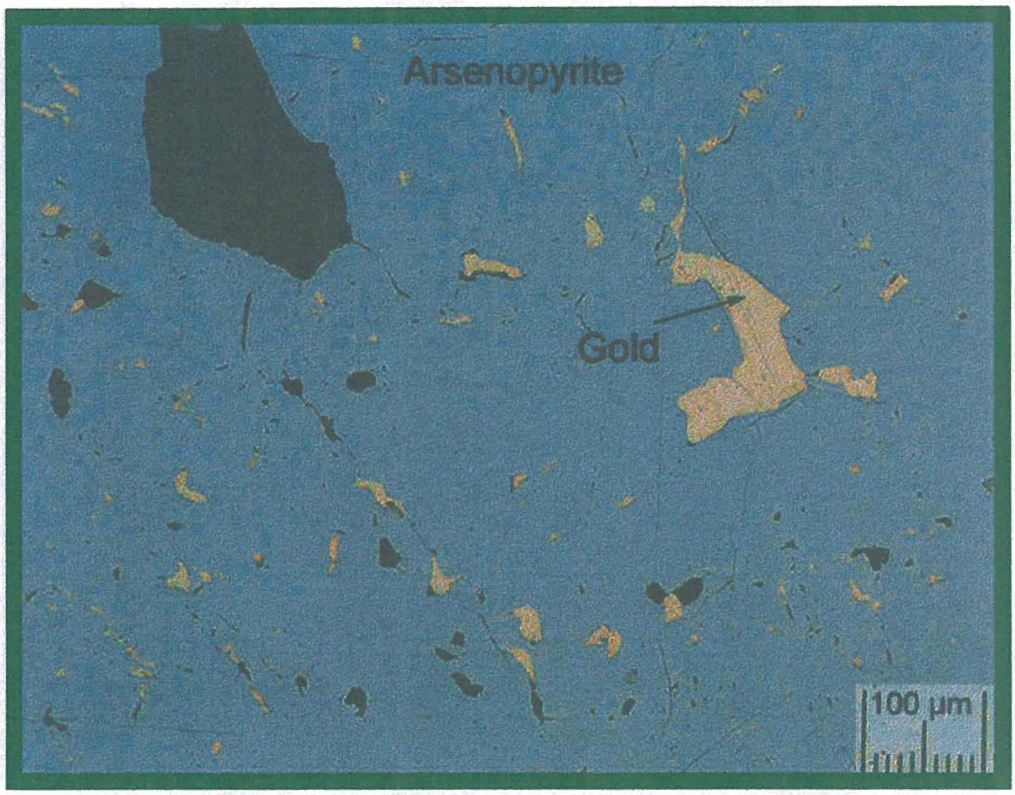

Figure 4.16 Polished mount of refractory Gold in arsenopyrite. Sample SV9733a (88.00m-88.05m); reflected light.

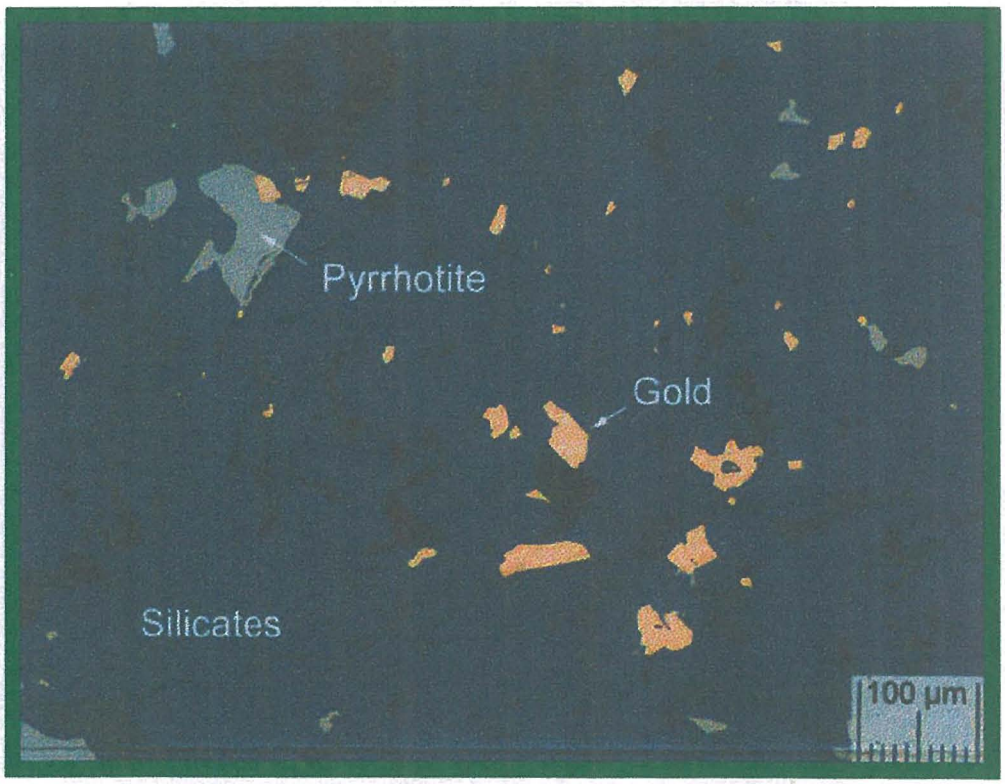

Figure 4.17 Polished mount of Gold grains within the calc-silicates (predominantly diopside). There is weak pyrrhotite growth around the gold grains. Sample SV9837a (19.70m-19.80m), reflected light.

4.6.3 Arsenopyrite/Loellingite

Arsenopyrite/Loellingite are the predominant sulphides within the ore zone. They have grown in aggregates of euhedral crystals along the ore zone banding (C-fabric). The coarser arsenopyrite crystals are pitted by the finer-grained loellingite, occasional pyrrhotite and trace niccolite (Townsend, 1999). The grain size ranges from 100 microns to 2mm (Figure 4.19 & 4.20).

In hand specimen, loellingite is indistinguishable from arsenopyrite. Loellingite ($FeAs_2$) is a high temperature version of arsenopyrite (FeAsS), suggesting that the alteration assemblage (including gold mineralisation) occurred at high temperatures (≥500°C). Arsenic has a concentration ~1000 times greater than gold. Arsenic has an excellent correlation with gold and is a potential pathfinder to help identify ore zones. (McCuaig, 2000).

4.6.4 Pyrrhotite

Pyrrhotite appears as fine-grained anhedral bands usually forming linear networks of polycrystalline veins crosscutting the ore banding or along the diopside and tremolite mineral contacts. The grain size is usually <50 microns (Figure 4.21).

The pyrrhotite is most likely derived from the carbonaceous pyrrhotitic shales. The pyrrhotite may have been dissolved into solution and assimilated with the hydrothermal fluids during the latter stages of the ductile deformation event. This mechanism would explain the anhedral, very fine-grained nature of the pyrrhotite grains.

Figure 4.18 Polished mount of Gold fines in graphite.
Sample SV9833b. reflected light; FOV = 0.54mm

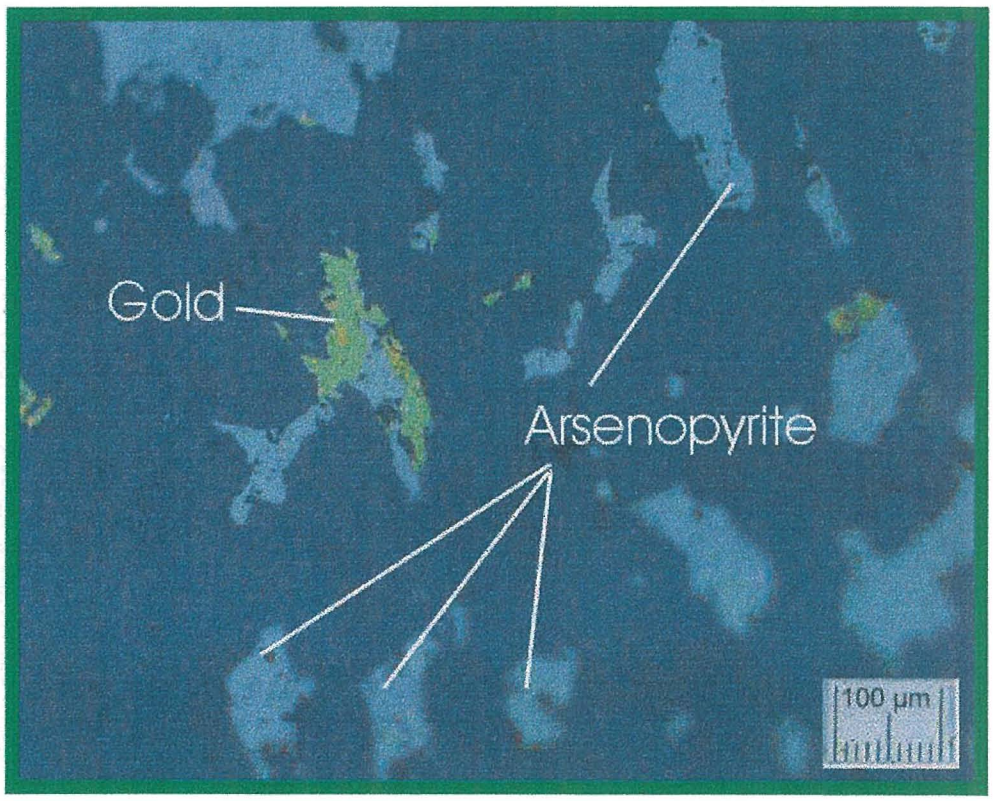

Figure 4.19 Polished mount of equigranular aggregates of arsenopyrite/loellingite. Note the gold development along the margins of the arsenopyrite crystals. Sample SV9723c (96.20m-96.25m) reflected light ; FOV = 1.935mm

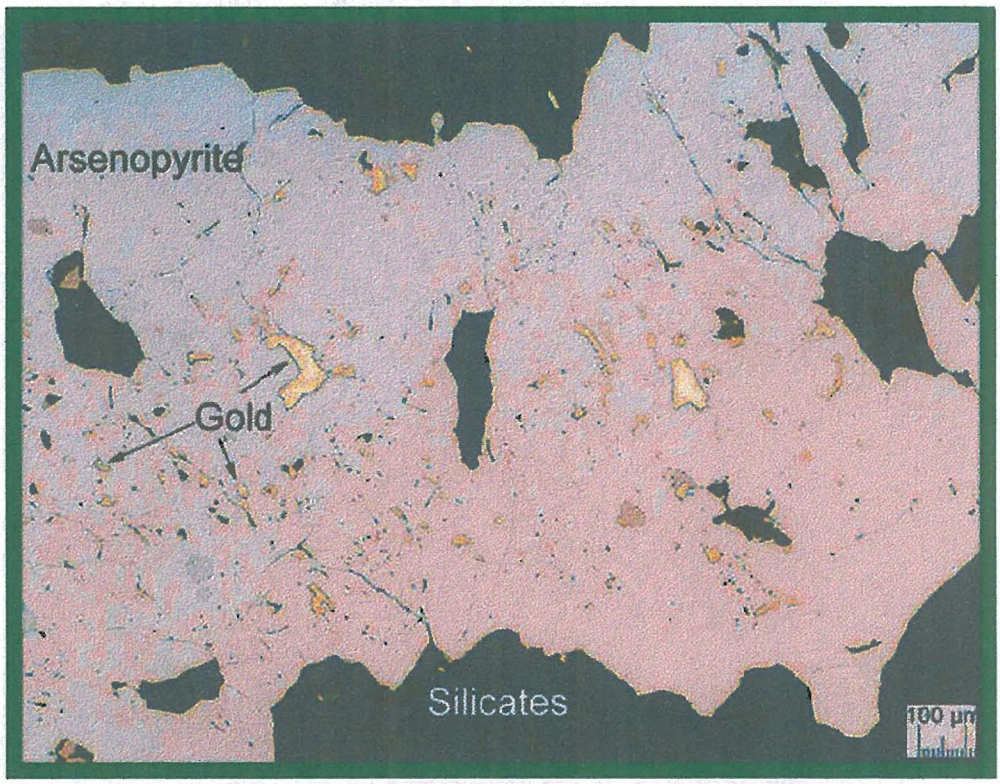

Figure 4.20 Polished mount of coarse-grained arsenopyrite with refractory gold inclusions. Sample SV9837a (19.70m-19.80m); reflected light

Figure 4.21 Polished mount of pyrrhotite vein cross-cutting the alteration assemblage, predominantly the arsenopyrite. Sample Sv9823d (96.20m –96.25m); reflected light ; FOV = 1.935m

The pyrrhotite is the last sulphide to crystallise within the ore zone. It is present mainly as veins, which crosscut the pre-existing alteration assemblage. This is a result of pyrrhotite requiring cooler temperatures in order to crystallise, which coincides, with the latter stages of the hydrothermal event. Towards the end of the hydrothermal event, the 'dilational zones' have been filled restricting hydrothermal fluid flow, allowing naturally cooler fluids to migrate through the shear zones, intruding along micro-fractures within the newly formed alteration assemblage, forming pyrrhotite microveinlets.

4.6.5 Accessory Sulphides and Tellurides

Chalcopyrite is a trace sulphide, which is closely associated with graphite. The anhedral chalcopyrite grains are <70 microns. Chalcopyrite is responsible for the Cu enrichment within the ore zone and Cu zonation along the margins of strong gold mineralisation.

Bismuth telluride is a trace mineral in the ore zone usually associated as inclusions within the calc-silicates. This telluride is subhedral and has a grain size <150 microns. The bismuth telluride is the main source of bismuth, which generally, correlates with the ore. There is a slight enrichment of bismuth on the western end of the mineralisation.

4.7 GEOLOGICAL MODEL

A geological model for the Svartliden Gold Project is proposed to explain the structural setting and mineralisation sequence. The following model will be used as a basis for the examination of the geophysical signatures of the deposit. This model can then be applied on a regional scale to identify other zones of potential gold mineralisation.

A schematic section of the structural setting, alteration and mineralisation sequence at the Svartliden Gold Deposit is described below (Figure 4.22). A geology plan of the Svartliden area shows an idealised model of the potential regional structural setting with respect to the controls of the alteration and gold mineralisation (Figure 4.23).

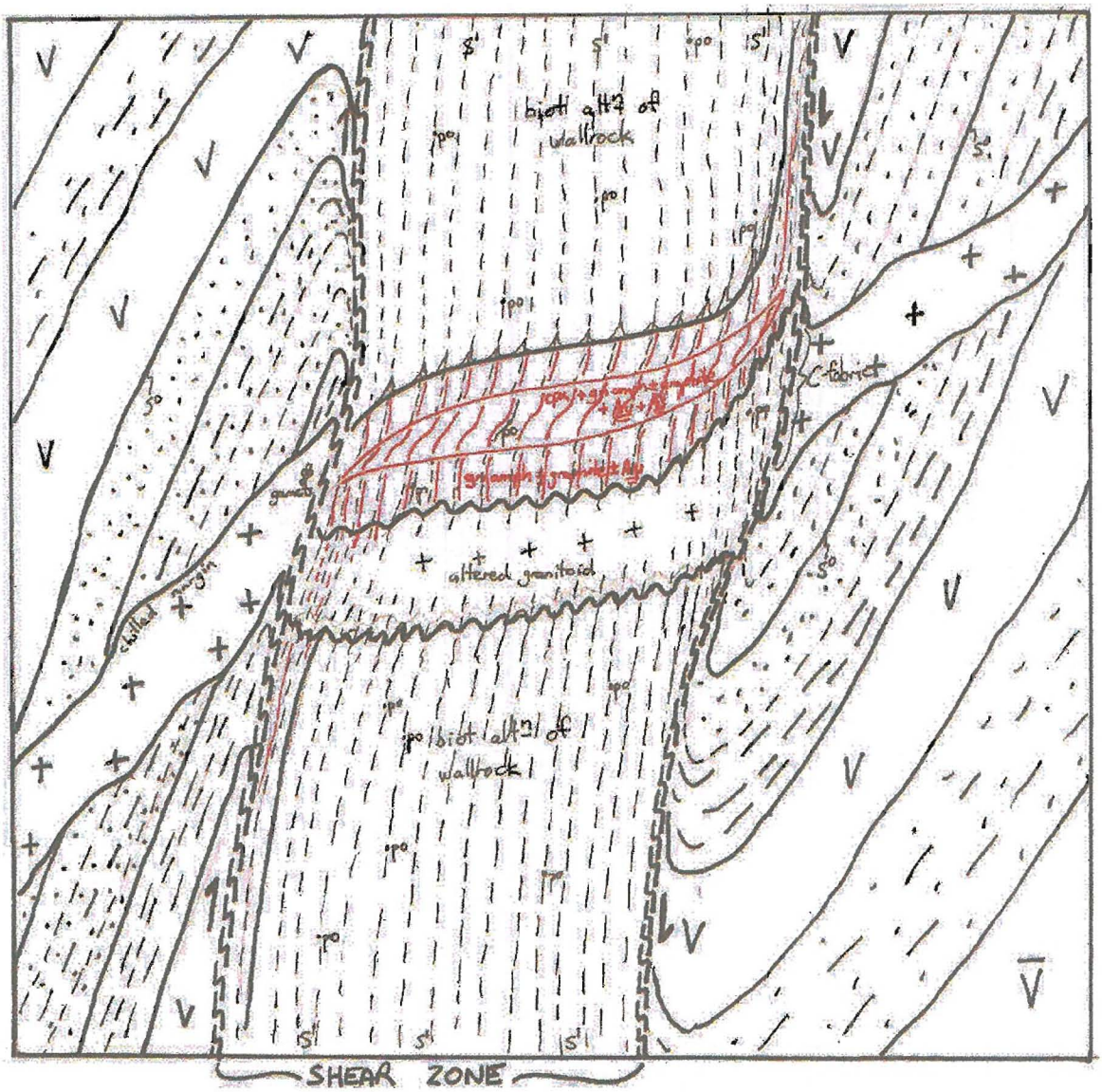

Figure 4.21 Schematic section of the structural setting and alteration sequence at the Svartliden Project.

The ore zone (red) in section is a shallow south-dipping 'lozenge'. The ore zone is formed in a 'dilational jog' within the dextral (reverse) ductile shear zone. The 'dilational jog' has opened along the shallow-plunging intersection lineation between the original bedding (S^0) and penetrative steep south-dipping fabric (S^1). Pervasive S-C fabric, pressure shadows on quartz and diopside boudins, fold axes and tension gashes all indicate reverse motion on shear zone. The variable degrees of deformation, combined with the 'dilational jog' on ore suggests that mineralisation occurred during ductile deformation.

The alteration assemblage within the shear zone consists of a distal zone of biotite ± pyrrhotite, and an ore-zone of clinopyroxene (diopside) + green amphibole (tremolite) + quartz + carbonate (± calcite) + pyrrhotite + arsenopyrite ± chalcopyrite ± graphite ± GOLD±SILVER. Within the ore zone, there is a core of clinopyroxene (diopside) rimmed predominantly by green amphibole (tremolite).

The granitoids have a moderate south dip (45°-60°) and appear to flatten through the shear zone whilst intruding during ductile shearing. Garnets have been rotated and cracked during the shearing event. Granitoids are weakly anomalous in gold where they coincide with the mineralised shear zone. This strongly suggests that the granitoids are syn-deformational, intruding during the latter parts of the deformational event but prior to the gold-bearing hydrothermal event. In fact the refraction of shear zone through the granite may control the development of ore positions.

At a project scale, mineralisation at Svartliden could only have formed in areas of dilation and low shear strain. Therefore, lithological heterogeneity is an important controlling factor of the mineralised zones and structures.

Strain partitioning around competent granitoid bodies creates pressure shadows, which may be potential trap sites for hydrothermal fluids. The Svartliden mineralisation may be the result of gold-bearing hydrothermal fluids coalescing in a pressure shadow zone created by the two major pre- or syn-deformational granitoids west and south of the Project area (Figure 4.23).

During the deformation event, the rotation of these granitoids may be responsible for the ductile shear event. Based on this model, other potential pressure shadow zones can be identified at Svartliden outside the current project area.

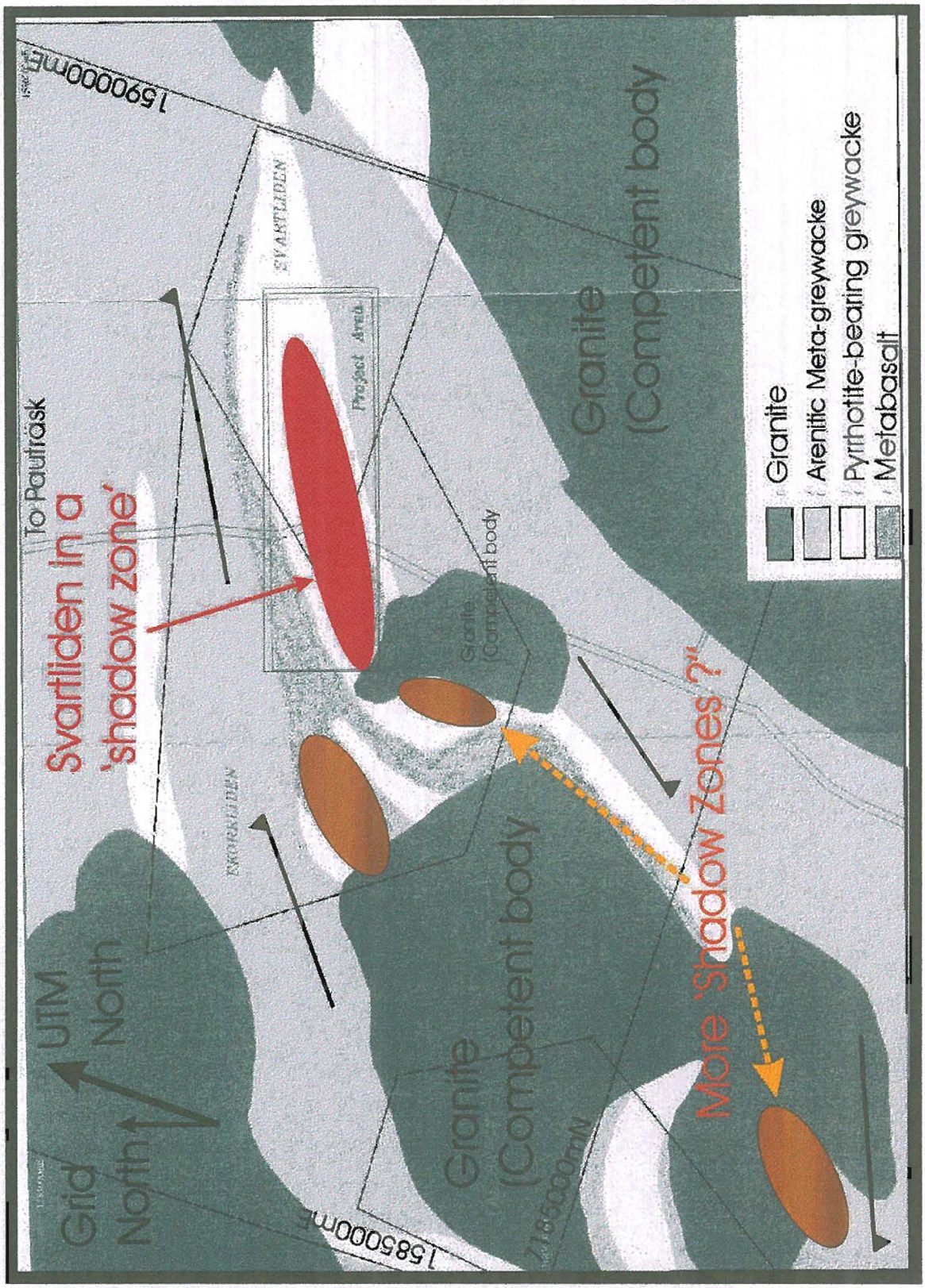

Figure 4.23 Schematic geology plan of the Svartliden Project. Strain partitioning around the granite body has created zones of low shear strain and dilation. The Svartliden mineralisation is interpreted as being located in such a dilational zone. The arrows (black) show the direction of the shear strain (sinistral).

4.8 ANALOGOUS DEPOSITS

The nature and style of mineralisation at Svartliden is analogous to the high-temperature gold deposits of the Southern Cross Greenstone Province of Western Australia (Ho, Groves & Bennett, 1990). The Southern Cross deposits have similar structural settings and mineralogy and often contain high gold grades in deposits of more than 1 million ounces of contained gold (Table 4.1).

Table 4.1. Gold deposits of the Southern Cross Province, Western Australia (Ho, Groves & Bennett,1990).

Deposit	**Tonnes (millions)**	**Grade (g/t Au)**	**Contained oz. (million)**
Big Bell	37	3.5	4.1
Copperhead/Frasers	13	4.3	1.8
Lancefield	7	8.3	1.8
Marvel Loch	37	2.4	2.8

There are structural, mineralogical and alteration similarities between Svartliden and the gold deposits of the Southern Cross Province. These include lithological heterogeneity, ductile deformation, and mineralogy.

Lithological heterogeneity acts as controlling factors in:-

(i) localising mineralised structures at the contact between two lithological units;

(ii) localising mineralisation within and parallel to narrow units with contrasting rheological properties;

(iii) localising mineralisation in structures which cross-cut lithological layering; and,

(iv) Localising mineralisation along structures where two lithological units with contrasting lithological properties are juxtaposed across the structure. All of which have been recognised within Svartliden and on a regional scale.

The Southern Cross and Svartliden deposits are both sited within broad regional (up to 1 km wide) ductile deformation zones, which trend parallel to gross lithological layering.

On a local scale, the ore zones form single or multiple lodes parallel to the overall trend of the deformation zone. The broad ductile shear zones are often completely silicified but have a lack of quartz-vein sets, suggesting that the Southern Cross deposits have formed at deep crustal levels at higher metamorphic grade ranging between mid-amphibolite and granulite facies (Groves *et al* 1995). From petrological evidence, the shear zone at Svartliden has also undergone complete silicification with a lack of quartz-vein sets. This suggests formation at a deep crustal level at a similar metamorphic grade (Marsh & Laurent, 1998) (Figure 4.24).

Common sulphide mineralogy includes pyrrhotite and arsenopyrite. Wallrock alteration comprise biotite ± K-feldspar ± quartz ± pyrrhotite with quartz ± diopside ± tremolite ± arsenopyrite ± calcite more abundant proximal to, and within, the ore zone.

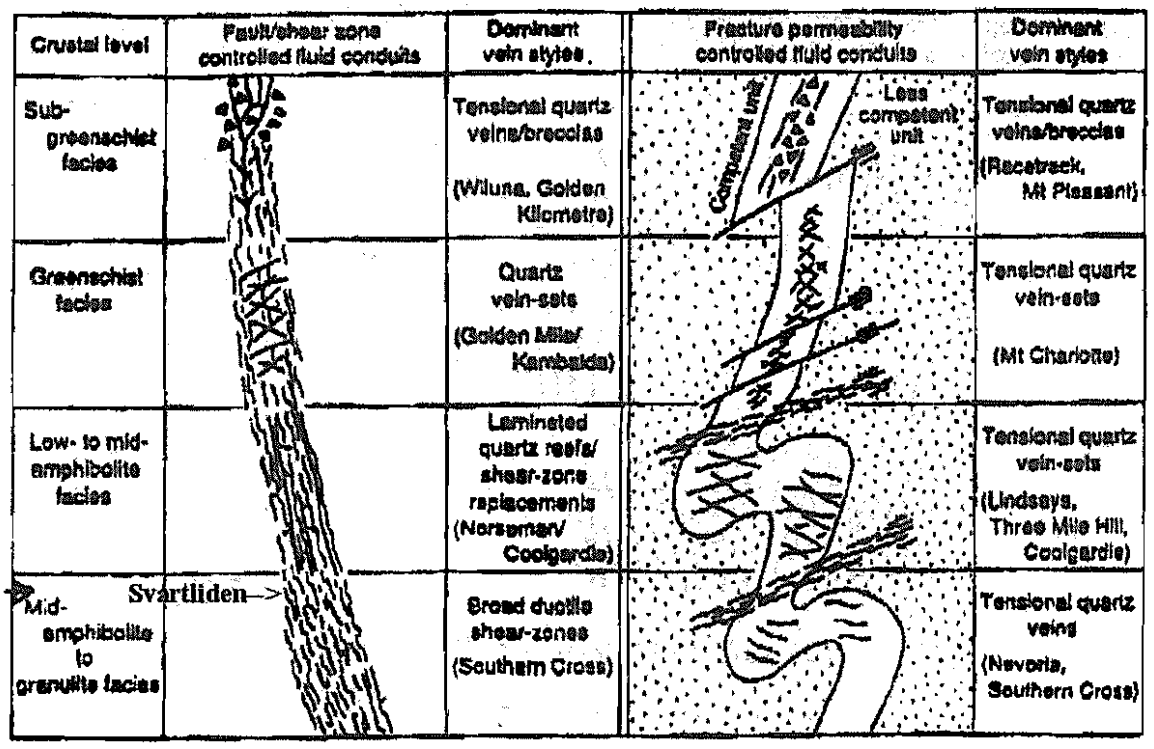

Figure 4.24 Schematic diagram showing a hypothetical fluid conduit system at different crustal levels. (modified from Groves et al. 1995). Svartliden lies within fault and shear zone hosted structures at deep crustal levels of mid-amphibolite to granulite facies.

4.9 SUMMARY

The Svartliden Project is situated on an east-northeast trending 'lozenge' of a north-south trending 'greenstone' belt. This 'greenstone' sequence consists of volcano-sedimentary rocks and lies beyond the western margin of the Skellefteå District.

The 'greenstone' belt is part of the supracrustal rocks deposited between 1.95Ga and 1.85Ga, and are part of the Svecofennian crustal growth during the Svecokarelian Orogeny.

The volcano-sedimentary rocks consist of a turbiditic sequence of mudstones, siltstones and sandstones intercalated with basalts exhibiting volcanic textures such as peperite, hyaloclastite, vesicles and pillow margins. This suggests that the sequence formed in a deep marine setting under reduced conditions. Granitoid dykes with constant composition range from pegmatitic to aplitic in texture and intruded prior to, or during the major deformation event.

During the principal deformation event, the volcano-sedimentary sequence was incorporated into a broad ductile shear zone at a deep crustal level. The more competent granitoid dykes within the shear zones became shortening compartments developing minor foliation at the margins. Rheological contrasts between the granitoids and volcano-sedimentary rocks are very important on the control of strain distribution. Mineralisation will form in areas of least strain (shadow zones).

The shear zone(s) are developed parallel to the axial-plane cleavage. Svartliden lies on an isoclinal anticline shallowly plunging east and west of 1500mE. Peak metamorphic grade during the ductile deformation event was mid- to upper-amphibolite facies.

Hydrothermal fluids migrated through the shear zone altering the host rocks, thus creating an outer or 'distal' zone surrounding a core or inner 'ore' zone. The ore zone has a mineral assemblage of clinopyroxene (diopside)+green amphibole (actinolite-tremolite) + quartz + carbonate (± calcite) + pyrrhotite + arsenopyrite ± chalcopyrite ± graphite ± GOLD±SILVER. The diopside is rimmed by the actinolite-tremolite.

The distal zone consists of biotite±quartz±pyrrhotite. There is a gradational facies change from the ore zone to the distal zone, whereby the tremolite is gradually replaced by biotite.

Economic gold mineralisation is restricted to the ore zone alteration assemblage within the shear zone(s) at Svartliden. Gold has a variable distribution including refractory gold in arsenopyrite/loellingite, non-refractory gold in silicates, and gold fines in fine-grained graphite.

Arsenopyrite is the major sulphide associated with gold. Pyrrhotite, although abundant, is a remobilised sulphide most likely derived from the carbonaceous siltstones and mudstones.

Mineralisation was concentrated in dilational jogs within the shear zone. The dilational jogs were best developed along the intersection lineation between bedding and the penetrative cleavage, spatially coinciding with the granitoid dykes within the shear zone.

The combination of highly sheared and less deformed veins, in close proximity to each other, indicates that alteration; ductile deformation and mineralisation have all been operating simultaneously.

5. REGIONAL GEOPHYSICS

The Swedish Geological Survey (SGU) has conducted several types of regional geophysical surveys over Sweden. Potential field measurements, such as gravity, were obtained from control points connected to a reference system established in the 1960's. Other potential fields, such as total magnetic intensity (TMI) were obtained from an aeromagnetic survey conducted in 1990 (Freden, 1994). The SGU carried out only limited airborne or ground surveys using electrical techniques, such as electromagnetism (EM) and electrical conductivity. An airborne radiometric survey was conducted in 1986, to measure Cesium-137 fallout after the Chernobyl Nuclear Reactor disaster.

5.1 GRAVITY

Gravity surveys were first carried out over Sweden in the 1960's, when the reference system was established. Control points, often located on the steps leading into a church, are used to connect the gravity measurements with this reference system. Gravity decreases away from the centre of the earth, therefore all measured values were corrected (free-air correction) to a reference area known as a geoid. A further reduction to compensate for the material between the geoid and earth's surface produces a Bouguer anomaly (measured in milligals). Measured gravity in Sweden ranges from –110 milligal to +15 milligal. The Caledonide Mountain Range, along the Norwegian border, has the lowest density of gravity stations mainly due to topography (Figure 5.1).

The Svartliden area has a Bouguer anomaly of between –30 milligals and –40 milligals. This density is a result of crystalline rocks, such as granite and basalts, reflecting the chemical composition. Sulphide-hosted ores have the highest densities.

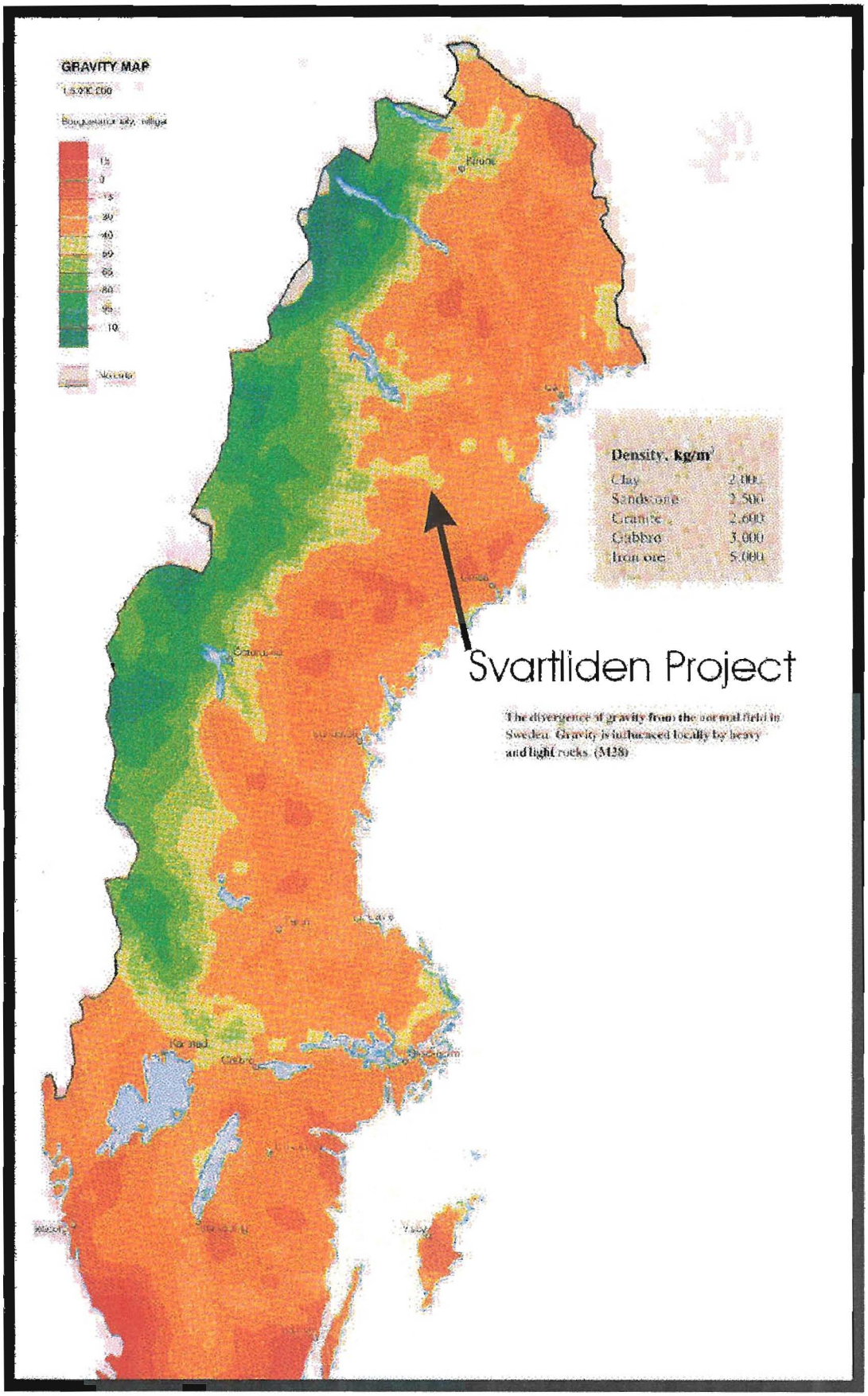

Figure 5.1 Gravity Map of Sweden (modified from Freden, 1994).

5.2 ELECTRICAL CONDUCTIVITY AND ELECTROMAGNETISM

Physical electrical propoerties, such as electrical conductivity and electromagnetism (EM), have had only limited use in Sweden to date. In the past, the highly resistive till cover often hindered effective electrical techniques. Prior to the use of Fixed-Loop and Moving-Loop ground Transient EM surveys, the SGU used measurements of low-frequency radio waves transmitted from a radio station in England. This technique is known as VLFEM. These VLFEM-waves penetrated the ground and when electrically conductive parts of the bedrock are encountered, they caused electrical currents that influenced the transmitted radio waves in a way that can be measured (Freden, 1994).

5.3 RADIOMETRICS

The whole of Sweden was measured by an airborne radiometric survey in 1986. The aerial survey had a line spacing of 50km and an altitude of 150m. The primary objective of this survey was to determine the amount of Cesium-137 fallout following the Chernobyl Nuclear Reactor accident in April 1986. The radiometric measurements were taken by a gamma spectrometer. These measurements recorded the flux of gamma-radiation in a number of energies, providing information about the distribution of naturally radioactive isotopes (eg. uranium, thorium and potassium) in the ground, and the occurrence of other, introduced, radioactive isotopes (eg. cesium and barium) (Freden, 1994).

5.4 SEISMIC SURVEYS

As sound waves move with different speeds through different rock types, the SGU conducted several seismic surveys before 1980 to provide information on the structure of the Earth and the processes related to earthquakes. Seismic waves are used to investigate the composition of the Earth's crust. When measuring how sound-waves are reflected in different layers and horizons with differing properties, it is possible to obtain extremely detailed information down to a depth of about 50km (Table 5.1) (Freden 1994).

Table 5.1 Velocity of seismic (sound) waves for the following rock types, determined by the SGU.

Rock Type	Seismic (sound) wave velocity (m/s)
Quartenary deposit	2,000
Sedimentary rock	4,000
Crystalline rock	>5,000
Earth's mantle	>8,000

5.5 MAGNETIC FIELD

5.5.1 Magnetic Inclination, Declination and Total Intensity

The magnetic field has both direction and magnitude. Two angles, the magnetic declination and the magnetic inclination give the direction. The magnetic declination is the angle in the horizontal plane measured from the north towards the east. This corresponds to the compass error. In Sweden, the magnetic declination varies between -1° and +6° (calculated in 1990). The Svartliden Project has a magnetic declination of between +2° and +3° (Figure 5.2).

The magnetic inclination is the angle downwards from the horizontal plane. In Sweden, the inclination of the magnetic field varies between 70° in the south to 78° in the north. The Svartliden Project has a magnetic inclination of between 75° and 76°.

The total magnetic intensity refers to the magnitude of the magnetic field. The magnetic field is directed vertically and is strongest at the magnetic poles. At the magnetic equator the field is horizontal and much weaker. Currently, the magnetic field is directed towards the centre of the earth in the Northern Hemisphere and outwards from the earth in the Southern Hemisphere. The unit of magnetic flux density is the *tesla* (T). The magnitude of the magnetic field in Sweden varies between 49,600nT in the south and 52,600nT in the north (Figure 5.3). The Svartliden Project has a total magnetic intensity of between 51,500nT and 52,000nT.

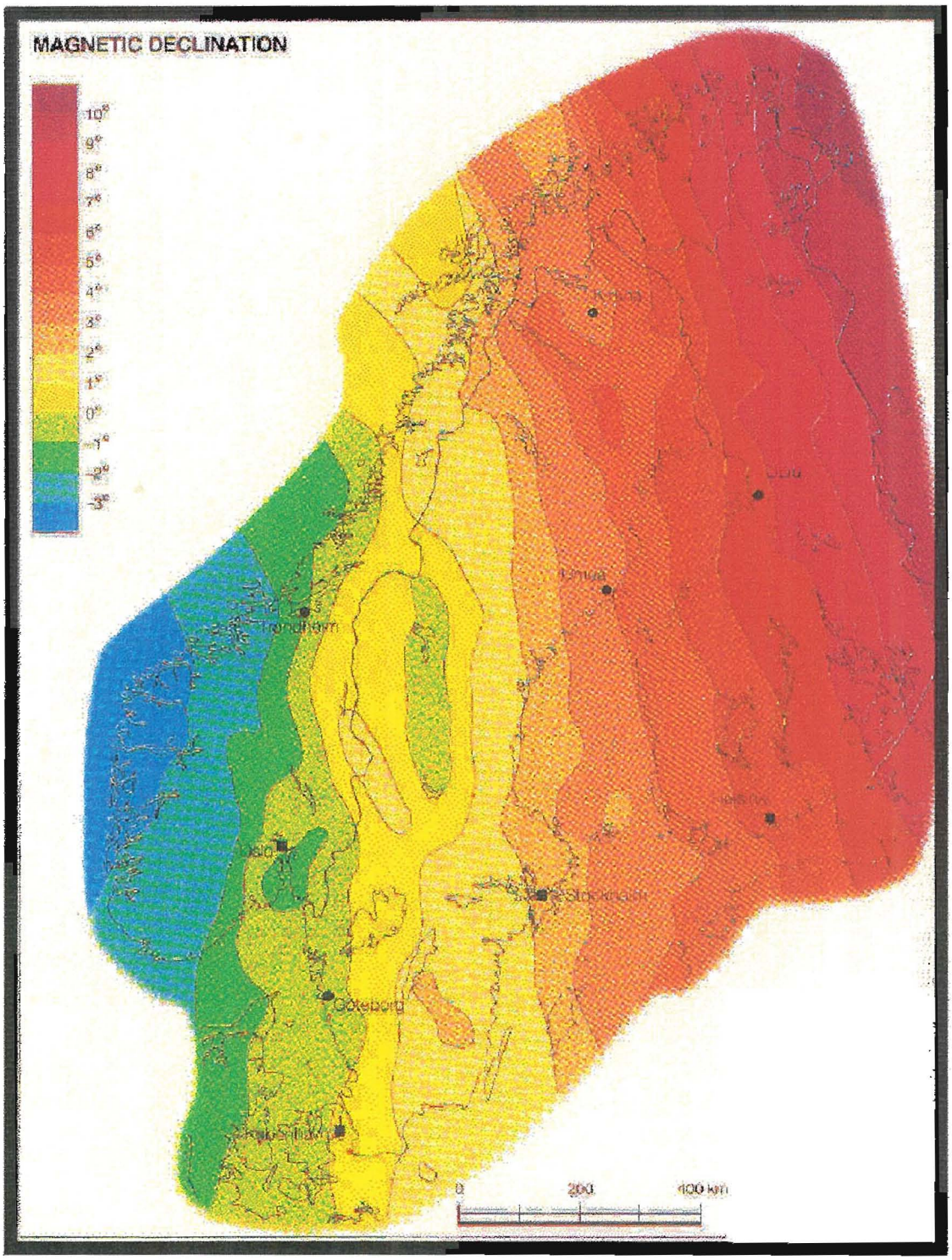

Figure 5.2 Magnetic Declination of Scandinavia (Freden, 1994)

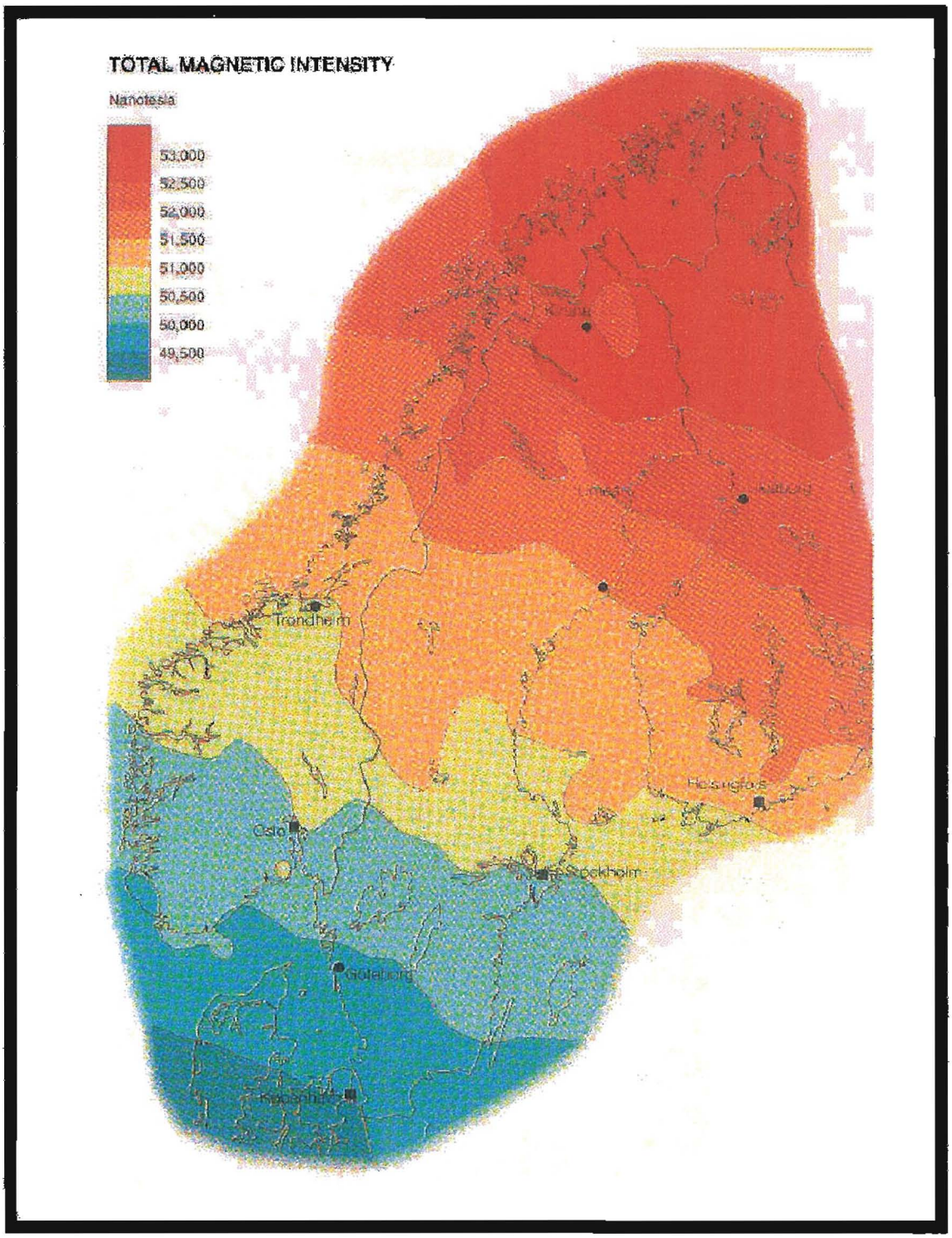

Figure 5.3 Total Magnetic Intensity (TMI) of Scandinavia (Freden 1994).

5.5.2 Magnetic Field of North Central Sweden

An aeromagnetic survey was conducted in 1990 over north central Sweden to show at a regional scale the magnetic variations caused by the bedrock. Measurements were made from an aircraft flying at an elevation of 30m with 200m line spacing. The Earth's normal magnetic field has been subtracted from the measured values (Freden, 1994). This produced a magnetic anomaly field, which is a pattern reflecting rock distribution on the surface and at greater depths. The crustal magnetic properties depend mainly on the content of magnetite and magnetic pyrrhotite in the rocks.

The Svartliden Project is part of discontinuous north-south trending belt of pyrrhotite-bearing volcano-sedimentary rocks. Immediately to the east and west of this 'greenstone' sequence lies large (upto 20km in diameter) magnetite-bearing domes or batholiths. These domes are most likely intermediate in composition, ranging from diorites to gabbros (Figure 5.4).

A magnetic anomaly map of Map 22H-NO was extracted from the regional aeromagnetic survey. The Svartliden Project is situated in the centre of map sheet 22H-NO. The project area is dominated by a magnetic-high lozenge trending in a South-southeast to North-northwest direction before flexing East-northeast. The Svartliden Project is part of a north-south trending discontinuous magnetic belt. The magnetic, east-west trending, granitoid unit appears to thin and pinch near the Svartliden area. This is a result of the poorly magnetic, syn- (post?-)deformational granitoid domes that have intruded north and south of the Svartliden area (Figure 5.5).

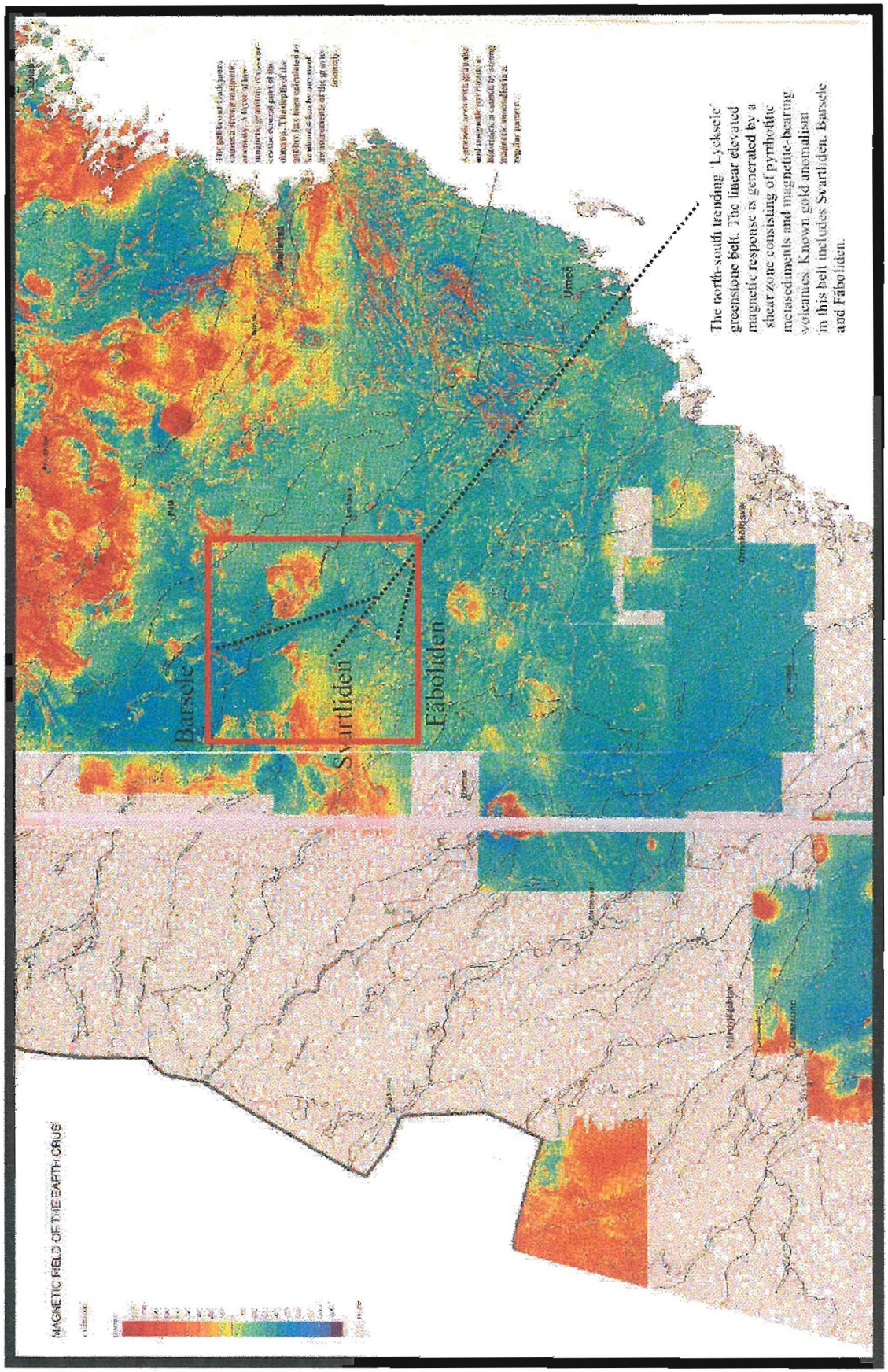

Figure 5.4 Magnetic anomaly map of North-central Sweden (modified after Freden 1994). The area within the red box is shown in detail in the top image of figure 5.5

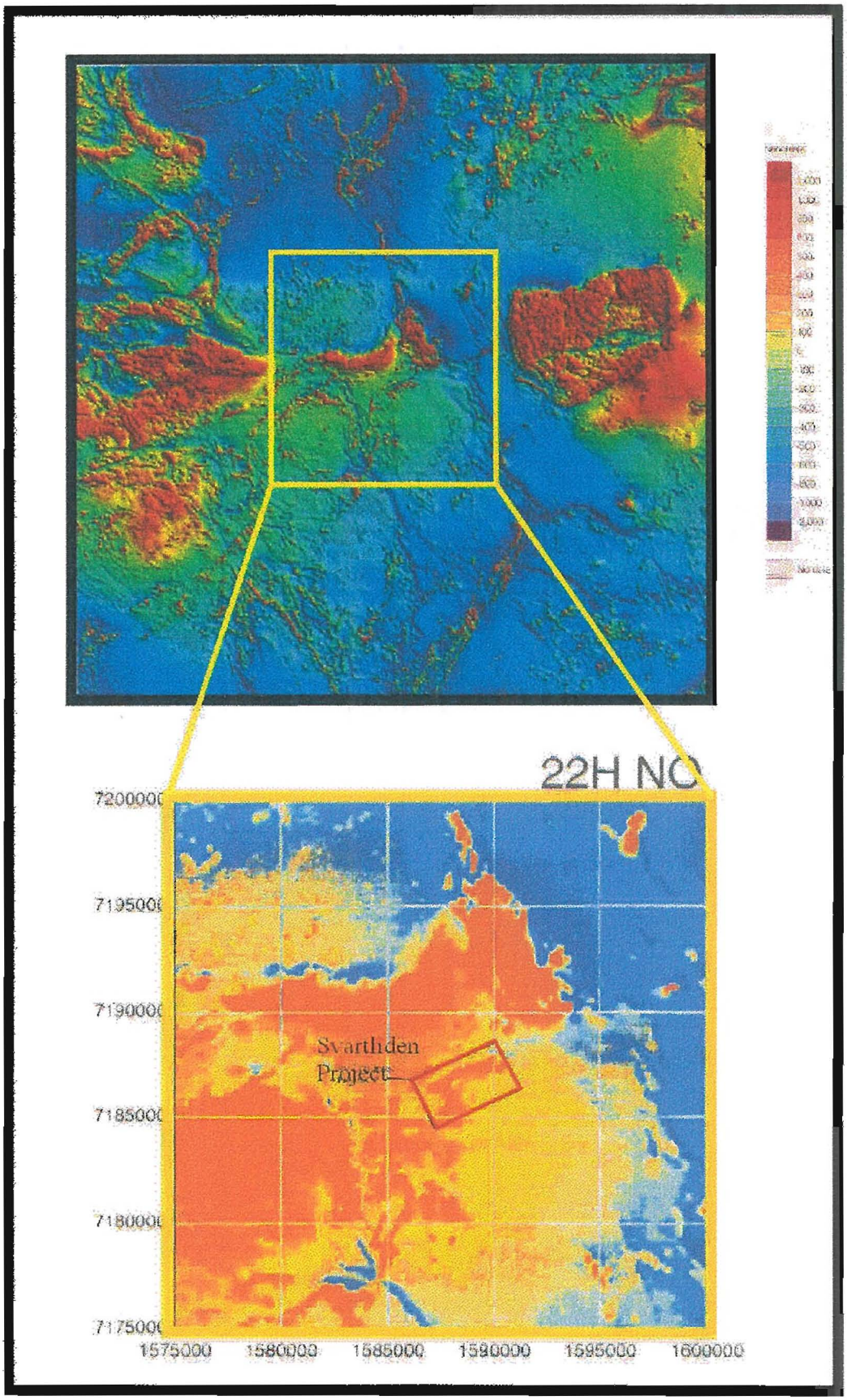

Figure 5.5 Detailed aeromagnetic anomaly map. The top image consists of Swedish Map Sheet 22H, 23H (southwest and southeast), and 22I (northwest and southwest). The bottom image is a blow up of Map Sheet 22H–NO (northeast), where the Svartliden Project is situated.

6. PROJECT GEOPHYSICS

Detailed geophysical surveys were commissioned over the Svartliden Project area following the discovery of significant gold mineralisation, in 1995. Geophysics was considered a suitable technique to identify the stratigraphy, mineralisation and structure beneath the extensive glacial till cover.

The preferred geophysical techniques were magnetic field and electromagnetics (EM). A survey was conducted in 1995, covering the Ekorrliden and Svartliden concessions. An infil magnetic and electromagnetic survey was carried out in 1997.

In 1997, three of the, then, fourteen drillholes were selected for downhole geophysics. The survey consisted of magnetic susceptibility, apparent resistivity, and induced polarisation.

6.1 GROUND GEOPHYSICS

Two ground-based magnetic and Slingram EM surveys were conducted at Svartliden in 1995 and 1997, respectively. The ground-based magnetic surveys were conducted using two GSM19 Overhauser magnetometers; one as a roaming unit the second as a base station unit. Diurnal values were registered every minute. The frequency-domain moving-loop EM surveys were conducted using an ABEM Slingram instrument at 18kHz with a horizontal, co-planar configuration using a 60m coil-separation recording in-phase and quadrature components. An ABEM GEOMAC II field computer did the data collection. (Geovista AB, 1997)

The first ground-based survey covered two areas, namely the western and northern areas. The detailed parts of the grids were surveyed on 20m x 10m centres, whereas the outer areas were surveyed on 10m centres but at variable line spacings. For this programme line azimuths varied from grid-NS in the northern area to grid-EW for the western area.

The second ground-based surveys were designed to a) infill the survey density to 20 x 10 m between 880mE - 1720mE & 1200mE – 1600mN; and b) cover the NW corner of the grid, between 360mE – 880mE & 1200mE – 1600mN. The line azimuths used were grid north-south for both surveys.

GEOVISTA AB of Luleå, Sweden conducted the initial and infil ground geophysical surveys. On both occasions the same geophysical instruments were used.

6.1.1 Survey Specification

The surveys were carried out using the Svartliden local grid system, which has specifications with reference to the Swedish National Grid (RT38/RT90). This is illustrated in Table 6.1.

Table 6.1 Local Grid specifications with respect to the Swedish National Grid (Geovista AB, 1997)

	Local Grid	RT38/RT90 Swedish National Grid
Base Co-ordinates	0mE/0mN	1587340mE; 7185270mN
Azimuth	341.4°East	360.0° (+1° mag. Declination)

6.1.2 Data Processing

GEOVISTA AB carried out the compilation, corrections, imaging, interpretation and reporting of the ground geophysical surveys (Geovista AB, 1997). Geological correlation was very difficult at the time of reporting. The geological setting and mineralisation was yet to be fully understood, and based on only 6 poorly exposed trenches, and 9 diamond holes drilled (with assays awaiting for 3 of these holes).

With this in mind, the bulk of the geophysical interpretation was based on understanding the geophysical properties and anomalies encountered over the project area. Initial target definition was broadly delineated based on magnetic and electromagnetic anomalies with coincident anomalous gold mineralisation and alteration found in the trenches, and in the 9 holes drilled at the time of the reporting.

6.1.3 Ground Magnetics

Ground magnetic data was corrected for diurnal drift. The magnetic data was measured in *nanoTeslas* (nT). A magnetic anomaly image for the Svartliden Project was produced on the local grid (Figure 6.1). The overall magnetic pattern consists of an east west linear belt that pinches and swells, varying in thickness and intensity.

In the western part of the surveyed area, the magnetic linear belt(s) bends to the south. At this flexure point, the linear magnetic bodies are dislocated and have reduced magnetic intensity. This broken-up or dislocated effect is caused by a series of crosscutting faults. A concentration of magnetic material has formed in the southwestern portion of the project (600mE; 900mN). This may be a result of a combination of magnetite-bearing volcanic rocks in contact with magnetic pyrrhotite-bearing sedimentary rocks.

The central western part of the project area (1200mE-1750mE) shows two distinct magnetic horizons trending east west. These two belts consist of magnetic pyrrhotite-bearing sediments and magnetite-bearing volcanics. A magnetic low between these two belts consists of magnetite-poor volcanics and granitoid intrusions.

At the 1750mE, a visible offset indicates either a zone of heterogeneous strain or a late-stage sinistral fault. East of this offset, the two magnetic horizons have coalesced. The coalesced magnetic horizon thickens and reduces in magnetic intensity as it trends east. The magnetic horizon consists of magnetic pyrrhotite-bearing sediments and magnetite-bearing volcanics.

The northern contact of the magnetic horizon is a strong magnetic low, clearly defining the magnetic volcano-sedimentary 'greenstone' sequence from the weakly deformed Vargfors Group (turbiditic sediments) within the Bottnian Basin.

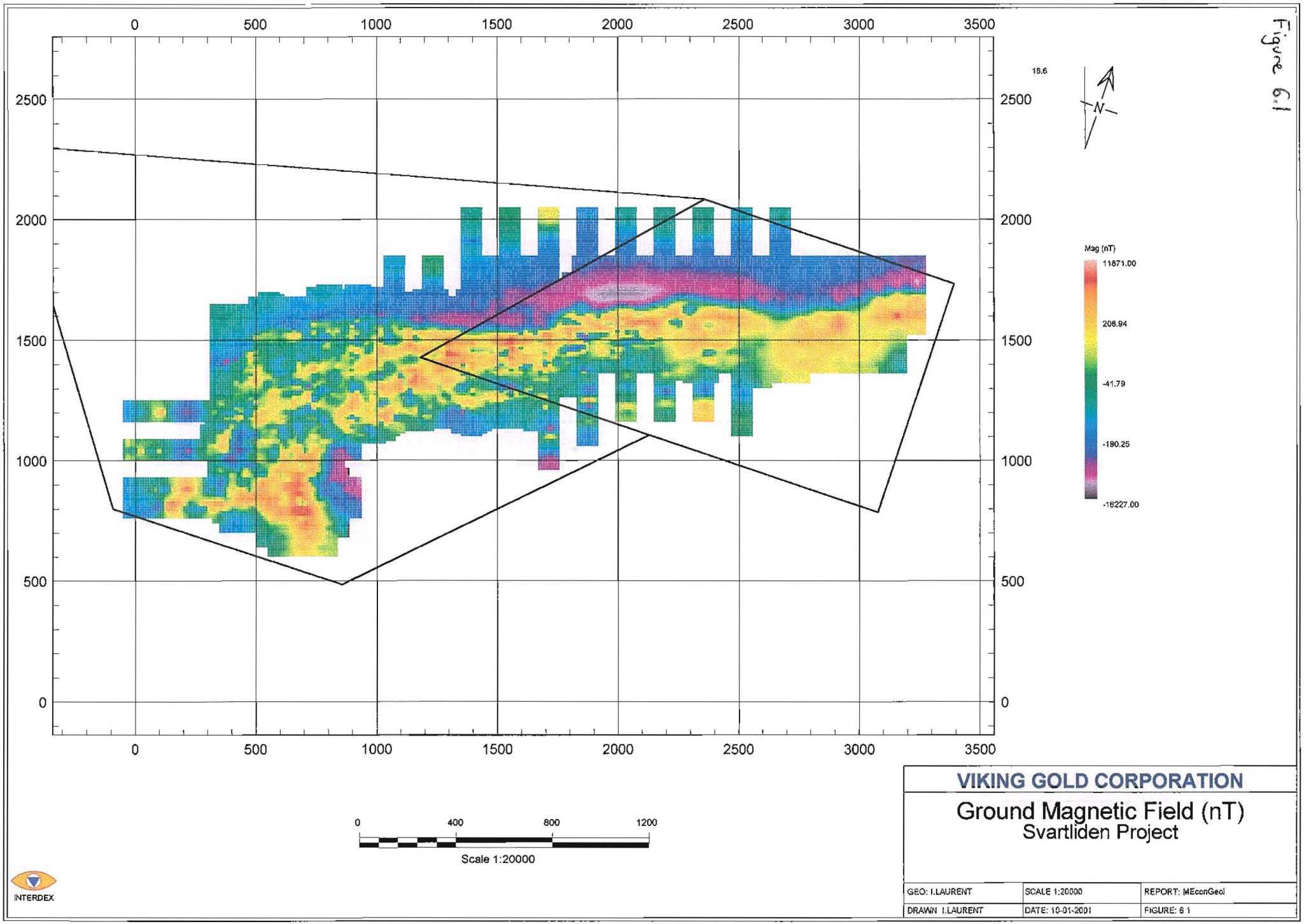
0
500
1000
1500
2000
2500
3000
3500
18.6
N
Mag (nT)
11871.00
208.94
-41.79
-190.25
-16227.00
0
400
800
1200
Scale 1:20000
INTERDEX
VIKING GOLD CORPORATION
Ground Magnetic Field (nT)
Svartliden Project
GEO: I.LAURENT
SCALE 1:20000
REPORT: MEconGeol
DRAWN I.LAURENT
DATE: 10-01-2001
FIGURE: 6 1

Figure 6.1

6.1.4 Ground Electromagnetics

The electromagnetic ground survey employed a frequency-domain moving loop system. A horizontal coplanar coil configuration was used with a base frequency of 18kHz. The charge was quite high so as to counter a) the very resistive nature of the till, and b) the Palaeoproterozoic rocks found in Sweden. A system frequency of 18kHz was selected to penetrate the till cover to map underlying conductive units (>20m). Both the in-phase and out-of-phase 'quadrature' components of the secondary magnetic field were recorded (in percent).

Two images were compiled from the electromagnetic ground survey, one for the in-phase component (figure 6.2), and one for the quadrature component (figure 6.3).

The in-phase image clearly defines the strongly conductive and resistive units. The in-phase image shows two linear belts trending east west across the project area. These two linear belts are coincident with the linear belts displayed on the magnetic anomaly image (figure 6.1).

These linear conductive belts consist of pyrrhotitic and graphitic sediments. To the east, the conductive anomalies are broader and lower in intensity. There is a large resistive break at 2600mE. This may be a granitic intrusion or very deep till cover. The linear conductive belts coalesce and form a large strongly conductive anomaly between the 2400mE to the 1750mE.

At the 1750mE, the conductive units have been offset. This may be a post-deformational sinistral fault or a heterogeneous zone within a ductile terrain. South of the large conductive anomaly on the eastern side of the 1750mE offset, there is a significant resistive break, which coincides with a granitoid encountered in drilling.

West of the 1750mE offset, the conductive unit separates into two distinct linear belts. From the 1200mE westwards, the conductive linear belts buckle and flex to the south. In this area, the belt becomes broken up and loses its conductivity. However, the belts are traceable as 3 narrow moderately conductive belts.

Figure 6.2

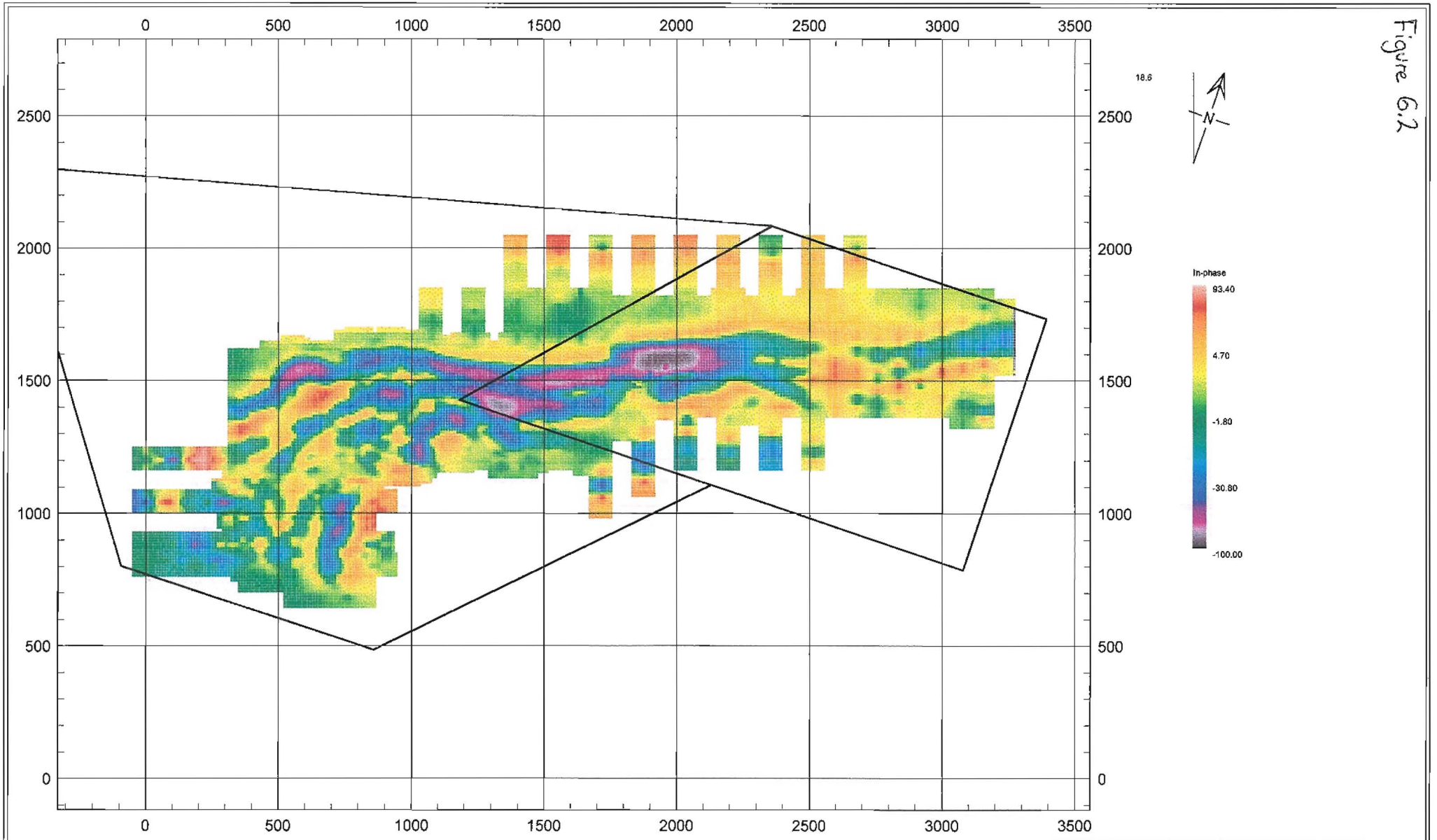

0 400 800 1200

Scale 1:20000

INTERDEX

VIKING GOLD CORPORATION		
Ground In-phase EM (%) Svartliden Project		
GEO: I.LAURENT	SCALE 1:20000	REPORT: MEconGeol
DRAWN: I.LAURENT	DATE: 10-01-2001	FIGURE: 6.2

Figure 6.3

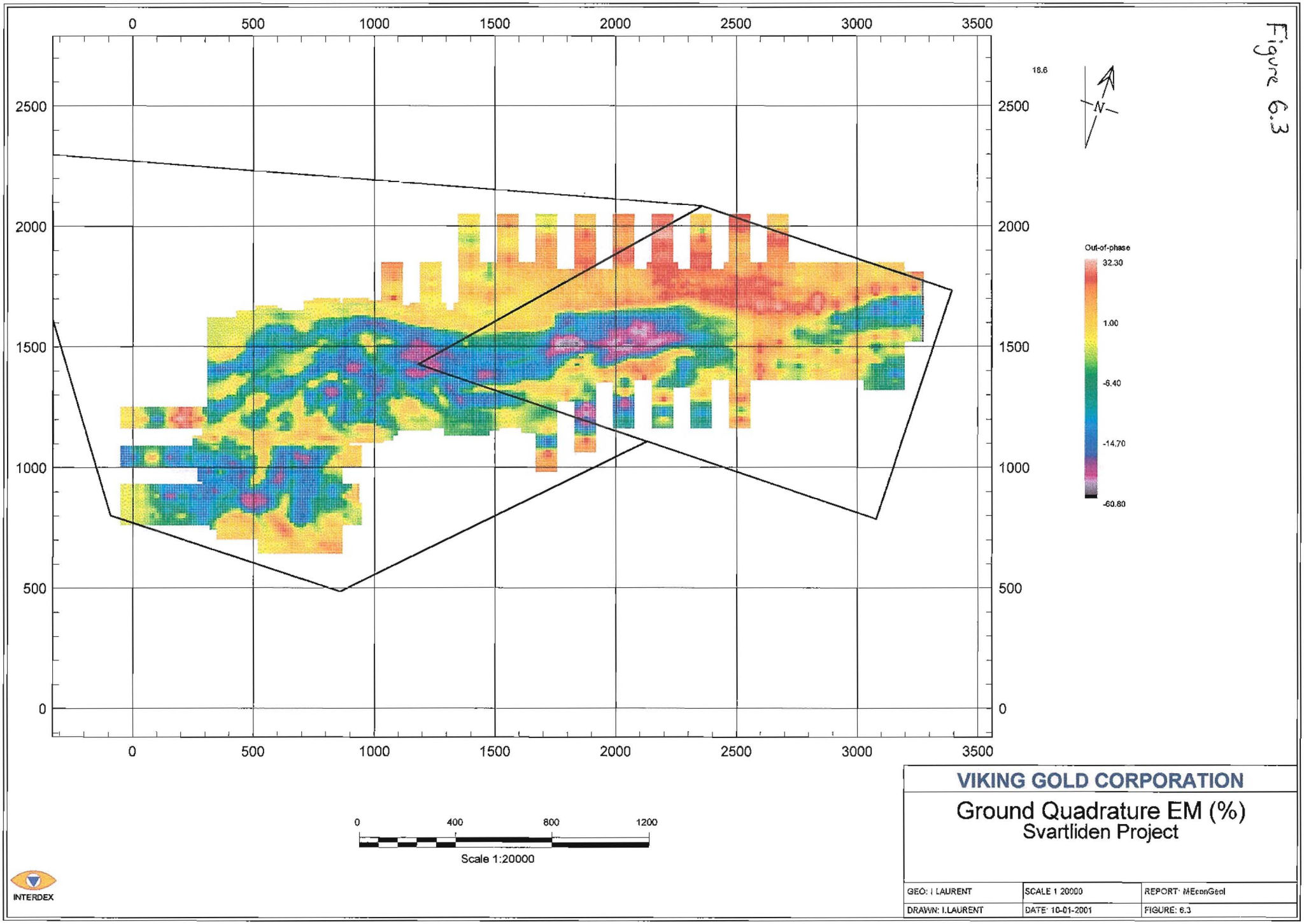

INTERDEX

VIKING GOLD CORPORATION

Ground Quadrature EM (%)
Svartliden Project

GEO: I LAURENT	SCALE 1 20000	REPORT: MEconGeol
DRAWN: I.LAURENT	DATE: 10-01-2001	FIGURE: 6.3

To the southwest, there is a large elongate conductive body that is most likely a concentration of pyrrhotite-rich carbonaceous sediments. This anomaly trends north-south and is part of the southern-most, linear belt that trends east-west before rotating to the south at the 1200mE. However, the quadrature image exhibits similar conductive anomalies to the in-phase image. The biggest difference is that the anomalies are not as pronounced, often exhibiting a broader gradational contact with the resistive units.

The quadrature image does show the linear conductive belts that have flexed to the south with higher conductivity than seen in the in-phase image. The northern contact with the non-'greenstone' sequence is clearly marked by both electromagnetic components.

6.2 DOWNHOLE GEOPHYSICS

Malå Geoscience AB conducted down-hole geophysical surveys on three drill holes in 1997 (Table 6.1). Physical properties measured included apparent resistivity, induced polarisation (IP) and magnetic susceptibility. Readings were taken at 0.1m intervals down hole. The resistivity and IP readings were taken using the same probe in a Wenner Configuration. The current electrode spacing was 0.75m with a measurement electrode spacing of 0.25m, giving average resistivity (Ωm) and IP (%) values within a radius of 0.2m-0.4m from the mid-point between the measurement electrodes. The magnetic susceptibility readings were taken from a separate probe with values recorded in SI x 10^{-5} units.

Table 6.1 List of drillholes with down-hole geophysical data

Hole number	Easting (m)	Northing (m)	Total depth (m)	Figure
SV9702	1700	1393	199.20	6.4
SV9703	1700	1437	200.00	6.5
SV9706	1698	1345	199.50	6.6

6.2.1 Drillhole SV9702

The downhole geophysical data for drillhole SV9702 is plotted on figure 6.4. Six discrete domains were identified based on correlating geophysical properties and signatures.

1) **Top of drillhole (TOH)–19m**. This is a domain of high apparent resistivity, low chargeability, and low magnetic susceptibility. This is a resistive unit such as granite or basalt.
2) **13m-46m**. This domain is moderately conductive with occasional resistive spikes, moderate to strong chargeability, moderate to high magnetic susceptibility with occasional magnetic spikes. This is a unit of pyrrhotite- and graphite-bearing silicified rock.
3) **46m-70m**. This is a domain of high apparent resistivity, low chargeability, and low magnetic susceptibility. This is a resistive unit such as granite or basalt.
4) **70m-135m**. This domain has moderate to strong apparent resistivity with occasional conductive troughs. IP spikes of moderate amplitude are coincident with the conductive troughs. There are magnetic susceptibility spikes in zones of strong apparent resistivity. This unit is overall quite resistive but does contain small proportions of minerals that are conductive, magnetic and/or chargeable. This unit is most likely a volcanic rock such as basalt.
5) **135m-180m**. High conductivity, high chargeability and magnetic susceptibility. The consistent series of peaks and troughs infers that the unit is layered (foliated). This is a pyrrhotite-bearing foliated sedimentary unit.
6) **180m- Bottom of Hole (BOH)**. This is a domain of high resistivity, low chargeability and low magnetic susceptibility. This unit is most likely a granitoid.

Readings from the surface to a depth of 3m (apparent resistivity and induced polarisation) and 6m (magnetic susceptibility) were affected by the metallic casing and hence subsequently removed from the data set.

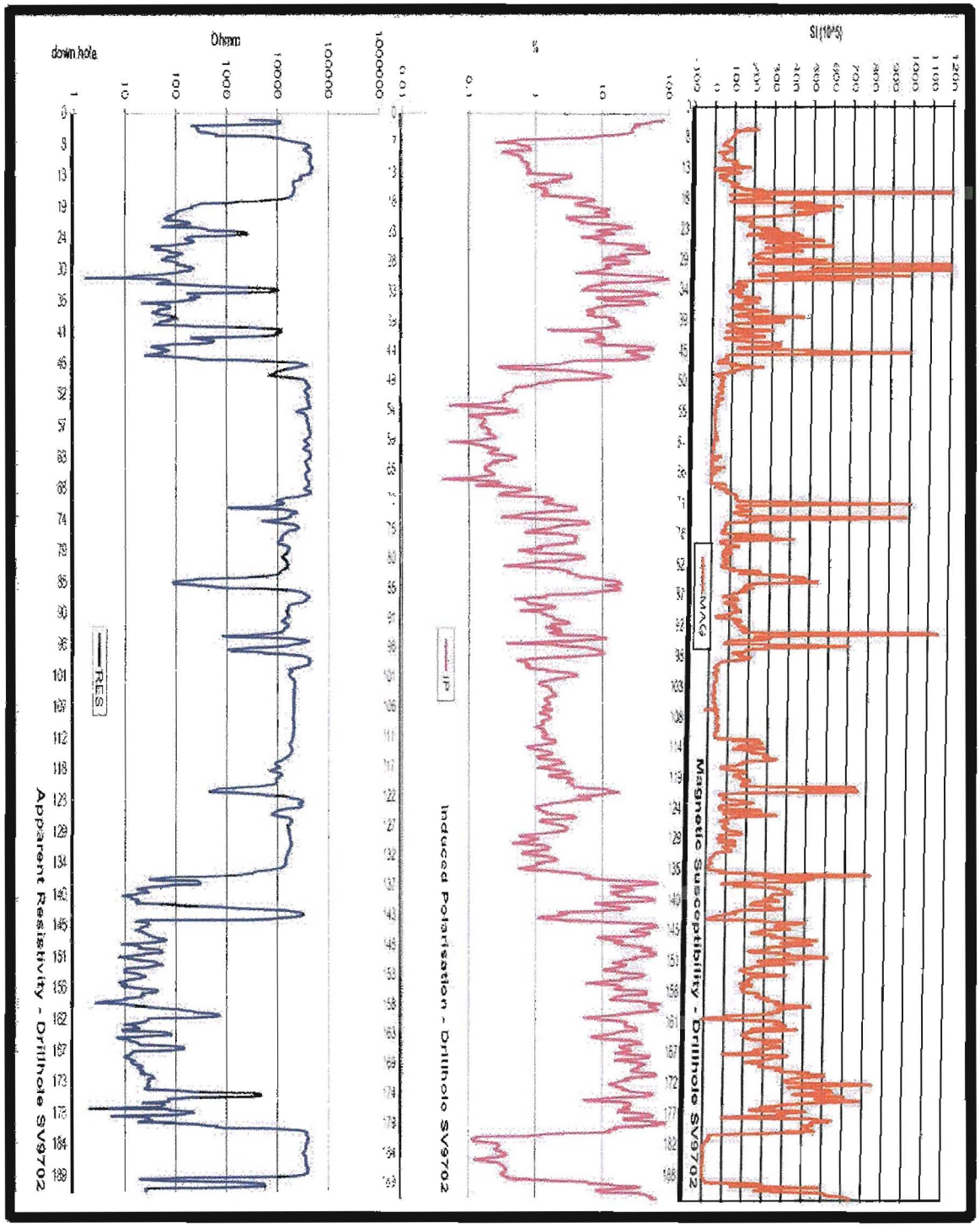

Figure 6.4 Plots for apparent resistivity (Ωm), induced polarisation (IP)(% of RP), and magnetic susceptibility (SI x 10^{-5} units) for drillhole SV9702.

6.2.2 Drillhole SV9703

The downhole geophysical data for drillhole SV9703 is plotted on figure 6.5. Four discrete domains were identified based on correlating geophysical properties and signatures.

1) **Top of drillhole (TOH)–61m**. This domain consists of a series of conductive zones within moderate to high apparent resistive material. There is coincident elevated chargeability, and high magnetic susceptibility, dominated by three peaks. This domain consists of a series of thin, intercalated units (<5m) such as magnetite-bearing volcanics, pyrrhotite-bearing sediments and silicified rock.
2) **61m-99m**. This is a domain of high apparent resistivity, low chargeability, and low magnetic susceptibility. This is a resistive unit such as granite or basalt.
3) **99m-150m**. This domain has a series of wide conductive zones in a moderately resistive terrain. The conductive zones are coincident with a wide series of magnetic material. The strongest chargeable unit is situated in this domain. The magnetic and conductive units are the result of large mass-percentage of magnetic-pyrrhotite in intercalated sediments and volcanics cut by wide, resistive units that may be the result of granitic intrusions.
4) **150m- Bottom of Hole (BOH)**. This is a domain of high apparent resistivity, poor chargeability, and poor magnetic susceptibility. This is a resistive unit such as granite or basalt.

Readings from the surface to a depth of 5m for magnetic susceptibility were affected by the metallic casing and hence subsequently removed from the data set.

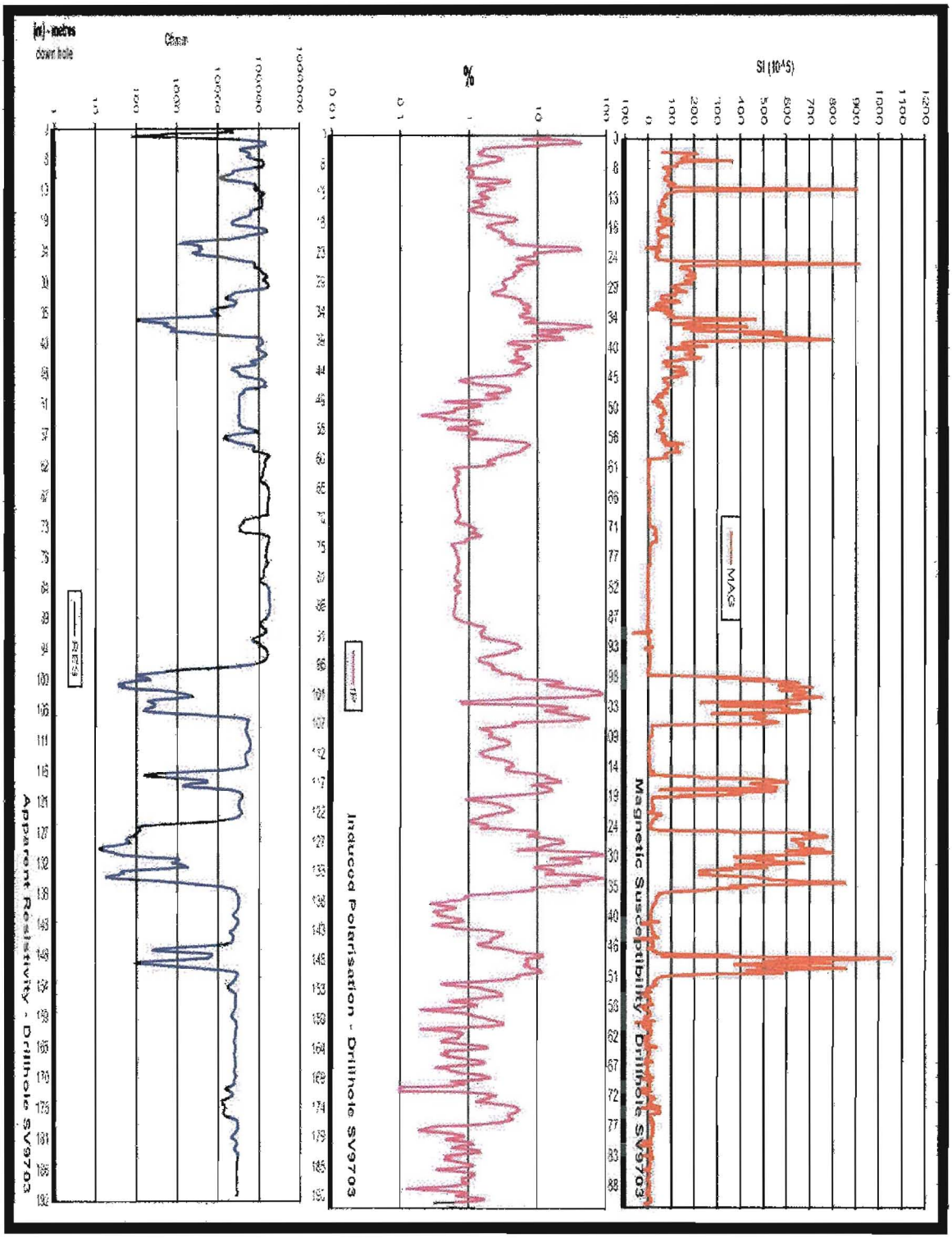

Figure 6.5 Plots for apparent resistivity (Ωm), induced polarisation (IP)(% of RP), and magnetic susceptibility (SI x 10^{-5} units) for drillhole SV9703.

6.2.3 Drillhole SV9706

The downhole geophysical data for drillhole SV9706 is plotted on figure 6.5. Four discrete domains were identified based on correlating geophysical properties and signatures.

1) **Top of drillhole (TOH)–80m**. This is a domain of high apparent resistivity, low chargeability, and low magnetic susceptibility. This is a resistive unit such as granite or basalt.
2) **80m-143m**. This domain consists of a series of conductive troughs coincident with strong chargeability. The magnetic susceptibility is moderate with occasional magnetic peaks. This unit is overall quite conductive. This series of peaks and troughs in all three types of geophysics suggests an intercalated zone of magnetite-bearing volcanics, pyrrhotite-bearing sediments and silicified rock.
3) **143m-180m**. This domain has moderate to high resistivity, moderate chargeability and magnetic susceptibility with occasional peaks. Moderate to high resistivity with coincident magnetic susceptibility suggests a magnetite-bearing crystalline rock. The moderate chargeability is a result of the pyrrhotite in this crystalline rock (most likely a volcanic).
4) **180m- Bottom of Hole (BOH)**. This is a domain of low resistivity (strongly conductive), the strongest chargeability in this hole and strong magnetic susceptibility with occasional magnetic spikes. A unit with coincident strong conductivity, chargeability and magnetism is due to a high concentration of pyrrhotite in foliated sediment.

Readings from the surface to a depth of 3m (apparent resistivity and induced polarisation) and 7.3m (magnetic susceptibility) were affected by the metallic casing and hence subsequently removed from the data set.

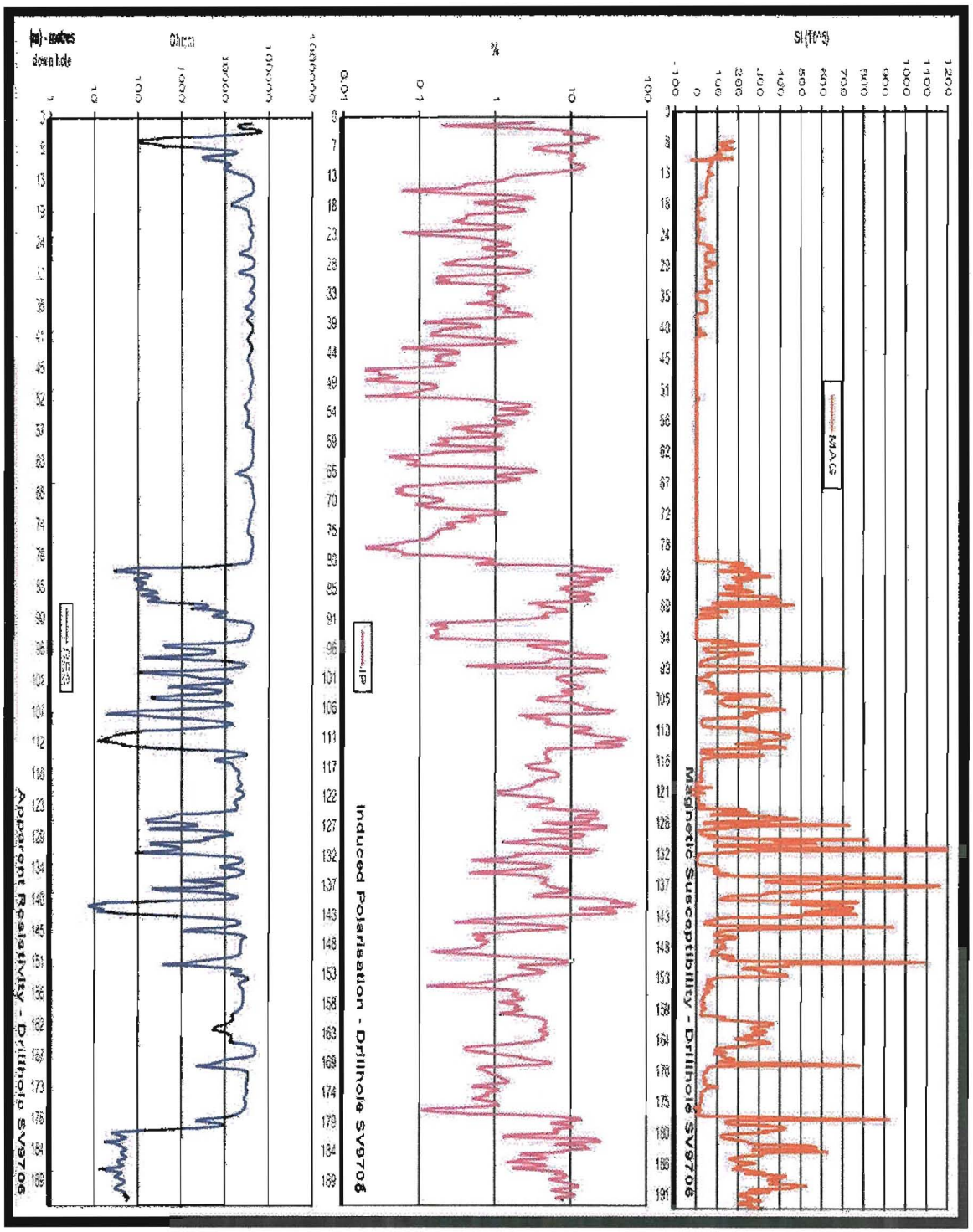

Figure 6.6 Plots for apparent resistivity (Ωm), induced polarisation (IP)(% of RP), and magnetic susceptibility (SI x 10^{-5} units) for drillhole SV9706.

6.3 SUMMARY

The ground-based magnetic field survey shows in detail the 'greenstone' belt of volcano-sedimentary rocks identified in the aeromagnetics.

The ground electromagnetic survey proved to be very useful in delineating conductive units in a known strongly resistive terrain. Due to the resistive nature of the bedrock and till in northern Sweden, the base frequency was set at 18kHz. Despite the high base frequency, there was a shallow, but sufficient, penetration of the primary field into the stratigraphic package at Svartliden, inducing eddy currents in the poorest of conductive units.

The in-phase image delineates quite clearly the conductive and resistive units. The conductive units mostly consist of pyrrhotite-bearing, carbonaceous shales and mudstones.

The downhole geophysical survey shows a strong negative correlation between the induced polarisation and apparent resistivity. This is logical as resistive units such as granitoids and basalts contain little if any minerals that have the potential to be chargeable.

Zones of chargeability with no correlating magnetic susceptibility are caused by the presence of graphite in sediments. Spikes of magnetic susceptibility within zones of high apparent resistivity are caused by magnetite found in crystalline rocks. Coincident high magnetic susceptibility and high IP is caused by pyrrhotite in foliated sediments.

7. QUALITATIVE GEOPHYSICAL INTERPRETATION

7.1 GROUND GEOPHYSICS

To identify first-order geophysical anomalies, the residual layer must be removed so as to leave only anomalous data. The method includes the log-transformation of the geophysical data and to produce an image. Probability plots of the log-transformed geophysical data statistically separates anomalous data from the background. An image is thus drawn showing first-order geophysical anomalies.

7.1.1 Ground Magnetics

The image created from the log-transformed magnetic data displays two strong magnetic anomalies (Figure 7.1). The first lies between 1500mE and 2150mE along the 1500mN. This anomaly has an average width of 20m. The second is a strong magnetic anomaly to the west along the 700mN between 700mE and 900mE. This anomaly is approximately 50m wide. Where the 'greenstone' belt flexes to the south, (between 1200mN and 1600mN, west of the 1000mE), there are only a few, small, disjointed magnetic bodies.

The probability plot for the log-transformed ground magnetic data shows a lower inflexion point at the 20^{th} percentile. The data population below the 20^{th} percentile represents poorly magnetic and non-magnetic units (such as granitoids or magnetite-depleted volcanics). The upper inflexion point at the 80^{th} percentile represents first-order ground magnetic anomalies (figure 7.2).

The first-order magnetic anomaly image shows a series of discontinuous magnetic bodies along the 1500mN and several broad anomalies to the southwest, notably along the 700mE (figure 7.3).

Figure 7.1

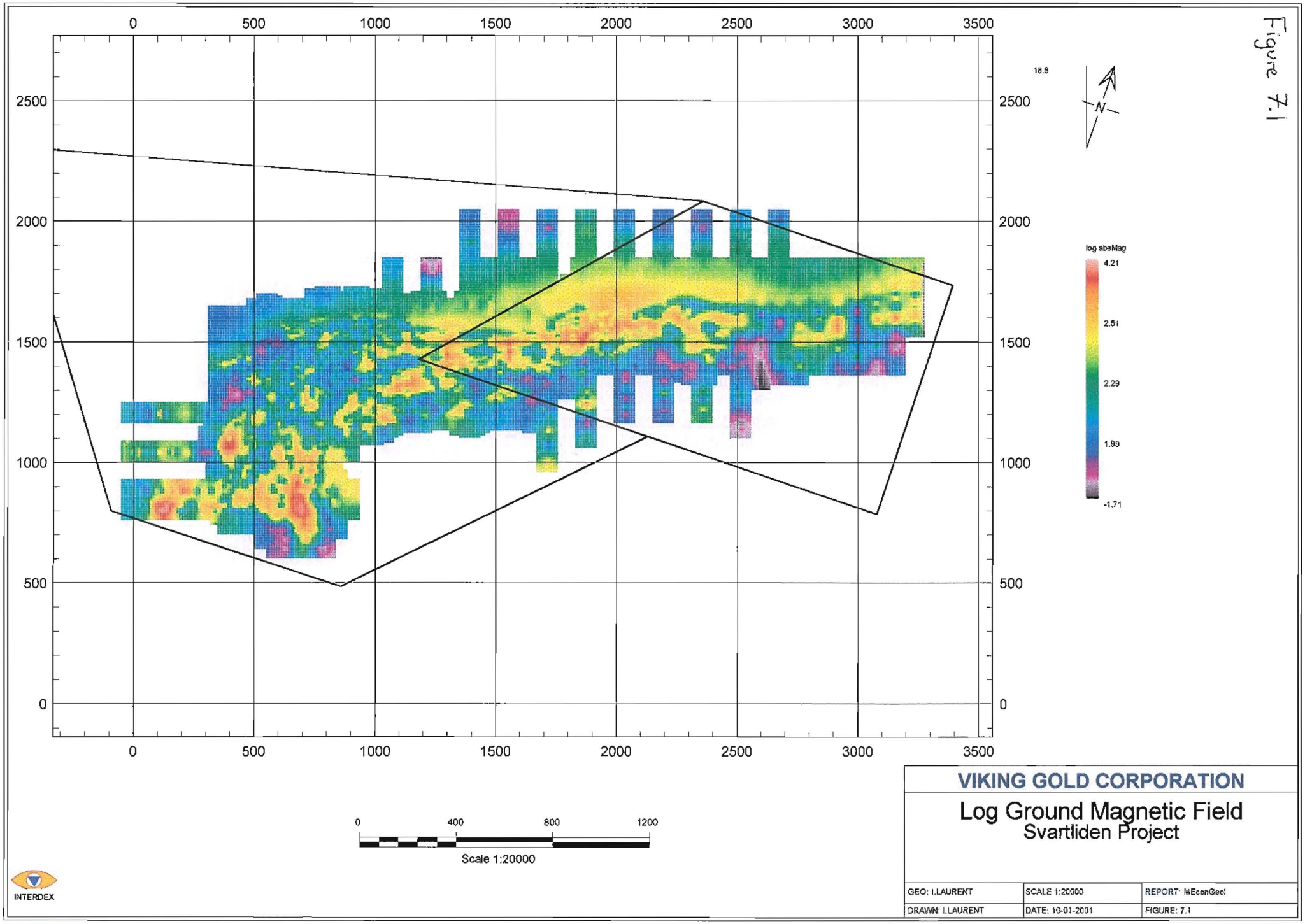

VIKING GOLD CORPORATION

Log Ground Magnetic Field
Svartliden Project

GEO: I.LAURENT	SCALE 1:20000	REPORT: MEconGeol
DRAWN: I.LAURENT	DATE: 10-01-2001	FIGURE: 7.1

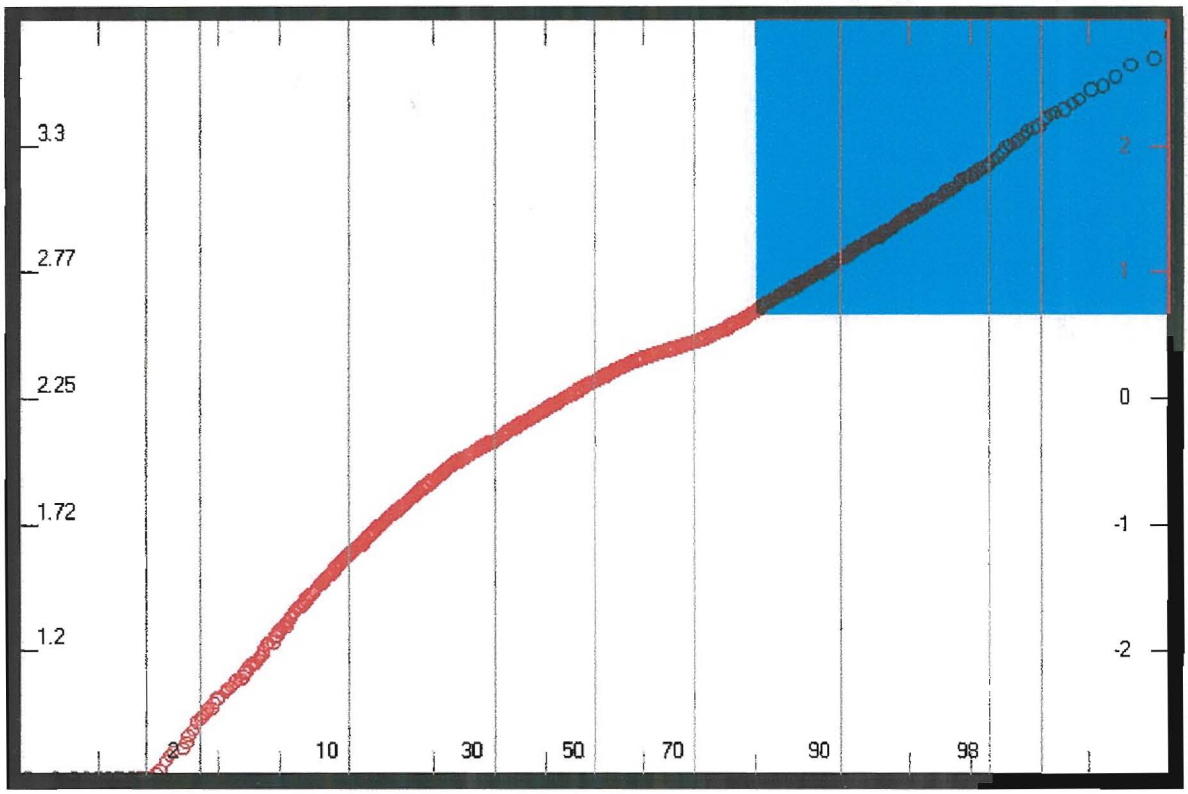

Figure 7.2 Probability plot of the log-transformed ground magnetic data.
The area in pale blue represents data above 80th percentile inflexion point. $\Sigma_x = 8,979$

7.1.2 Ground EM (in-phase component)

The linear 'greenstone' belt in figure 6.2 is represented by a conductive zone that breaks up into 3 or 4 thin conductive belts as the sequence flexes to the south (west of the 1000mE).

The log-transformed image emphasises the conductive highs (figure 7.4). The in-phase EM anomalies are strong and continuous, ranging from 1000mE to 2300mE. East of the 2300mE, the in-phase anomaly remains continuous but is weaker in intensity. Along the 700mE (between 600mN and 1000mN), there is a broad, strong, in-phase EM anomaly.

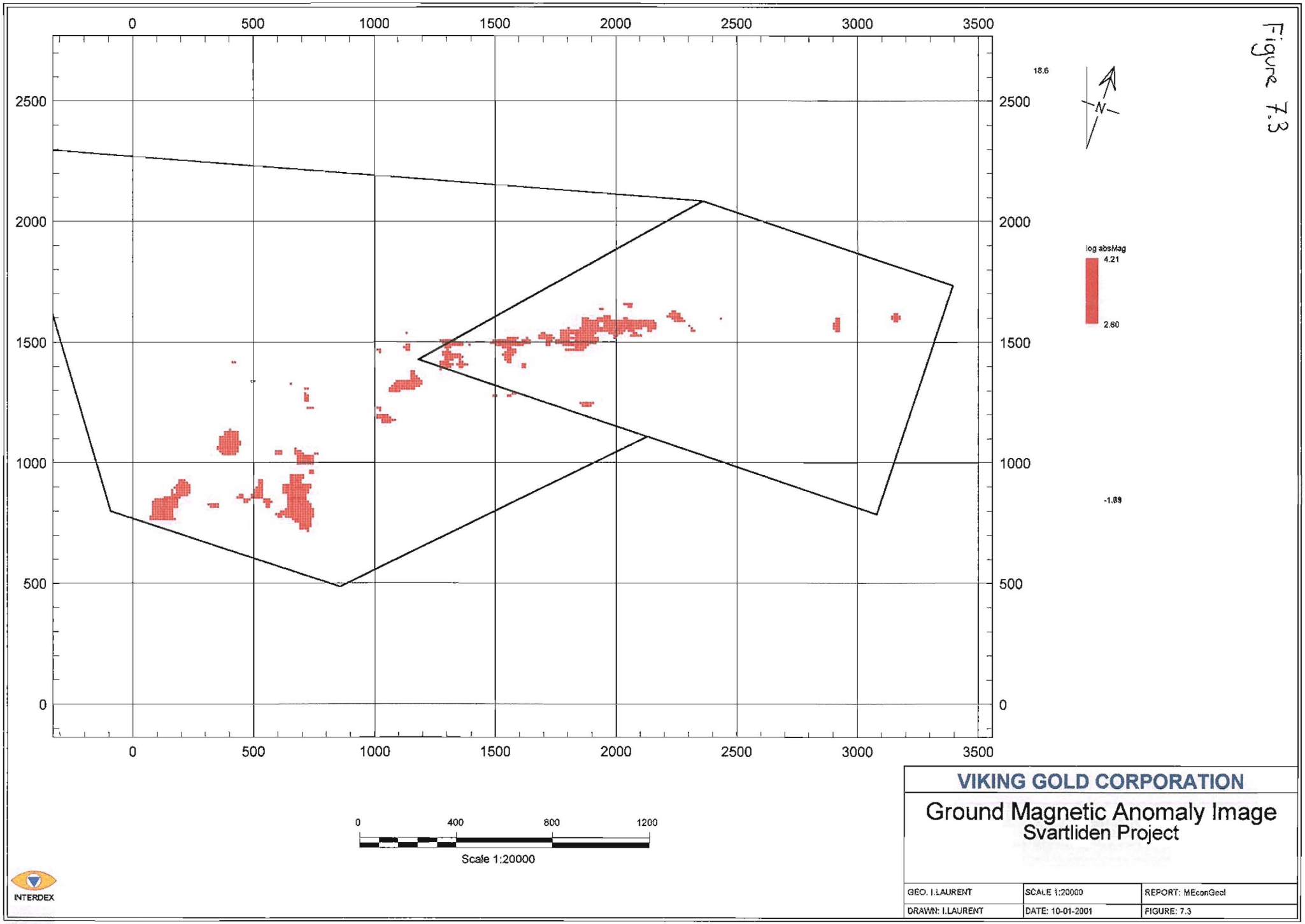
0
500
1000
1500
2000
2500
3000
3500
18.6
log absMag
4.21
2.60
-1.89
0
400
800
1200
Scale 1:20000
INTERDEX
VIKING GOLD CORPORATION
Ground Magnetic Anomaly Image
Svartliden Project
GEO. I.LAURENT
SCALE 1:20000
REPORT: MEconGeol
DRAWN: I.LAURENT
DATE: 10-01-2001
FIGURE: 7.3

Figure 7.3

Figure 7.4

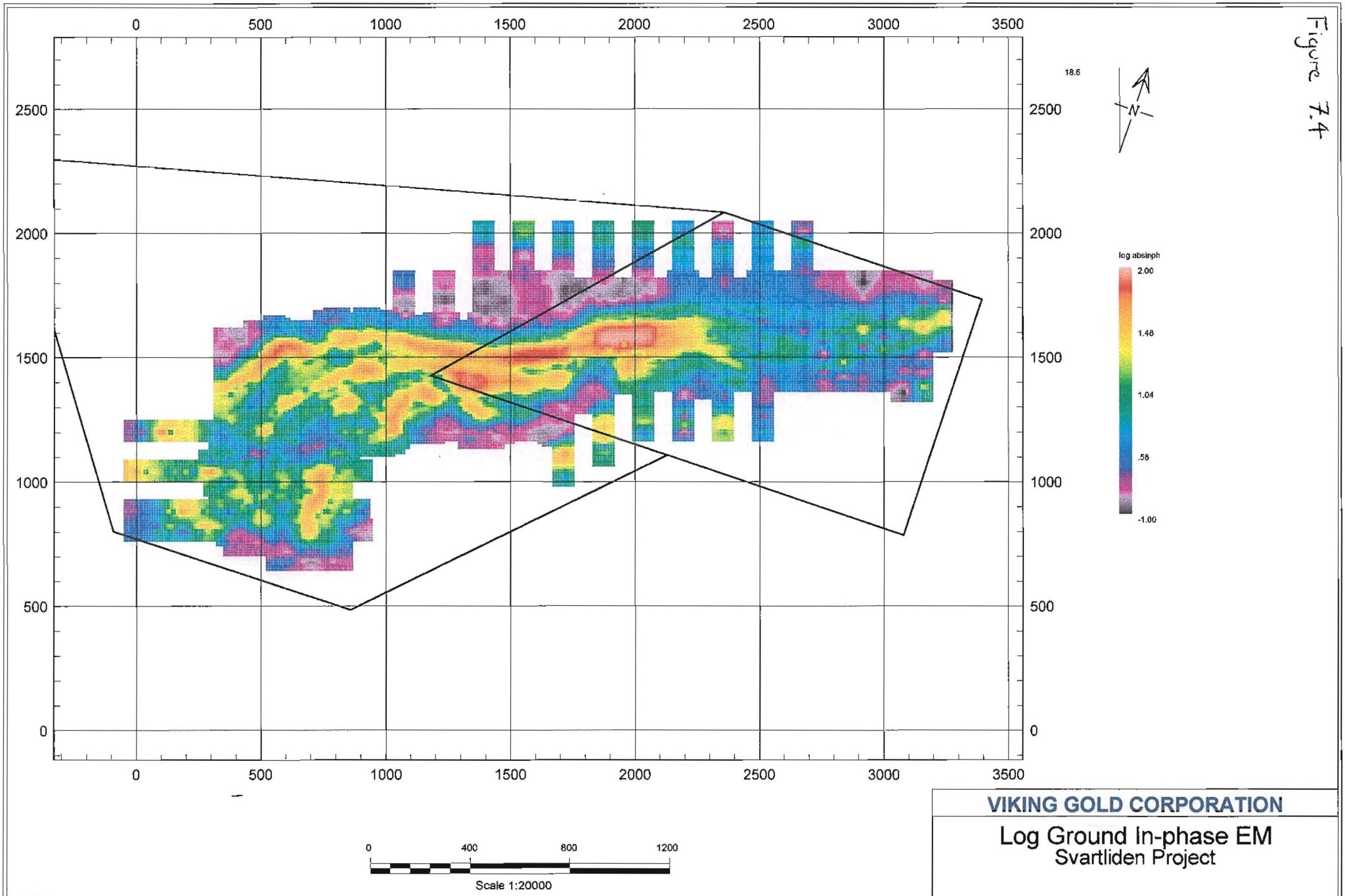

INTERDEX

VIKING GOLD CORPORATION

Log Ground In-phase EM
Svartliden Project

GEO. I.LAURENT	SCALE 1:20000	REPORT: MEconGeol
DRAWN. I.LAURENT	DATE: 10-01-2001	FIGURE: 7.4

The probability plot shows an inflexion point at the 80th percentile (figure 7.5). The data population above the 80th percentile represents first-order, in-phase EM anomalies. The plot shows a normal distribution up to the inflexion point. From the inflexion point, the graph plateau's out suggesting that the conductive units have a uniform, high EM response.

The first-order in-phase EM anomaly image shows three linear bodies along the 1600mN, between the 1100mE and 2200mE (figure 7.6). There is one linear body along the 1400mN, between the 1200mE and 1600mE and a linear anomaly along the 700mE, between the 900mN and 1000mN.

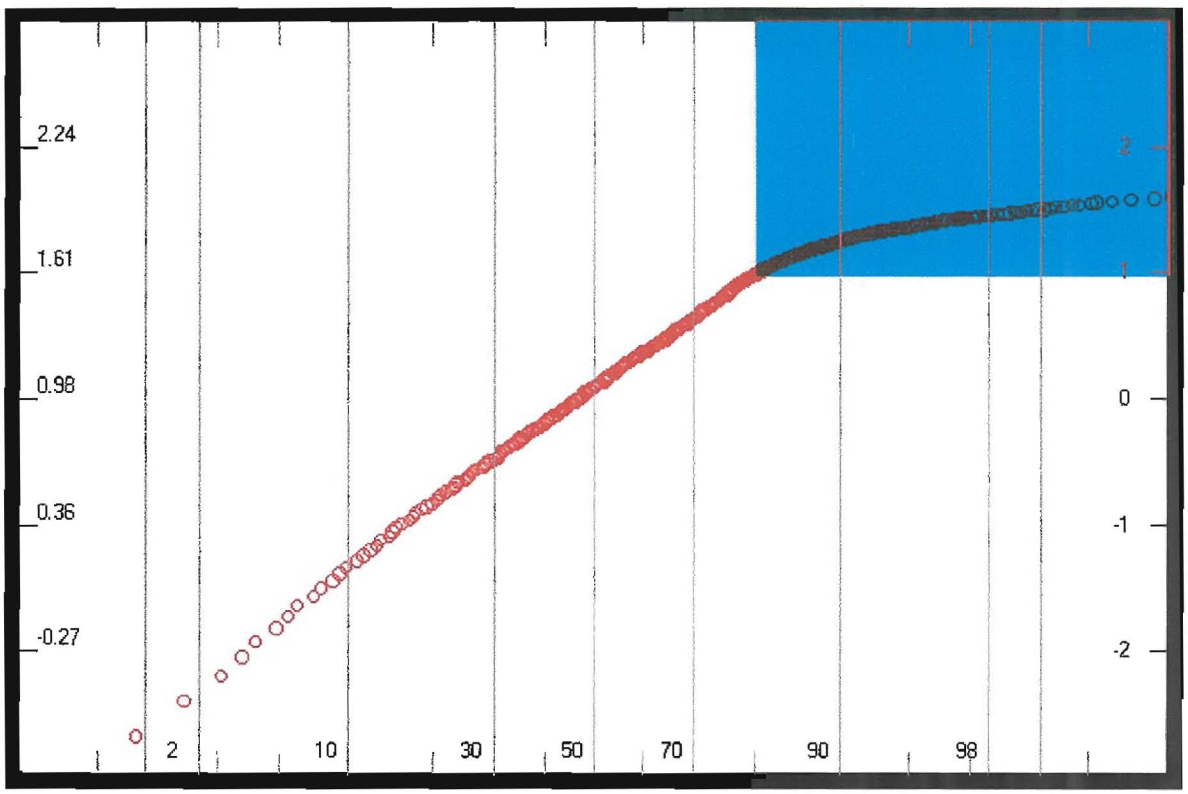

Figure 7.5 Probability plot of the log-transformed ground magnetic data. The area in pale blue represents data above 80th percentile inflexion point. $\Sigma_x = 6{,}324$

Figure 7.6

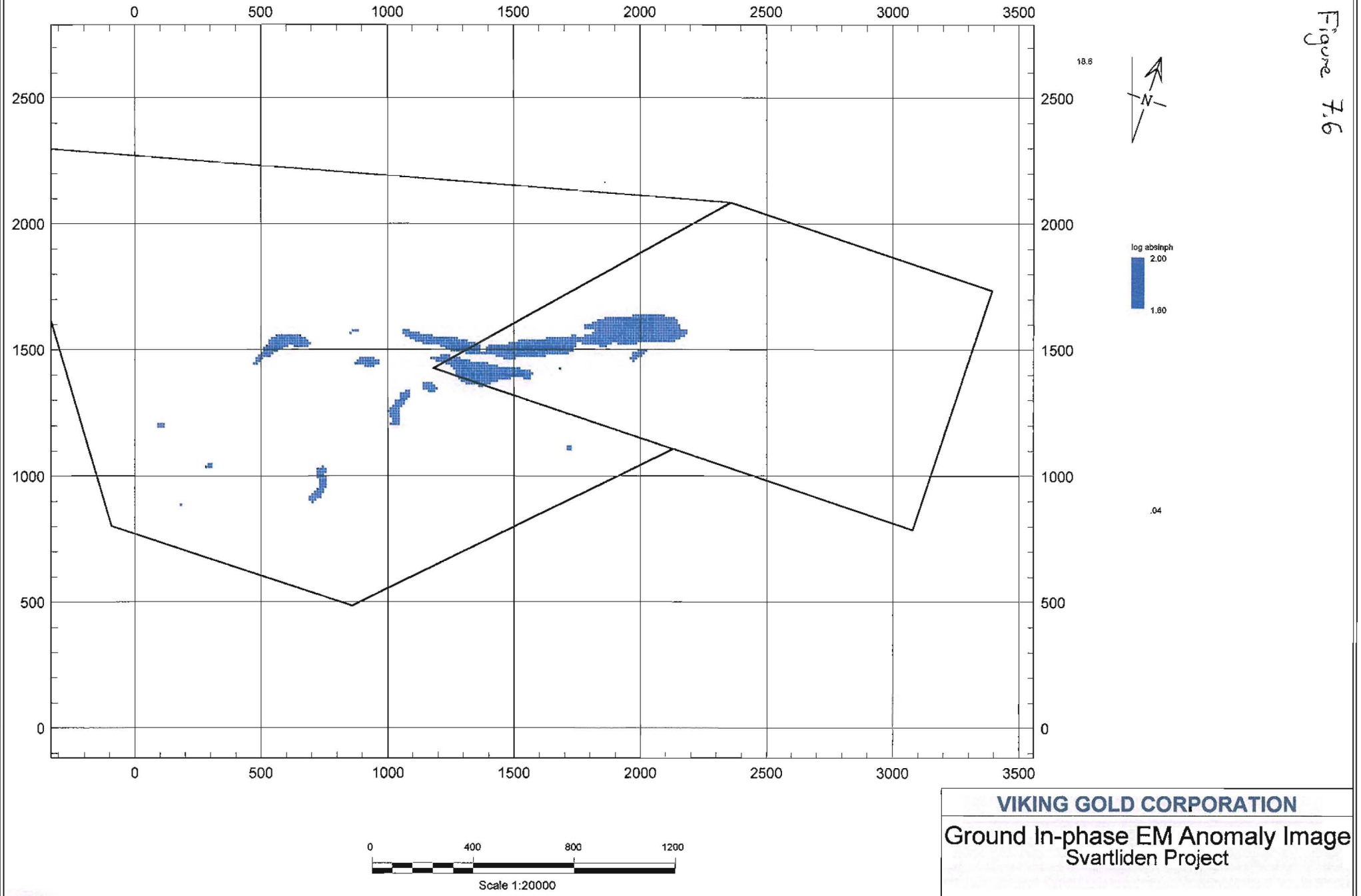

INTERDEX

VIKING GOLD CORPORATION

Ground In-phase EM Anomaly Image
Svartliden Project

GEO: I.LAURENT	SCALE 1:20000	REPORT: MEconGeol
DRAWN: I.LAURENT	DATE: 10-01-2001	FIGURE: 7.6

7.1.3 Ground EM (quadrature component)

A conductive zone marks the broad linear 'greenstone' belt, seen in figure 6.3. The quadrature component displays the Svartliden 'greenstone' belt as a broader, moderately conductive unit.

The log-transformed quadrature EM image shows anomalies that are discrete and representative of the conductive unit below surface (figure 7.7). East of the 2300mE, the quadrature anomaly weakens and disappears.

The western part of the project area is marked by a broad conductive anomaly. The south-trending, linear conductive units delineated in the log-transformed in-phase EM image appear as a combined, moderately conductive body in the log-transformed quadrature EM image.

The probability plot statistically identified the first-order, quadrature EM anomalies at Svartliden (figure 7.8). The plot shows a gradational increase in the data rather than several data populations separated by inflexion points. This gradational increase in the data explains the broad anomalism displayed by the quadrature EM image. There is a weak inflexion point at the 70^{th} percentile. Above the 70^{th} percentile, the data population represents first-order, quadrature EM anomalies (figure 7.9).

A 150m-wide, irregular body dominates the first-order, quadrature EM, anomaly image. This body is located along the 1500mN, between the 1600mE and 2200mE. There is an irregular shaped body along the 1400mN, between the 1400mE and 1600mE and is surrounded by several small, irregular, first-order quadrature EM anomalies.

Figure 7.7

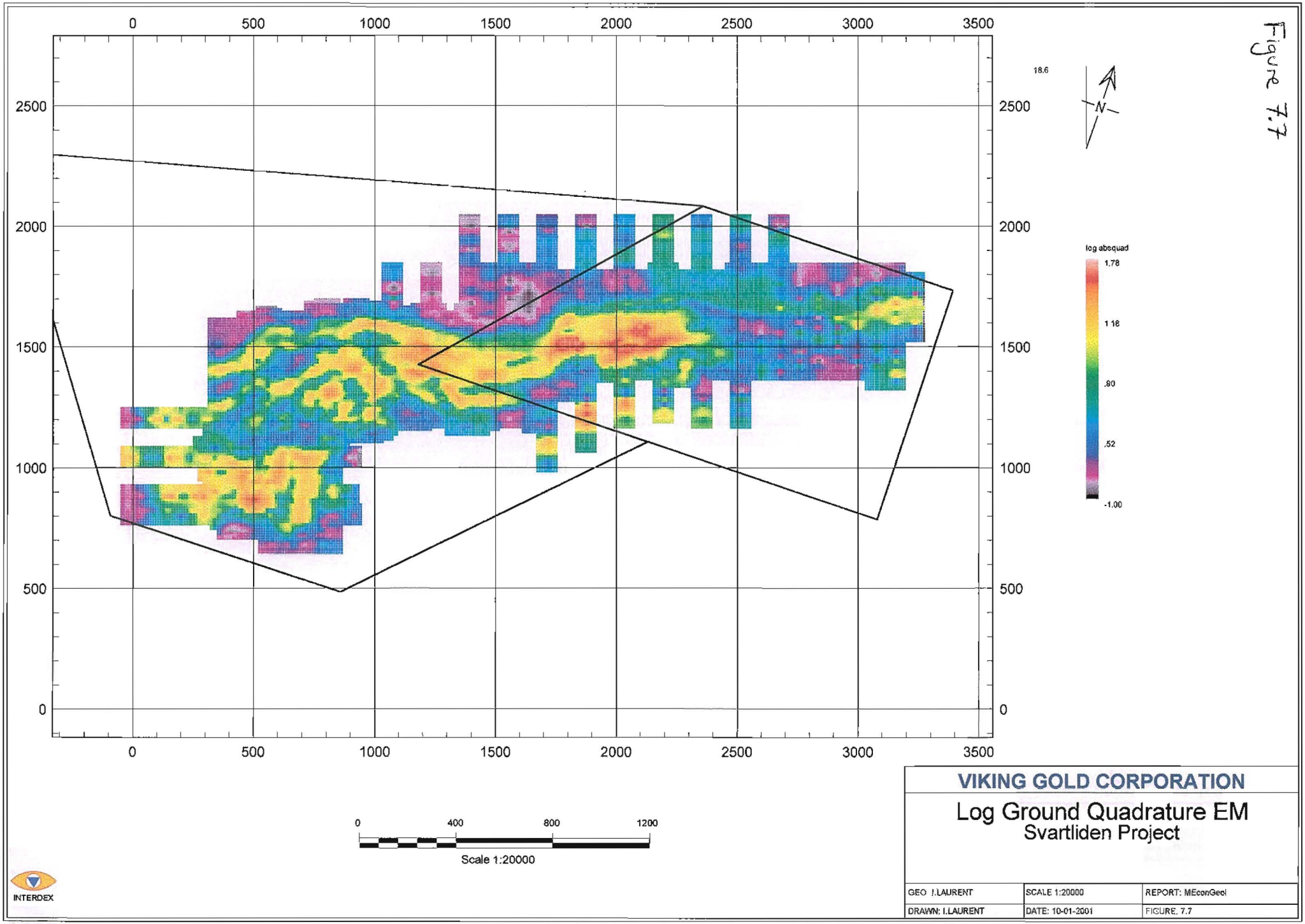

VIKING GOLD CORPORATION

Log Ground Quadrature EM
Svartliden Project

GEO I.LAURENT	SCALE 1:20000	REPORT: MEconGeol
DRAWN: I.LAURENT	DATE: 10-01-2001	FIGURE. 7.7

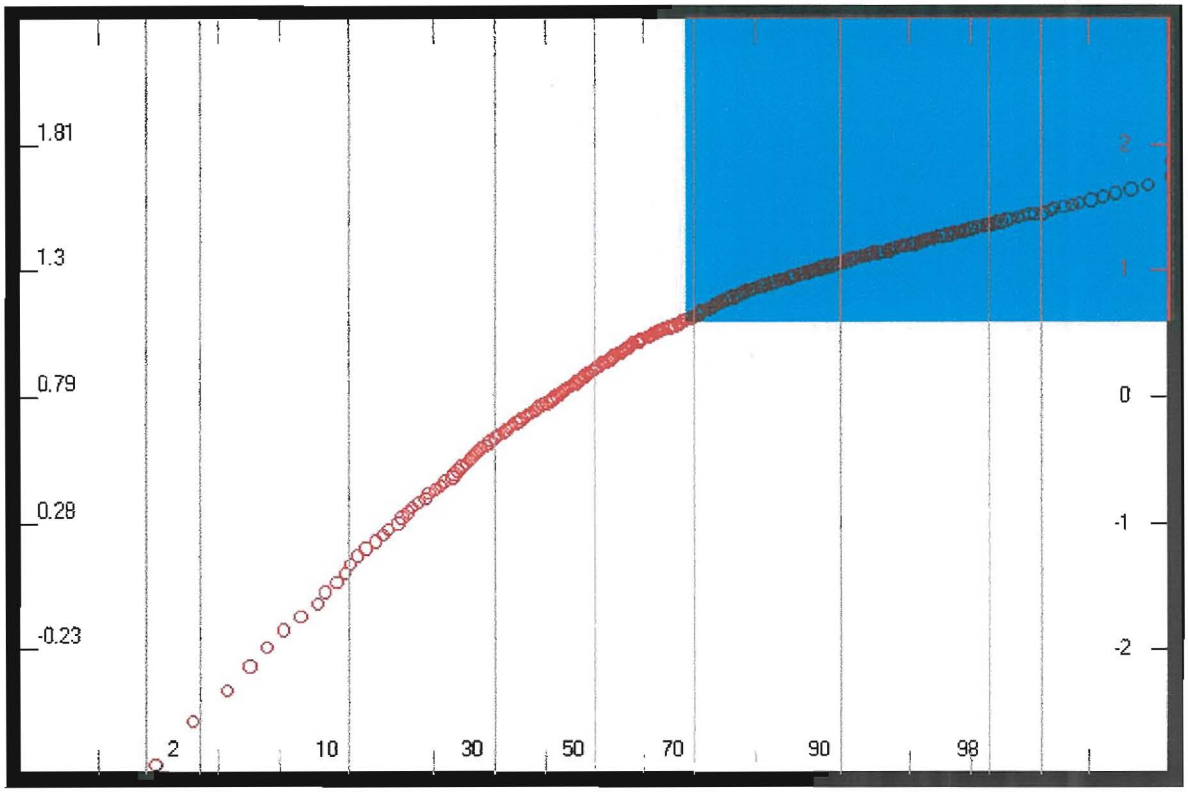

Figure 7.8 Probability plot of the log-transformed ground magnetic data.
The area in pale blue represents data above 70th percentile inflexion point. $\Sigma_x = 6{,}324$

7.1.4 Ground EM (inphase/quadrature ratio)

A ratio between the in-phase and quadrature component of the ground EM was calculated to accentuate the strong in-phase EM anomalies

The ratio-EM image delineates clearly a northern conductive unit, averaging 50m in width. The unit trends east-west along the 1600mN (±50m) between the 400mE and the 3000mE. Within this belt there are zones of highly conductive material and small pockets of resistive material (figure 7.10).

A second conductive unit is also clearly delineated on the ratio-EM image. A 50m wide conductive unit trending east-west is situated along the 1400mN from the 1200mE to the 1700mE. From the 1200mE westward, this conductive unit breaks up as the stratigraphy rotates from an east-west orientation to a north-south orientation.

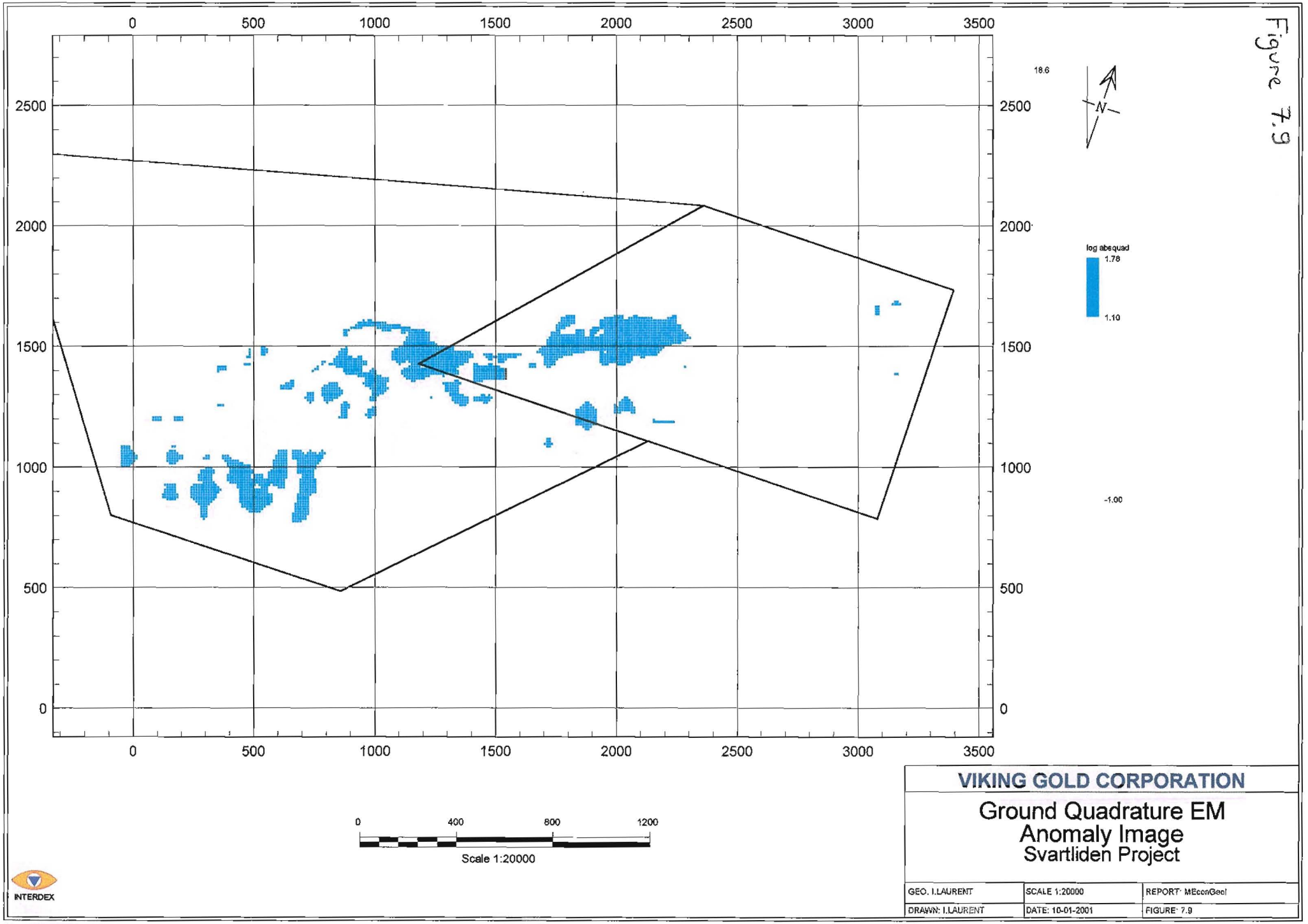
0
500
1000
1500
2000
2500
3000
3500
18.6
N
log absquad
1.78
1.10
-1.00
0
400
800
1200
Scale 1:20000
INTERDEX
VIKING GOLD CORPORATION
Ground Quadrature EM
Anomaly Image
Svartliden Project
GEO. I.LAURENT
SCALE 1:20000
REPORT: MEconGeol
DRAWN: I.LAURENT
DATE: 10-01-2001
FIGURE: 7.9

Figure 7.9

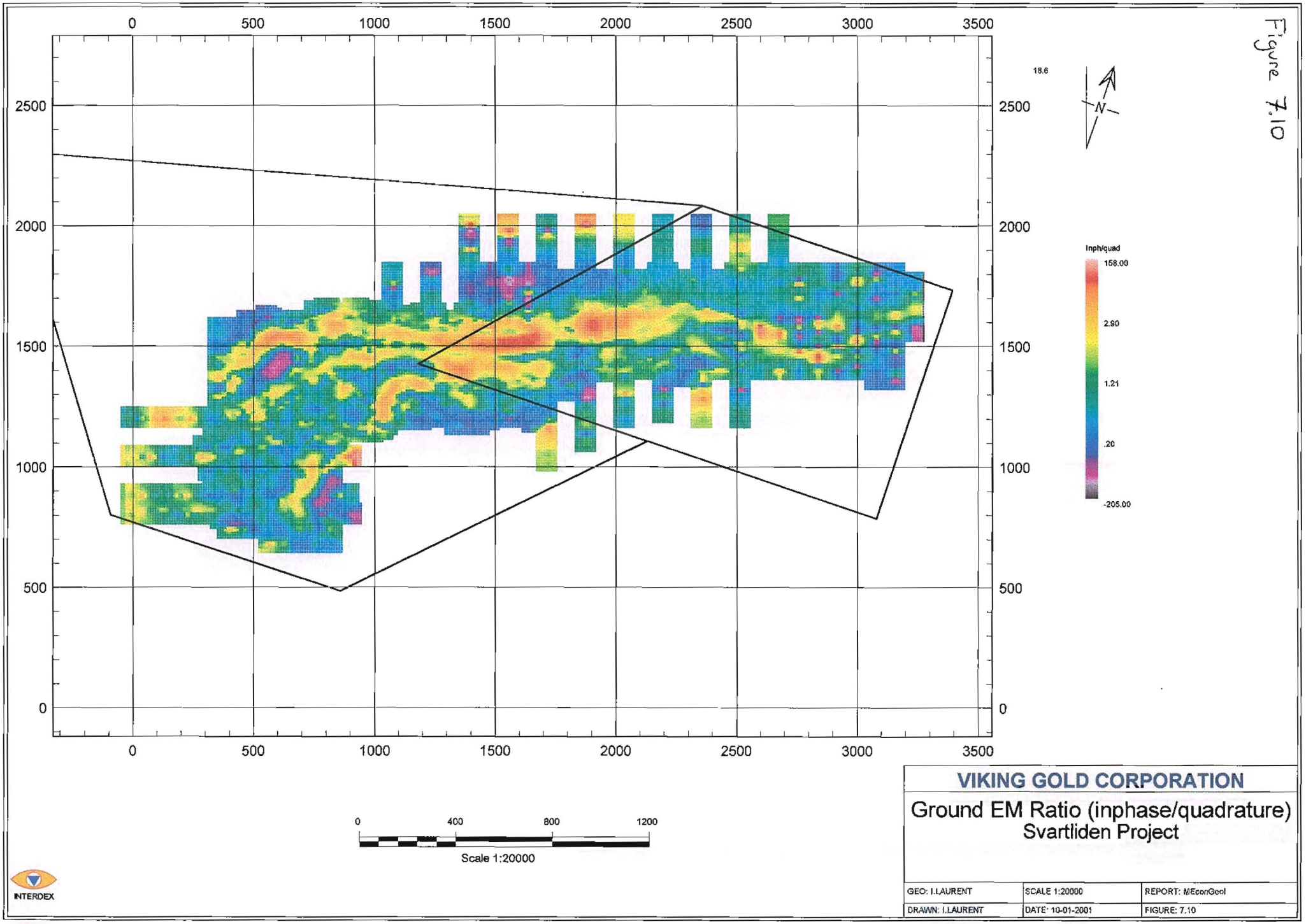
0
500
1000
1500
2000
2500
3000
3500
18.6
N
Inph/quad
158.00
2.90
1.21
.20
-205.00
0
400
800
1200
Scale 1:20000
INTERDEX
VIKING GOLD CORPORATION
Ground EM Ratio (inphase/quadrature)
Svartliden Project
GEO: I.LAURENT
SCALE 1:20000
REPORT: MEconGeol
DRAWN: I.LAURENT
DATE: 10-01-2001
FIGURE: 7.10

Figure 7.10

A significant ratio-EM anomaly exists along the 700mE, between the 800mN and 1100mN. The anomaly reflects the coincident anomaly in, both, the in-phase EM image and the quadrature EM image.

The probability plot shows a curvi-linear pattern indicating a gradational increase to an inflexion point at the 90th percentile (figure 7.11). The data population above the 90th percentile represents first-order, ratio-EM anomalies.

The first-order ratio-EM anomalies are the highly conductive pockets identified in the conductive linear belt (figure 7.12). The dominant lens is +50m wide and is situated on the 1500mN, between the 1400mE and 1700mE. There is another irregular shaped anomaly along the 1500mN, between the 1800mE and 2000mE. These anomalies are surrounded by small, irregular, first-order ratio-EM anomalies.

In the western part of the project, there are a few highly conductive, first-order ratio-EM anomalies, averaging 200m^2. The ratio-EM anomalies do not differentiate pyrrhotite-only bearing rocks from graphite-only bearing rocks but do show units with significant concentrations of interlocking conductive sulphides.

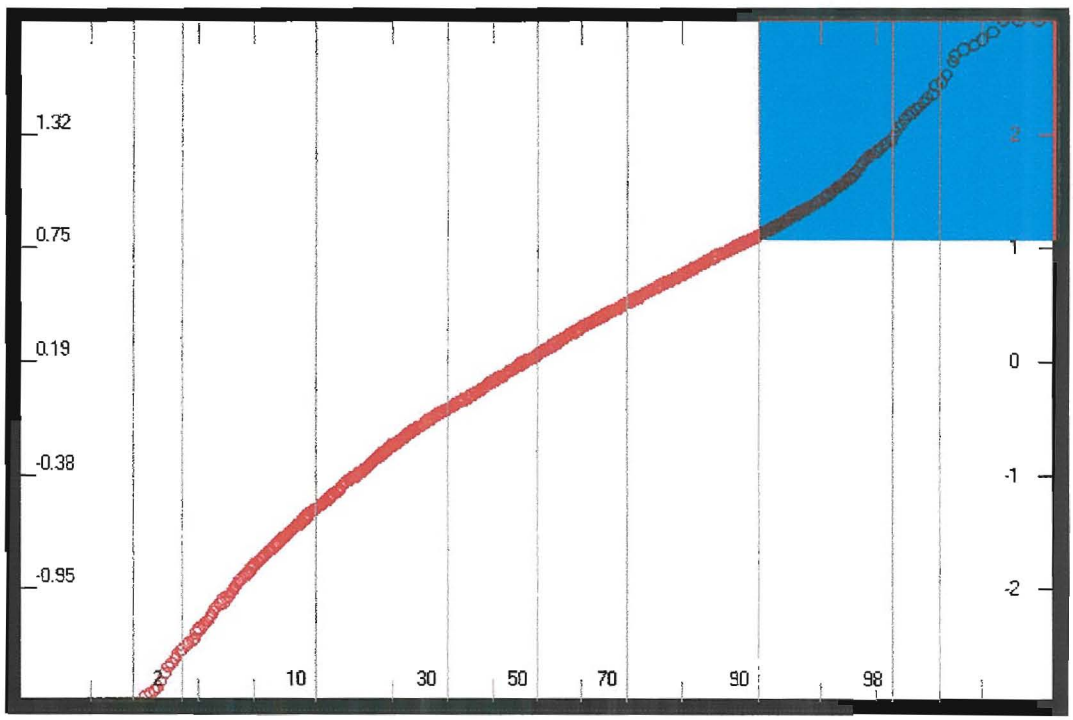

Figure 7.11 Probability plot of the log-transformed ground magnetic data.
The area in pale blue represents data above 90th percentile inflexion point. $\Sigma_x = 6{,}324$

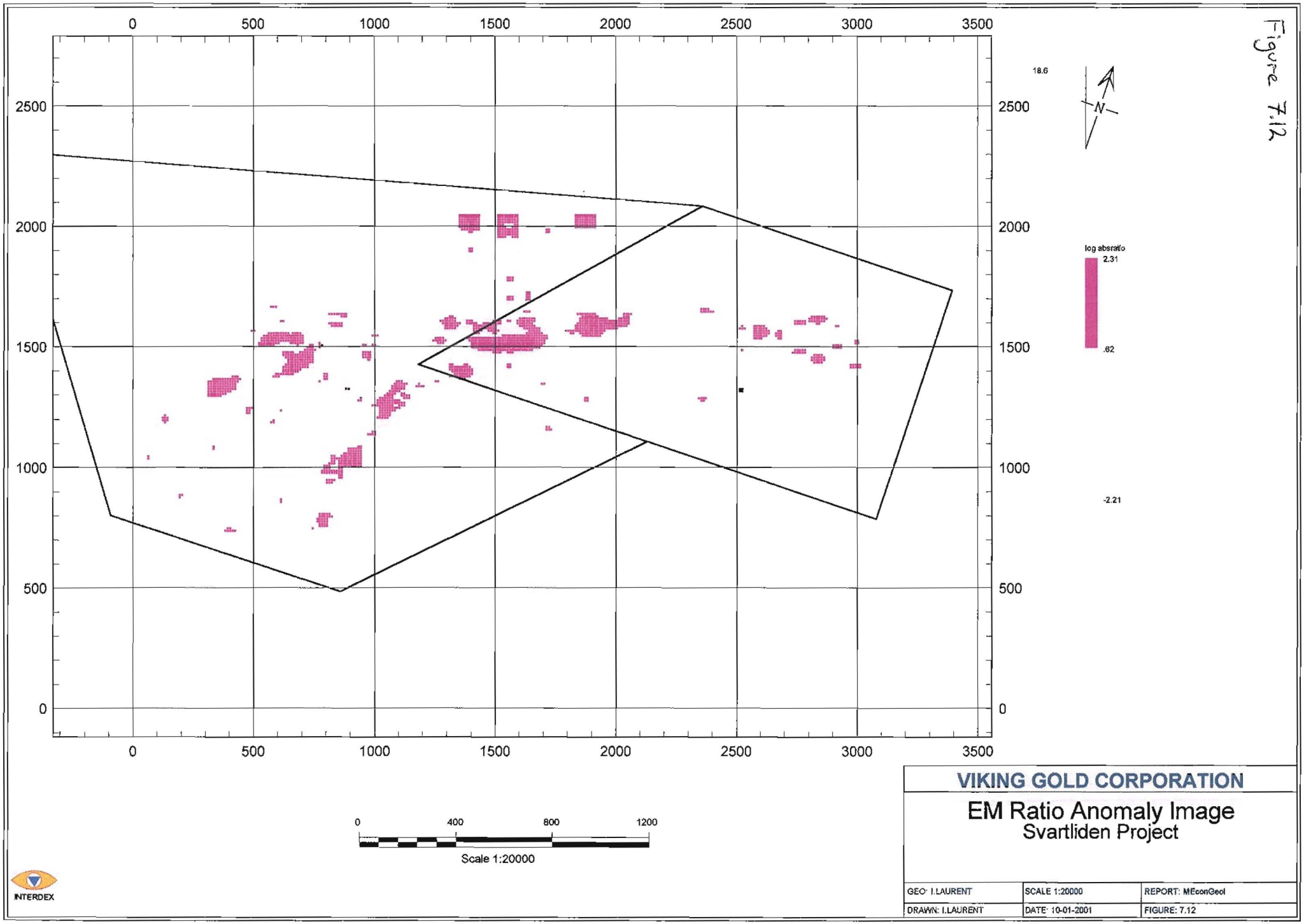
0
500
1000
1500
2000
2500
3000
3500
18.6
N
log absratio
2.31
.62
-2.21
0
400
800
1200
Scale 1:20000
INTERDEX
VIKING GOLD CORPORATION
EM Ratio Anomaly Image
Svartliden Project
GEO: I.LAURENT
SCALE 1:20000
REPORT: MEconGeol
DRAWN: I.LAURENT
DATE: 10-01-2001
FIGURE: 7.12

Figure 7.12

7.1.5 Synthesis of the Ground Magnetics and Ground EM

The ground magnetic anomalies are based on different criteria to the ground EM anomalies. These magnetic anomalies do not differentiate pyrrhotite-bearing rocks from magnetite-bearing rocks.

In the southwestern part of the project, there are four sub-parallel linear bodies, between the 900mN and 1100mN. The presence of these conductive anomalies in the quadrature EM image, which are not present in the in-phase EM image, may be caused by either:

a) The coil configuration, although deemed constant, not taking into account the change in stratigraphy from east-west to north-south; or,
b) The quadrature response may sample to a greater depth.

The quadrature EM anomalies, like the in-phase EM anomalies, do not differentiate pyrrhotite-only bearing rocks from graphite-only bearing rocks. The in-phase EM anomalies do not differentiate pyrrhotite-only bearing rocks from graphite-only bearing rocks.

When the magnetic data is plotted against the corresponding in-phase and quadrature EM components, two distinct populations are apparent (figure 7.13).

The larger anomaly has coincident strong magnetism and strong EM (in-phase and quadrature). This indicates that the strongly conductive units also have magnetic properties exhibited by sulphides such as pyrrhotite, and pentlandite.

The second zone of anomalous magnetism in figure 7.13 has coincident low EM response (in-phase and quadrature). Magnetite is a common mineral in the volcanic rocks that has high magnetic susceptibility but is not conductive.

The in-phase EM response delineates the discrete conductive units near surface, whereas the quadrature response is broader and slightly less conductive, possibly representing features at greater depth. The ratio-EM response was able to identify the highly conductive units.

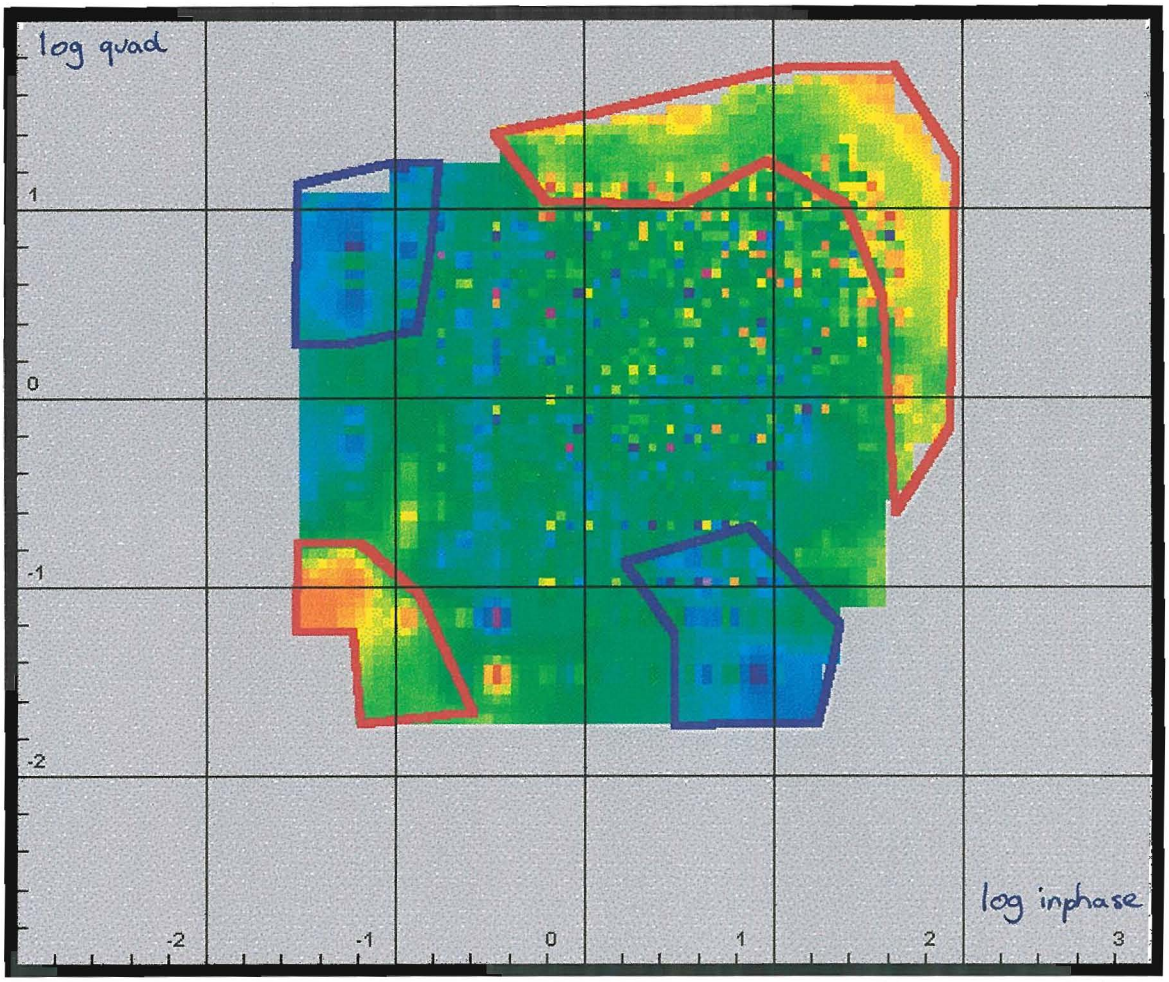

Figure 7.13 Plot of the log-transformed in-phase component against the log-transformed quadrature component. The Z value is log-transformed ground magnetics.
Red domains are magnetic highs, Blue domains are magnetic lows. $\Sigma_x = 6{,}277$

The EM and magnetic anomalies identified were combined to produce an image (figure 7.14). The coincident EM and magnetic anomalies, EM-only anomalies, and magnetic-only anomalies can be separated.

The coincident EM and magnetic anomalies are shown in red/purple and represent a concentration of magnetic-pyrrhotite. The EM-only anomalies are shown in grey/blue and represent graphite-bearing or non-magnetic sulphides (eg. cubic pyrite, galena). The magnetic-only anomalies are shown in yellow and represent magnetite-bearing units.

7.2 DOWNHOLE GEOPHYSICS

The downhole geophysical data is plotted against its corresponding drillholes along section 1700mE. The aim of plotting the geophysics in section was to correlate like domains identified in each hole and delineate the vertical distribution of anomalous geophysical bodies.

7.2.1 Magnetic Susceptibility

Zones of high magnetic susceptibility in each drillhole have been extrapolated to create an image illustrating these anomalies along section 1700mE (Figure 7.15). There are three south-dipping zones of high magnetic susceptibility and three discrete zones of low magnetic susceptibility. Zones of high magnetic susceptibility are due to concentrations of magnetite and magnetic pyrrhotite.

7.2.2 Apparent Resistivity

Three resistive zones and two conductive zones are delineated along the 1700mE (Figure 7.16). Above the 400mRL, there are two highly resistive bodies cut by a conductive unit. The conductive unit thickens down dip (as seen in drill hole SV9706). At depth (below the 380mRL), there is another highly conductive, south-dipping unit. This unit thickens down dip but is lithologically and/or structurally constrained. Zones of low apparent resistivity are due to concentrations of conductive pyrrhotite and graphite.

7.2.3 Induced Polarisation

Two zones of high chargeability and three zones of low chargeability were delineated along the 1700mE (Figure 7.17). The two chargeable zones are subparallel and dip to the south. The upper body thickens with depth (as seen in drill hole SV9706). The lower, south dipping, body is traceable across all three holes. This unit is lithologically and/or structurally constrained. Zones of high chargeability are due to concentrations of graphite and chargeable pyrrhotite and chalcopyrite.

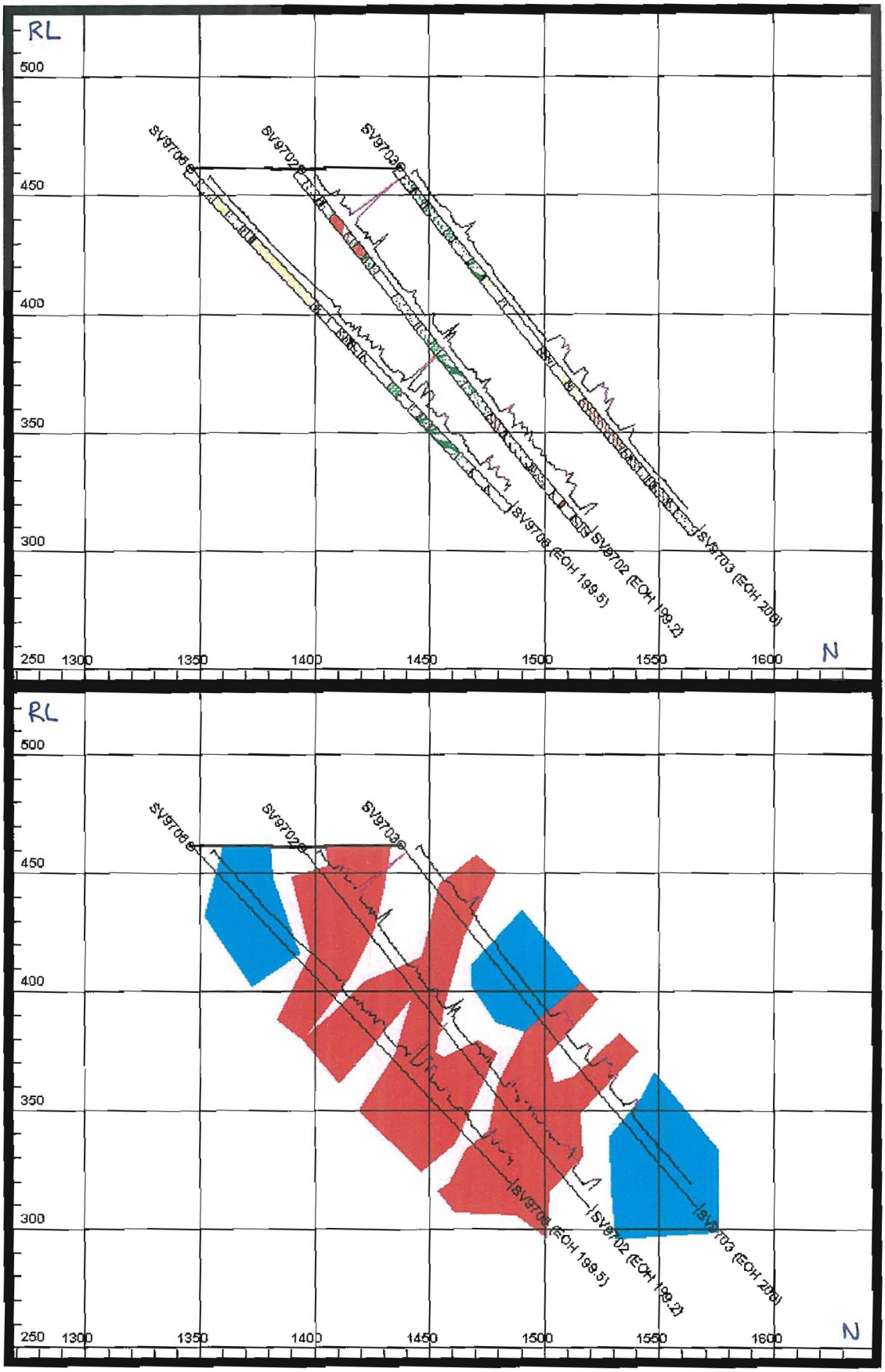

Figure 7.15 Anomalies of magnetic susceptibility delineated along the 1700mE Section.

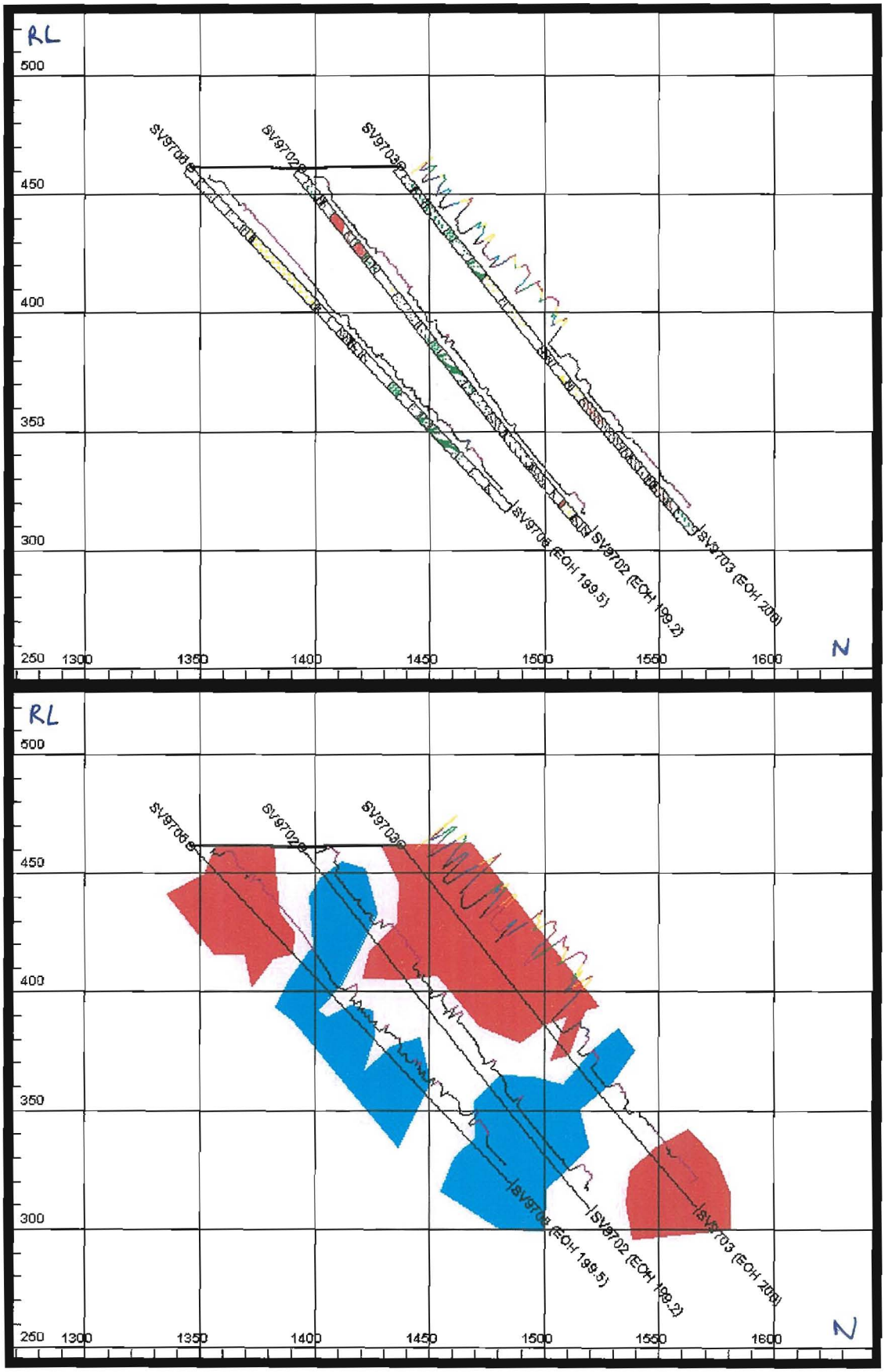

Figure 7.16 Anomalies of apparent resistivity delineated along the 1700mE Section.

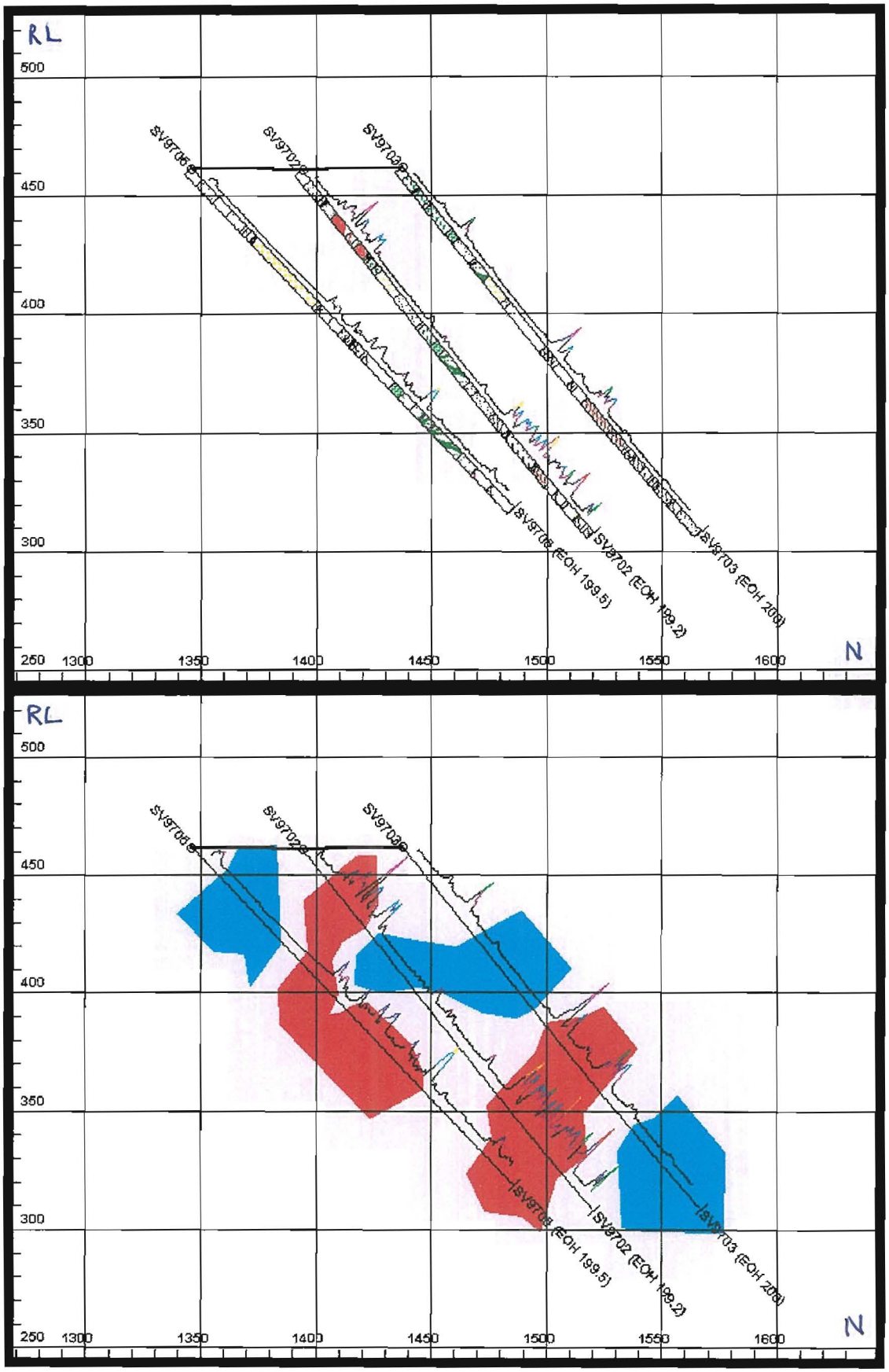

Figure 7.17 Anomalies of induced polarisation delineated along the 1700mE Section.

7.2.4 Synthesis of the downhole geophysics

When comparing the three downhole geophysical anomaly maps, there is a significant overlap between highly conductive, highly chargeable and high magnetic susceptibility zones. An anomaly map displaying all coincident zones is shown in figure 7.18.

There are five coincident zones identified. The two red domains represent strongly conductive, highly chargeable, high magnetic susceptibility units. The upper unit is predominantly structurally controlled. The lower unit is lithologically controlled. The three blue domains represent resistive, poorly chargeable, non-magnetic units.

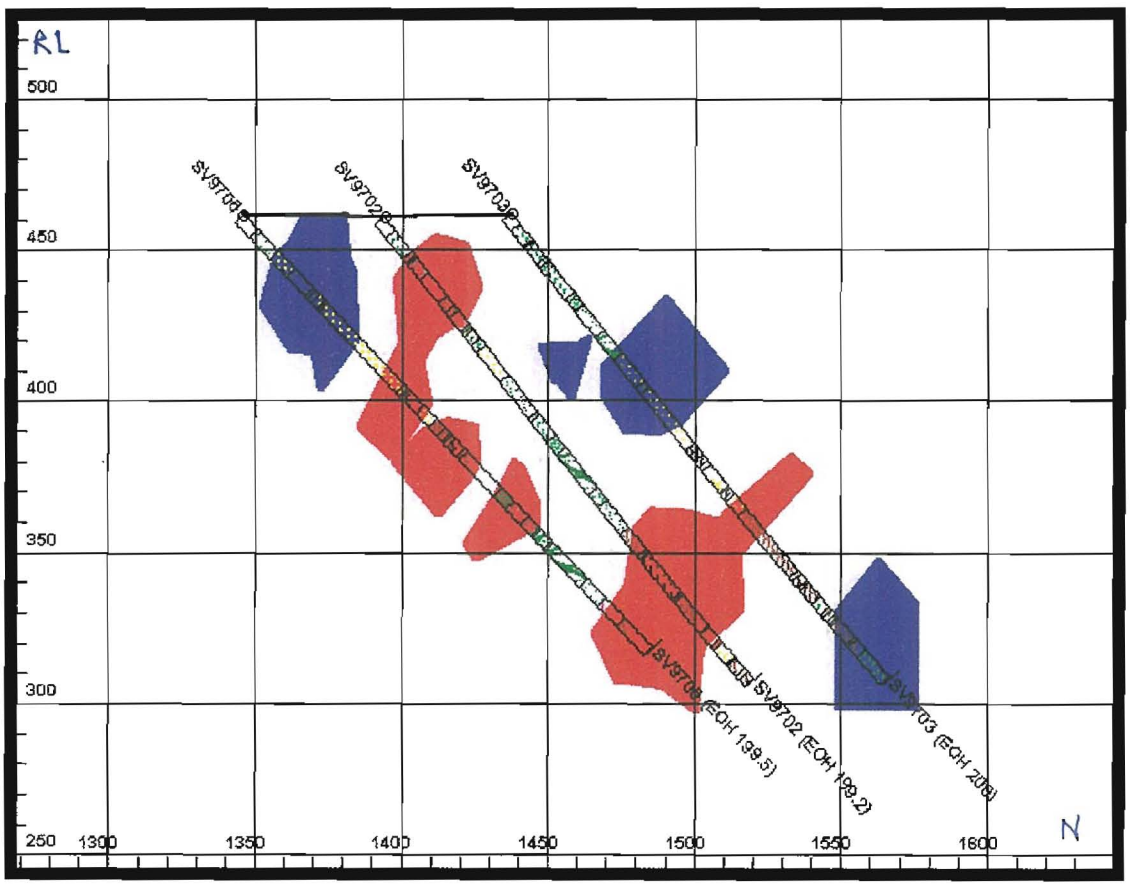

Figure 7.18 Anomaly map of strong (red domains) and weak (blue domains) coincident magnetic susceptibility, chargeability, and conductivity.

The downhole geophysical data has been log-tranformed[1] to statistically display the properties of the three different geophysical methods with respect to each other.

The log apparent resistivity (log α) is plotted on a log magnetic susceptibility (log k)-log induced polarisation (log IP) graph (figure 7.19). The weakest conductivity (red domain) is situated in low to moderate magnetic susceptibility zones with corresponding low chargeability. The strongest conductivity (blue domain) is located within the zone of high magnetic susceptibility and chargeability.

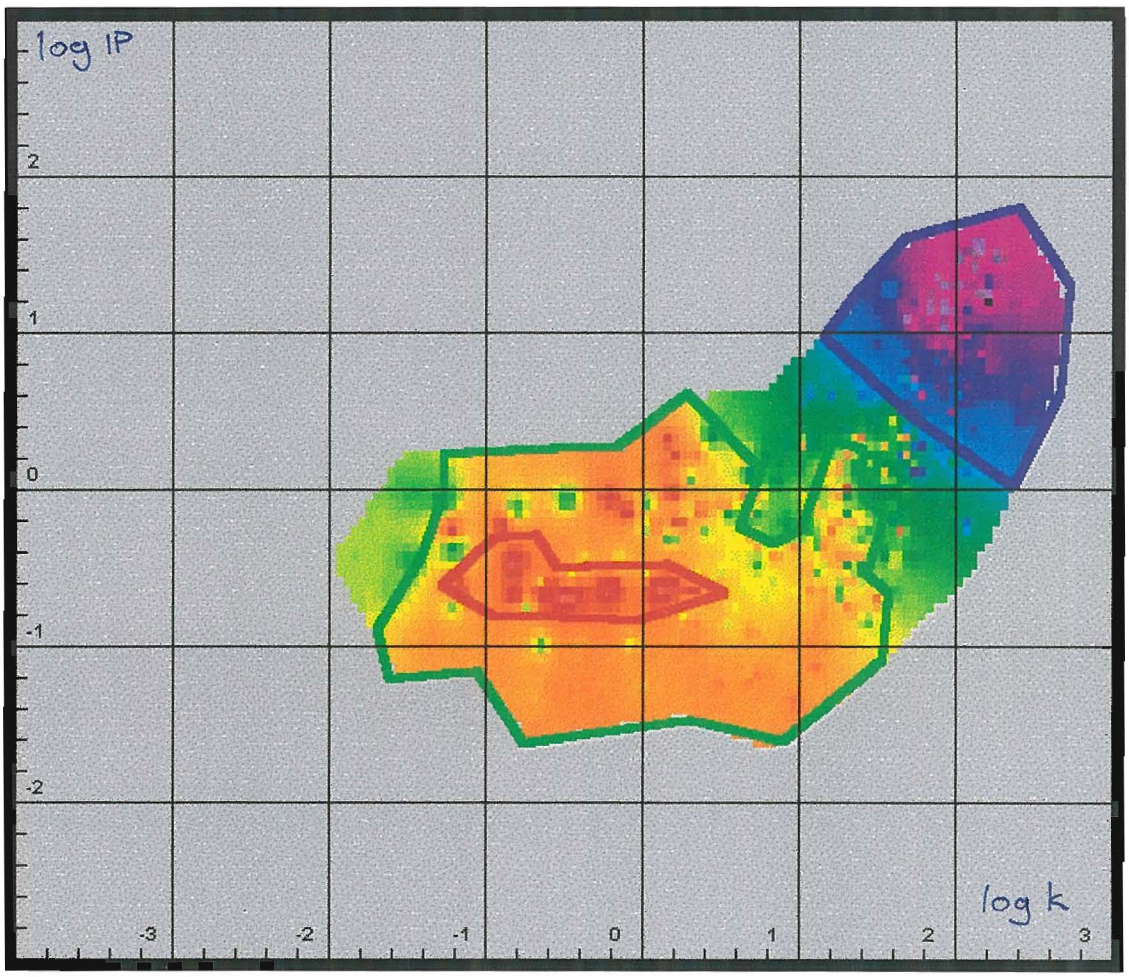

Figure 7.19 Apparent resistivity (log α) plotted on a log k-log IP graph. $\Sigma_x = 5{,}709$

[1] Log transformation to the base 10

The log-transformed induced polarisation data (log IP) is plotted on a log k-log α graph (figure 7.20). Zones of highest chargeability (red domain) correlates with zones of highest magnetic susceptibility and highest conductivity. The lowest chargeability (blue domain) is situated in the zones of lowest conductivity and low magnetic susceptibility. This plot shows clearly the inverse relation between chargeability and apparent resistivity.

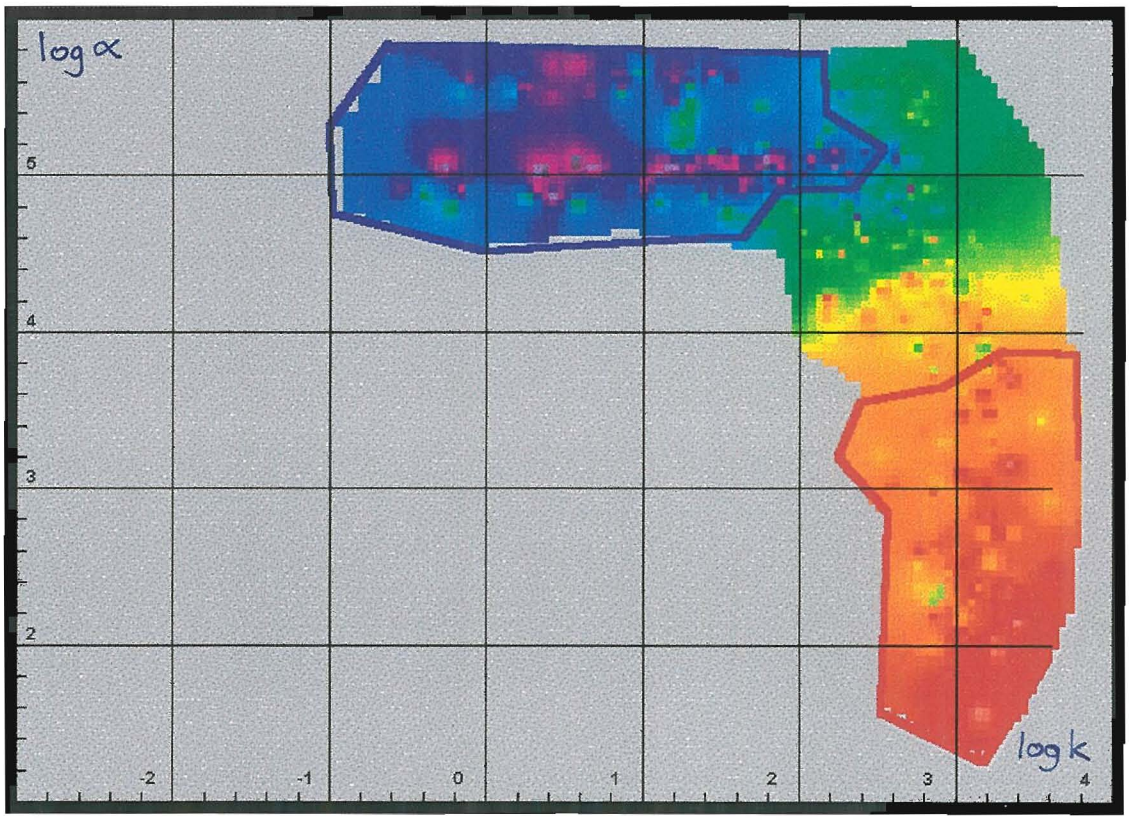

Figure 7.20 Induce Polarisation (log IP) plotted on a log k- log α graph. $\Sigma_x = 5{,}709$

The log-transformed magnetic susceptibility data (log k) is plotted on a log α-log IP graph (figure 7.21). The strongest magnetically susceptible zone (red domain) correlates with zones of highest conductivity and highest chargeability. Lowest magnetic susceptible values (blue domain) are apparent in the zone of high resistivity and low chargeability.

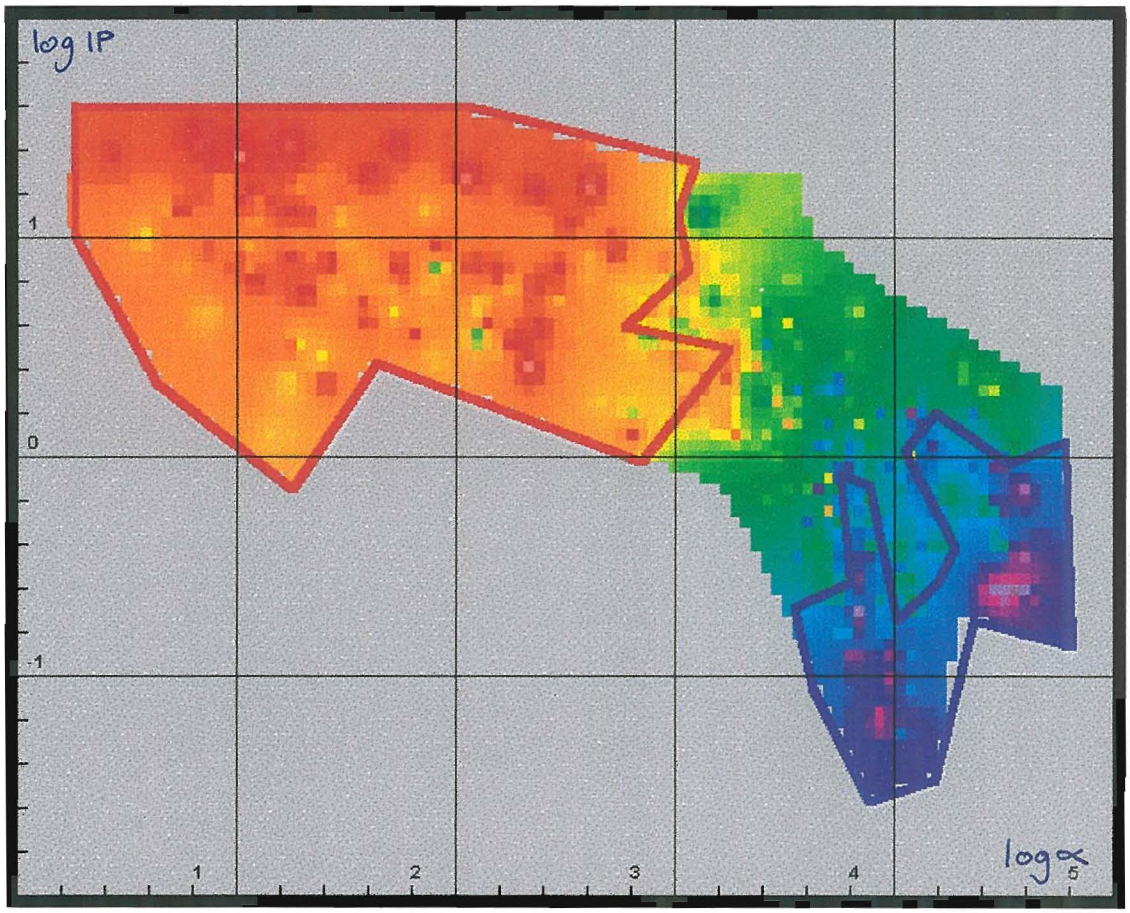

Figure 7.21 Magnetic Susceptibility (log k) plotted on a log α-log IP graph. $\Sigma_x = 5{,}709$

7.3 SUMMARY

Log-transformation and thresholding the ground magnetic data delineates discrete anomalies (referred to as 'first-order' anomalies) rather than a broad, continuous magnetic belt ('second-order' anomaly) as seen in the magnetic anomaly field image (figure 6.1).

The uniformity and continuity in the in-phase EM anomalies suggests a lithological or alteration control rather than structural. The EM ratio image delineates quite clearly a linear conductive unit. In a shear zone with less than 50% sulphides, the greater the EM ratio, the higher the conductive thickness.

The quadrature EM defines with better resolution the electromagnetic anomalies in the southwestern part of the project. This may be a result of a change of stratigraphy from east-west to north-south without the coil separation being adjusted accordingly.

From the downhole geophysical data, zones of coincident high chargeability, high conductivity and high magnetic susceptibility define two south-dipping units. The major constituent that displays these geophysical properties is pyrrhotite. The non-magnetic areas with high apparent resistivity and low chargeability delineate sulphide-poor siliceous rocks.

There are zones of high chargeability and high conductivity but with poor magnetic susceptibility. These zones represent graphite-only units. Areas of high magnetic susceptibility with no coincident chargeability or conductivity represent magnetite-only units.

8. GEOPHYSICAL MODELLING

8.1 GEOLOGICAL RELATIONSHIPS

Geological plans and sections were interpreted from the drillhole geological logs and correlated with the ground and downhole geophysics. The greatest concentration of drilling is located between the 1200mE and 2000mE. In Section 8.1.2, a detailed geological interpretation of Section 1700mE is overlain with the downhole geophysics.

Four stacked sections were created to best illustrate the ground geophysical profiles with respect to the drillhole geology and alteration. The four stacked sections have a window of ± 100m, capturing all the ground geophysical profiles and drillholes within a 5ha area. Details of the four stacked sections are described below:-

a) 1200mE – 1400mE (Section 1300mE ± 100m)
b) 1400mE – 1600mE (Section 1500mE ± 100m)
c) 1600mE – 1800mE (Section 1700mE ± 100m)
d) 1800mE – 2000mE (Section 1900mE ± 100m)

8.1.1 Ground Geophysics

The ground magnetic profiles are plotted against the drillhole geology (figure 8.1a-d). High magnetic responses overlie a combination of foliated volcanics, carbonaceous sediments and "Mineralised Zone". Low magnetic responses overlie thick sequences of weakly foliated volcanic and granitic rocks.

The profiles of the log-transformed magnetic data show discrete magnetic anomalies (figure 8.2a-d). The strong magnetic responses represent the foliated volcanics and pyrrhotite-bearing sediments. The log-transformed magnetic data displays only second-order anomalism for the "Mineralised Zone". From the log-transformed data, the weakly foliated volcanic and granitic rocks retain their low magnetic response.

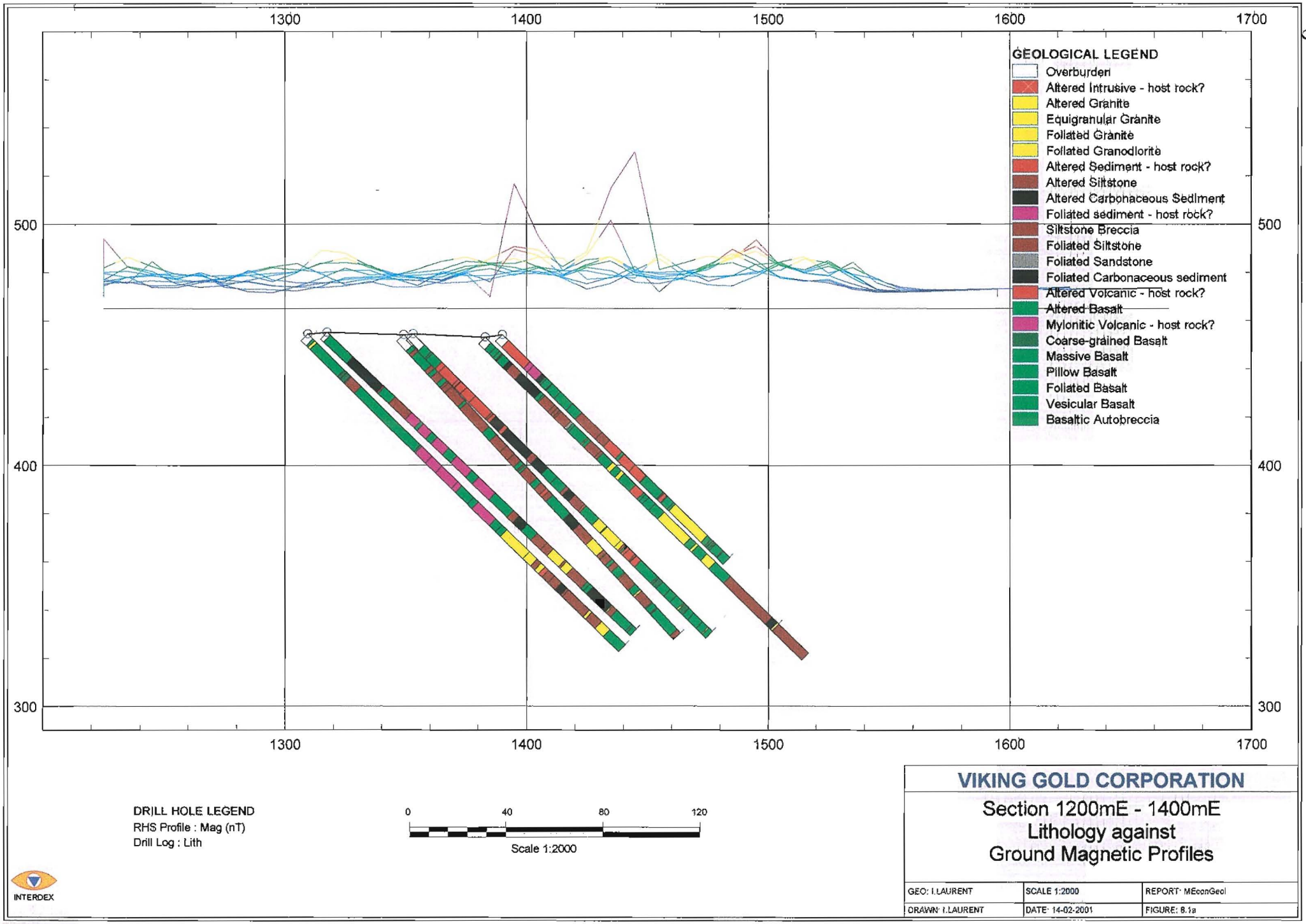
1300
1400
1500
1600
1700
500
400
300
GEOLOGICAL LEGEND
Overburden
Altered Intrusive - host rock?
Altered Granite
Equigranular Granite
Foliated Granite
Foliated Granodiorite
Altered Sediment - host rock?
Altered Siltstone
Altered Carbonaceous Sediment
Foliated sediment - host rock?
Siltstone Breccia
Foliated Siltstone
Foliated Sandstone
Foliated Carbonaceous sediment
Altered Volcanic - host rock?
Altered Basalt
Mylonitic Volcanic - host rock?
Coarse-grained Basalt
Massive Basalt
Pillow Basalt
Foliated Basalt
Vesicular Basalt
Basaltic Autobreccia
DRILL HOLE LEGEND
RHS Profile : Mag (nT)
Drill Log : Lith
0
40
80
120
Scale 1:2000
INTERDEX
VIKING GOLD CORPORATION
Section 1200mE - 1400mE
Lithology against
Ground Magnetic Profiles
GEO: I.LAURENT
SCALE 1:2000
REPORT: MEconGeol
DRAWN: I.LAURENT
DATE: 14-02-2001
FIGURE: 8.1a

Figure 8.1a

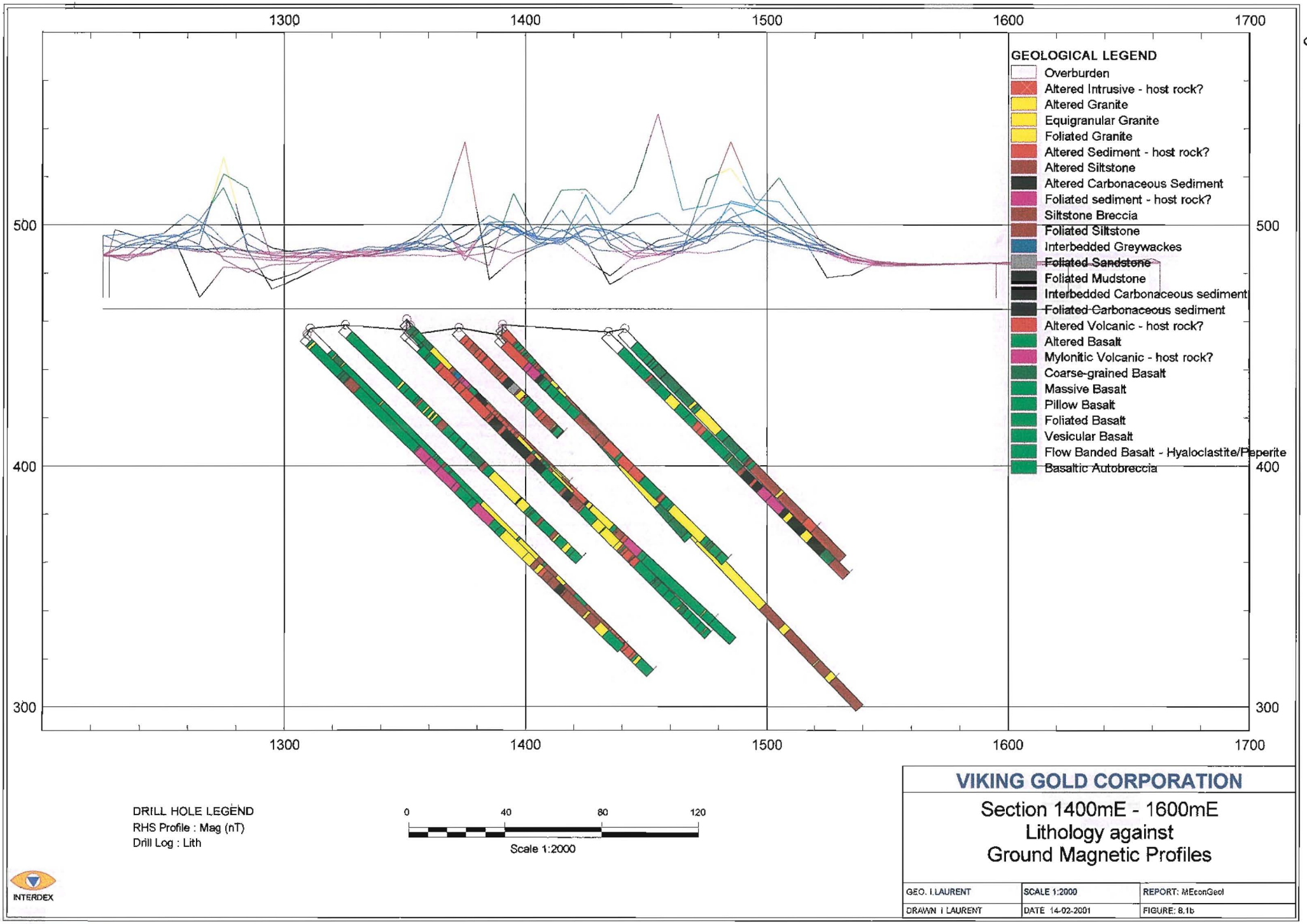
1300
1400
1500
1600
1700
500
400
300
GEOLOGICAL LEGEND
Overburden
Altered Intrusive - host rock?
Altered Granite
Equigranular Granite
Foliated Granite
Altered Sediment - host rock?
Altered Siltstone
Altered Carbonaceous Sediment
Foliated sediment - host rock?
Siltstone Breccia
Foliated Siltstone
Interbedded Greywackes
Foliated Sandstone
Foliated Mudstone
Interbedded Carbonaceous sediment
Foliated Carbonaceous sediment
Altered Volcanic - host rock?
Altered Basalt
Mylonitic Volcanic - host rock?
Coarse-grained Basalt
Massive Basalt
Pillow Basalt
Foliated Basalt
Vesicular Basalt
Flow Banded Basalt - Hyaloclastite/Peperite
Basaltic Autobreccia
DRILL HOLE LEGEND
RHS Profile : Mag (nT)
Drill Log : Lith
0
40
80
120
Scale 1:2000
INTERDEX
VIKING GOLD CORPORATION
Section 1400mE - 1600mE
Lithology against
Ground Magnetic Profiles
GEO. I.LAURENT
SCALE 1:2000
REPORT: MEconGeol
DRAWN I LAURENT
DATE 14-02-2001
FIGURE: 8.1b

Figure 8.1b

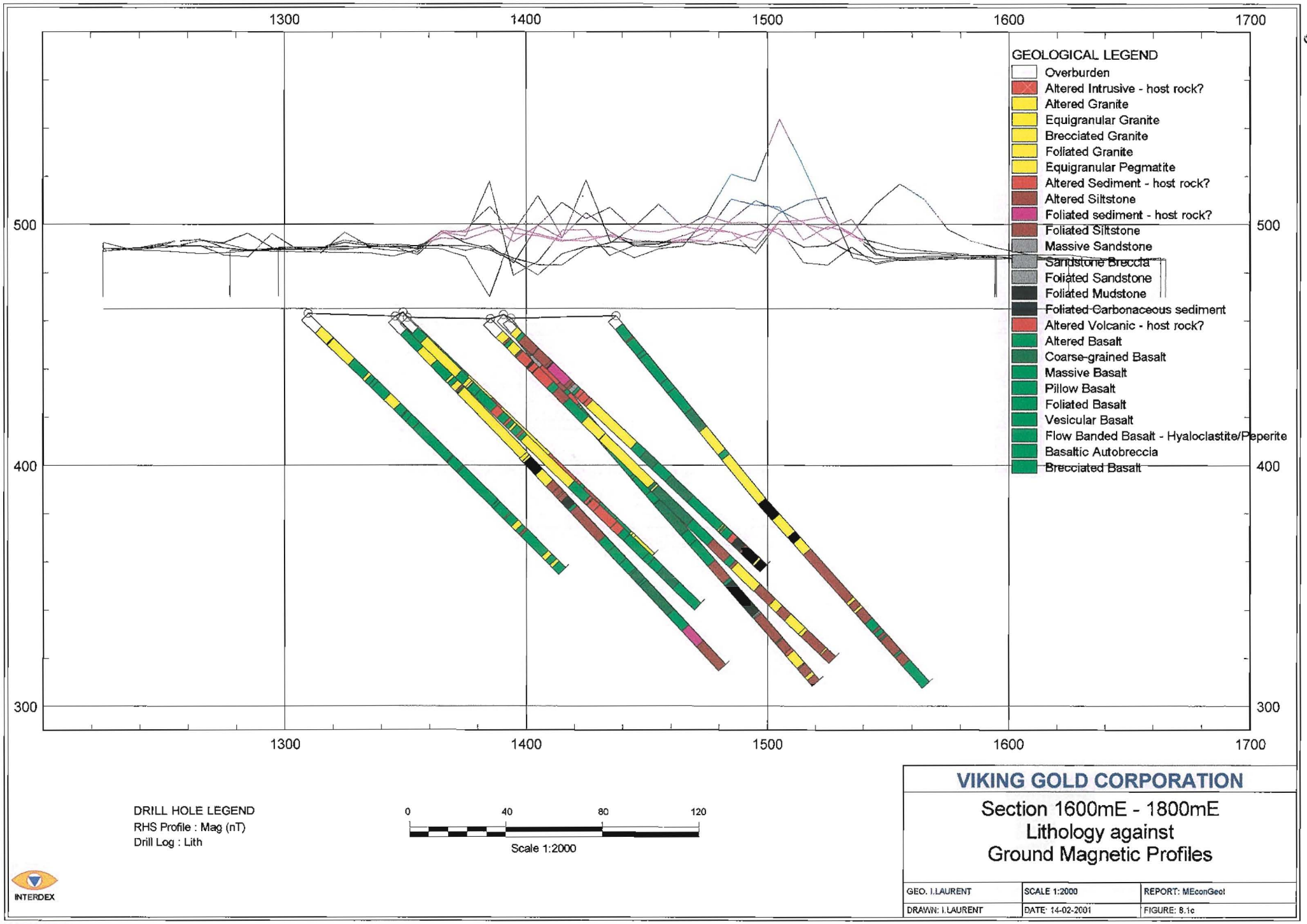
1300
1400
1500
1600
1700
500
400
300
GEOLOGICAL LEGEND
Overburden
Altered Intrusive - host rock?
Altered Granite
Equigranular Granite
Brecciated Granite
Foliated Granite
Equigranular Pegmatite
Altered Sediment - host rock?
Altered Siltstone
Foliated sediment - host rock?
Foliated Siltstone
Massive Sandstone
Sandstone Breccia
Foliated Sandstone
Foliated Mudstone
Foliated Carbonaceous sediment
Altered Volcanic - host rock?
Altered Basalt
Coarse-grained Basalt
Massive Basalt
Pillow Basalt
Foliated Basalt
Vesicular Basalt
Flow Banded Basalt - Hyaloclastite/Peperite
Basaltic Autobreccia
Brecciated Basalt
DRILL HOLE LEGEND
RHS Profile : Mag (nT)
Drill Log : Lith
0
40
80
120
Scale 1:2000
INTERDEX
VIKING GOLD CORPORATION
Section 1600mE - 1800mE
Lithology against
Ground Magnetic Profiles
GEO. I.LAURENT
SCALE 1:2000
REPORT: MEconGeol
DRAWN: I.LAURENT
DATE: 14-02-2001
FIGURE: 8.1c

Figure 8.1c

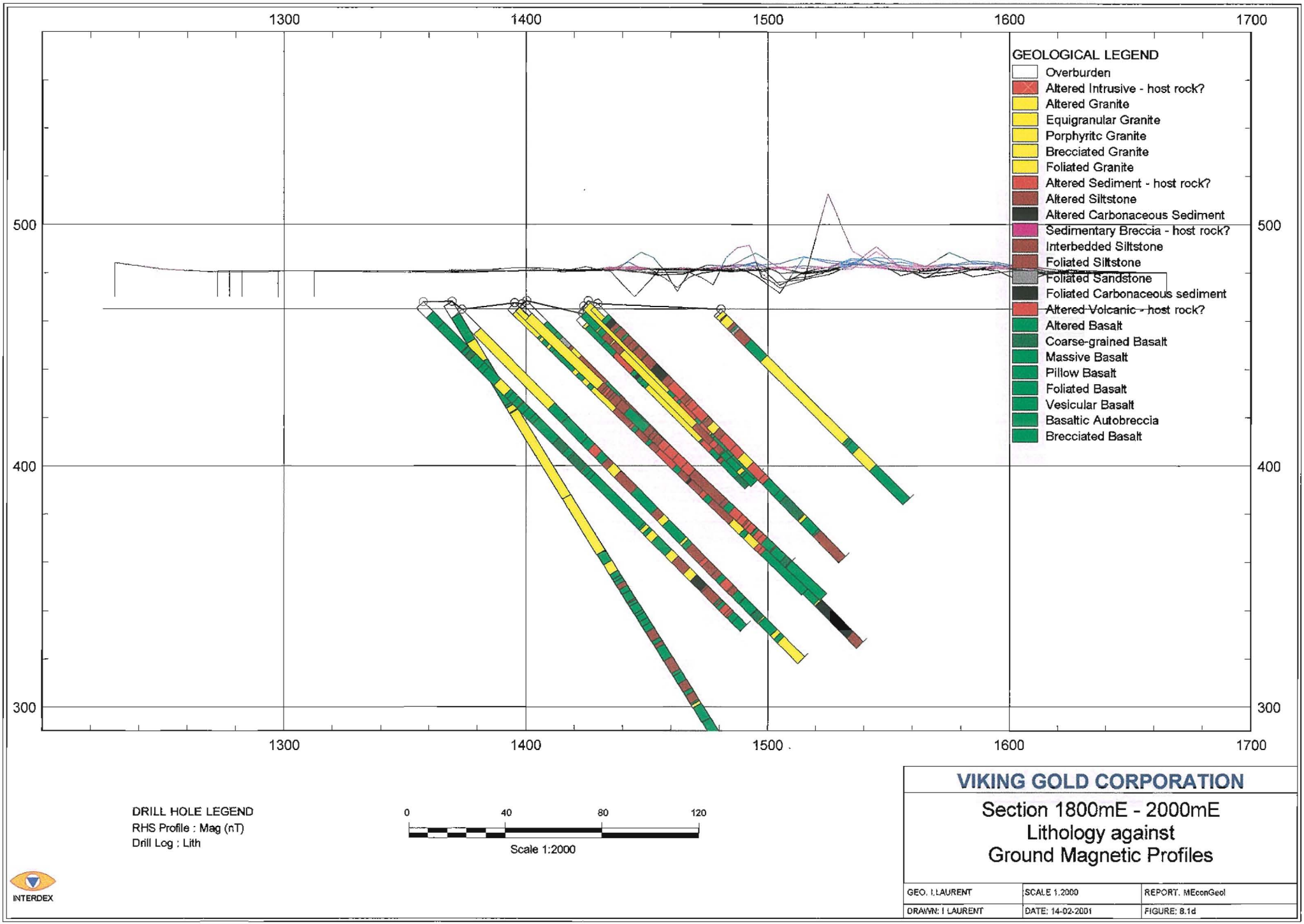
1300
1400
1500
1600
1700
500
400
300
GEOLOGICAL LEGEND
Overburden
Altered Intrusive - host rock?
Altered Granite
Equigranular Granite
Porphyritc Granite
Brecciated Granite
Foliated Granite
Altered Sediment - host rock?
Altered Siltstone
Altered Carbonaceous Sediment
Sedimentary Breccia - host rock?
Interbedded Siltstone
Foliated Siltstone
Foliated Sandstone
Foliated Carbonaceous sediment
Altered Volcanic - host rock?
Altered Basalt
Coarse-grained Basalt
Massive Basalt
Pillow Basalt
Foliated Basalt
Vesicular Basalt
Basaltic Autobreccia
Brecciated Basalt
DRILL HOLE LEGEND
RHS Profile : Mag (nT)
Drill Log : Lith
0
40
80
120
Scale 1:2000
INTERDEX
VIKING GOLD CORPORATION
Section 1800mE - 2000mE
Lithology against
Ground Magnetic Profiles
GEO. I.LAURENT
SCALE 1:2000
REPORT. MEconGeol
DRAWN: I LAURENT
DATE: 14-02-2001
FIGURE: 8.1d

Figure 8.1d

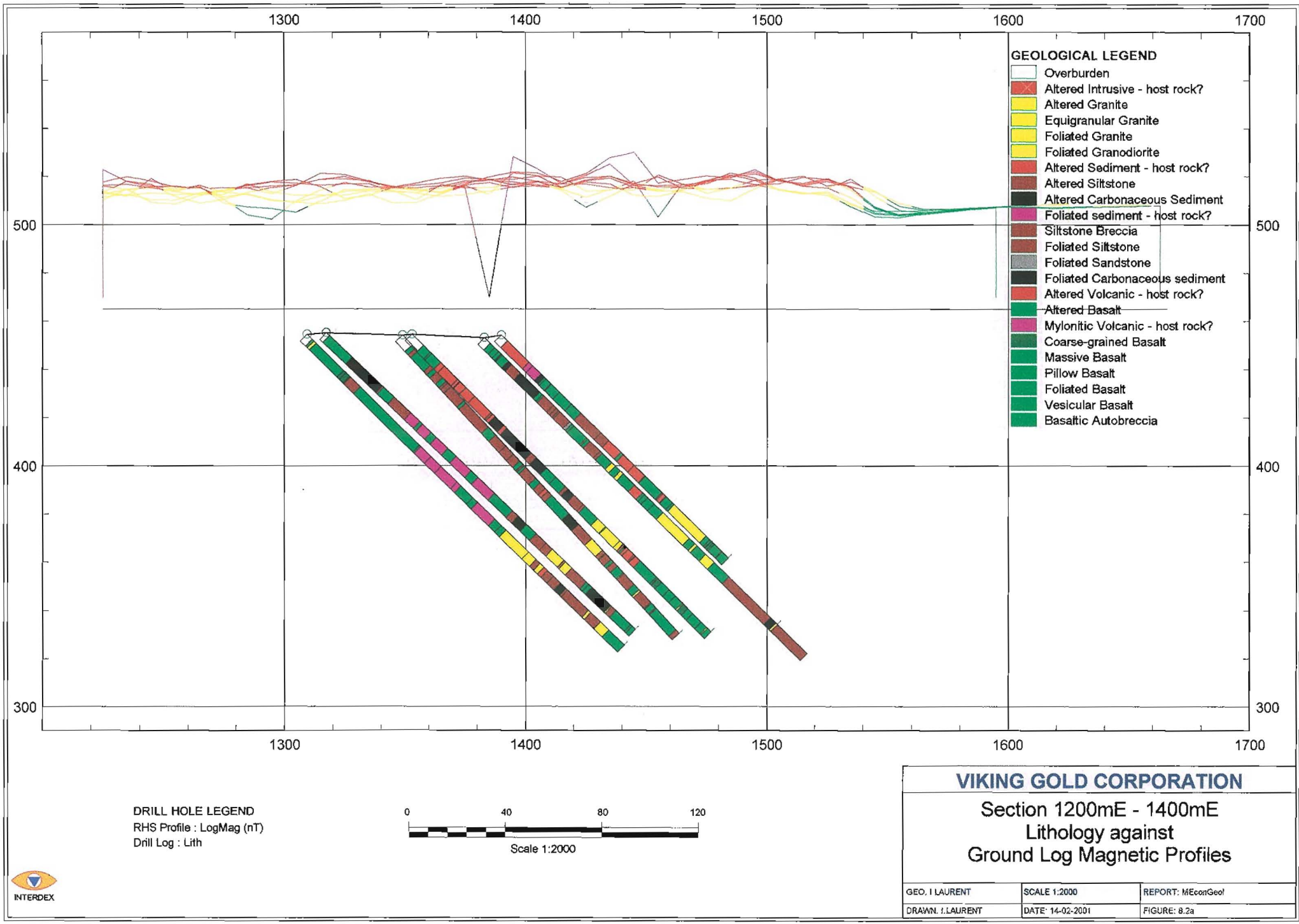
1300
1400
1500
1600
1700
500
400
300
GEOLOGICAL LEGEND
Overburden
Altered Intrusive - host rock?
Altered Granite
Equigranular Granite
Foliated Granite
Foliated Granodiorite
Altered Sediment - host rock?
Altered Siltstone
Altered Carbonaceous Sediment
Foliated sediment - host rock?
Siltstone Breccia
Foliated Siltstone
Foliated Sandstone
Foliated Carbonaceous sediment
Altered Volcanic - host rock?
Altered Basalt
Mylonitic Volcanic - host rock?
Coarse-grained Basalt
Massive Basalt
Pillow Basalt
Foliated Basalt
Vesicular Basalt
Basaltic Autobreccia
DRILL HOLE LEGEND
RHS Profile : LogMag (nT)
Drill Log : Lith
0
40
80
120
Scale 1:2000
INTERDEX
VIKING GOLD CORPORATION
Section 1200mE - 1400mE
Lithology against
Ground Log Magnetic Profiles
GEO. I LAURENT
SCALE 1:2000
REPORT: MEconGeol
DRAWN. I.LAURENT
DATE: 14-02-2001
FIGURE: 8.2a

Figure 8.2a

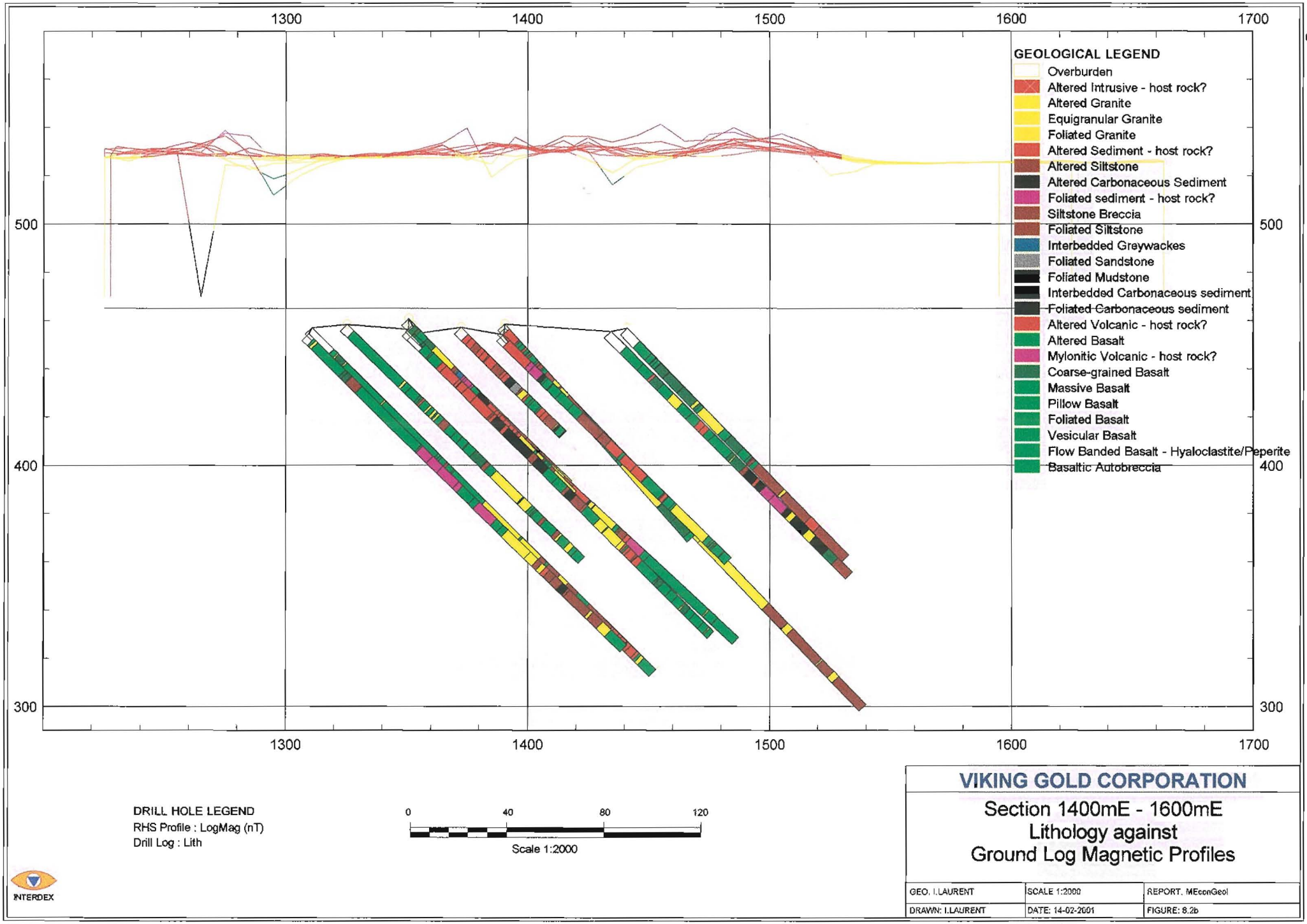
1300
1400
1500
1600
1700
500
400
300
GEOLOGICAL LEGEND
Overburden
Altered Intrusive - host rock?
Altered Granite
Equigranular Granite
Foliated Granite
Altered Sediment - host rock?
Altered Siltstone
Altered Carbonaceous Sediment
Foliated sediment - host rock?
Siltstone Breccia
Foliated Siltstone
Interbedded Greywackes
Foliated Sandstone
Foliated Mudstone
Interbedded Carbonaceous sediment
Foliated Carbonaceous sediment
Altered Volcanic - host rock?
Altered Basalt
Mylonitic Volcanic - host rock?
Coarse-grained Basalt
Massive Basalt
Pillow Basalt
Foliated Basalt
Vesicular Basalt
Flow Banded Basalt - Hyaloclastite/Peperite
Basaltic Autobreccia
DRILL HOLE LEGEND
RHS Profile : LogMag (nT)
Drill Log : Lith
0
40
80
120
Scale 1:2000
INTERDEX
VIKING GOLD CORPORATION
Section 1400mE - 1600mE
Lithology against
Ground Log Magnetic Profiles
GEO. I.LAURENT
SCALE 1:2000
REPORT. MEconGeol
DRAWN: I.LAURENT
DATE: 14-02-2001
FIGURE: 8.2b

Figure 8.2b

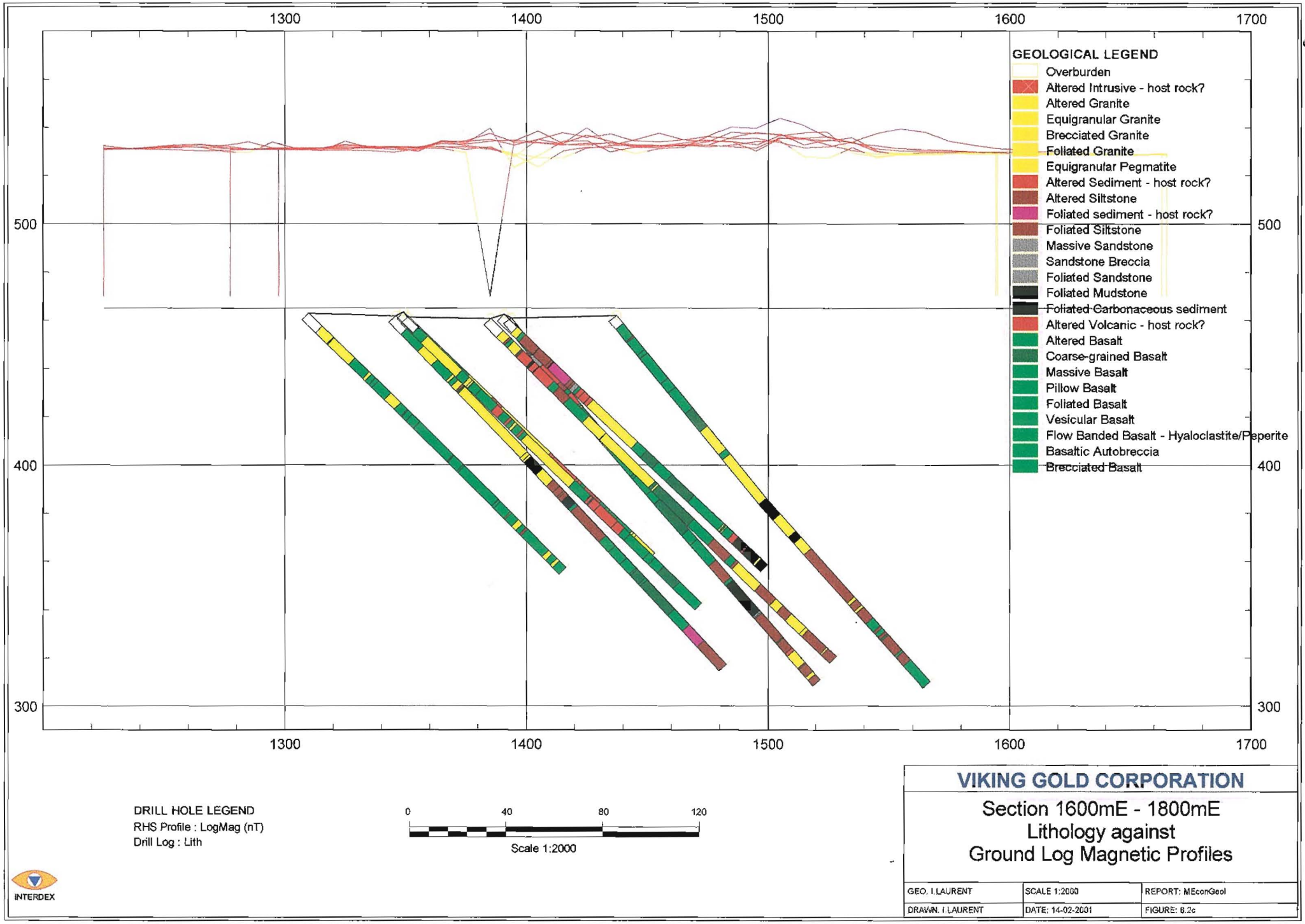
1300
1400
1500
1600
1700
500
400
300
GEOLOGICAL LEGEND
Overburden
Altered Intrusive - host rock?
Altered Granite
Equigranular Granite
Brecciated Granite
Foliated Granite
Equigranular Pegmatite
Altered Sediment - host rock?
Altered Siltstone
Foliated sediment - host rock?
Foliated Siltstone
Massive Sandstone
Sandstone Breccia
Foliated Sandstone
Foliated Mudstone
Foliated Carbonaceous sediment
Altered Volcanic - host rock?
Altered Basalt
Coarse-grained Basalt
Massive Basalt
Pillow Basalt
Foliated Basalt
Vesicular Basalt
Flow Banded Basalt - Hyaloclastite/Peperite
Basaltic Autobreccia
Brecciated Basalt
DRILL HOLE LEGEND
RHS Profile : LogMag (nT)
Drill Log : Lith
0
40
80
120
Scale 1:2000
INTERDEX
VIKING GOLD CORPORATION
Section 1600mE - 1800mE
Lithology against
Ground Log Magnetic Profiles
GEO. I.LAURENT
SCALE 1:2000
REPORT: MEconGeol
DRAWN. I.LAURENT
DATE: 14-02-2001
FIGURE: 8.2c

Figure 8.2c

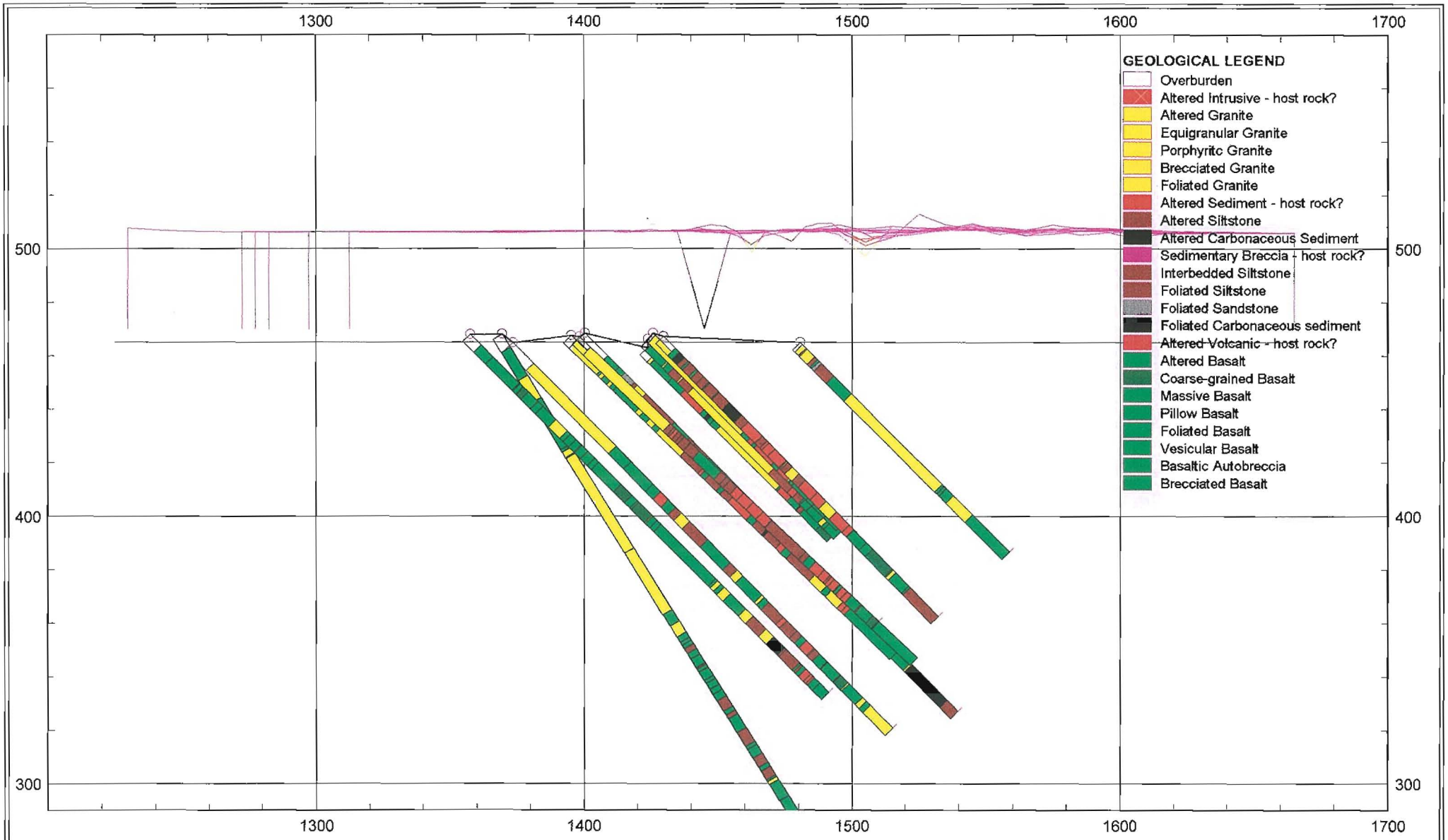

DRILL HOLE LEGEND
RHS Profile : LogMag (nT)
Drill Log : Lith

0 40 80 120
Scale 1:2000

INTERDEX

VIKING GOLD CORPORATION

Section 1800mE - 2000mE
Lithology against
Ground Log Magnetic Profiles

GEO I.LAURENT	SCALE 1:2000	REPORT: MEconGeol
DRAWN: I.LAURENT	DATE: 14-02-2001	FIGURE: 8.2d

Figure 8.2d

The interpreted geology is overlain with the magnetic anomaly map, which was defined in Section 7 (figure 8.3). The magnetic anomalies represent the combination of magnetite-bearing volcanics and the pyrrhotite-bearing sediments on the northern (footwall) contact of the shear zone

The in-phase EM profiles are plotted against the drillhole geology (figure 8.4a-d). There are two 800m long in-phase EM conductive anomalies between the 1200mE and 2000mE. The southern anomaly overlies the "Mineralised Zone" and altered wallrock. The northern anomaly overlies the pyrrhotite-bearing sediments.

The log-transformed, in-phase electromagnetic data reveals a difference between the two anomalies (figure 8.5a-d). The northern anomaly is a first-order EM anomaly suggesting very high conductivity through the pyrrhotite-bearing sediments. The southern anomaly, after log-transformation, is a second-order EM anomaly. The "Mineralised Zone" and altered wallrock display moderate conductivity due to insufficient graphite, lack of interlocking pyrrhotite and high degree of silicification. Following log-transformation of the data, the southern anomaly from the 1200mE to 1500mE retains its first-order in-phase EM anomalism. The "Mineralised Zone" is near surface and in contact with the water table, the sulphides within the "Mineralised Zone" are slowly broken down into solution adding salts to the water table.

The interpreted geological plan is overlain onto the in-phase EM anomaly map, which was delineated in Section 7 (figure 8.6). The in-phase EM anomalies correlate almost exclusively with the pyrrhotite-bearing sediments in both length and width. The "Mineralised Zone" does not correlate with the first-order in-phase EM anomalies, except to the west (between 1200mE and 1550mE) where the "Mineralised Zone" trends along the rim of the in-phase EM anomaly. The volcanic and granitic rocks are strongly resistive.

The quadrature EM profiles are plotted against the drillhole geology (figure 8.7a-d). The quadrature anomalies are weaker and broader. The quadrature EM anomalism covers the entire shear zone (between 1350mN and 1550mN), ranging from zones of moderate to high conductivity across all lithologies.

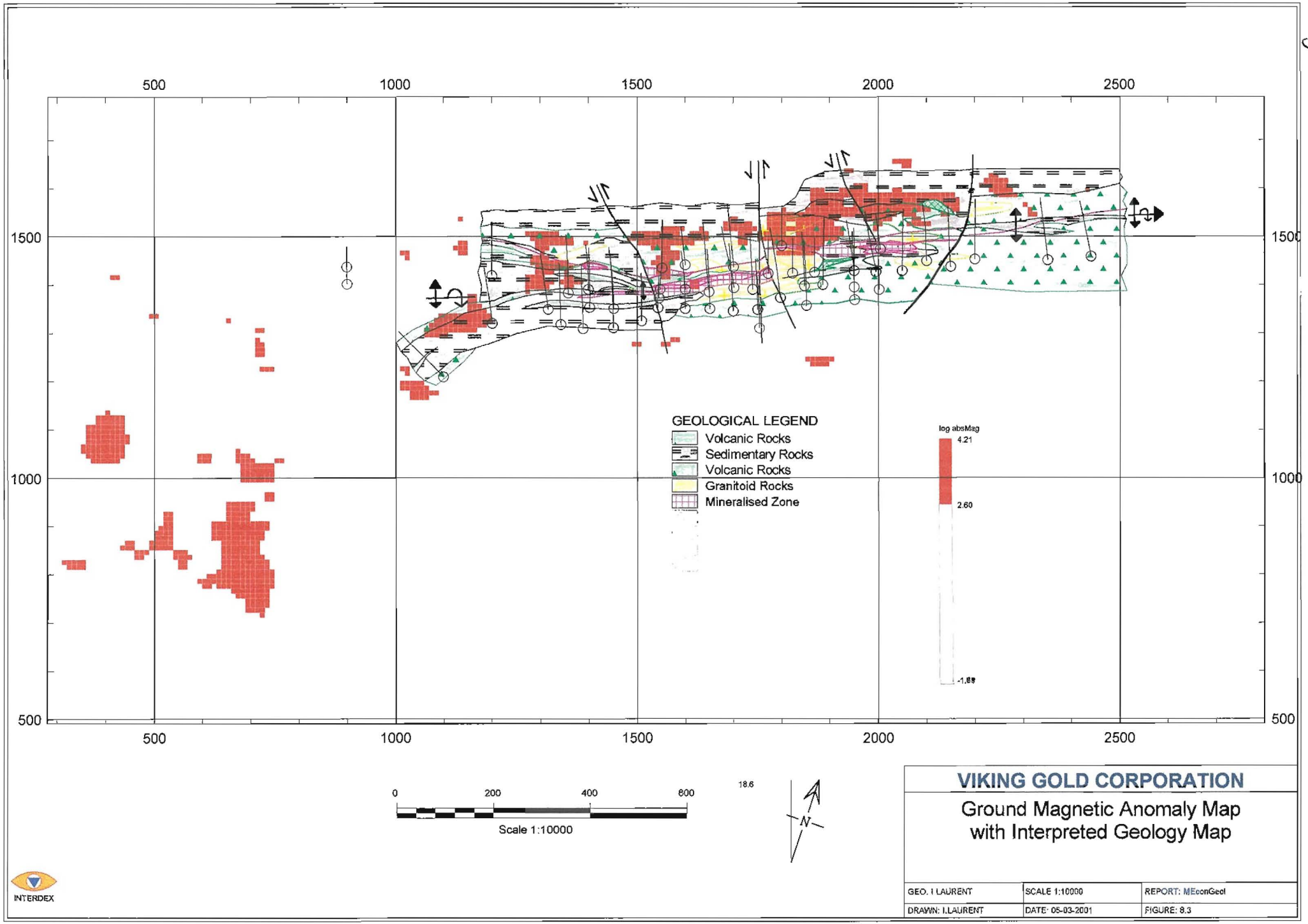
500
1000
1500
2000
2500
GEOLOGICAL LEGEND
Volcanic Rocks
Sedimentary Rocks
Volcanic Rocks
Granitoid Rocks
Mineralised Zone
log absMag
4.21
2.60
-1.88
0
200
400
800
Scale 1:10000
18.6
N
INTERDEX
VIKING GOLD CORPORATION
Ground Magnetic Anomaly Map
with Interpreted Geology Map
GEO. I LAURENT
SCALE 1:10000
REPORT: MEconGeol
DRAWN: I.LAURENT
DATE: 05-03-2001
FIGURE: 8.3

Figure 8.3

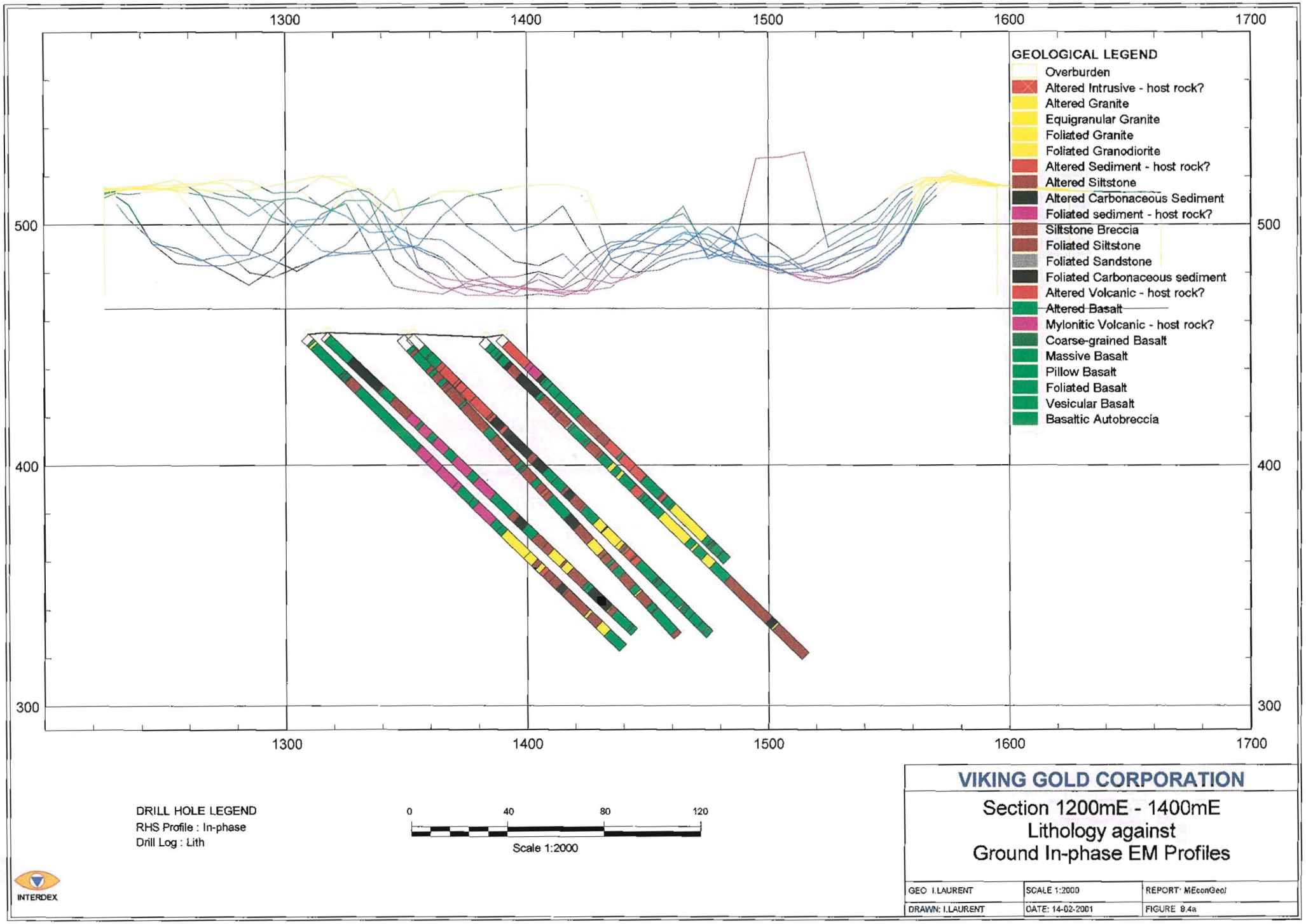
1300
1400
1500
1600
1700
500
400
300
GEOLOGICAL LEGEND
Overburden
Altered Intrusive - host rock?
Altered Granite
Equigranular Granite
Foliated Granite
Foliated Granodiorite
Altered Sediment - host rock?
Altered Siltstone
Altered Carbonaceous Sediment
Foliated sediment - host rock?
Siltstone Breccia
Foliated Siltstone
Foliated Sandstone
Foliated Carbonaceous sediment
Altered Volcanic - host rock?
Altered Basalt
Mylonitic Volcanic - host rock?
Coarse-grained Basalt
Massive Basalt
Pillow Basalt
Foliated Basalt
Vesicular Basalt
Basaltic Autobreccia
DRILL HOLE LEGEND
RHS Profile : In-phase
Drill Log : Lith
0
40
80
120
Scale 1:2000
INTERDEX
VIKING GOLD CORPORATION
Section 1200mE - 1400mE
Lithology against
Ground In-phase EM Profiles
GEO I.LAURENT
SCALE 1:2000
REPORT: MEconGeol
DRAWN: I.LAURENT
DATE: 14-02-2001
FIGURE 8.4a

Figure 8.4a

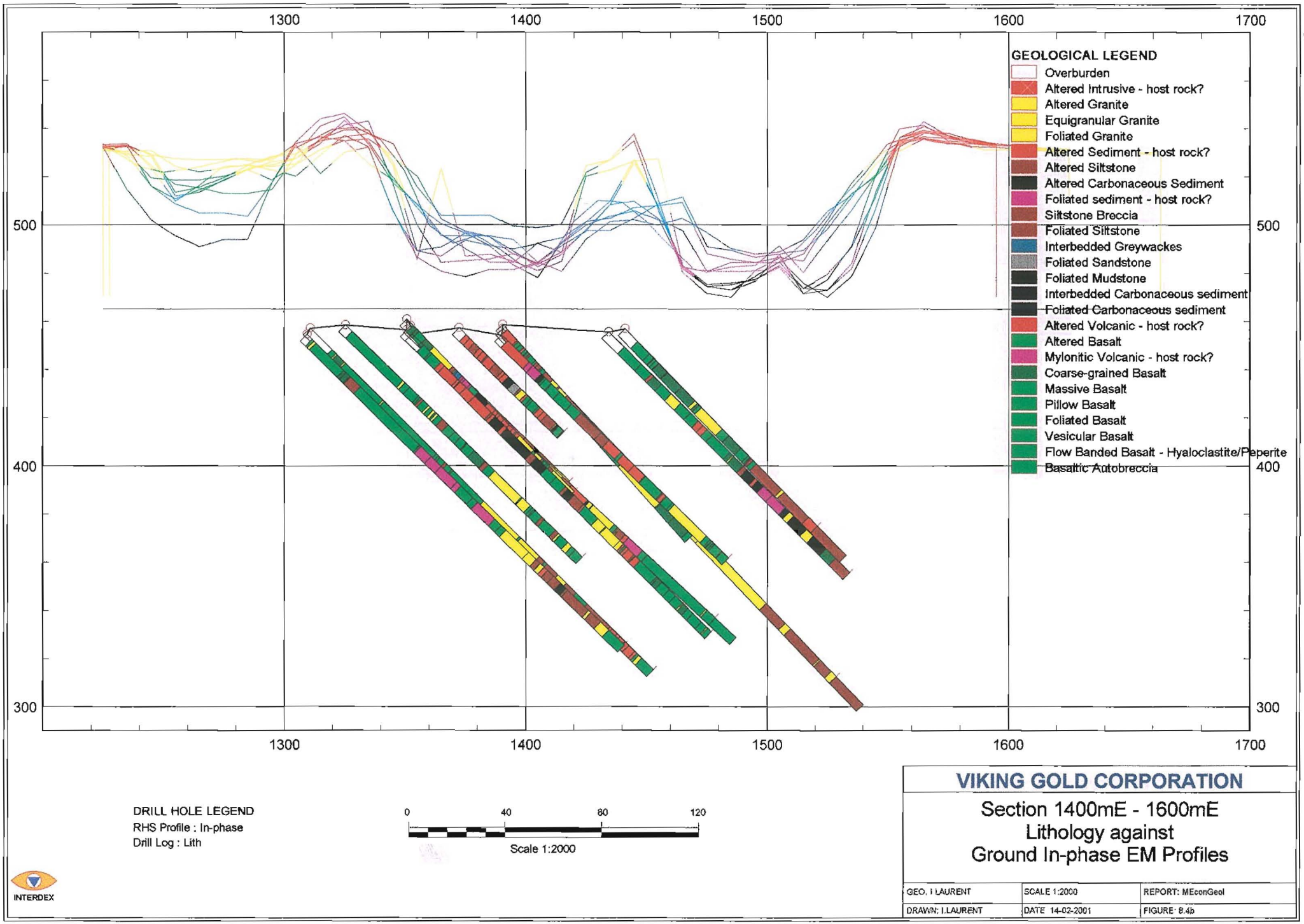
1300
1400
1500
1600
1700
500
400
300
GEOLOGICAL LEGEND
Overburden
Altered Intrusive - host rock?
Altered Granite
Equigranular Granite
Foliated Granite
Altered Sediment - host rock?
Altered Siltstone
Altered Carbonaceous Sediment
Foliated sediment - host rock?
Siltstone Breccia
Foliated Siltstone
Interbedded Greywackes
Foliated Sandstone
Foliated Mudstone
Interbedded Carbonaceous sediment
Foliated Carbonaceous sediment
Altered Volcanic - host rock?
Altered Basalt
Mylonitic Volcanic - host rock?
Coarse-grained Basalt
Massive Basalt
Pillow Basalt
Foliated Basalt
Vesicular Basalt
Flow Banded Basalt - Hyaloclastite/Peperite
Basaltic Autobreccia
DRILL HOLE LEGEND
RHS Profile : In-phase
Drill Log : Lith
0
40
80
120
Scale 1:2000
INTERDEX
VIKING GOLD CORPORATION
Section 1400mE - 1600mE
Lithology against
Ground In-phase EM Profiles
GEO. I LAURENT
SCALE 1:2000
REPORT: MEconGeol
DRAWN: I.LAURENT
DATE 14-02-2001
FIGURE 8.4b

Figure 8.4b

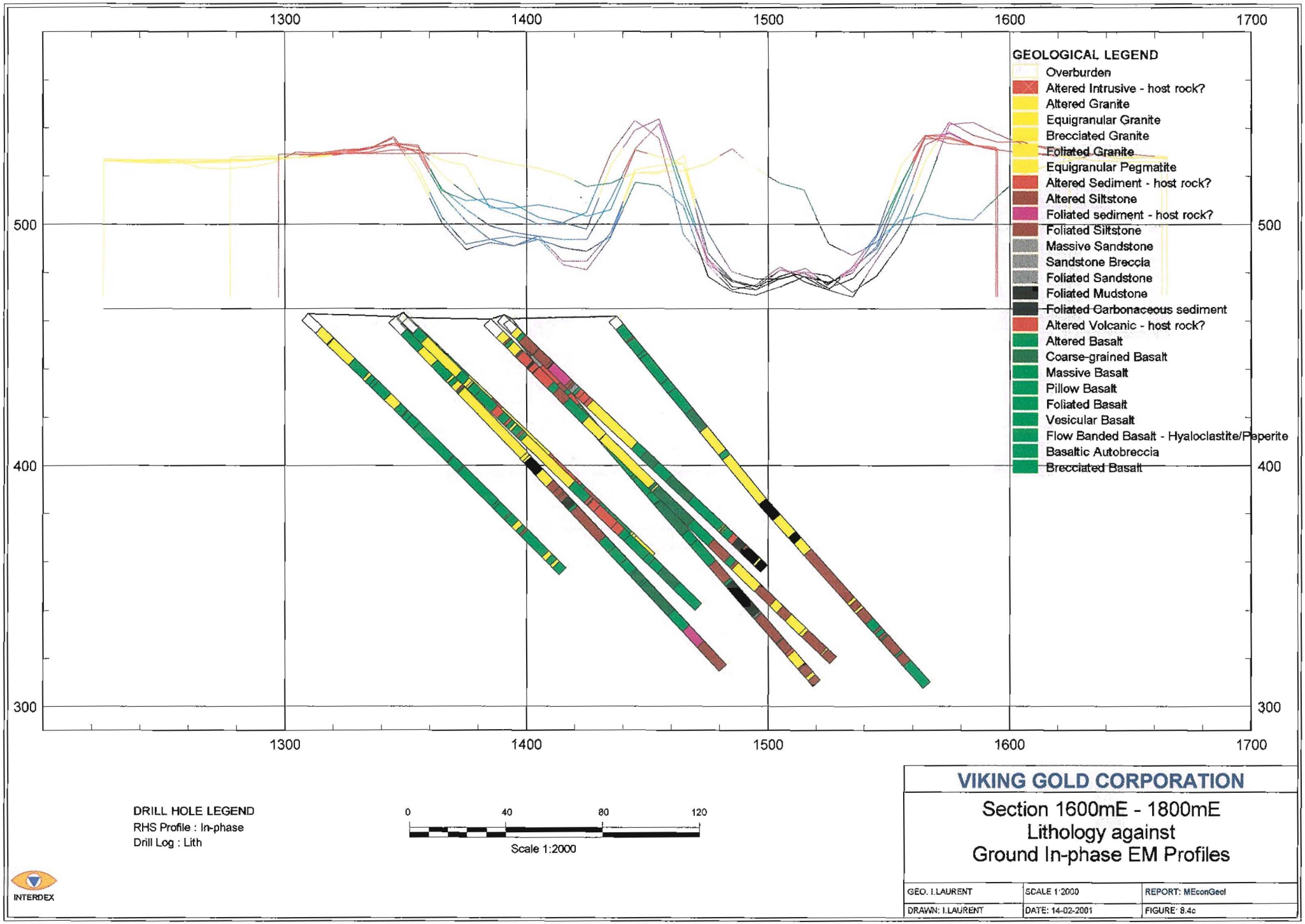
1300
1400
1500
1600
1700
500
400
300
GEOLOGICAL LEGEND
Overburden
Altered Intrusive - host rock?
Altered Granite
Equigranular Granite
Brecciated Granite
Foliated Granite
Equigranular Pegmatite
Altered Sediment - host rock?
Altered Siltstone
Foliated sediment - host rock?
Foliated Siltstone
Massive Sandstone
Sandstone Breccia
Foliated Sandstone
Foliated Mudstone
Foliated Carbonaceous sediment
Altered Volcanic - host rock?
Altered Basalt
Coarse-grained Basalt
Massive Basalt
Pillow Basalt
Foliated Basalt
Vesicular Basalt
Flow Banded Basalt - Hyaloclastite/Peperite
Basaltic Autobreccia
Brecciated Basalt
DRILL HOLE LEGEND
RHS Profile : In-phase
Drill Log : Lith
0
40
80
120
Scale 1:2000
INTERDEX
VIKING GOLD CORPORATION
Section 1600mE - 1800mE
Lithology against
Ground In-phase EM Profiles
GEO. I.LAURENT
SCALE 1:2000
REPORT: MEconGeol
DRAWN: I.LAURENT
DATE: 14-02-2001
FIGURE: 8.4c

Figure 8.4c

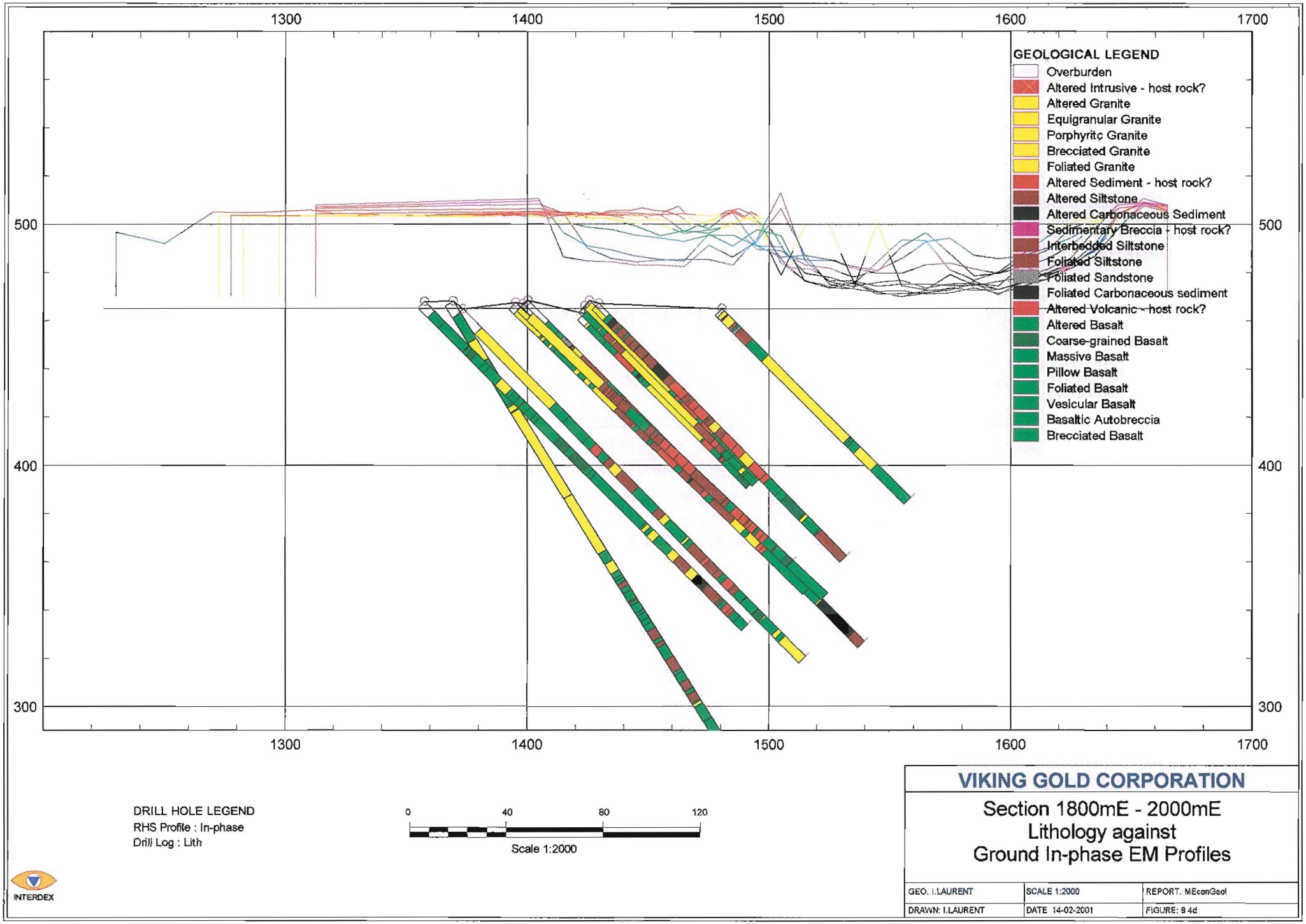
1300
1400
1500
1600
1700
500
400
300
GEOLOGICAL LEGEND
Overburden
Altered Intrusive - host rock?
Altered Granite
Equigranular Granite
Porphyritc Granite
Brecciated Granite
Foliated Granite
Altered Sediment - host rock?
Altered Siltstone
Altered Carbonaceous Sediment
Sedimentary Breccia - host rock?
Interbedded Siltstone
Foliated Siltstone
Foliated Sandstone
Foliated Carbonaceous sediment
Altered Volcanic - host rock?
Altered Basalt
Coarse-grained Basalt
Massive Basalt
Pillow Basalt
Foliated Basalt
Vesicular Basalt
Basaltic Autobreccia
Brecciated Basalt
DRILL HOLE LEGEND
RHS Profile : In-phase
Drill Log : Lith
0
40
80
120
Scale 1:2000
INTERDEX
VIKING GOLD CORPORATION
Section 1800mE - 2000mE
Lithology against
Ground In-phase EM Profiles
GEO. I.LAURENT
SCALE 1:2000
REPORT. MEconGeol
DRAWN: I.LAURENT
DATE 14-02-2001
FIGURE: 8.4d

Figure 8.4d

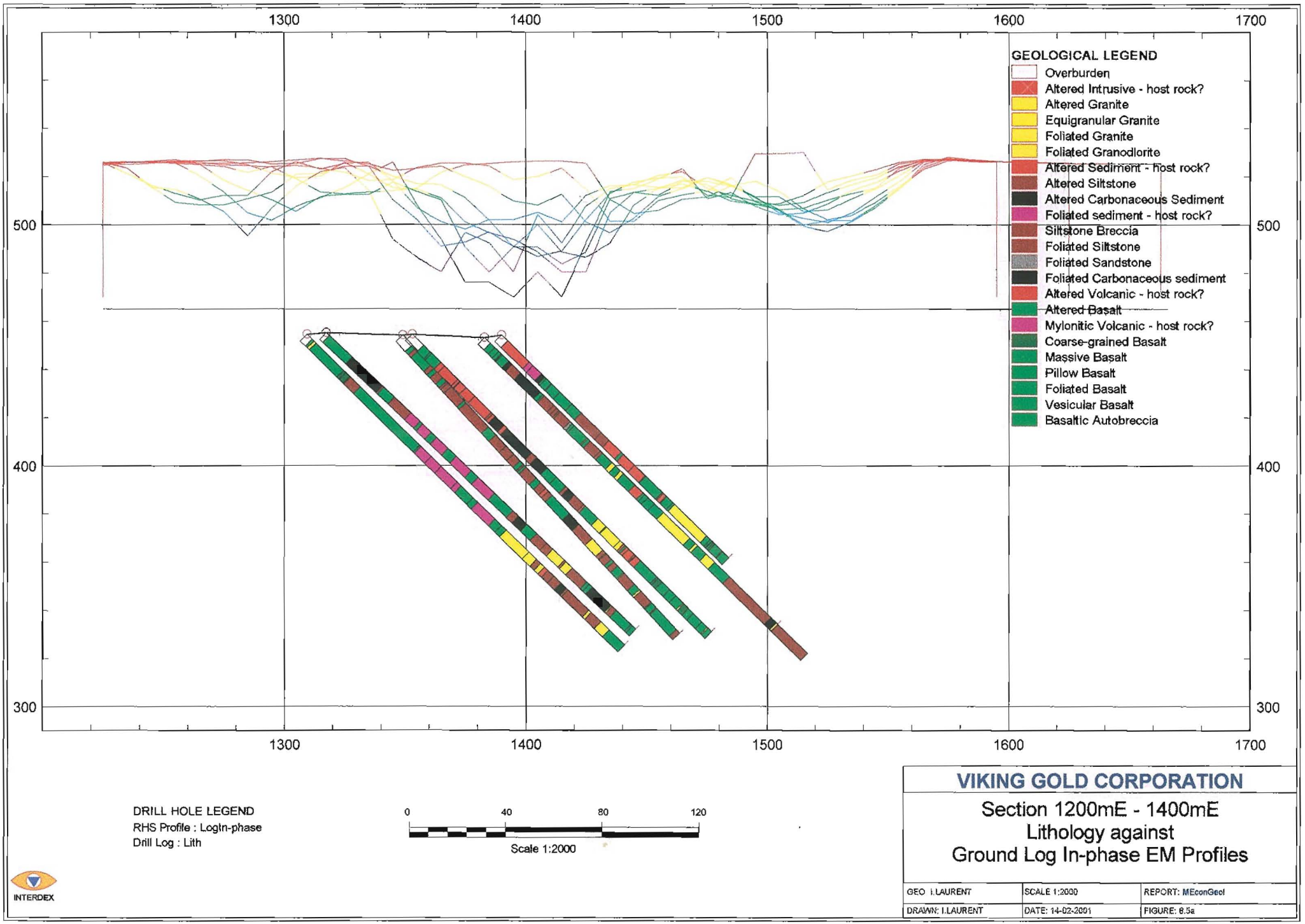
1300
1400
1500
1600
1700
500
400
300
GEOLOGICAL LEGEND
Overburden
Altered Intrusive - host rock?
Altered Granite
Equigranular Granite
Foliated Granite
Foliated Granodiorite
Altered Sediment - host rock?
Altered Siltstone
Altered Carbonaceous Sediment
Foliated sediment - host rock?
Siltstone Breccia
Foliated Siltstone
Foliated Sandstone
Foliated Carbonaceous sediment
Altered Volcanic - host rock?
Altered Basalt
Mylonitic Volcanic - host rock?
Coarse-grained Basalt
Massive Basalt
Pillow Basalt
Foliated Basalt
Vesicular Basalt
Basaltic Autobreccia
DRILL HOLE LEGEND
RHS Profile : LogIn-phase
Drill Log : Lith
0
40
80
120
Scale 1:2000
INTERDEX
VIKING GOLD CORPORATION
Section 1200mE - 1400mE
Lithology against
Ground Log In-phase EM Profiles
GEO I.LAURENT
SCALE 1:2000
REPORT: MEconGeol
DRAWN: I.LAURENT
DATE: 14-02-2001
FIGURE: 8.5a

Figure 8.5a

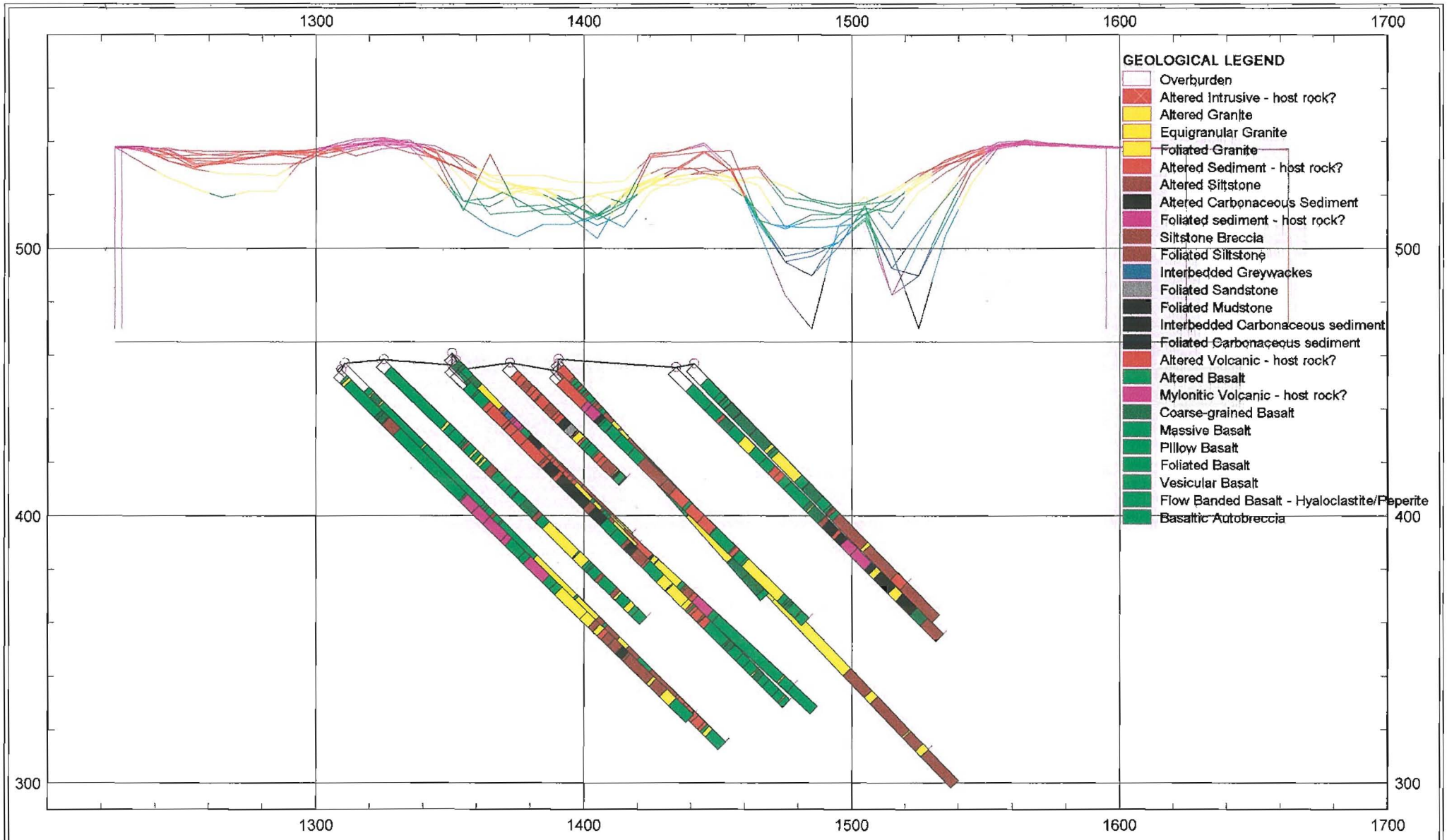

DRILL HOLE LEGEND
RHS Profile : LogIn-phase
Drill Log : Lith

0 40 80 120
Scale 1:2000

INTERDEX

VIKING GOLD CORPORATION

Section 1400mE - 1600mE
Lithology against
Ground Log In-phase EM Profiles

GEO. I.LAURENT	SCALE 1:2000	REPORT: MEconGeol
DRAWN: I.LAURENT	DATE: 14-02-2001	FIGURE: 8.5b

Figure 8.5b

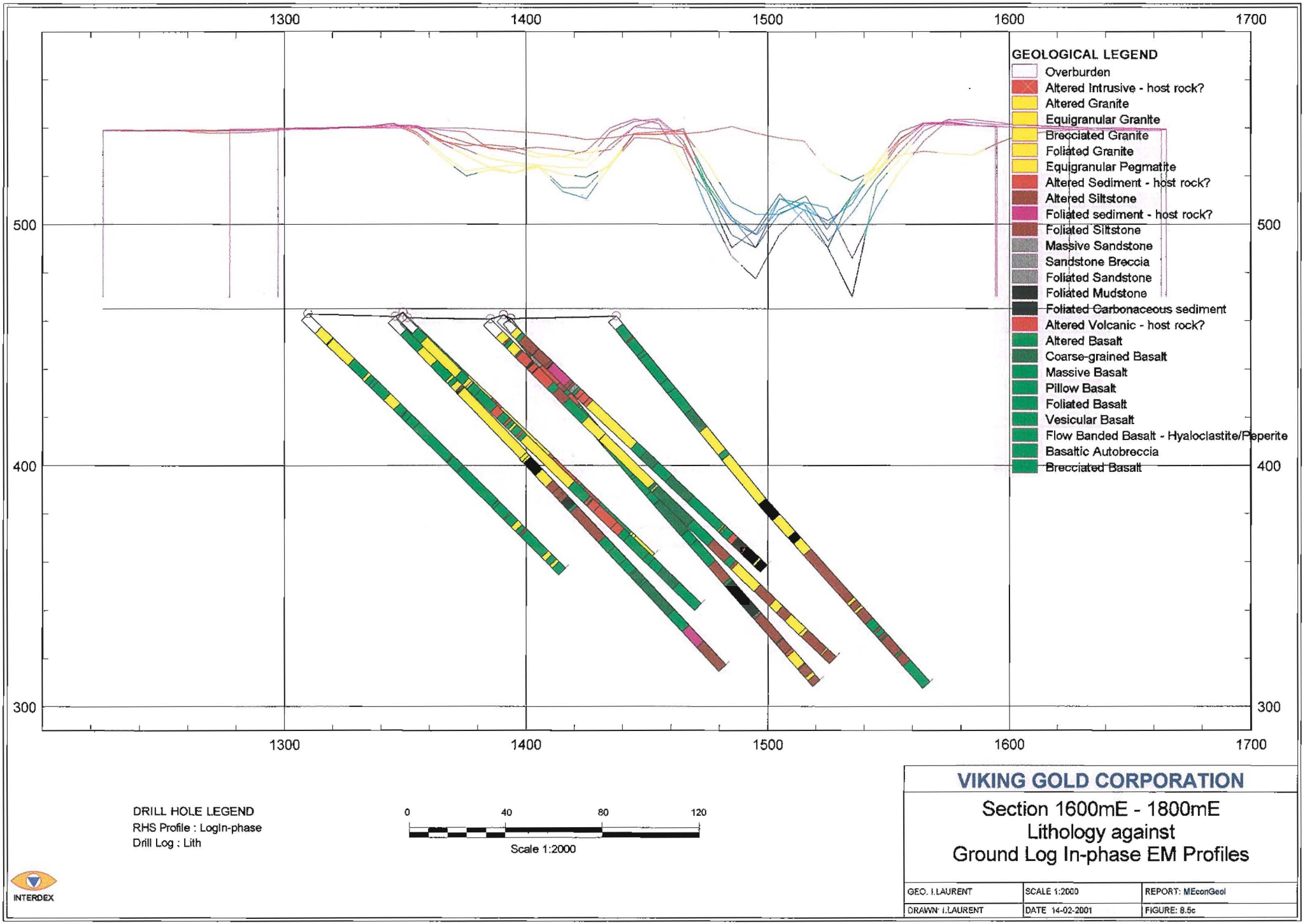
1300
1400
1500
1600
1700
500
400
300
GEOLOGICAL LEGEND
Overburden
Altered Intrusive - host rock?
Altered Granite
Equigranular Granite
Brecciated Granite
Foliated Granite
Equigranular Pegmatite
Altered Sediment - host rock?
Altered Siltstone
Foliated sediment - host rock?
Foliated Siltstone
Massive Sandstone
Sandstone Breccia
Foliated Sandstone
Foliated Mudstone
Foliated Carbonaceous sediment
Altered Volcanic - host rock?
Altered Basalt
Coarse-grained Basalt
Massive Basalt
Pillow Basalt
Foliated Basalt
Vesicular Basalt
Flow Banded Basalt - Hyaloclastite/Peperite
Basaltic Autobreccia
Brecciated Basalt
DRILL HOLE LEGEND
RHS Profile : LogIn-phase
Drill Log : Lith
0
40
80
120
Scale 1:2000
INTERDEX
VIKING GOLD CORPORATION
Section 1600mE - 1800mE
Lithology against
Ground Log In-phase EM Profiles
GEO. I.LAURENT
SCALE 1:2000
REPORT: MEconGeol
DRAWN: I.LAURENT
DATE 14-02-2001
FIGURE: 8.5c

Figure 8.5c

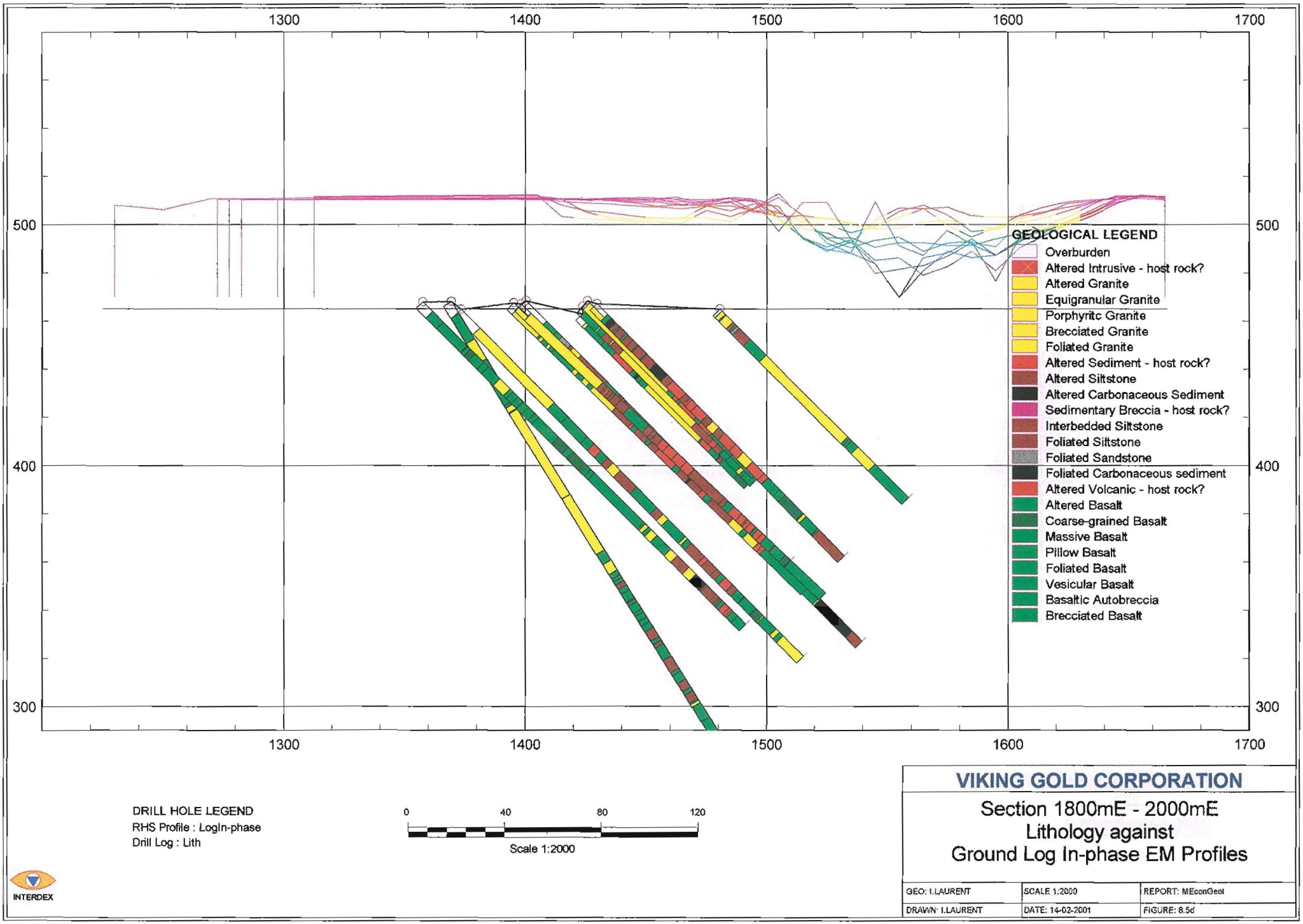
1300
1400
1500
1600
1700
500
400
300
GEOLOGICAL LEGEND
Overburden
Altered Intrusive - host rock?
Altered Granite
Equigranular Granite
Porphyritc Granite
Brecciated Granite
Foliated Granite
Altered Sediment - host rock?
Altered Siltstone
Altered Carbonaceous Sediment
Sedimentary Breccia - host rock?
Interbedded Siltstone
Foliated Siltstone
Foliated Sandstone
Foliated Carbonaceous sediment
Altered Volcanic - host rock?
Altered Basalt
Coarse-grained Basalt
Massive Basalt
Pillow Basalt
Foliated Basalt
Vesicular Basalt
Basaltic Autobreccia
Brecciated Basalt
DRILL HOLE LEGEND
RHS Profile : LogIn-phase
Drill Log : Lith
0
40
80
120
Scale 1:2000
INTERDEX
VIKING GOLD CORPORATION
Section 1800mE - 2000mE
Lithology against
Ground Log In-phase EM Profiles
GEO: I.LAURENT
SCALE 1:2000
REPORT: MEconGeol
DRAWN: I.LAURENT
DATE: 14-02-2001
FIGURE: 8.5d

Figure 8.5d

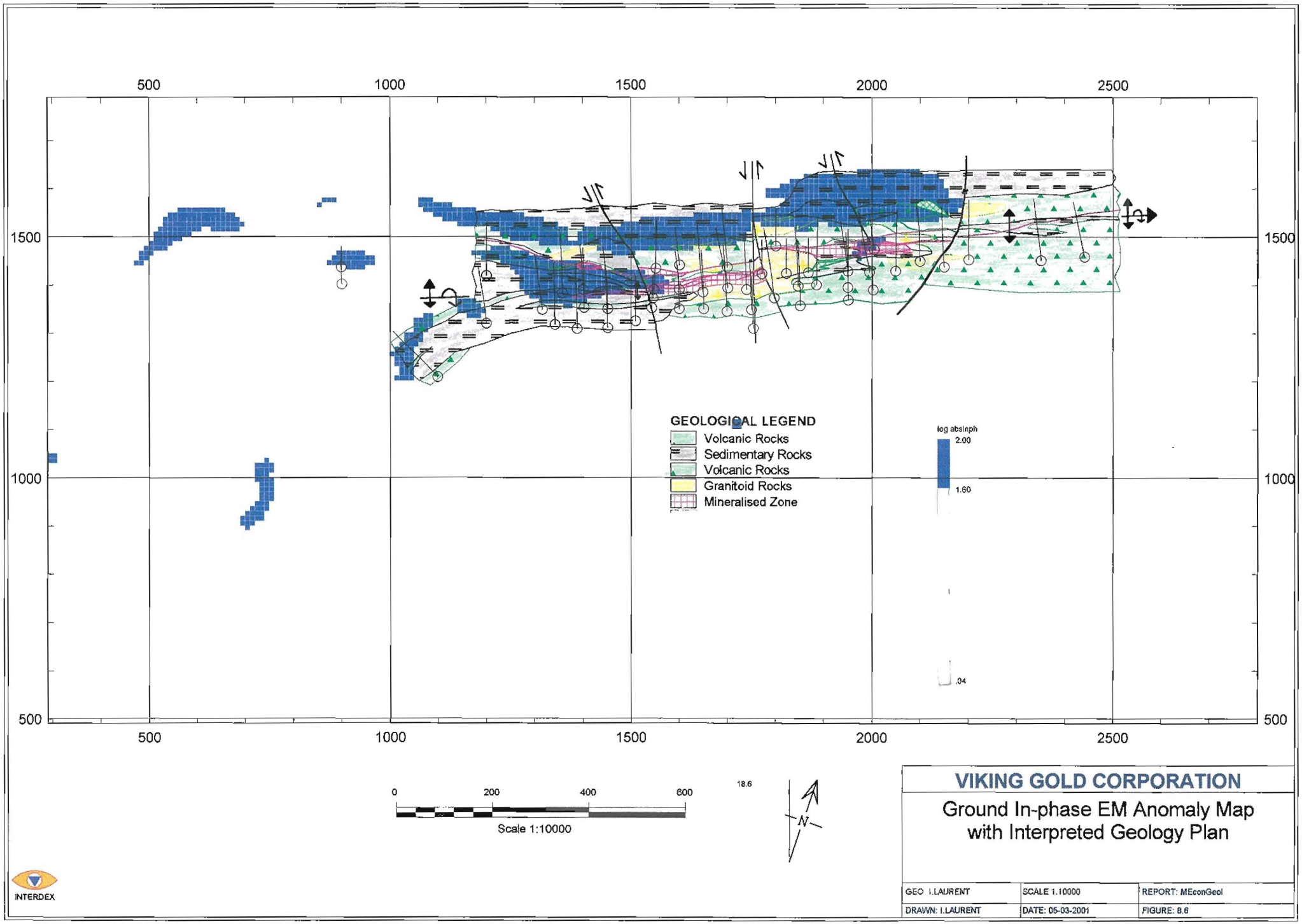
500
1000
1500
2000
2500
GEOLOGICAL LEGEND
Volcanic Rocks
Sedimentary Rocks
Volcanic Rocks
Granitoid Rocks
Mineralised Zone
log absinph
2.00
1.60
.04
0
200
400
600
Scale 1:10000
18.6
N
INTERDEX
VIKING GOLD CORPORATION
Ground In-phase EM Anomaly Map
with Interpreted Geology Plan
GEO I.LAURENT
SCALE 1.10000
REPORT: MEconGeol
DRAWN: I.LAURENT
DATE: 05-03-2001
FIGURE: 8.6

Figure 8.6

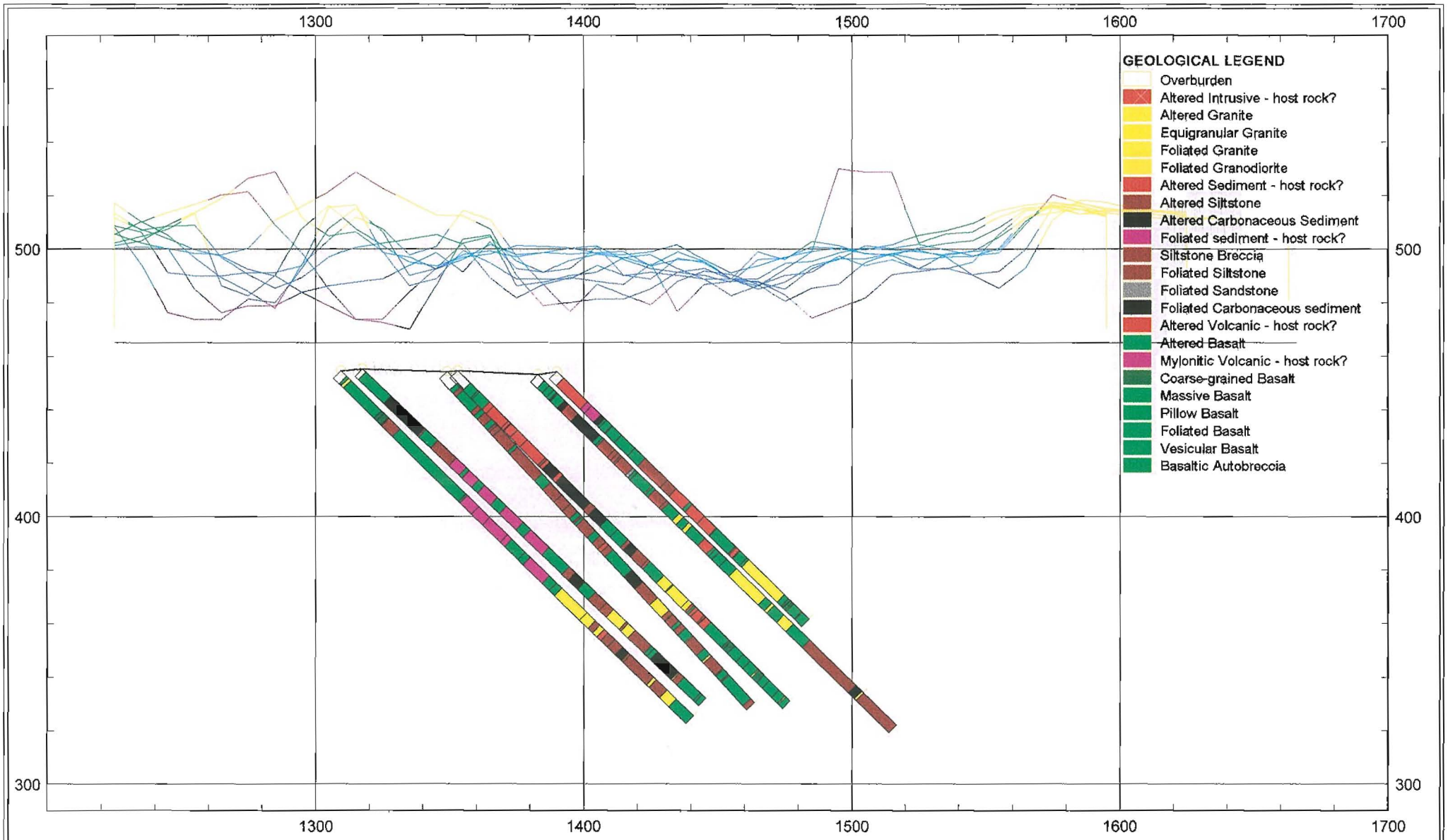

DRILL HOLE LEGEND
RHS Profile : Quadrature
Drill Log : Lith

0 40 80 120
Scale 1:2000

INTERDEX

VIKING GOLD CORPORATION

Section 1200mE - 1400mE
Lithology against
Ground Quadrature EM Profiles

GEO: I.LAURENT	SCALE 1:2000	REPORT: MEconGeol
DRAWN I.LAURENT	DATE: 14-02-2001	FIGURE: 8.7a

Figure 8.7a

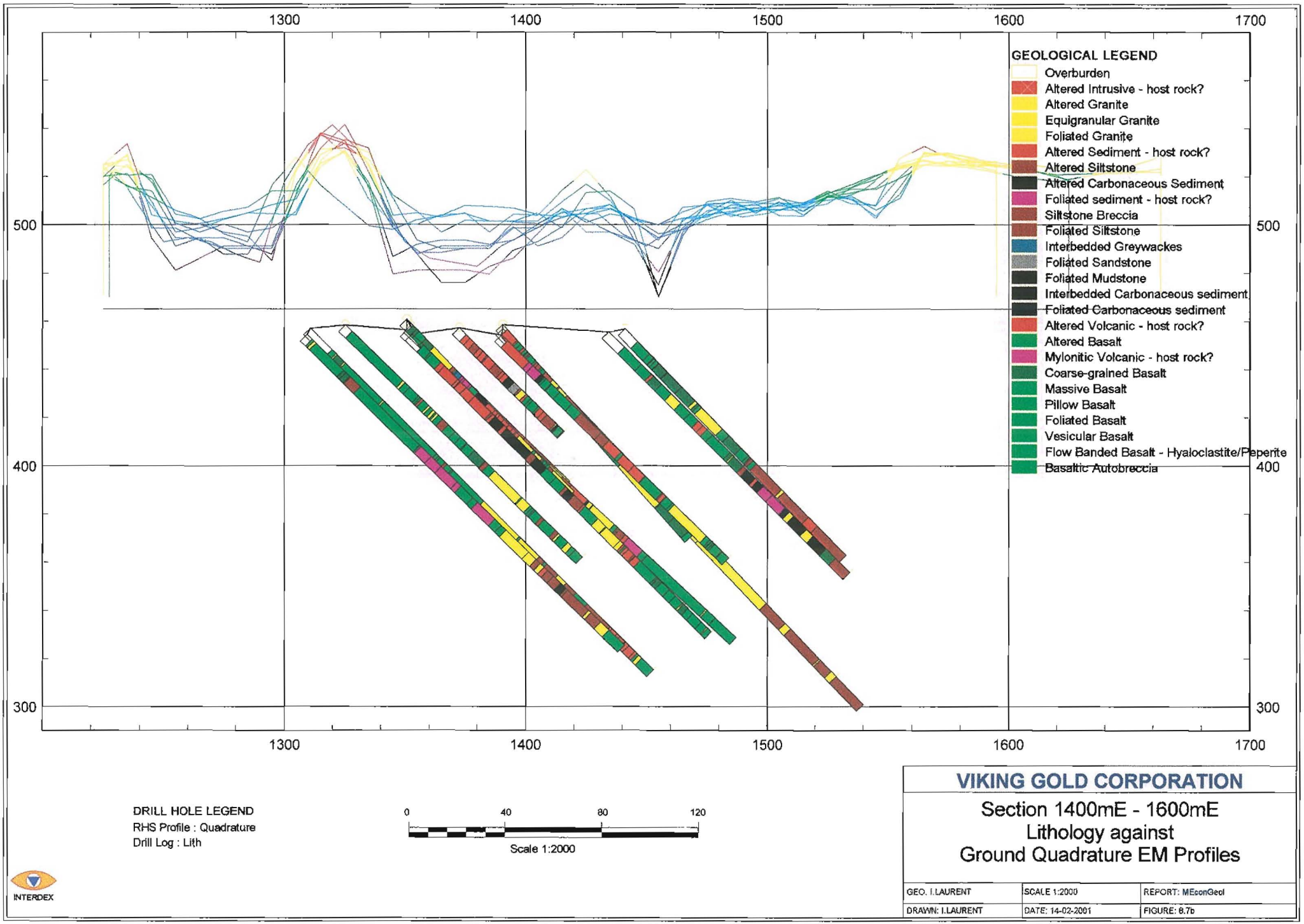
1300
1400
1500
1600
1700
500
400
300
GEOLOGICAL LEGEND
Overburden
Altered Intrusive - host rock?
Altered Granite
Equigranular Granite
Foliated Granite
Altered Sediment - host rock?
Altered Siltstone
Altered Carbonaceous Sediment
Foliated sediment - host rock?
Siltstone Breccia
Foliated Siltstone
Interbedded Greywackes
Foliated Sandstone
Foliated Mudstone
Interbedded Carbonaceous sediment
Foliated Carbonaceous sediment
Altered Volcanic - host rock?
Altered Basalt
Mylonitic Volcanic - host rock?
Coarse-grained Basalt
Massive Basalt
Pillow Basalt
Foliated Basalt
Vesicular Basalt
Flow Banded Basalt - Hyaloclastite/Peperite
Basaltic Autobreccia
DRILL HOLE LEGEND
RHS Profile : Quadrature
Drill Log : Lith
0
40
80
120
Scale 1:2000
INTERDEX
VIKING GOLD CORPORATION
Section 1400mE - 1600mE
Lithology against
Ground Quadrature EM Profiles
GEO. I.LAURENT
SCALE 1:2000
REPORT: MEconGeol
DRAWN: I.LAURENT
DATE: 14-02-2001
FIGURE: 8.7b

Figure 8.7b

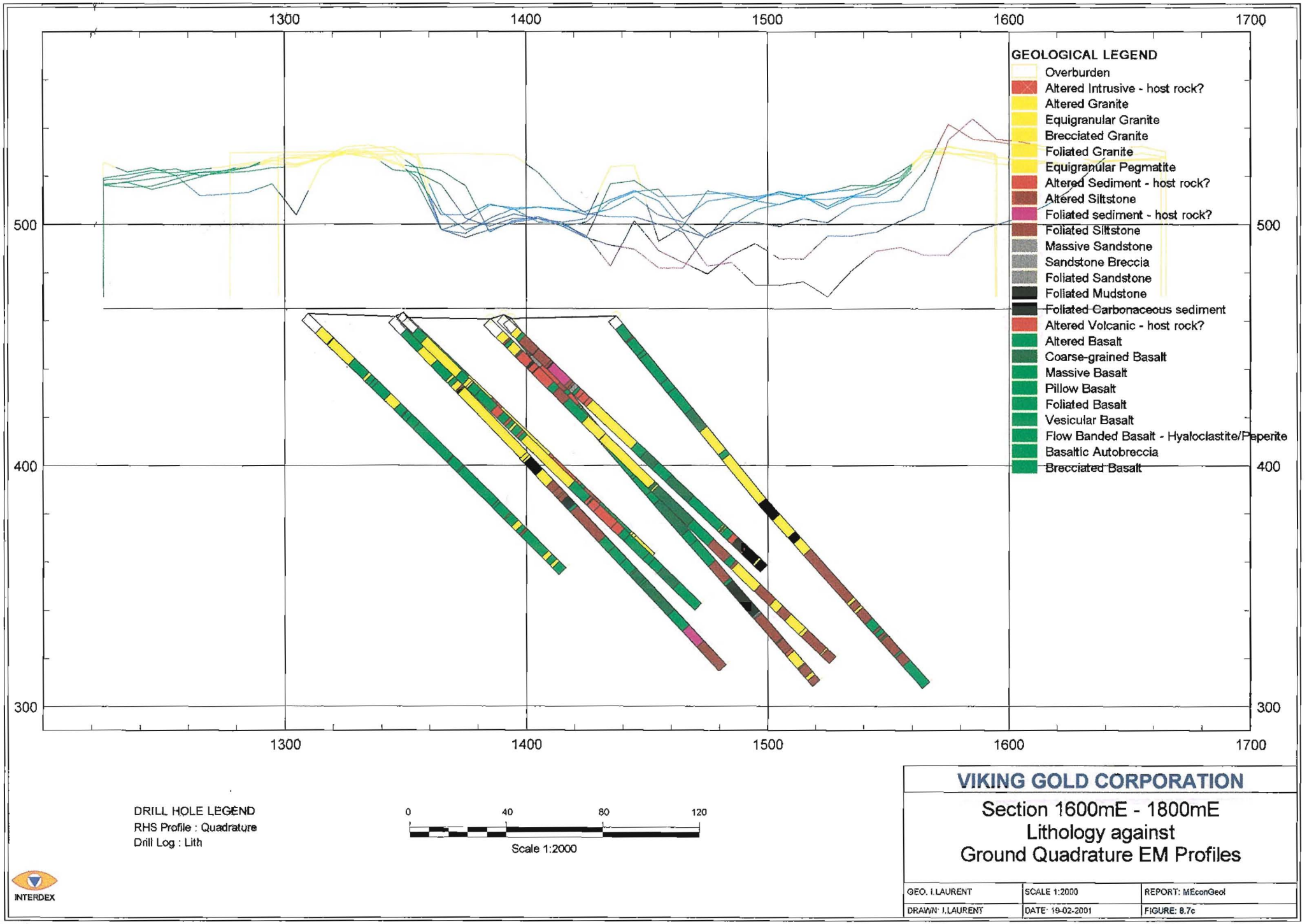
1300
1400
1500
1600
1700
500
400
300
GEOLOGICAL LEGEND
Overburden
Altered Intrusive - host rock?
Altered Granite
Equigranular Granite
Brecciated Granite
Foliated Granite
Equigranular Pegmatite
Altered Sediment - host rock?
Altered Siltstone
Foliated sediment - host rock?
Foliated Siltstone
Massive Sandstone
Sandstone Breccia
Foliated Sandstone
Foliated Mudstone
Foliated Carbonaceous sediment
Altered Volcanic - host rock?
Altered Basalt
Coarse-grained Basalt
Massive Basalt
Pillow Basalt
Foliated Basalt
Vesicular Basalt
Flow Banded Basalt - Hyaloclastite/Peperite
Basaltic Autobreccia
Brecciated Basalt
DRILL HOLE LEGEND
RHS Profile : Quadrature
Drill Log : Lith
0
40
80
120
Scale 1:2000
INTERDEX
VIKING GOLD CORPORATION
Section 1600mE - 1800mE
Lithology against
Ground Quadrature EM Profiles
GEO. I.LAURENT
SCALE 1:2000
REPORT: MEconGeol
DRAWN: I.LAURENT
DATE: 19-02-2001
FIGURE: 8.7c

Figure 8.7c

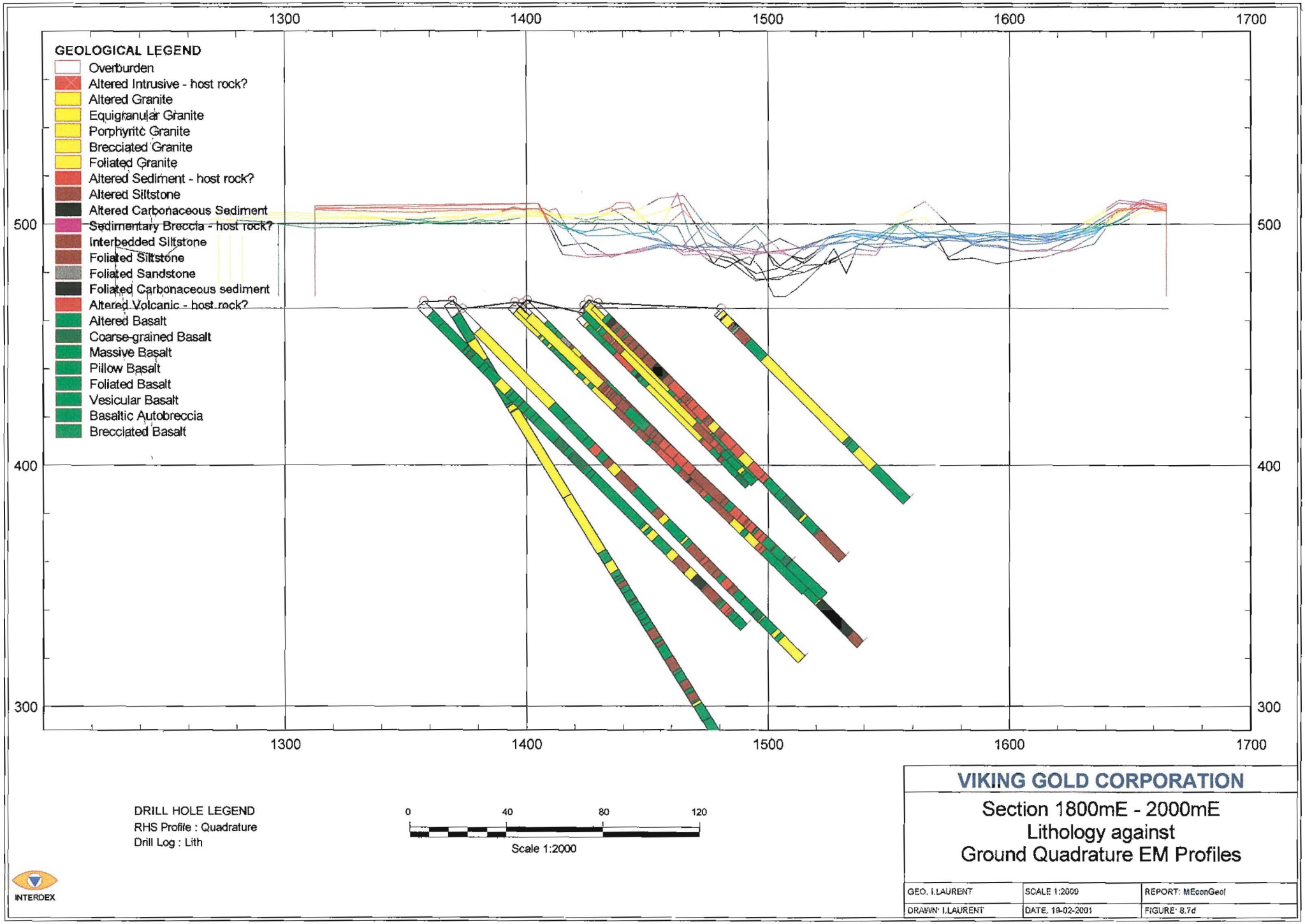
1300
1400
1500
1600
1700
500
400
300
GEOLOGICAL LEGEND
Overburden
Altered Intrusive - host rock?
Altered Granite
Equigranular Granite
Porphyritic Granite
Brecciated Granite
Foliated Granite
Altered Sediment - host rock?
Altered Siltstone
Altered Carbonaceous Sediment
Sedimentary Breccia - host rock?
Interbedded Siltstone
Foliated Siltstone
Foliated Sandstone
Foliated Carbonaceous sediment
Altered Volcanic - host rock?
Altered Basalt
Coarse-grained Basalt
Massive Basalt
Pillow Basalt
Foliated Basalt
Vesicular Basalt
Basaltic Autobreccia
Brecciated Basalt
DRILL HOLE LEGEND
RHS Profile : Quadrature
Drill Log : Lith
0
40
80
120
Scale 1:2000
INTERDEX
VIKING GOLD CORPORATION
Section 1800mE - 2000mE
Lithology against
Ground Quadrature EM Profiles
GEO. I.LAURENT
SCALE 1:2000
REPORT: MEconGeol
DRAWN: I.LAURENT
DATE: 19-02-2001
FIGURE: 8.7d

Figure 8.7d

The log-transformed, quadrature electromagnetic data separates the first-order from the second-order anomalies within the shear zone (figure 8.8a-d). Between the 1400mE and 1600mE, the pyrrhotite-bearing sediments generate a second-order quadrature anomaly.

The first-order anomalies are found west of the 1400mE and east of the 1600mE. The anomalies derive from a combination of foliated volcanics and granitoids, carbonaceous sediments and the "Mineralised Zone".

The interpreted geological plan is overlain onto the quadrature EM anomaly map, which was delineated in Section 7 (figure 8.9). High quadrature EM anomalies overlie most of the stratigraphy at Svartliden and suggest no lithological or structural control.

The EM ratio profiles are plotted against the drillhole geology (figure 8.10a-d). The EM ratio anomalies are quite discrete and correlate with the in-phase EM anomalies, overlying primarily the pyrrhotite-bearing sediments. Weak EM ratio anomalies overlie the "Mineralised Zone".

The interpreted geological plan is overlain onto the EM ratio anomaly map, which was delineated in Section 7 (figure 8.11). The EM ratio anomalies overlie most of the stratigraphy at Svartliden and suggest no lithological or structural control.

The interpreted geological plan is overlain onto the combined ground geophysical anomaly map (figure 8.12). There are two major coincident geophysical anomalies between the 1100mE and 1400mE, and 1700mE and 2200mE represented by pyrrhotite-bearing sediments.

Between 1400mE and 1700mE, there is a strong magnetic-only anomaly coincident with the magnetite-bearing volcanics. For an unexplained reason the pyrrhotite-bearing sediments within this zone, on the northern contact of the shear zone, displays only in-phase EM anomalism. The "Mineralised Zone" straddles the different geophysical anomalies.

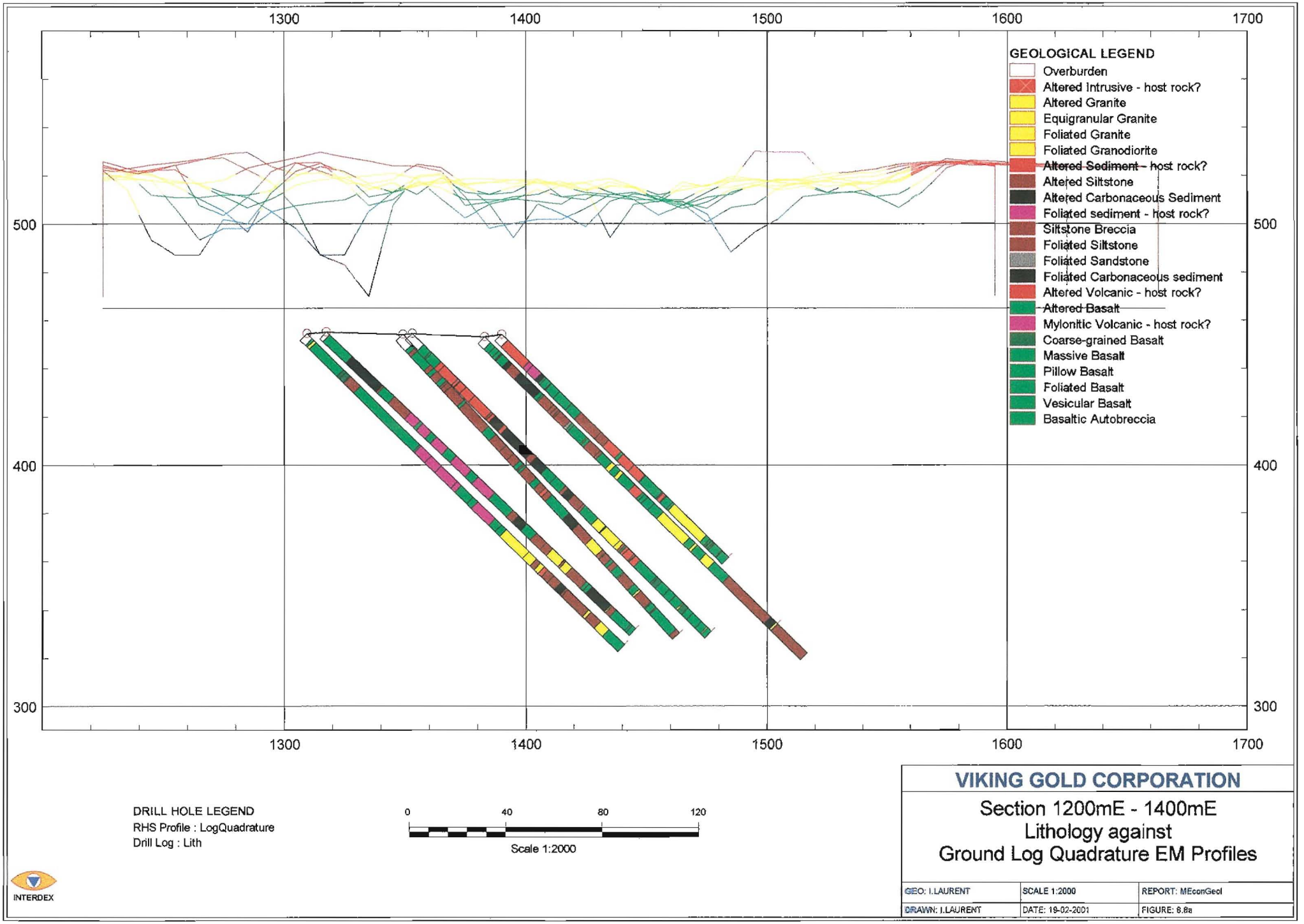
1300
1400
1500
1600
1700
500
400
300
GEOLOGICAL LEGEND
Overburden
Altered Intrusive - host rock?
Altered Granite
Equigranular Granite
Foliated Granite
Foliated Granodiorite
Altered Sediment - host rock?
Altered Siltstone
Altered Carbonaceous Sediment
Foliated sediment - host rock?
Siltstone Breccia
Foliated Siltstone
Foliated Sandstone
Foliated Carbonaceous sediment
Altered Volcanic - host rock?
Altered Basalt
Mylonitic Volcanic - host rock?
Coarse-grained Basalt
Massive Basalt
Pillow Basalt
Foliated Basalt
Vesicular Basalt
Basaltic Autobreccia
DRILL HOLE LEGEND
RHS Profile : LogQuadrature
Drill Log : Lith
0
40
80
120
Scale 1:2000
INTERDEX
VIKING GOLD CORPORATION
Section 1200mE - 1400mE
Lithology against
Ground Log Quadrature EM Profiles
GEO: I.LAURENT
SCALE 1:2000
REPORT: MEconGeol
DRAWN: I.LAURENT
DATE: 19-02-2001
FIGURE: 8.8a

Figure 8.8a

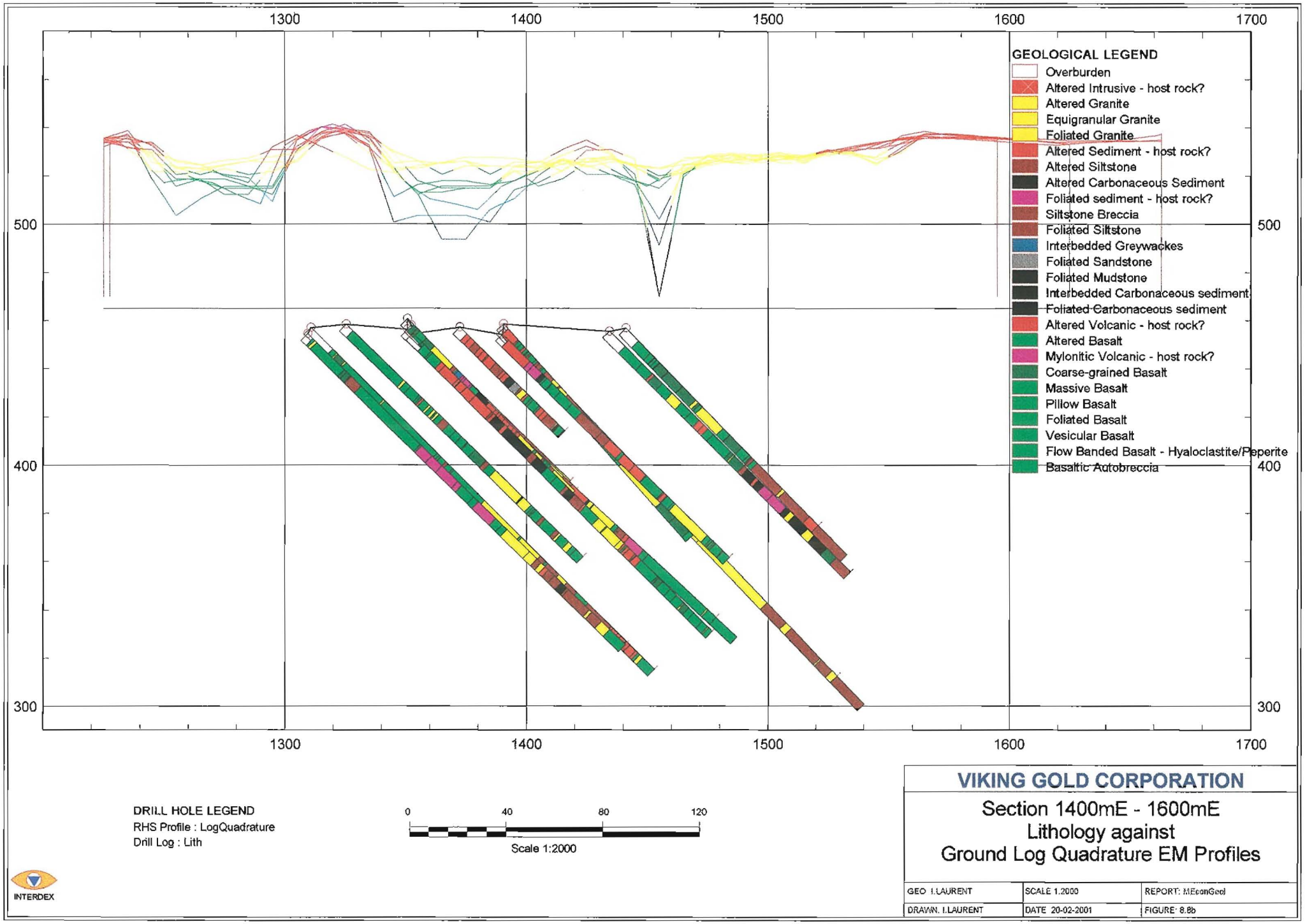
1300
1400
1500
1600
1700
500
400
300
GEOLOGICAL LEGEND
Overburden
Altered Intrusive - host rock?
Altered Granite
Equigranular Granite
Foliated Granite
Altered Sediment - host rock?
Altered Siltstone
Altered Carbonaceous Sediment
Foliated sediment - host rock?
Siltstone Breccia
Foliated Siltstone
Interbedded Greywackes
Foliated Sandstone
Foliated Mudstone
Interbedded Carbonaceous sediment
Foliated Carbonaceous sediment
Altered Volcanic - host rock?
Altered Basalt
Mylonitic Volcanic - host rock?
Coarse-grained Basalt
Massive Basalt
Pillow Basalt
Foliated Basalt
Vesicular Basalt
Flow Banded Basalt - Hyaloclastite/Peperite
Basaltic Autobreccia
DRILL HOLE LEGEND
RHS Profile : LogQuadrature
Drill Log : Lith
0
40
80
120
Scale 1:2000
INTERDEX
VIKING GOLD CORPORATION
Section 1400mE - 1600mE
Lithology against
Ground Log Quadrature EM Profiles
GEO I.LAURENT
SCALE 1:2000
REPORT: MEconGeol
DRAWN. I.LAURENT
DATE 20-02-2001
FIGURE 8.8b

Figure 8.8b

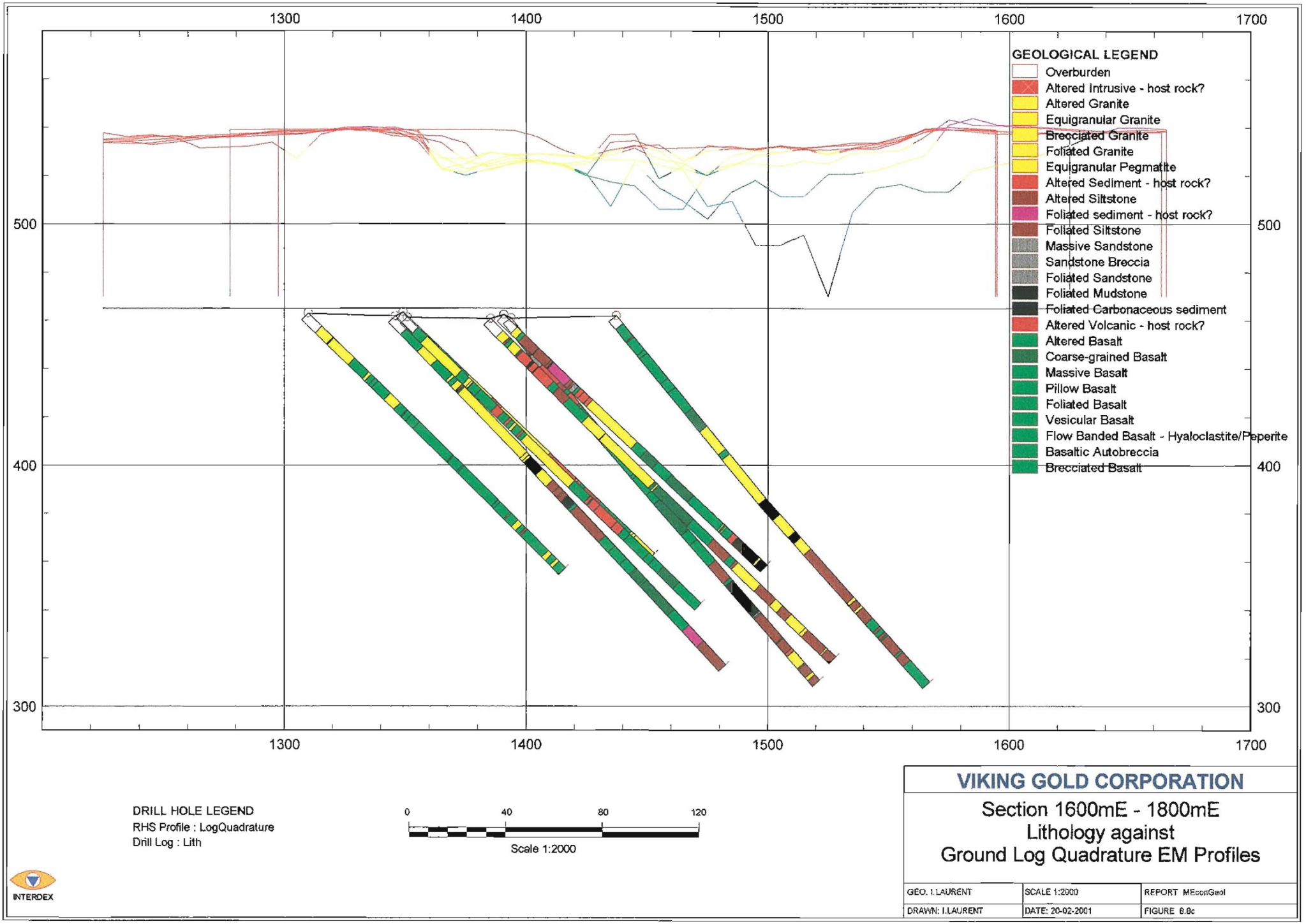
1300
1400
1500
1600
1700
500
400
300
GEOLOGICAL LEGEND
Overburden
Altered Intrusive - host rock?
Altered Granite
Equigranular Granite
Brecciated Granite
Foliated Granite
Equigranular Pegmatite
Altered Sediment - host rock?
Altered Siltstone
Foliated sediment - host rock?
Foliated Siltstone
Massive Sandstone
Sandstone Breccia
Foliated Sandstone
Foliated Mudstone
Foliated Carbonaceous sediment
Altered Volcanic - host rock?
Altered Basalt
Coarse-grained Basalt
Massive Basalt
Pillow Basalt
Foliated Basalt
Vesicular Basalt
Flow Banded Basalt - Hyaloclastite/Peperite
Basaltic Autobreccia
Brecciated Basalt
DRILL HOLE LEGEND
RHS Profile : LogQuadrature
Drill Log : Lith
0
40
80
120
Scale 1:2000
INTERDEX
VIKING GOLD CORPORATION
Section 1600mE - 1800mE
Lithology against
Ground Log Quadrature EM Profiles
GEO. I.LAURENT
SCALE 1:2000
REPORT MEconGeol
DRAWN: I.LAURENT
DATE: 20-02-2001
FIGURE 8.8c

Figure 8.8c

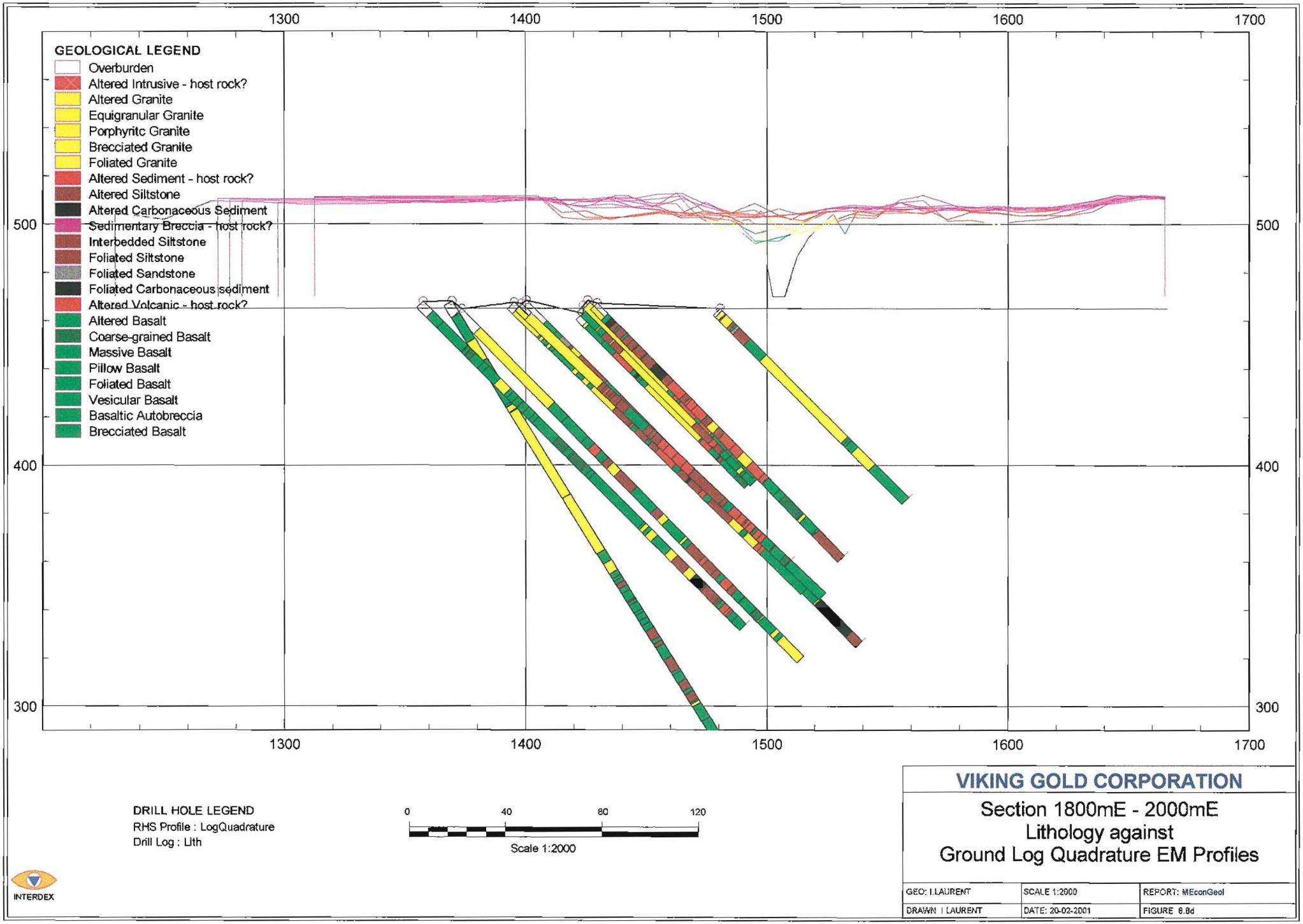
1300
1400
1500
1600
1700
500
400
300
GEOLOGICAL LEGEND
Overburden
Altered Intrusive - host rock?
Altered Granite
Equigranular Granite
Porphyritc Granite
Brecciated Granite
Foliated Granite
Altered Sediment - host rock?
Altered Siltstone
Altered Carbonaceous Sediment
Sedimentary Breccia - host rock?
Interbedded Siltstone
Foliated Siltstone
Foliated Sandstone
Foliated Carbonaceous sediment
Altered Volcanic - host rock?
Altered Basalt
Coarse-grained Basalt
Massive Basalt
Pillow Basalt
Foliated Basalt
Vesicular Basalt
Basaltic Autobreccia
Brecciated Basalt
DRILL HOLE LEGEND
RHS Profile : LogQuadrature
Drill Log : Lith
0
40
80
120
Scale 1:2000
INTERDEX
VIKING GOLD CORPORATION
Section 1800mE - 2000mE
Lithology against
Ground Log Quadrature EM Profiles
GEO: I.LAURENT
SCALE 1:2000
REPORT: MEconGeol
DRAWN : LAURENT
DATE: 20-02-2001
FIGURE 8.8d

Figure 8.8d

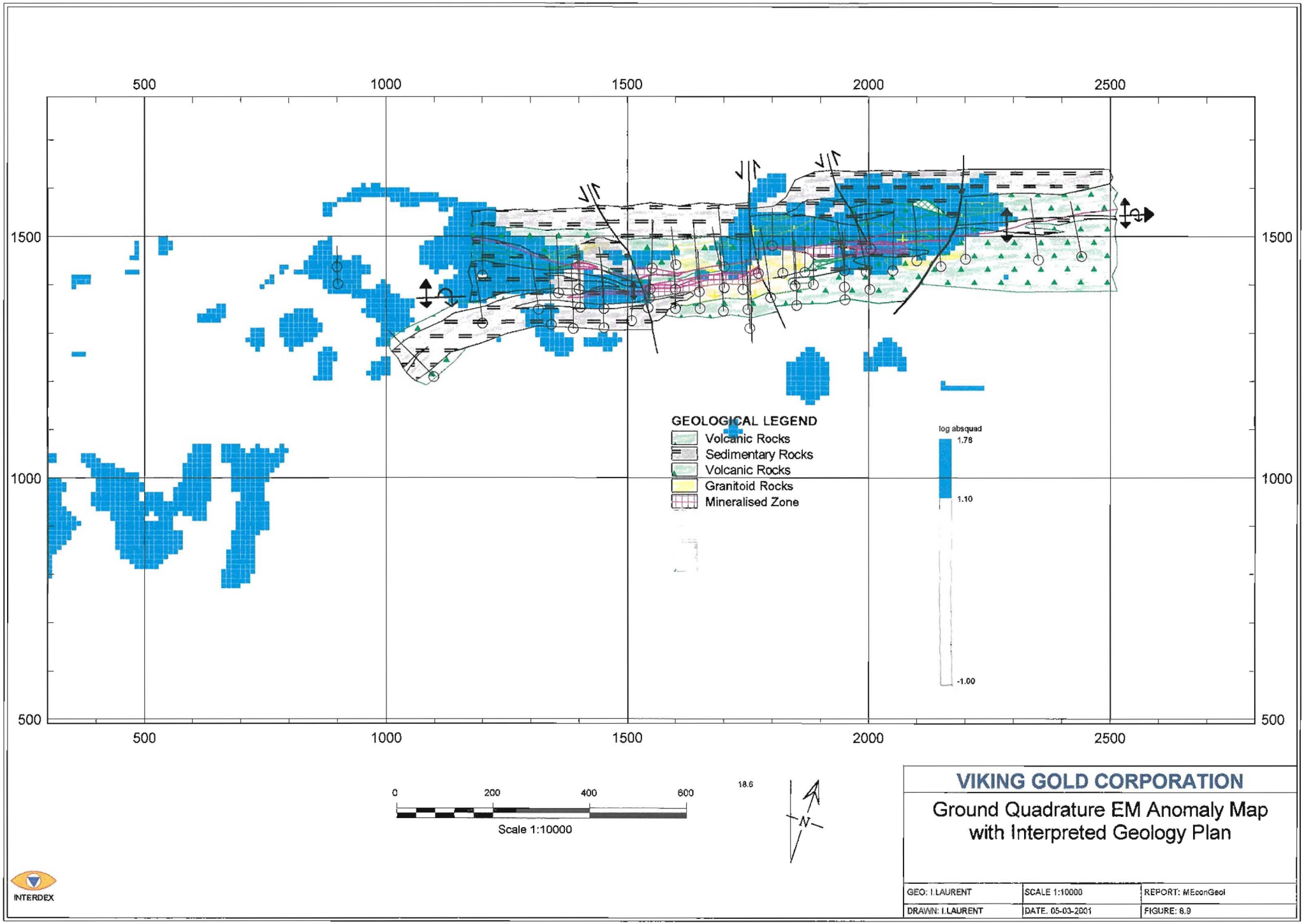
500
1000
1500
2000
2500
GEOLOGICAL LEGEND
Volcanic Rocks
Sedimentary Rocks
Volcanic Rocks
Granitoid Rocks
Mineralised Zone
log absquad
1.78
1.10
-1.00
0
200
400
600
Scale 1:10000
18.6
N
INTERDEX
VIKING GOLD CORPORATION
Ground Quadrature EM Anomaly Map
with Interpreted Geology Plan
GEO: I.LAURENT
SCALE 1:10000
REPORT: MEconGeol
DRAWN: I.LAURENT
DATE. 05-03-2001
FIGURE: 8.9

Figure 8.9

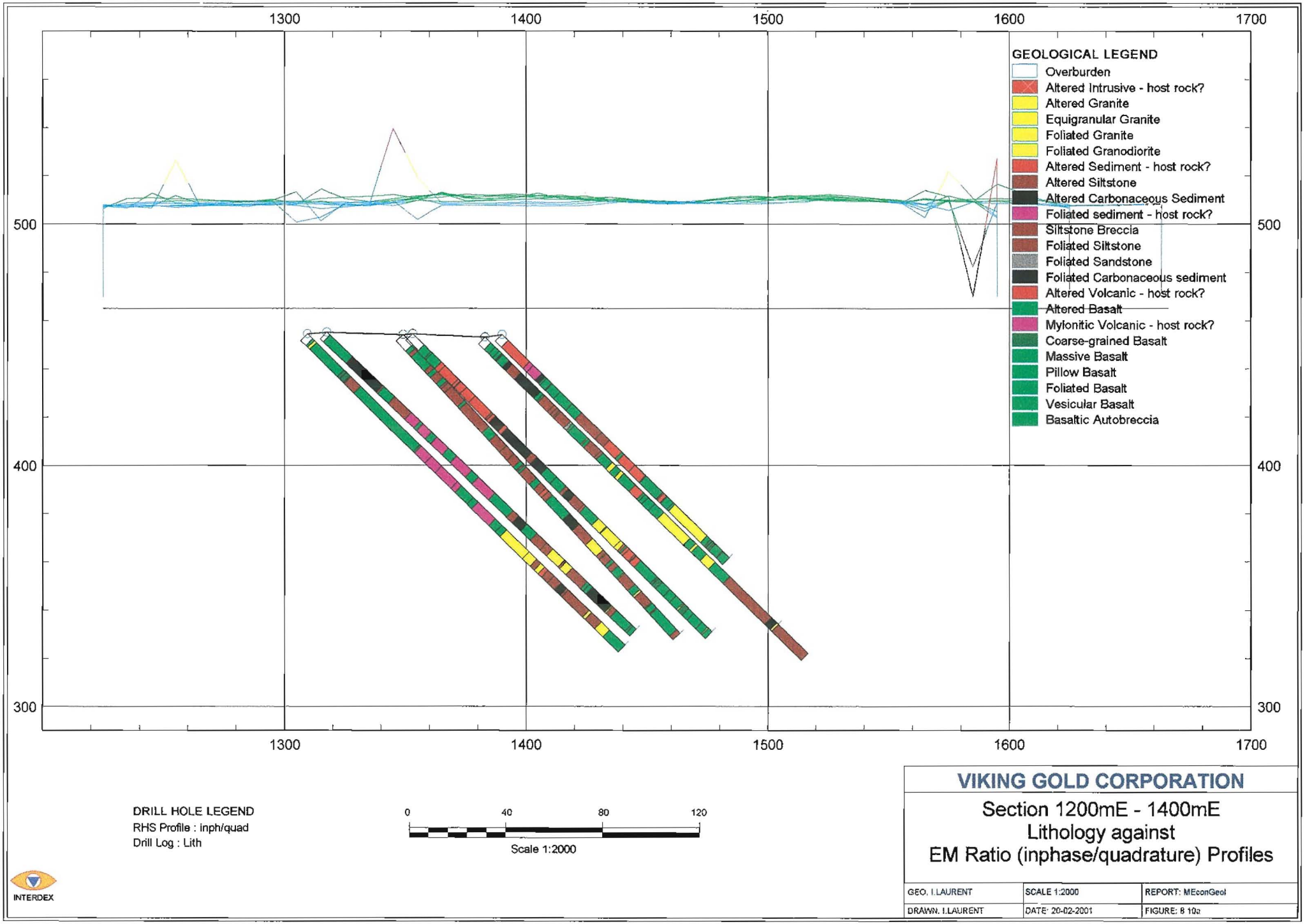
1300
1400
1500
1600
1700
500
400
300
GEOLOGICAL LEGEND
Overburden
Altered Intrusive - host rock?
Altered Granite
Equigranular Granite
Foliated Granite
Foliated Granodiorite
Altered Sediment - host rock?
Altered Siltstone
Altered Carbonaceous Sediment
Foliated sediment - host rock?
Siltstone Breccia
Foliated Siltstone
Foliated Sandstone
Foliated Carbonaceous sediment
Altered Volcanic - host rock?
Altered Basalt
Mylonitic Volcanic - host rock?
Coarse-grained Basalt
Massive Basalt
Pillow Basalt
Foliated Basalt
Vesicular Basalt
Basaltic Autobreccia
DRILL HOLE LEGEND
RHS Profile : inph/quad
Drill Log : Lith
0
40
80
120
Scale 1:2000
INTERDEX
VIKING GOLD CORPORATION
Section 1200mE - 1400mE
Lithology against
EM Ratio (inphase/quadrature) Profiles
GEO. I.LAURENT
SCALE 1:2000
REPORT: MEconGeol
DRAWN. I.LAURENT
DATE: 20-02-2001
FIGURE: 8 10a

Figure 8.10a

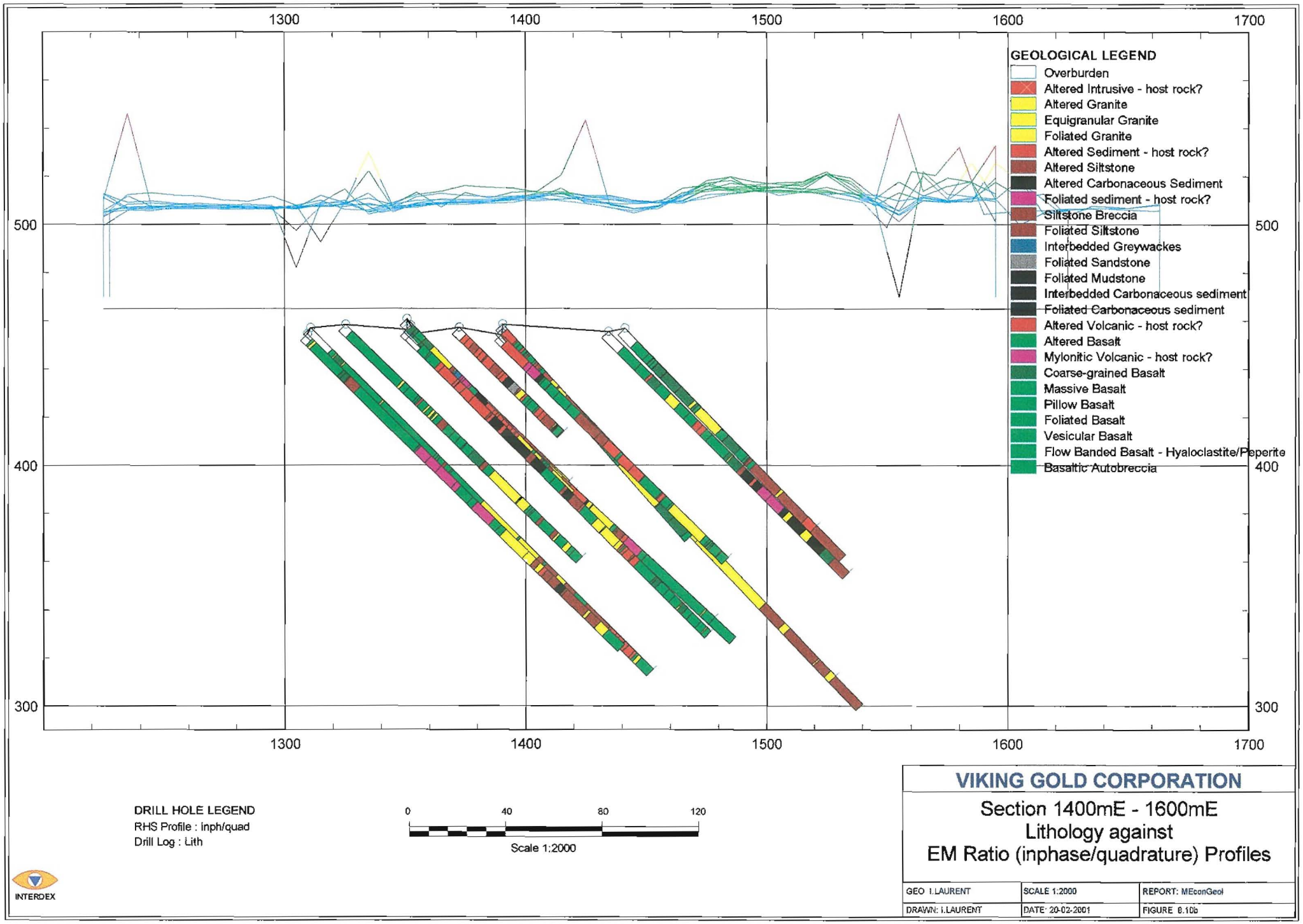
1300
1400
1500
1600
1700
500
400
300
GEOLOGICAL LEGEND
Overburden
Altered Intrusive - host rock?
Altered Granite
Equigranular Granite
Foliated Granite
Altered Sediment - host rock?
Altered Siltstone
Altered Carbonaceous Sediment
Foliated sediment - host rock?
Siltstone Breccia
Foliated Siltstone
Interbedded Greywackes
Foliated Sandstone
Foliated Mudstone
Interbedded Carbonaceous sediment
Foliated Carbonaceous sediment
Altered Volcanic - host rock?
Altered Basalt
Mylonitic Volcanic - host rock?
Coarse-grained Basalt
Massive Basalt
Pillow Basalt
Foliated Basalt
Vesicular Basalt
Flow Banded Basalt - Hyaloclastite/Peperite
Basaltic Autobreccia
DRILL HOLE LEGEND
RHS Profile : inph/quad
Drill Log : Lith
0
40
80
120
Scale 1:2000
INTERDEX
VIKING GOLD CORPORATION
Section 1400mE - 1600mE
Lithology against
EM Ratio (inphase/quadrature) Profiles
GEO I.LAURENT
SCALE 1:2000
REPORT: MEconGeol
DRAWN: I.LAURENT
DATE: 20-02-2001
FIGURE 8.10b

Figure 8.10b

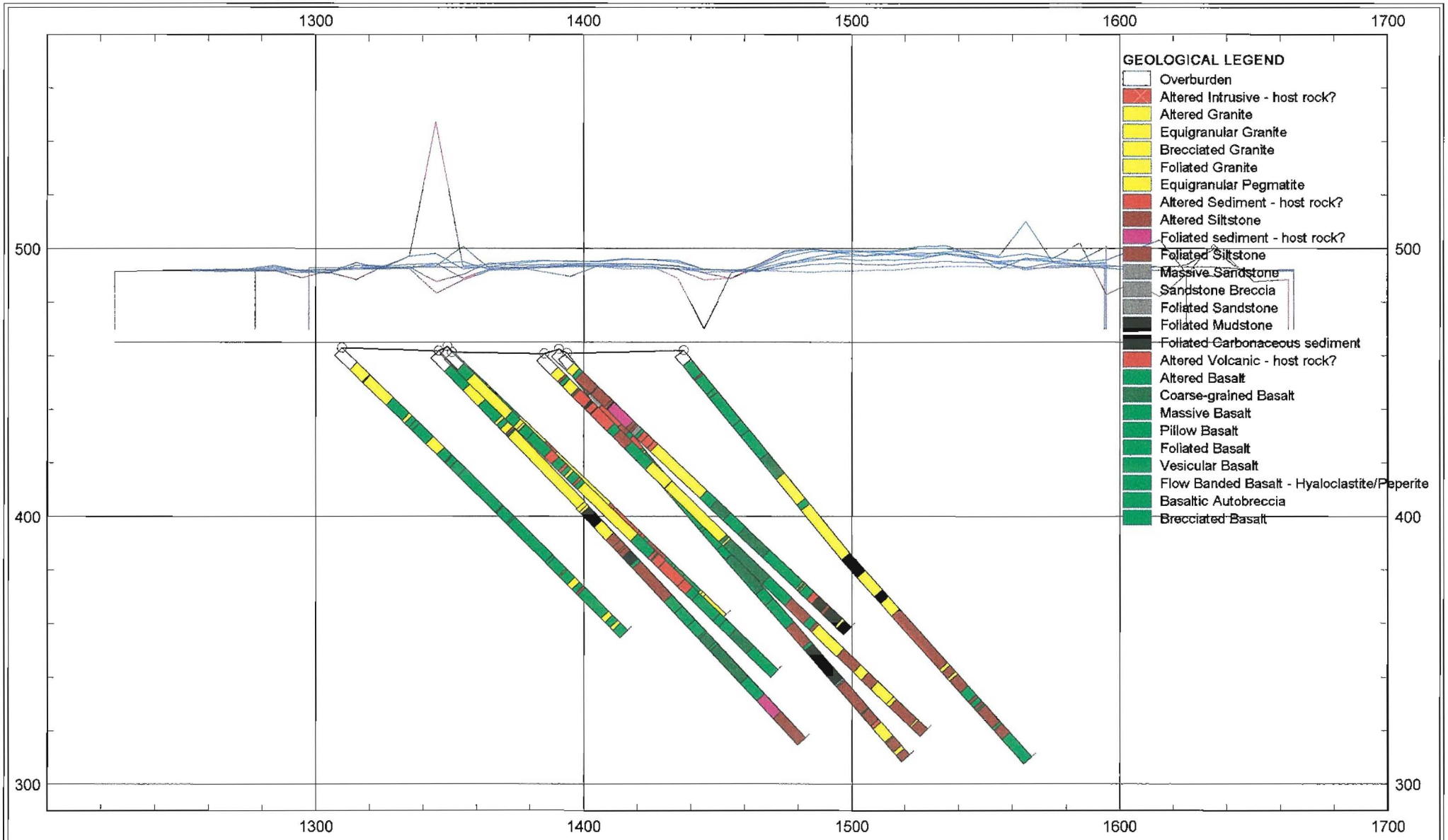

DRILL HOLE LEGEND
RHS Profile : inph/quad
Drill Log : Lith

0 40 80 120
Scale 1:2000

INTERDEX

VIKING GOLD CORPORATION

Section 1600mE - 1800mE
Lithology against
EM Ratio (inphase/quadrature) Profiles

GEO: I LAURENT	SCALE 1 2000	REPORT. MEconGeol
DRAWN. I.LAURENT	DATE: 20-02-2001	FIGURE: 8 10c

8.10c

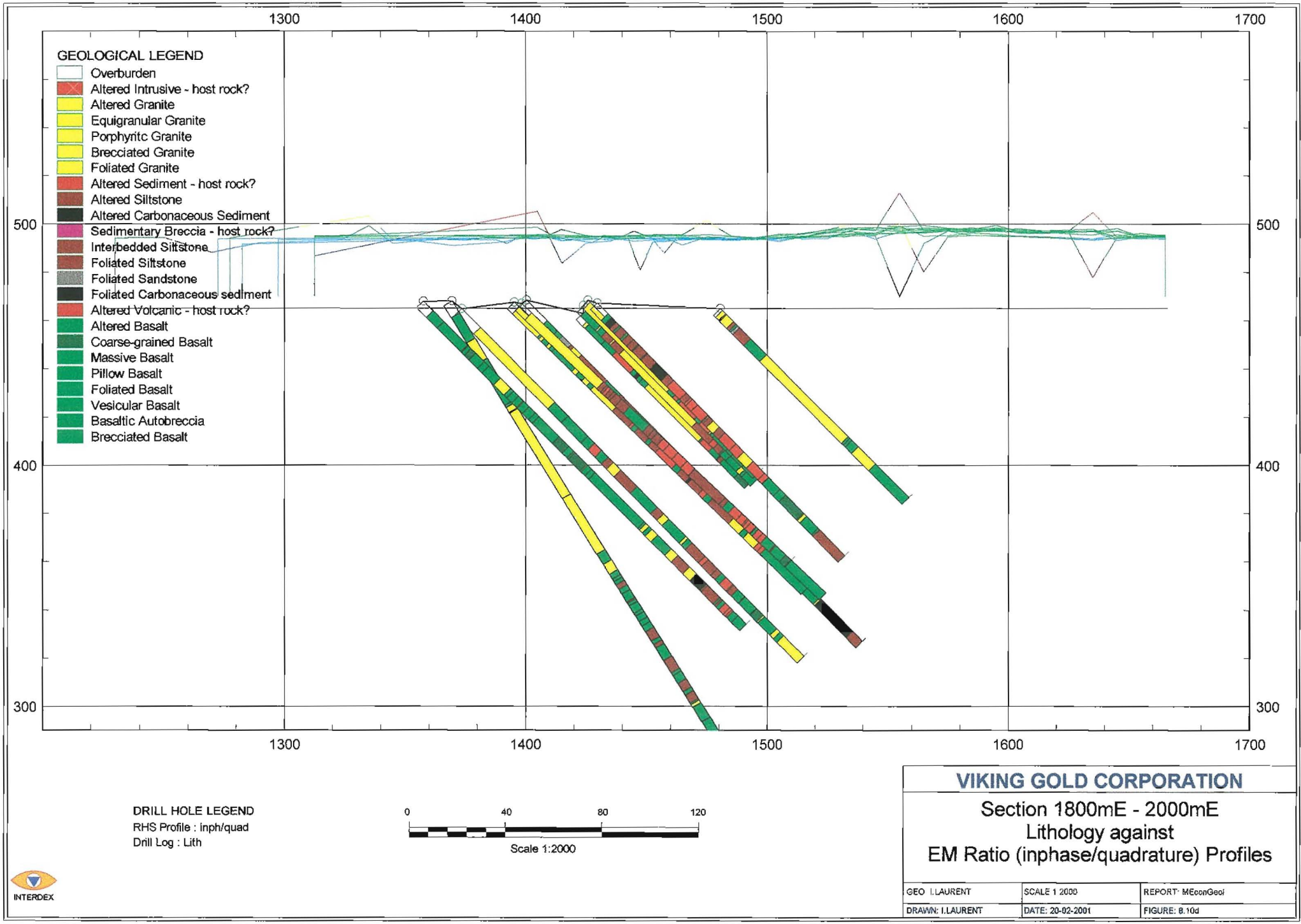
1300
1400
1500
1600
1700
500
400
300
GEOLOGICAL LEGEND
Overburden
Altered Intrusive - host rock?
Altered Granite
Equigranular Granite
Porphyritc Granite
Brecciated Granite
Foliated Granite
Altered Sediment - host rock?
Altered Siltstone
Altered Carbonaceous Sediment
Sedimentary Breccia - host rock?
Interbedded Siltstone
Foliated Siltstone
Foliated Sandstone
Foliated Carbonaceous sediment
Altered Volcanic - host rock?
Altered Basalt
Coarse-grained Basalt
Massive Basalt
Pillow Basalt
Foliated Basalt
Vesicular Basalt
Basaltic Autobreccia
Brecciated Basalt
DRILL HOLE LEGEND
RHS Profile : inph/quad
Drill Log : Lith
0
40
80
120
Scale 1:2000
INTERDEX
VIKING GOLD CORPORATION
Section 1800mE - 2000mE
Lithology against
EM Ratio (inphase/quadrature) Profiles
GEO I.LAURENT
SCALE 1 2000
REPORT: MEconGeol
DRAWN: I.LAURENT
DATE: 20-02-2001
FIGURE: 8.10d

Figure 8.10d

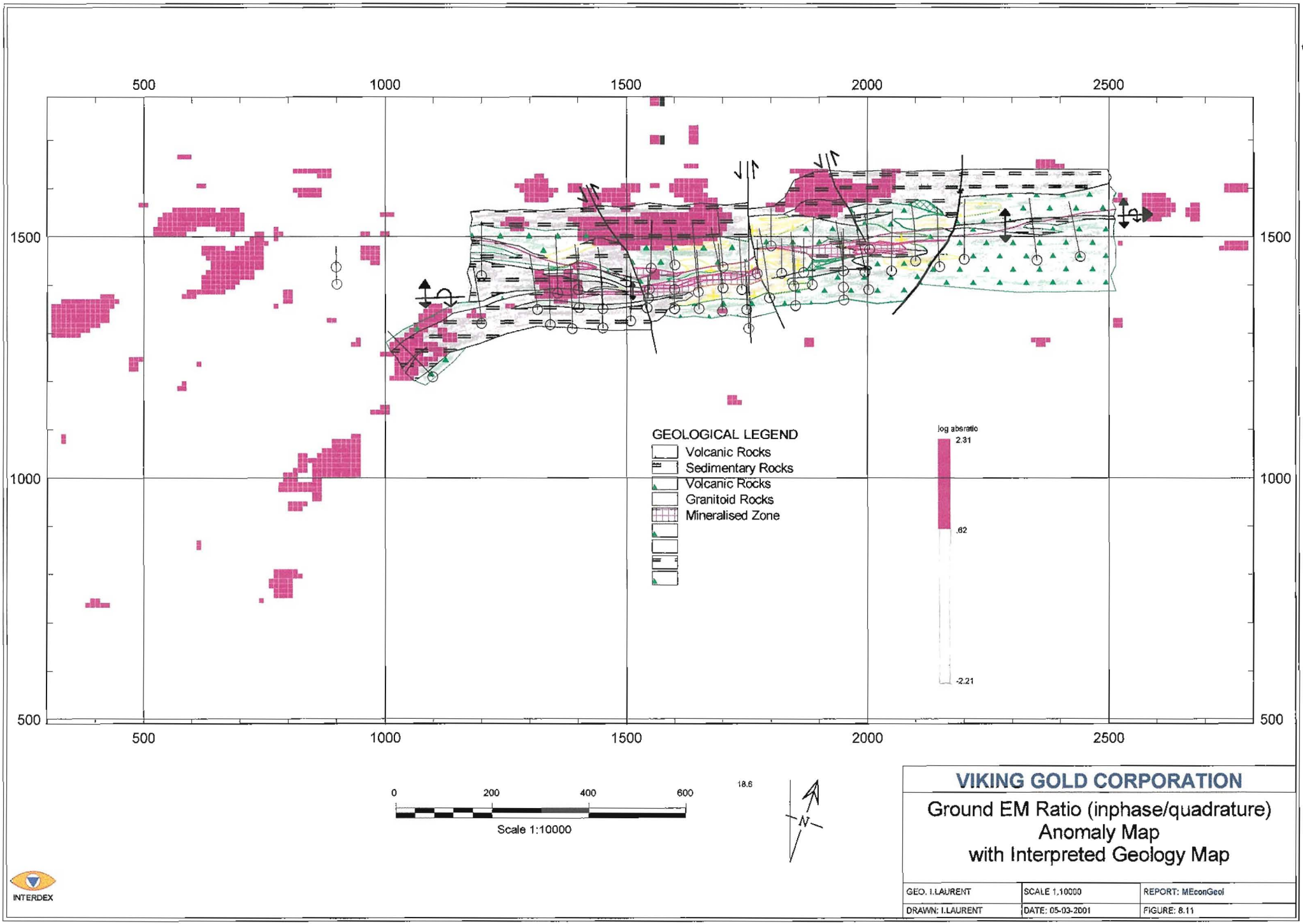
500
1000
1500
2000
2500
GEOLOGICAL LEGEND
Volcanic Rocks
Sedimentary Rocks
Volcanic Rocks
Granitoid Rocks
Mineralised Zone
log absratio
2.31
.62
-2.21
0
200
400
600
Scale 1:10000
18.6
N
INTERDEX
VIKING GOLD CORPORATION
Ground EM Ratio (inphase/quadrature)
Anomaly Map
with Interpreted Geology Map
GEO. I.LAURENT
SCALE 1:10000
REPORT: MEconGeol
DRAWN: I.LAURENT
DATE: 05-03-2001
FIGURE: 8.11

Figure 8.11

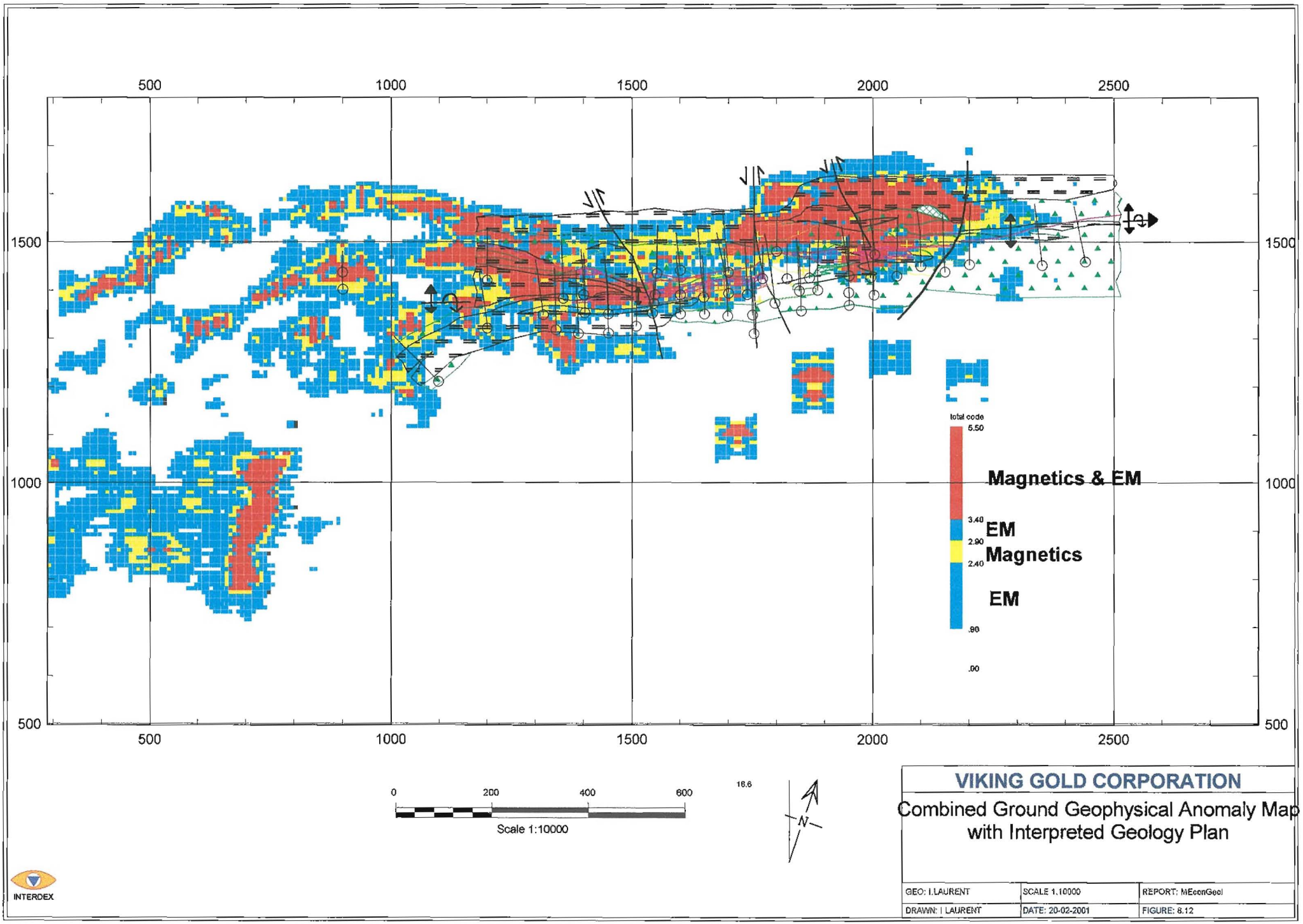
500
1000
1500
2000
2500
total code
5.50
Magnetics & EM
3.40
EM
2.90
2.40
Magnetics
EM
.90
.00
0
200
400
600
Scale 1:10000
16.6
N
VIKING GOLD CORPORATION
Combined Ground Geophysical Anomaly Map
with Interpreted Geology Plan
GEO: I.LAURENT
SCALE 1:10000
REPORT: MEconGeol
DRAWN: I LAURENT
DATE: 20-02-2001
FIGURE: 8.12
INTERDEX

Figure 8.12

8.1.2 Downhole Geophysics

A geological section along the 1700mE was interpreted from the geological logs of drillholes SV9702, SV9703 and SV9706 (Appendix 5). The geological section is plotted against the downhole geophysical anomaly maps (defined in Section 7).

The magnetic susceptibility anomaly map is overlain onto the interpreted geological section (figure 8.13). There are three zones of low magnetic susceptibility. The southern zone (1350mN to 1380mN) found at the top of drillhole SV9706 consists of weakly foliated basalts and medium-grained granitic rocks. A granitic unit present in the middle of drillhole SV9703 dominates the central zone (1480mN to 1510mN). The northern zone (1530mN to 1570mN) consists of a mix of weakly foliated basalts and pyrrhotite-poor siliciclastic sediments present at the base of drillhole SV9703.

The positive magnetic susceptibility anomalies can also be separated into three zones. The southern zone (1400mN to 1440mN) correlates with the "Mineralised Zone" (top of drillhole SV9702) and altered wallrock (middle of drillhole SV9706). The central zone (1440mN to 1460mN) has a strong correlation with the magnetite-bearing foliated basalt traceable along all three drillholes. The anomaly is lithologically constrained by the coarse-grained basalt on the footwall. The northern zone (1480mN to 1520mN) is confined to the pyrrhotite-bearing carbonaceous sediments found at the base of drillholes SV9702 and SV9706 and the middle of drillhole SV9703.

The apparent resistivity anomaly map is overlain onto the interpreted geological section (figure 8.14). The southern high conductivity zone (1390mN to 1430mN) corresponds to the "Mineralised Zone" in drillhole SV9702 and altered wallrock in drillhole SV9706. The northern conductive zone (1480mN to 1520mN) correlates with the pyrrhotite-bearing carbonaceous sediments. The major resistive zone (1430mN to 1510mN) is situated in the upper part of drillhole SV9703 within foliated volcanic and massive granitic rocks. A parallel resistive zone is situated in the upper part of drillhole SV9706 within weakly foliated basalts and granitoids. The weakly foliated volcanics at the base of drillhole SV9706 are also highly resistive.

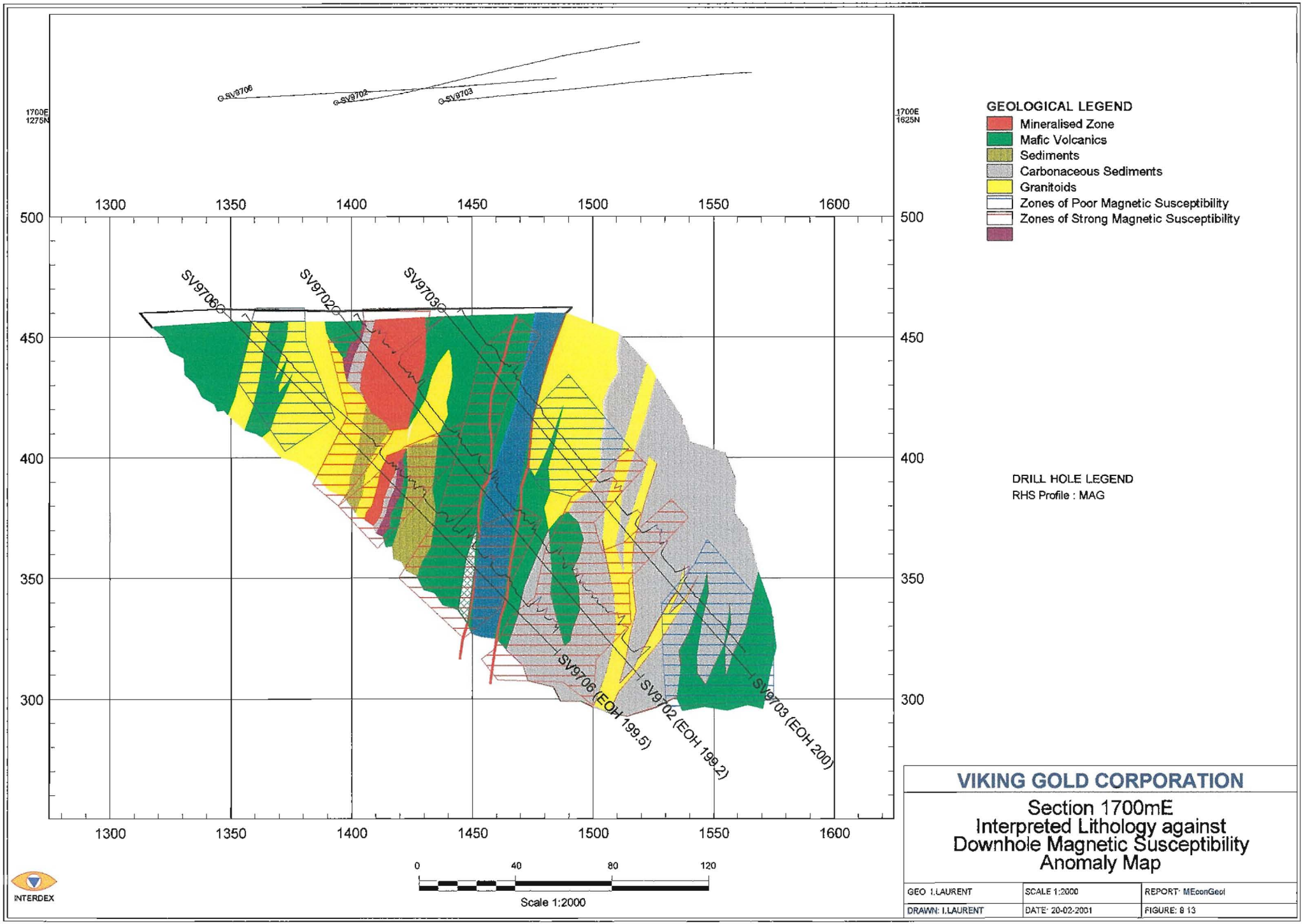
1700E
1275N
1700E
1625N
SV9706
SV9702
SV9703
1300
1350
1400
1450
1500
1550
1600
500
450
400
350
300
SV9706 (EOH 199.5)
SV9702 (EOH 199.2)
SV9703 (EOH 200)
0
40
80
120
Scale 1:2000
INTERDEX
GEOLOGICAL LEGEND
Mineralised Zone
Mafic Volcanics
Sediments
Carbonaceous Sediments
Granitoids
Zones of Poor Magnetic Susceptibility
Zones of Strong Magnetic Susceptibility
DRILL HOLE LEGEND
RHS Profile : MAG
VIKING GOLD CORPORATION
Section 1700mE
Interpreted Lithology against
Downhole Magnetic Susceptibility
Anomaly Map
GEO: I.LAURENT
SCALE 1:2000
REPORT: MEconGeol
DRAWN: I.LAURENT
DATE: 20-02-2001
FIGURE: 8.13

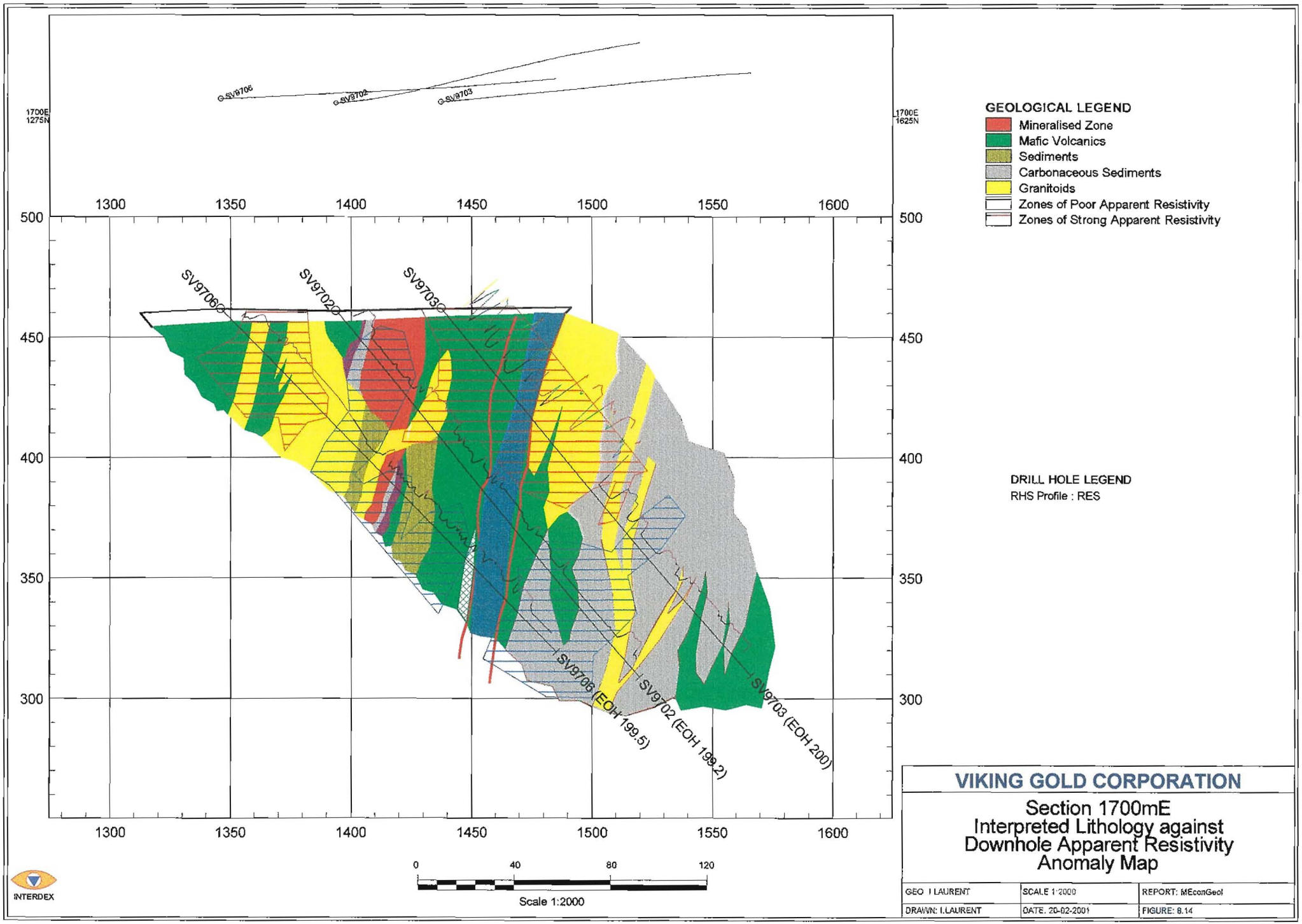
1700E
1275N
1700E
1625N
SV9706
SV9702
SV9703
1300
1350
1400
1450
1500
1550
1600
500
450
400
350
300
SV9706 (EOH 199.5)
SV9702 (EOH 199.2)
SV9703 (EOH 200)
0
40
80
120
Scale 1:2000
INTERDEX
GEOLOGICAL LEGEND
Mineralised Zone
Mafic Volcanics
Sediments
Carbonaceous Sediments
Granitoids
Zones of Poor Apparent Resistivity
Zones of Strong Apparent Resistivity
DRILL HOLE LEGEND
RHS Profile : RES
VIKING GOLD CORPORATION
Section 1700mE
Interpreted Lithology against
Downhole Apparent Resistivity
Anomaly Map
GEO I.LAURENT
SCALE 1:2000
REPORT: MEconGeol
DRAWN: I.LAURENT
DATE: 20-02-2001
FIGURE: 8.14

The induced polarisation anomaly map is overlain onto the interpreted geological section (figure 8.15). The southern zone of low chargeability correlates with the weakly foliated basalts and granitoids situated in the upper part of drillhole SV9706. The central zone (1480mN to 1520mN) represents the granitic unit located in the middle of drillhole SV9703. The northern zone (1530mN to 1570mN) consists of a mix of weakly foliated basalts and pyrrhotite-poor siliciclastic sediments present at the base of drillhole SV9703.

There is a southern and northern zone of high chargeability along section 1700mN. The southern zone (1390mN to 1440mN) correlates with the "Mineralised Zone" in drillhole SV9702 and altered wallrock in drillhole SV9706. The northern zone (1480mN to 1520mN) is confined to the pyrrhotite-bearing carbonaceous sediments found at the base of drillholes SV9702 and SV9706 and the middle of drillhole SV9703.

The combined downhole geophysical anomaly map defined in Section 7 is overlain onto the interpreted geological section (figure 8.16). There are two anomalies with red hatching representing zones of high chargeability, high magnetic susceptibility and low apparent resistivity. The southern anomaly (1390mN to 1440mN) represents the "Mineralised Zone" in drillhole SV9702 and altered wallrock in drillhole SV9706. The northern anomaly (1480mN to 1520mN) overlies pyrrhotite-bearing carbonaceous sediments found at the base of drillholes SV9702 and SV9706 and the middle of drillhole SV9703.

There are three anomalies with blue hatching representing resistive zones of low chargeability and low magnetic susceptibility. The southern and central anomalies represent predominantly granitic rocks with minor weakly foliated basalts situated in the upper part of drillhole SV9706 and middle of drillhole SV9703. The northern anomaly represents by weakly foliated basalt and pyrrhotite-poor siliciclastic sediments present at the base of drillhole SV9703.

To illustrate the correlation between downhole geophysics with lithology, lithology is plotted on a log k-log ip graph (figure 8.17), log k –log α graph (figure 8.18), and log α-log ip graph (figure 8.19).

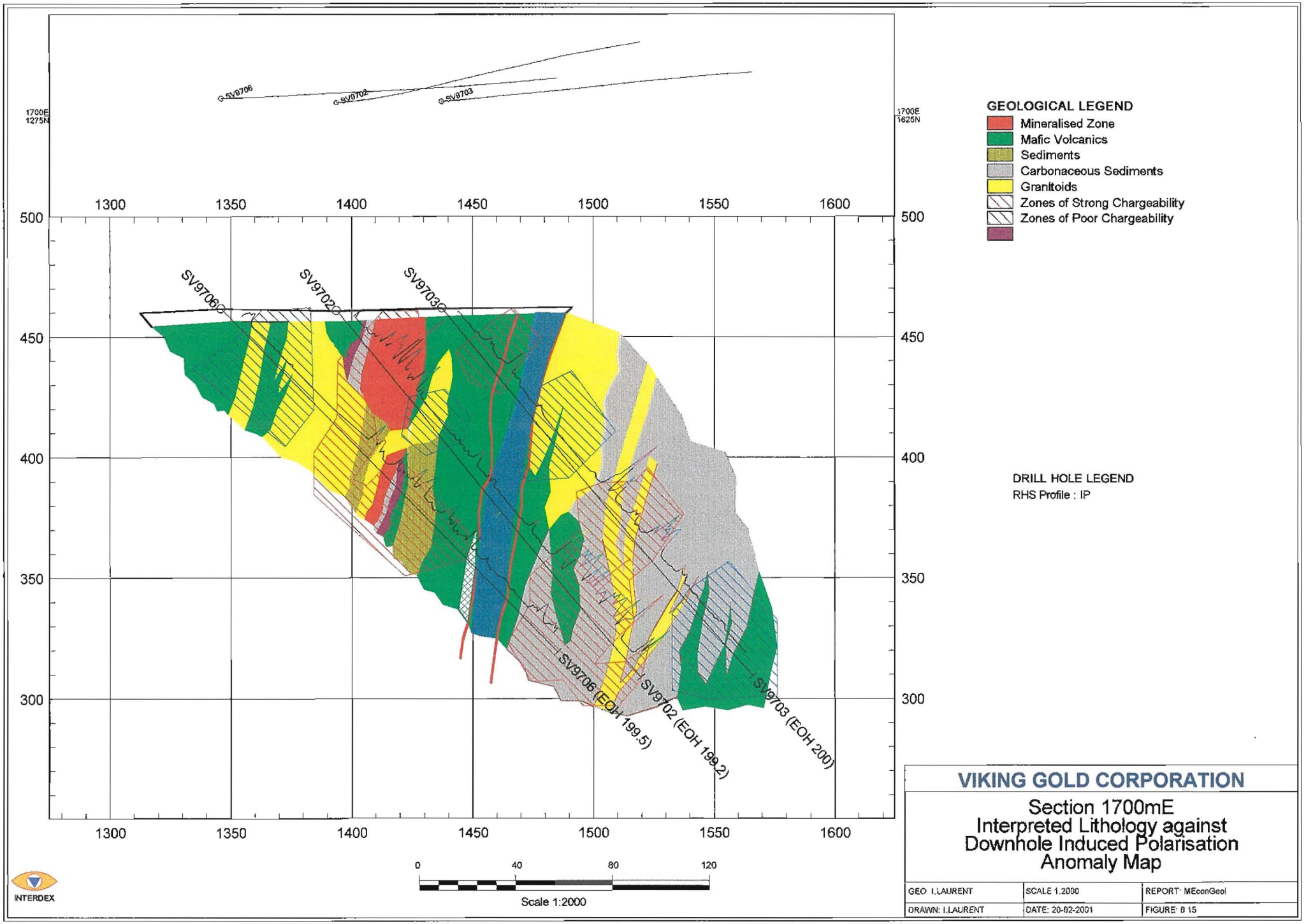
1700E
1275N
1700E
1625N
G-SV9706
G-SV9702
G-SV9703
1300
1350
1400
1450
1500
1550
1600
500
450
400
350
300
SV9706
SV9702
SV9703
SV9706 (EOH 199.5)
SV9702 (EOH 199.2)
SV9703 (EOH 200)
GEOLOGICAL LEGEND
Mineralised Zone
Mafic Volcanics
Sediments
Carbonaceous Sediments
Granitoids
Zones of Strong Chargeability
Zones of Poor Chargeability
DRILL HOLE LEGEND
RHS Profile : IP
0
40
80
120
Scale 1:2000
INTERDEX
VIKING GOLD CORPORATION
Section 1700mE
Interpreted Lithology against
Downhole Induced Polarisation
Anomaly Map
GEO I.LAURENT
SCALE 1:2000
REPORT: MEconGeol
DRAWN: I.LAURENT
DATE: 20-02-2001
FIGURE: 8.15

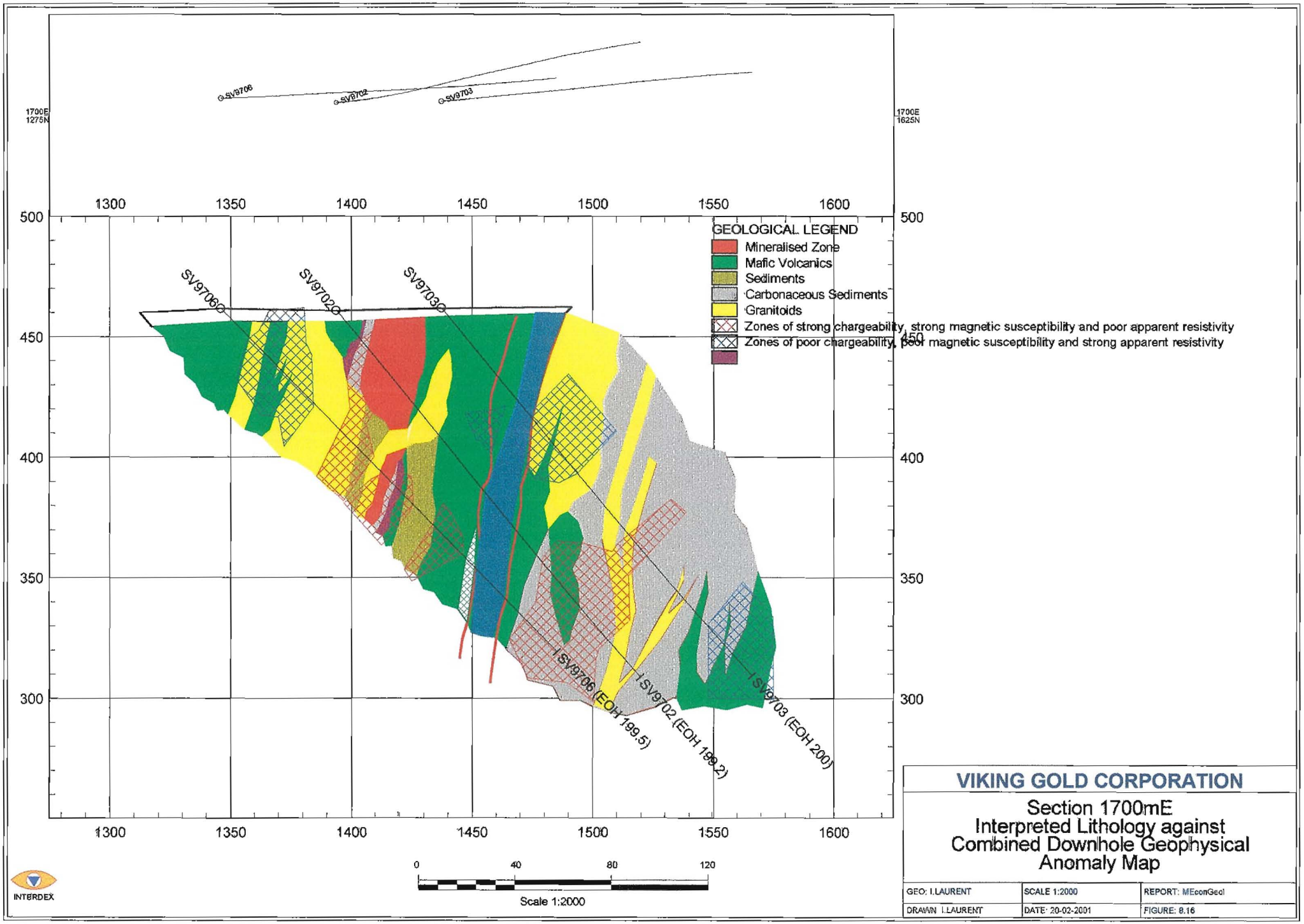
1700E
1275N
1700E
1625N
SV9706
SV9702
SV9703
1300
1350
1400
1450
1500
1550
1600
500
450
400
350
300
GEOLOGICAL LEGEND
Mineralised Zone
Mafic Volcanics
Sediments
Carbonaceous Sediments
Granitoids
Zones of strong chargeability, strong magnetic susceptibility and poor apparent resistivity
Zones of poor chargeability, poor magnetic susceptibility and strong apparent resistivity
SV9706 (EOH 199.5)
SV9702 (EOH 199.2)
SV9703 (EOH 200)
0
40
80
120
Scale 1:2000
INTERDEX
VIKING GOLD CORPORATION
Section 1700mE
Interpreted Lithology against
Combined Downhole Geophysical
Anomaly Map
GEO: I.LAURENT
SCALE 1:2000
REPORT: MEconGeol
DRAWN I.LAURENT
DATE: 20-02-2001
FIGURE: 8.16

On the log k-log IP graph, the lithology separates into 4 domains (figure 8.17). Weakly foliated volcanic rocks have low chargeability and low magnetic susceptibility. This unit is found at the top of drillhole SV9706 and at the base of drillhole SV9703. This unit represents the southern and northern limits of the Svartliden Shear Zone. The granitic rocks form in a domain of expected poor chargeability with a small range of magnetic susceptibility. This small range of magnetic susceptibility in the granitic rocks represent the strongly altered, pyrrhotite-bearing granitic dykes strongly associated with the "Mineralised Zone".

Basaltic rocks have a moderate to high magnetic susceptibility and low to moderate chargeability. The rocks with lowest chargeability represent the magnetite-bearing foliated basalts. Whereas the basaltic rocks that have moderate chargeability are associated with the pyrrhotite-bearing "Mineralised Zone" as part of the altered wallrock. The sedimentary rocks and the "Mineralised Zone" have the highest chargeability and magnetic susceptibility. The sedimentary rocks cannot be separated from the pyrrhotite-bearing sedimentary unit, and the altered sediments associated with the "Mineralised Zone" on the basis of their geophysical characteristics.

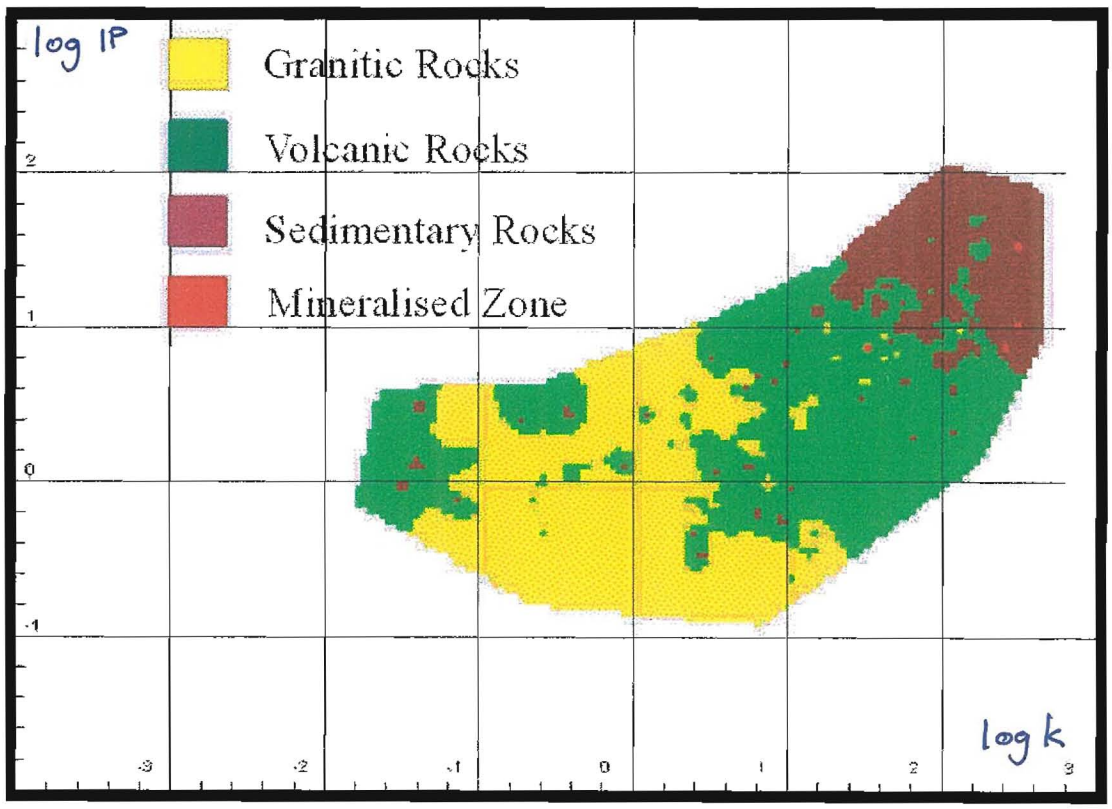

Figure 8.17 Lithology from drillholes SV9702, SV9703 & SV9706 plotted on a log k-log ip graph.
$\Sigma_x = 5{,}709$

On the log k-log α graph, the lithology can be separated into three domains (figure 8.18). The granitic rocks have the highest apparent resistivity and have a small range in magnetic susceptibility. The volcanic rocks have a moderate to high apparent resistivity, and a wide range of magnetic susceptibility.

The resistive volcanic rocks fall within the Svartliden Shear Zone but are not directly associated with the "Mineralised Zone". The volcanic rocks with moderate apparent resistivity have high magnetic susceptibility due to wallrock alteration associated with the "Mineralised Zone".

The sedimentary rocks and the "Mineralised Zone" have the highest magnetic susceptibility and lowest apparent resistivity. The conductive nature of the sedimentary rocks is due to a) the elevated pyrrhotite and graphite content, and b) the high porosity not found in the other lithologies.

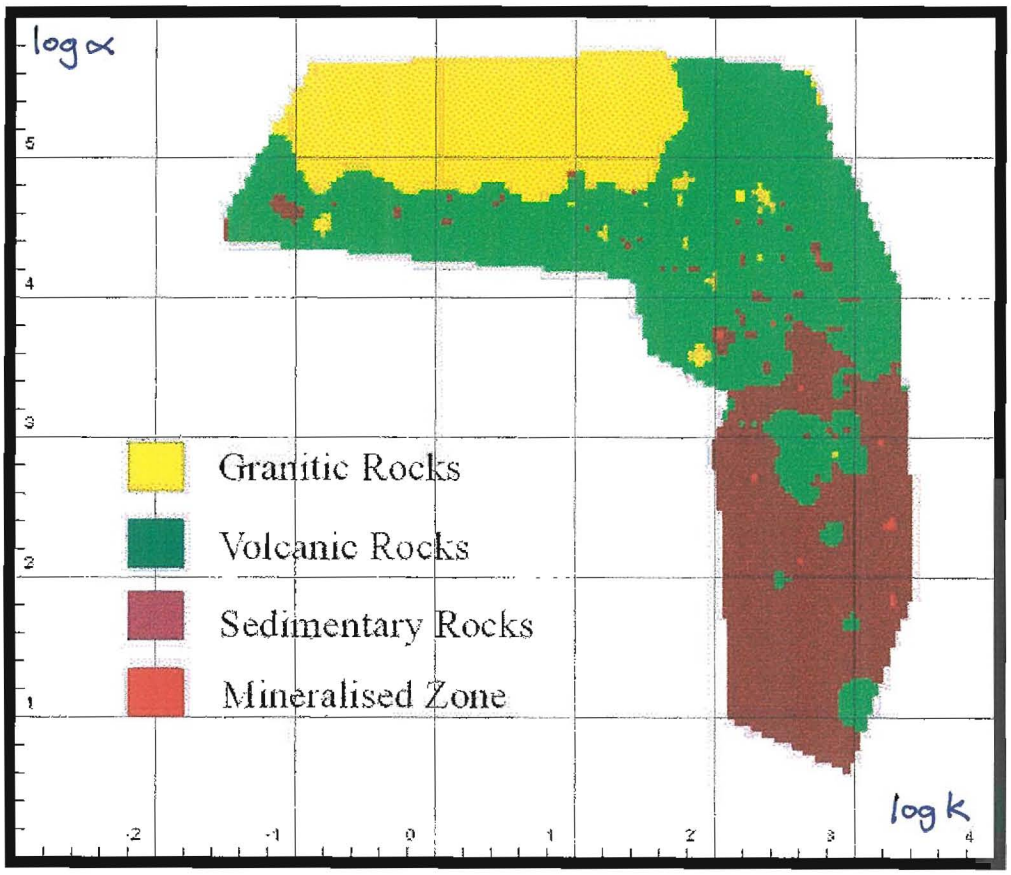

Figure 8.18 Lithology from drillholes SV9702, SV9703 & SV9706 plotted on a log k-log α graph. $\Sigma_x = 5{,}709$

There were three clear domains in the log α-log ip graph (figure 8.19). The sedimentary rocks and the "Mineralised Zone" have low to moderate apparent resistivity with a zone of high chargeability. The amount of pyrrhotite determines the conductive nature of the sedimentary rocks and hence influences the apparent resistivity.

The volcanic rocks decrease in chargeability as they increase in apparent resistivity. The least altered sulphide-poor volcanic rocks are highly resistive. The moderate chargeabilities observed in volcanic rocks result from an increase in alteration and introduction of remobilised pyrrhotite. These volcanic rocks are part of the altered wallrock (strongly associated to the "Mineralised Zone").

The granitic rocks have the highest apparent resistivity and corresponding low chargeability. The crystalline nature and inherent lack of sulphides in the granitic rocks explains its resistive response.

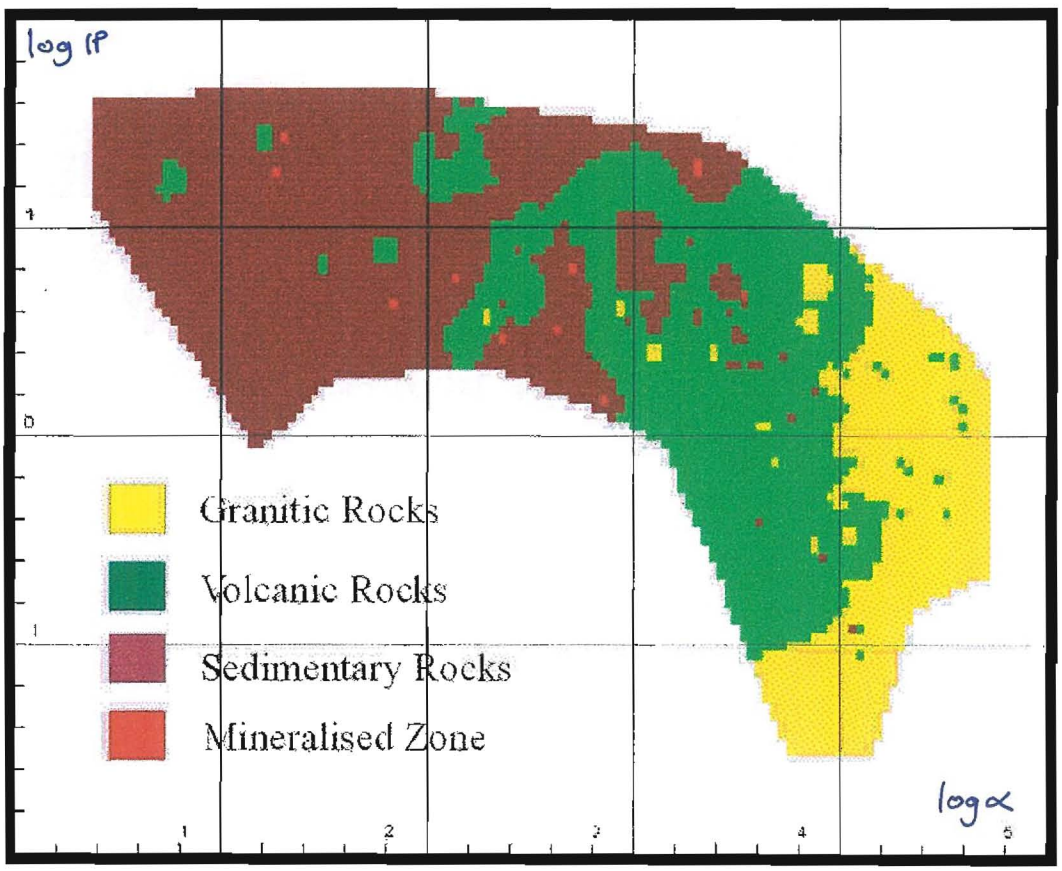

Figure 8.19 Lithology from drillholes SV9702, SV9703 & SV9706 plotted on a log α-log ip graph. $\Sigma_x = 5{,}709$

8.1.3 Synthesis

Magnetic and log magnetic profiles of ground geophysical data show that the anomalous magnetic areas overlap stratigraphic units. The magnetic field is dependent on a combination of the magnetite and magnetic-pyrrhotite content and there is no simple lithological or structural control.

The in-phase EM profiles distinguish the "Mineralised Zone" and carbonaceous sediments from the remaining lithologies within the shear zone. The log in-phase EM profiles delineate the anomalous conductivity of the carbonaceous sediments from the less conductive "Mineralised Zone". The pyrrhotite-bearing carbonaceous sediments produce a first-order in-phase EM anomaly, whilst the "Mineralised Zone" produces a second-order in-phase EM response. The limits of the second-order signal were statistically defined using probablility plots, and used to produce a second-order in-phase EM anomaly map that is overlain by the interpreted geological map (figure 8.20).

West of the 1750mE, there is a strong correlation between the "Mineralised Zone" (traceable from drillhole to drillhole) and the second-order anomalies. The quadrature and log quadrature profiles delineate the shear zone but the response is too broad to clearly identify the individual conductive units such as the carbonaceous sediments or the "Mineralised Zone". The EM ratio profiles accentuate the strong in-phase anomalies such as the carbonaceous sediments. The overall conductivity east of 1750mE is low because of the granitoid units are thicker and near surface. On Section 1700mE, the interpreted geological section was confirmed by three downhole geophysical techniques. The carbonaceous sediments and the "Mineralised Zone" have coincident high chargeability and magnetic susceptibility. These units are also highly conductive. The granitic units, in contrast, have low chargeability and magnetic susceptibility and are highly resistive. The IP anomalies inversely correlate with the apparent resistivity anomalies.

The ground in-phase EM conductive anomalies display a positive correlation with downhole IP anomalies but a negative correlation with the downhole apparent resistivity anomalies. Both EM and IP methods can distinguish the carbonaceous sediments on the northern footwall and the "Mineralised Zone" from the remaining lithologies.

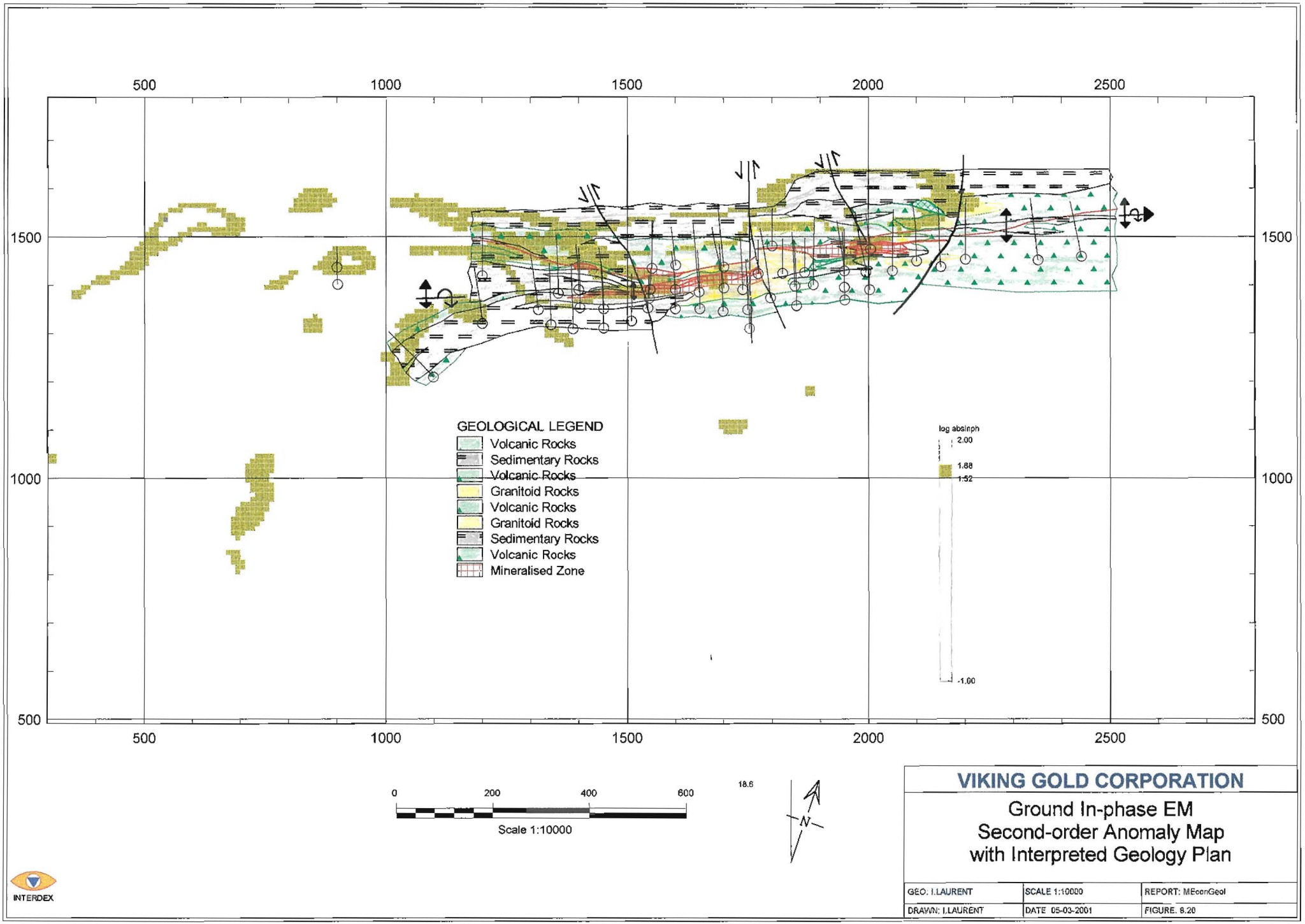

INTERDEX

VIKING GOLD CORPORATION

Ground In-phase EM Second-order Anomaly Map with Interpreted Geology Plan

GEO. I.LAURENT	SCALE 1:10000	REPORT: MEconGeol
DRAWN: I.LAURENT	DATE 05-03-2001	FIGURE. 8.20

8.2 MINERALISATION AND ALTERATION

The alteration system, defined in Section 6, consists of five discrete domains. Alteration is important since it readily delineates the sub-vertical shear zone that cross-cuts lithological boundaries.

Four stacked sections were created to best illustrate the relationship between ground geophysical profiles and drillhole alteration and mineralisation. An interpretation of the mineralisation and alteration on Section 1700mE is correlated with the downhole geophysics. The four stacked sections have a window of ±100m, capturing all the ground geophysical profiles and drillholes within a 5ha area.

The 32 multi-element ICP assay data was used to determine the mass proportion, in parts per million (ppm), of pyrrhotite, arsenopyrite, loellingite, and argentite per metre in each drillhole to enable direct correlation with geophysical data. Pyrite is only a trace sulphide and hence only pyrrhotite was calculated. Calculations are tabulated in Appendix 8.

Pyrrhotite was calculated, as this is the most pervasive sulphide encountered through the entire shear zone. Pyrrhotite is present as a primary magmatic/sedimentary mineral in the carbonaceous sediments and as a remobilised hydrothermal mineral in the "Mineralised Zone" (predominantly in Type A and B alteration) and altered wallrock (Type C1 and C2 alteration). Pyrrhotite is a magnetic mineral, which can be chargeable. High conductivity is possible if the pyrrhotite has an interlocking platy crystal morphology. Cubic pyrrhotite is not as conductive or chargeable.

Arsenopyrite and Loellingite are the primary indicator sulphide minerals associated with gold mineralisation. The presence of arsenopyrite indicates Type A and B alteration.

Argentite was calculated to determine the amount of silver and its distribution within the alteration system. Argentite is usually associated with trace galena and forms at lower pressures and temperatures than gold. At a project scale, silver mineralisation is enriched around the margins of the shear zone (McCuaig, 2000).

8.2.1 Ground Geophysics

Stacked sections showing drillhole alteration and images, calculated for pyrrhotite and "Total Mineralisation", are plotted against the ground geophysical profiles. The "Total Mineralisation" combines gold, arsenopyrite, loellingite and argentite. The pyrrhotite and "Total Mineralisation" are measured in parts per million (ppm). The pyrrhotite and "Total Mineralisation" images are used only as an indication of the concentration of these metals over a 5ha area. The 50m spacing between drill sections is too wide to allow definition of the volume or mass content of metals between each section. The anomalies generated from these images, however, can be used to explain the ground geophysical anomalies.

The magnetic field displays positive anomalies across the entire shear zone. There is weak magnetic anomalism over the Type A and B alteration zones due to the magnetic-pyrrhotite content that has remobilised into the shear zone. The strongest peaks correspond with the Type C1 and C2 alteration (blue and yellow field in figure 8.21). This strong magnetic anomalism corresponds to the northern pyrrhotite zone, situated along the 1500mN (figure 8.22). The zones of highest "Total Mineralisation" correlate poorly with the ground magnetic anomalies and this is primarily dependent on the pyrrhotite content within the "Mineralised Zone" (figure 8.23).

The log magnetic profiles display an elevated response across the shear zone covering Type A, B and C1 alteration (figure 8.24). The northern pyrrhotite-bearing sedimentary unit is of a Type C2 alteration and, also, displays a strong log magnetic response. The strongest log magnetic peaks correlate with the pyrrhotite-rich anomalies (figure 8.25). There is little correlation between the strongest log magnetic anomalies and the zones of highest "Total Mineralisation" (figure 8.26).

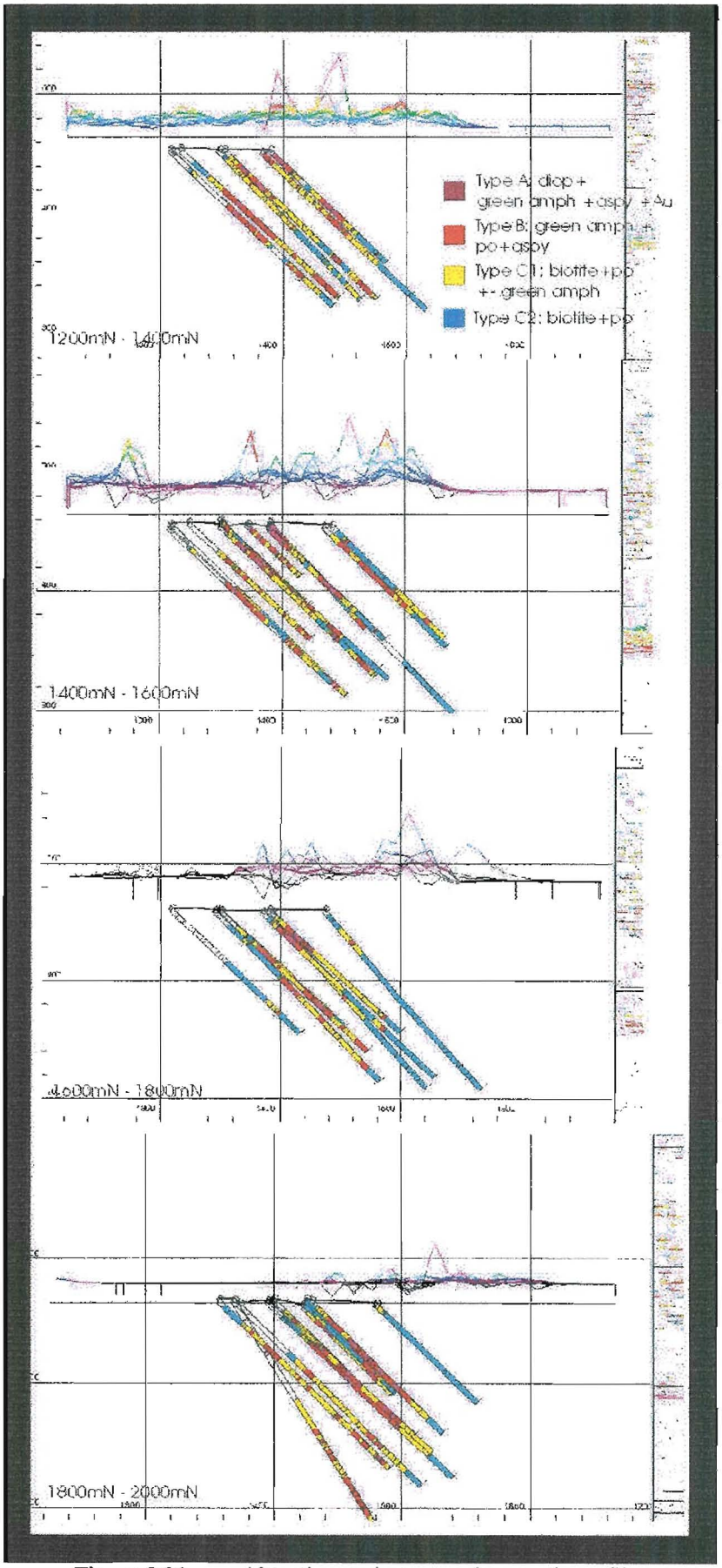

Figure 8.21 Alteration against ground magnetic profiles

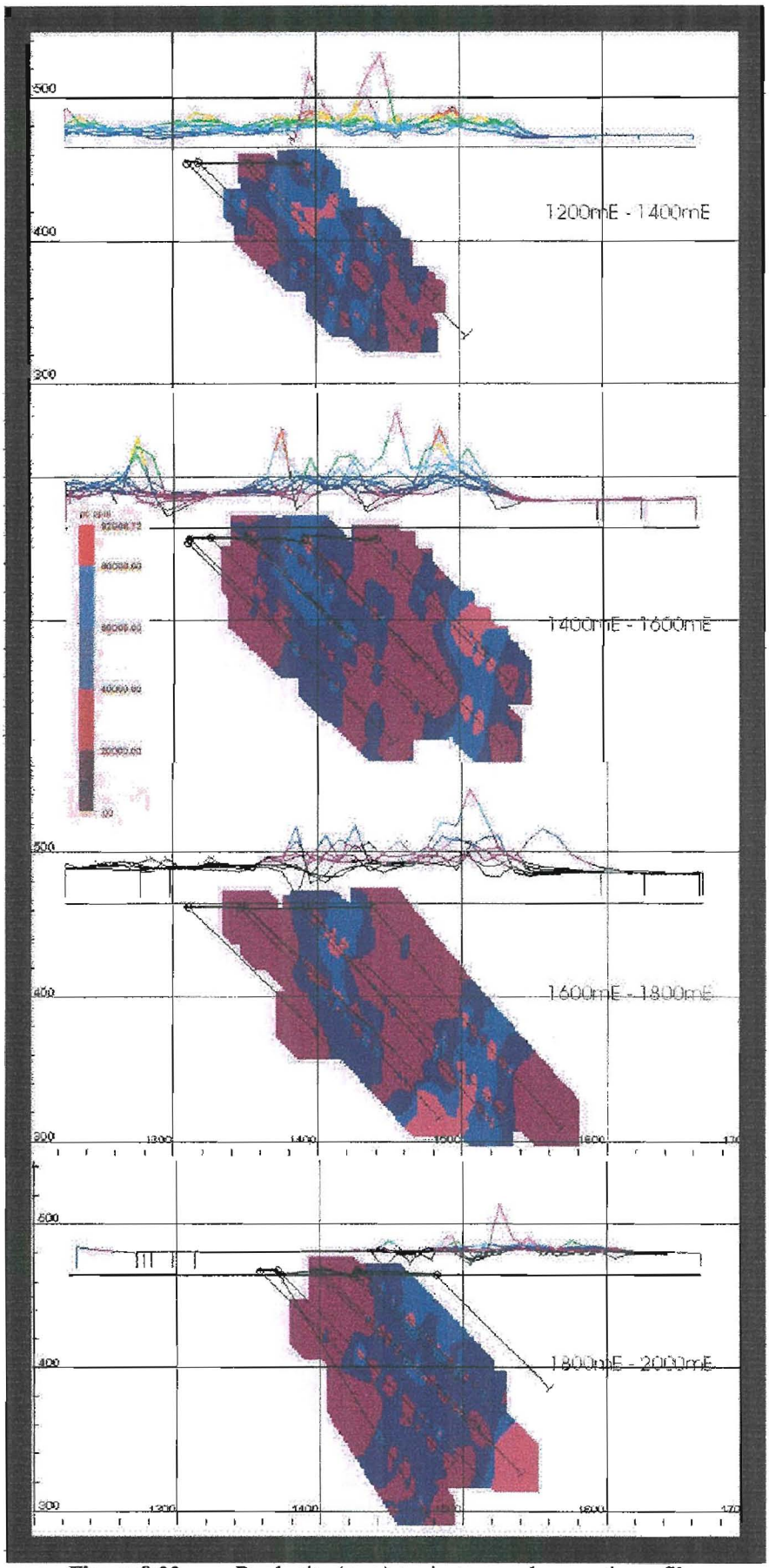

Figure 8.22 Pyrrhotite (ppm) against ground magnetic profiles

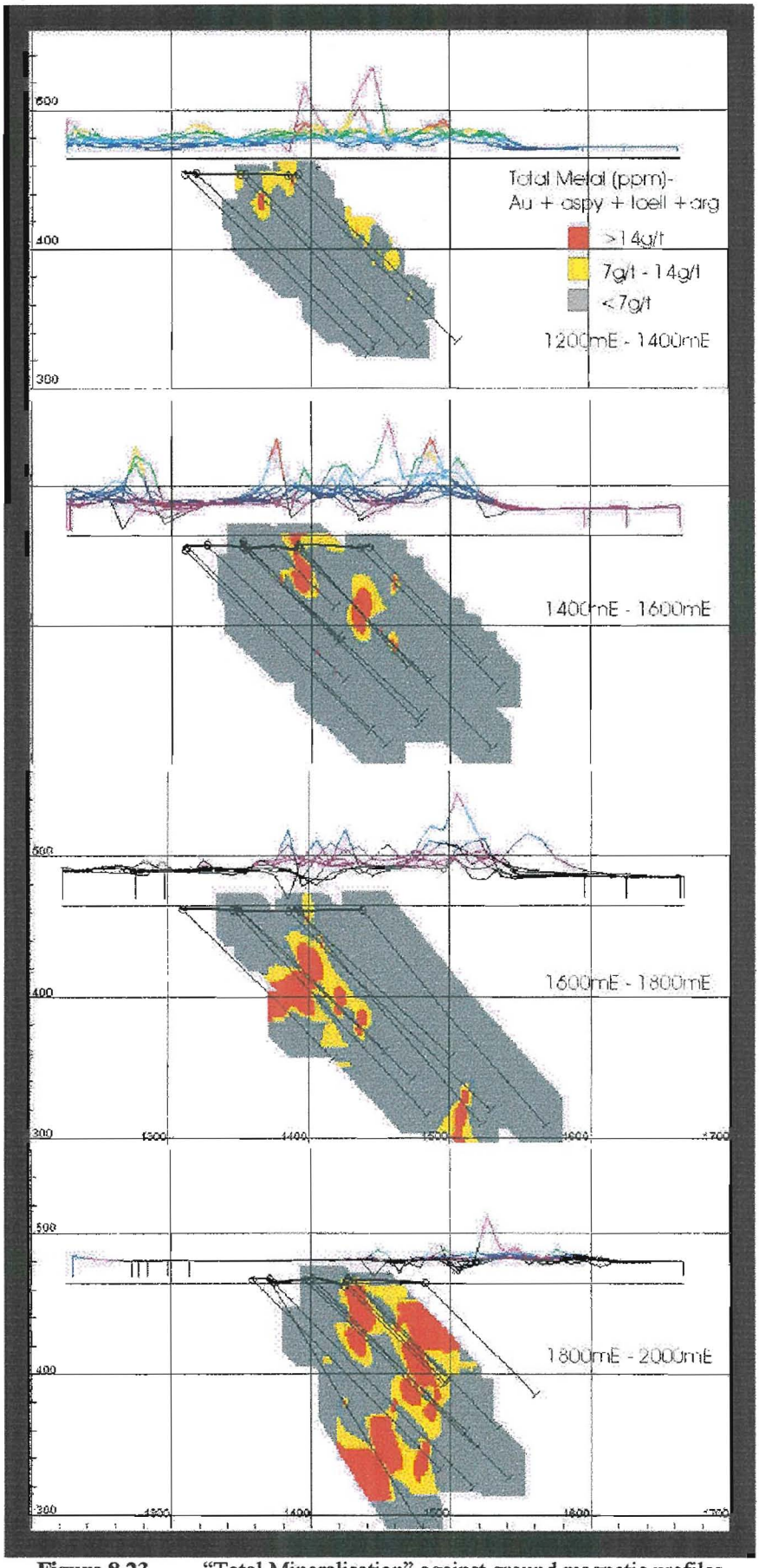

Figure 8.23 "Total Mineralisation" against ground magnetic profiles

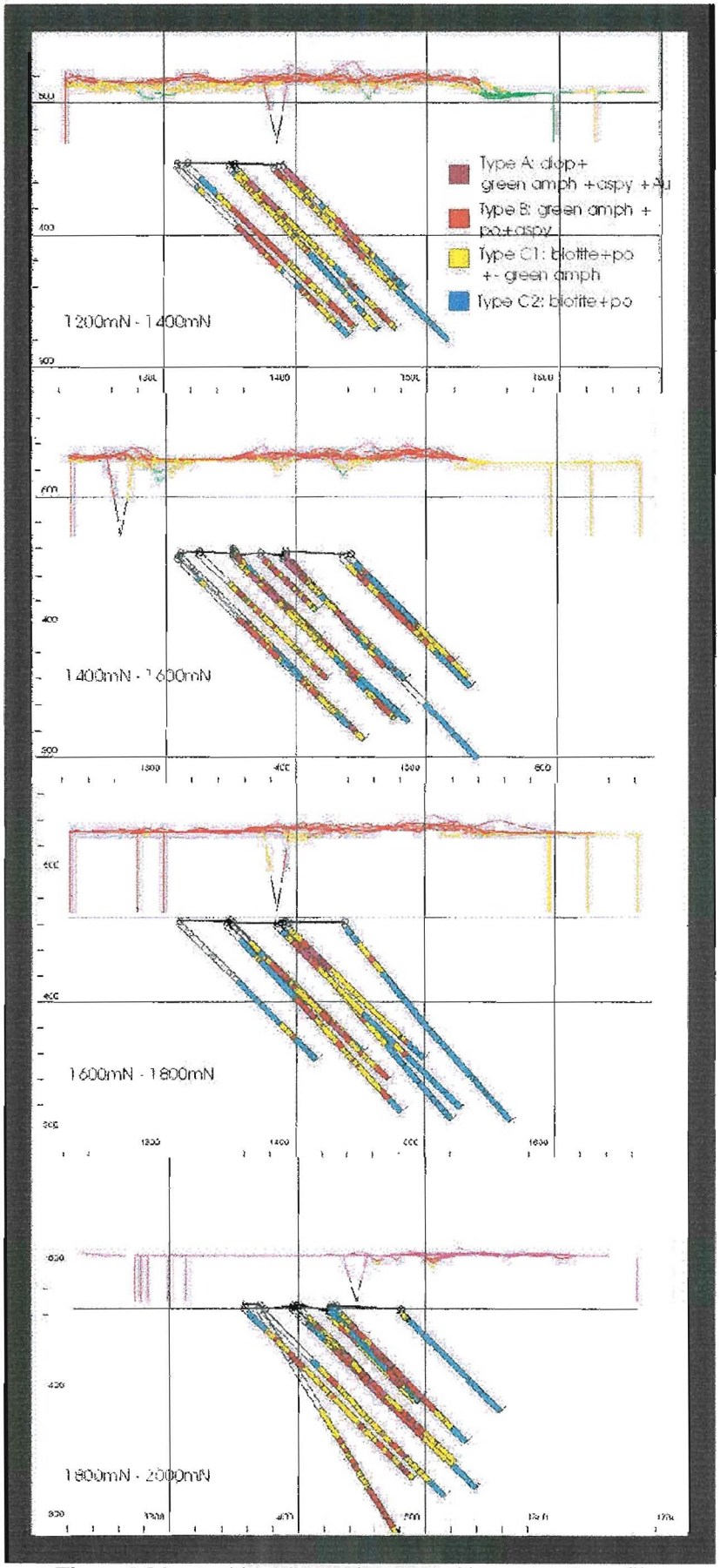

Figure 8.24 Alteration against ground log magnetic profiles

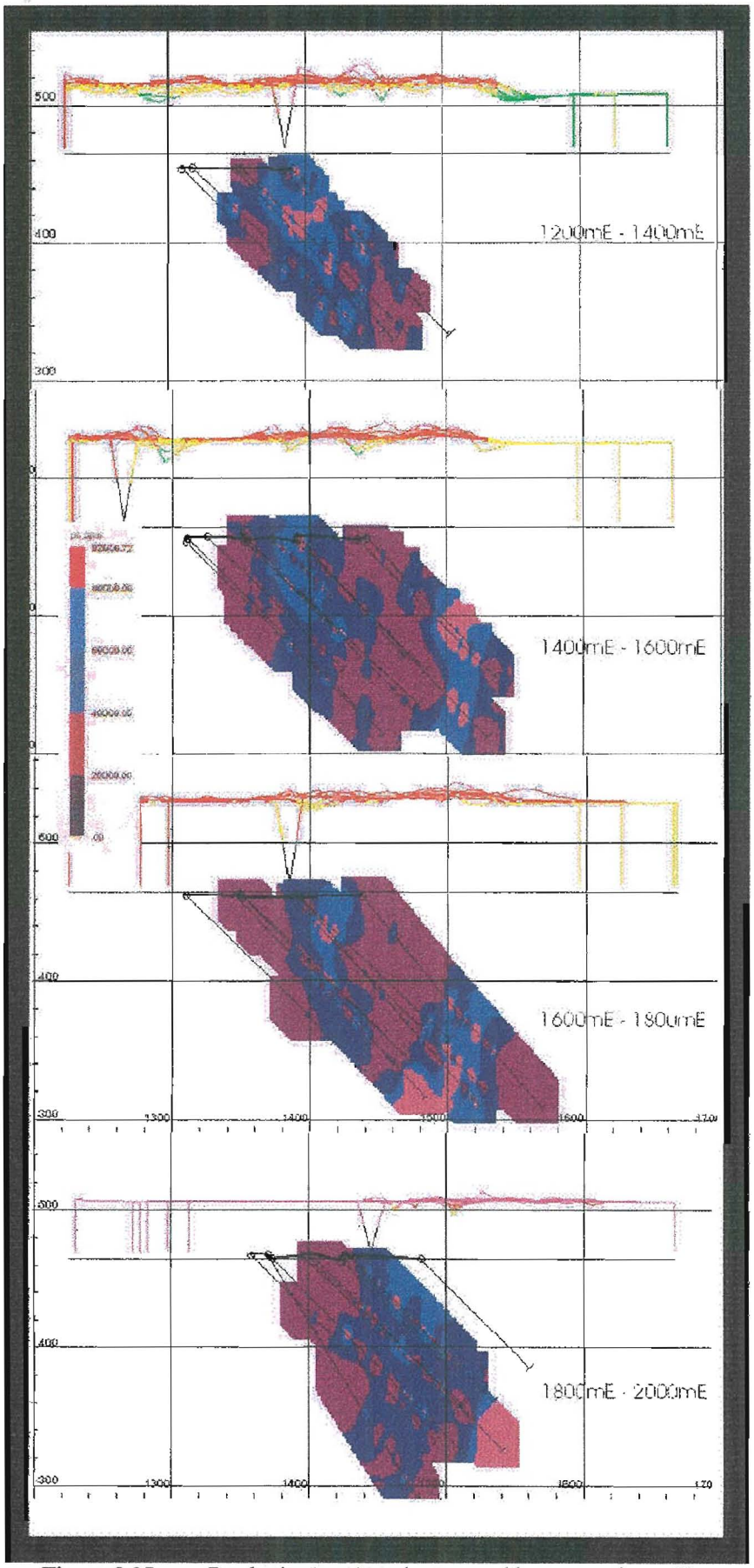

Figure 8.25 Pyrrhotite (ppm) against ground log magnetic profiles

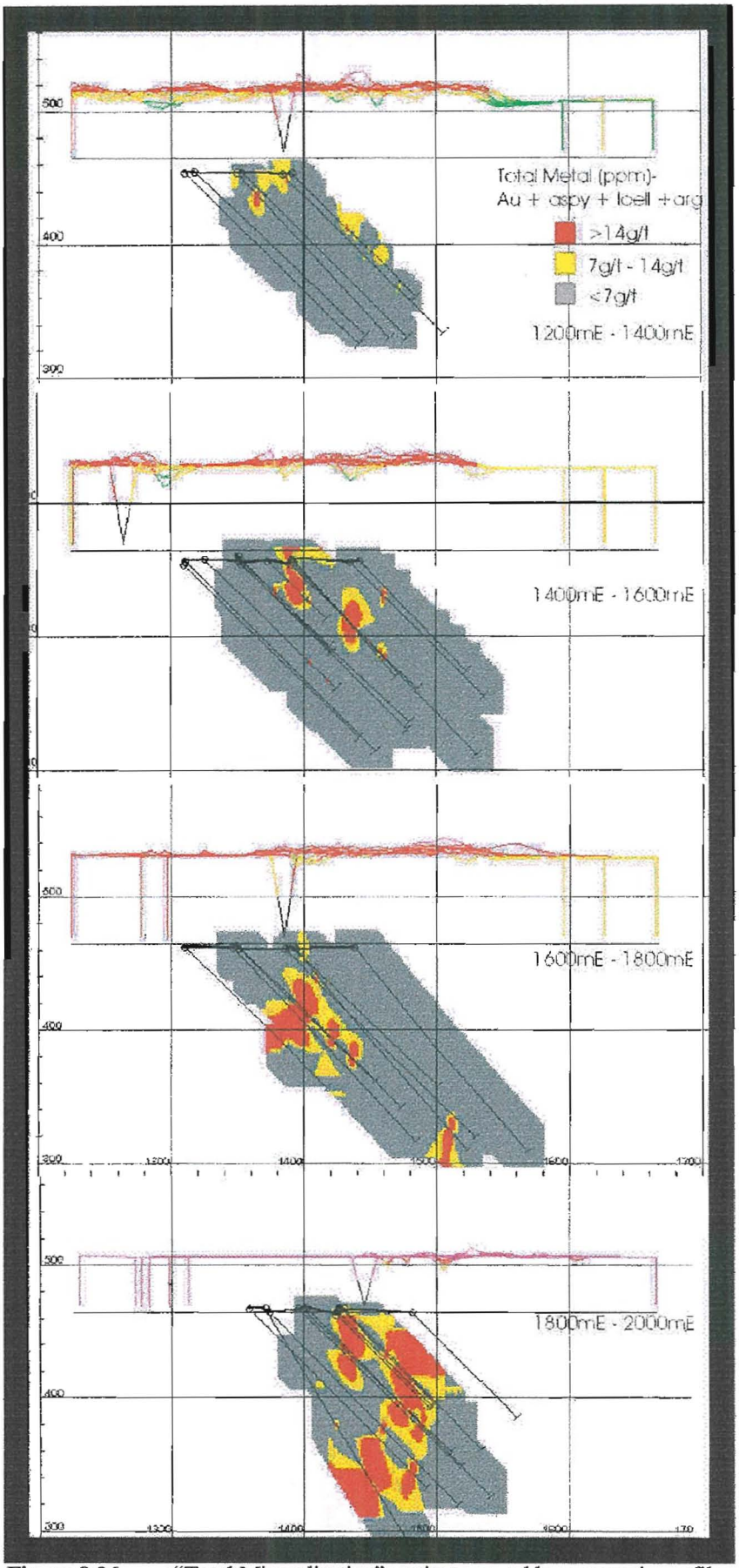

Figure 8.26 "Total Mineralisation" against ground log magnetic profiles

The in-phase EM profiles delineate two highly conductive zones. The southern zone correlates with Type A and B alteration. The northern zone is coincident with Type C2 alteration (figure 8.27). The two conductive zones correlate clearly with the two distinct pyrrhotite-rich anomalies (figure 8.28). The highest concentration of "Total Mineralisation" is situated within the southern conductive zone around the 1400mN (figure 8.29).

The log in-phase EM profiles delineate and differentiate the two highly strong conductive zones. The northern conductive zone is a first-order anomaly and the southern conductive zone is a second order anomaly. The southern zone is represented by Type A and B alteration, whilst the northern zone displays C1 and C2 alteration (figure 8.30). The pyrrhotite content in both zones is comparable. The pyrrhotite is aligned along the foliation plane within the more porous carbonaceous sediments along the 1500mN and therefore allows greater conductivity through this unit than in the strongly siliceous second-order southern conductive anomaly (figure 8.31). The "Total Mineralisation" is coincident with the second-order log in-phase EM anomaly (figure 8.32).

The quadrature and log quadrature EM profiles display a broad conductive anomaly that covers the entire shear zone with Type A, B and C1 alteration (figure 8.33 & figure 8.36). The stronger conductive zones are coincident with the pyrrhotite-rich zones much like the in-phase EM conductive anomalies (figure 8.34 & figure 8.37). The "Total Mineralisation" is coincident with the southern end of the broad conductive anomaly (figure 8.35 & figure 8.38).

The EM ratio profiles show an overall conductive response across the entire shear zone. The strongest EM ratio responses represent zones of high in-phase EM response but lower quadrature EM. The entire alteration sequence is within the strong EM ratio response (figure 8.39). The pyrrhotite-rich zones are coincident with the elevated EM ratio response (figure 8.40). "Total Mineralisation" does not have a direct correlation with the EM ratio response (figure 8.41).

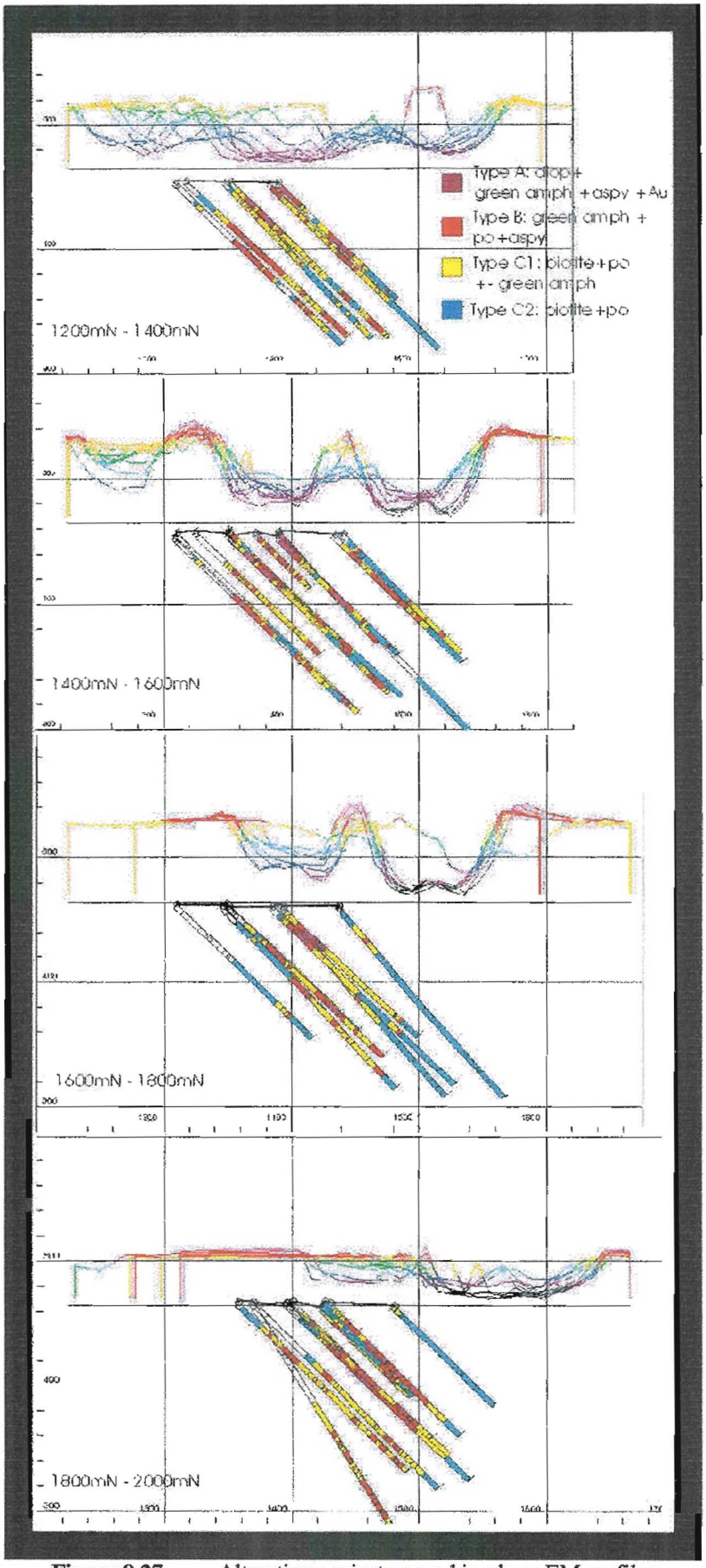

Figure 8.27 Alteration against ground in-phase EM profiles

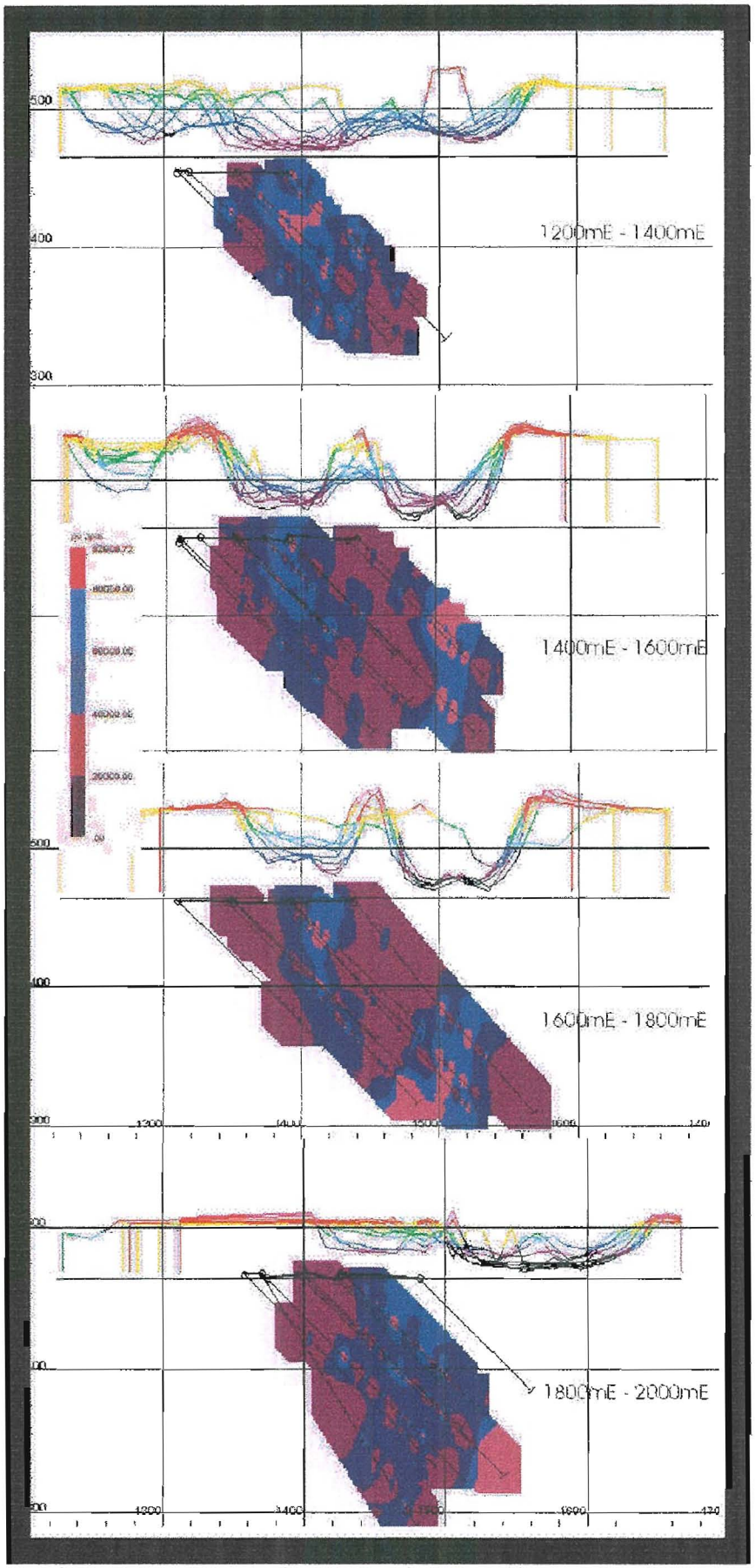

Figure 8.28 Pyrrhotite (ppm) against ground in-phase EM profiles

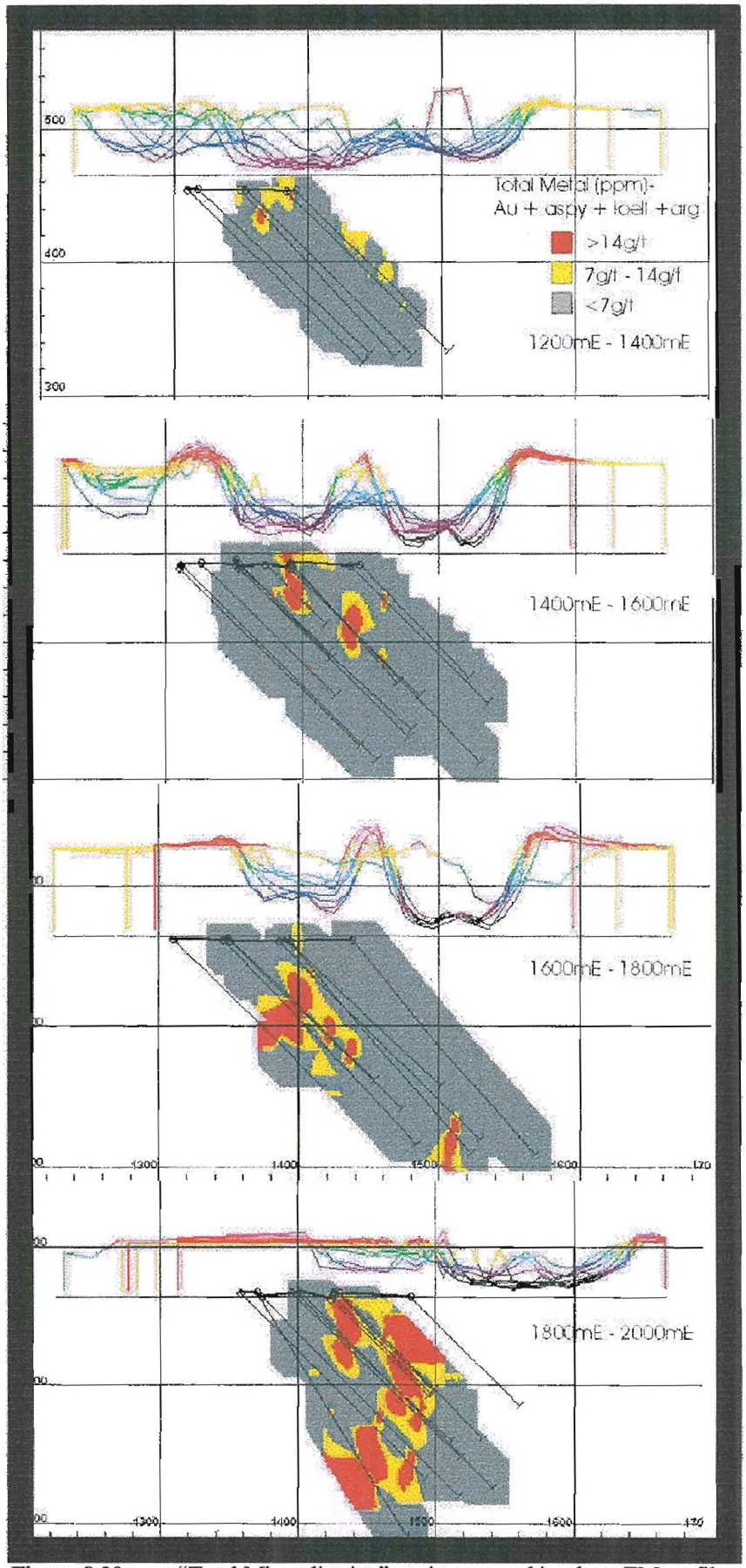

Figure 8.29 "Total Mineralisation" against ground in-phase EM profiles

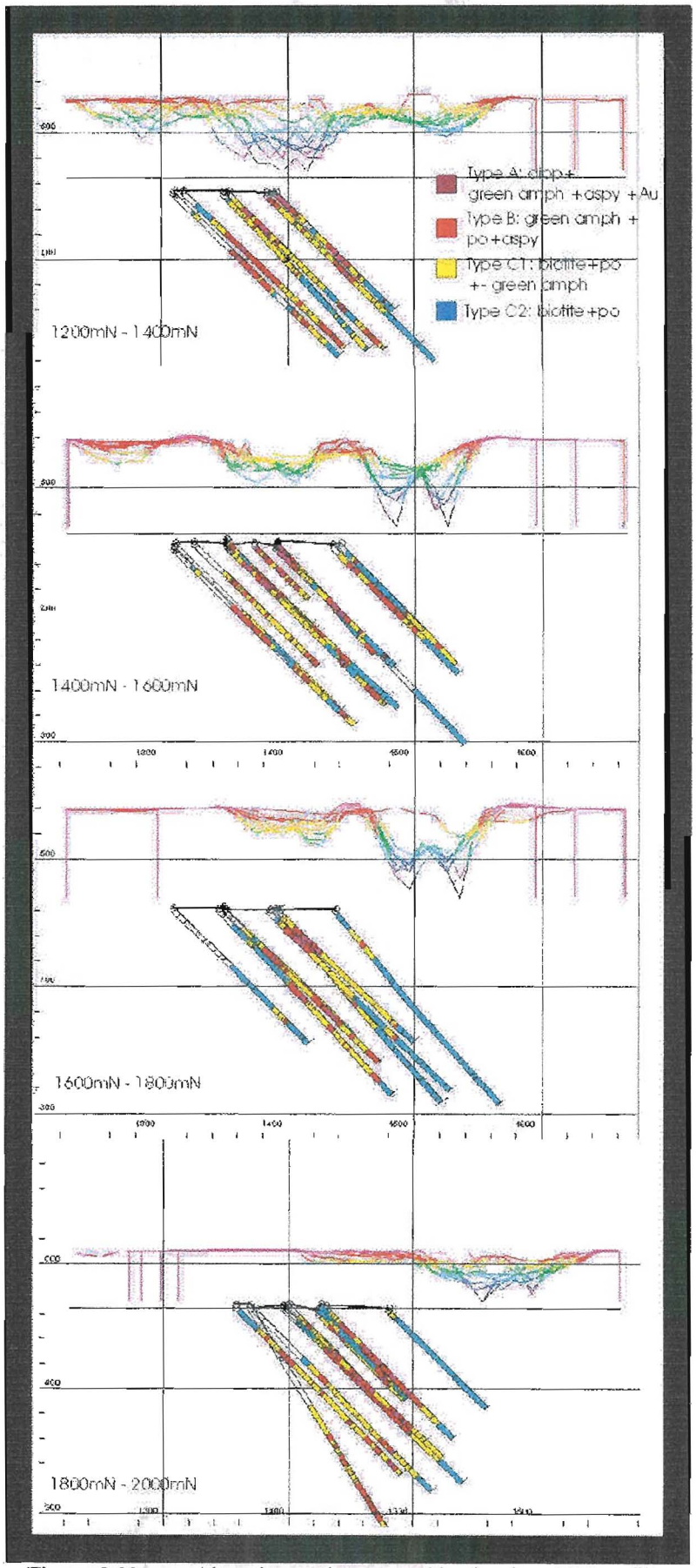

Figure 8.30 Alteration against ground log in-phase EM profiles

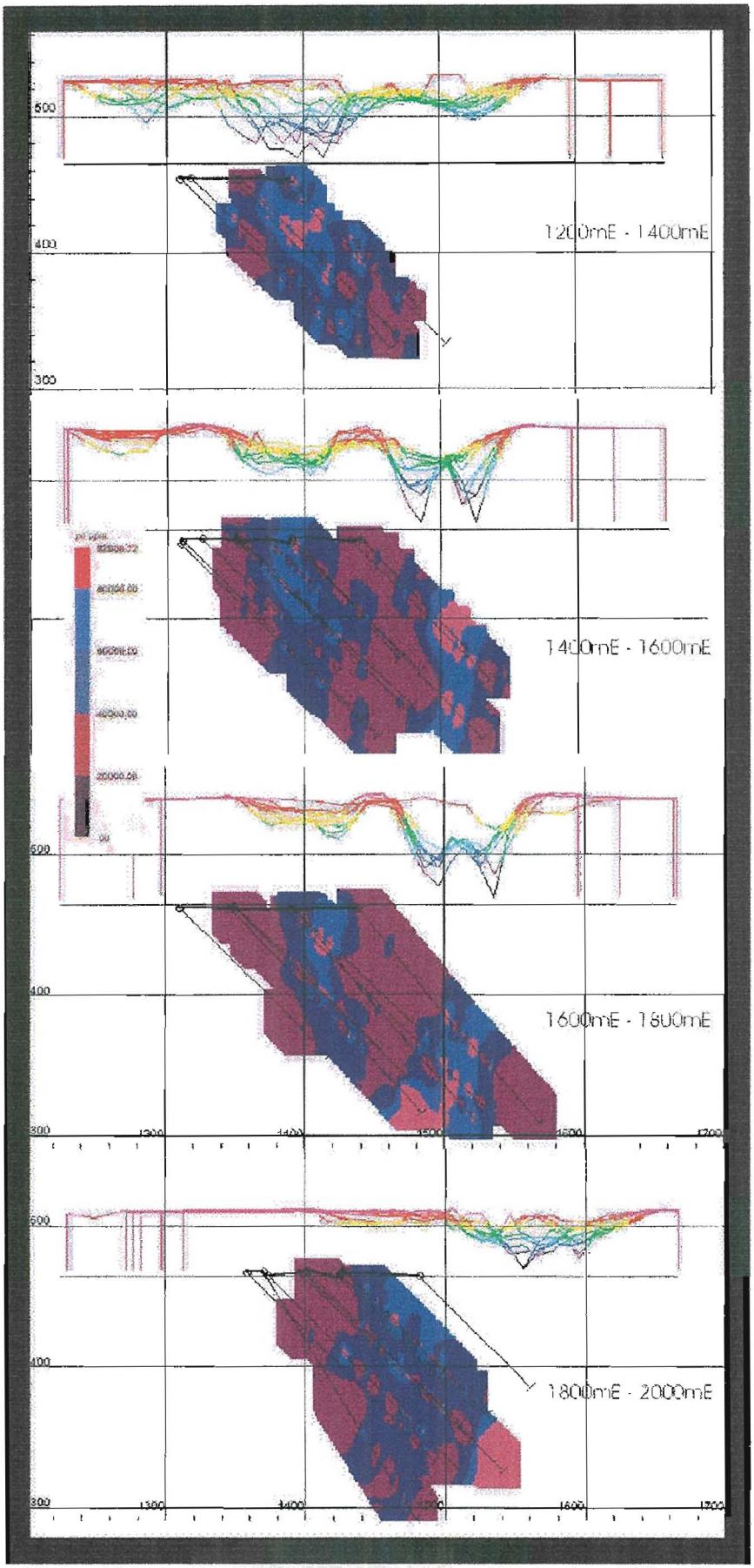

Figure 8.31 Pyrrhotite (ppm) against ground log in-phase EM profiles

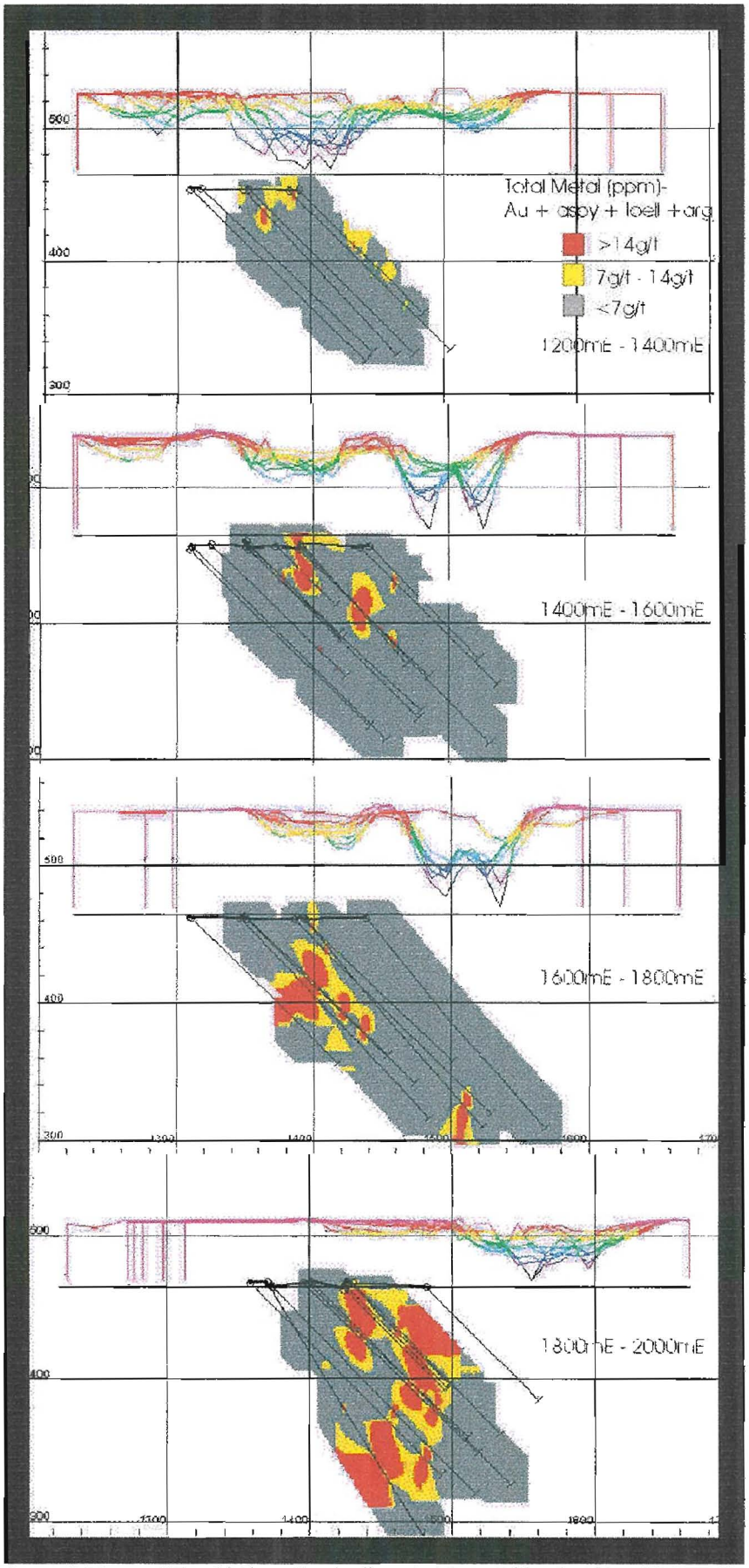

Figure 8.32 "Total Mineralisation" against ground log in-phase EM profiles

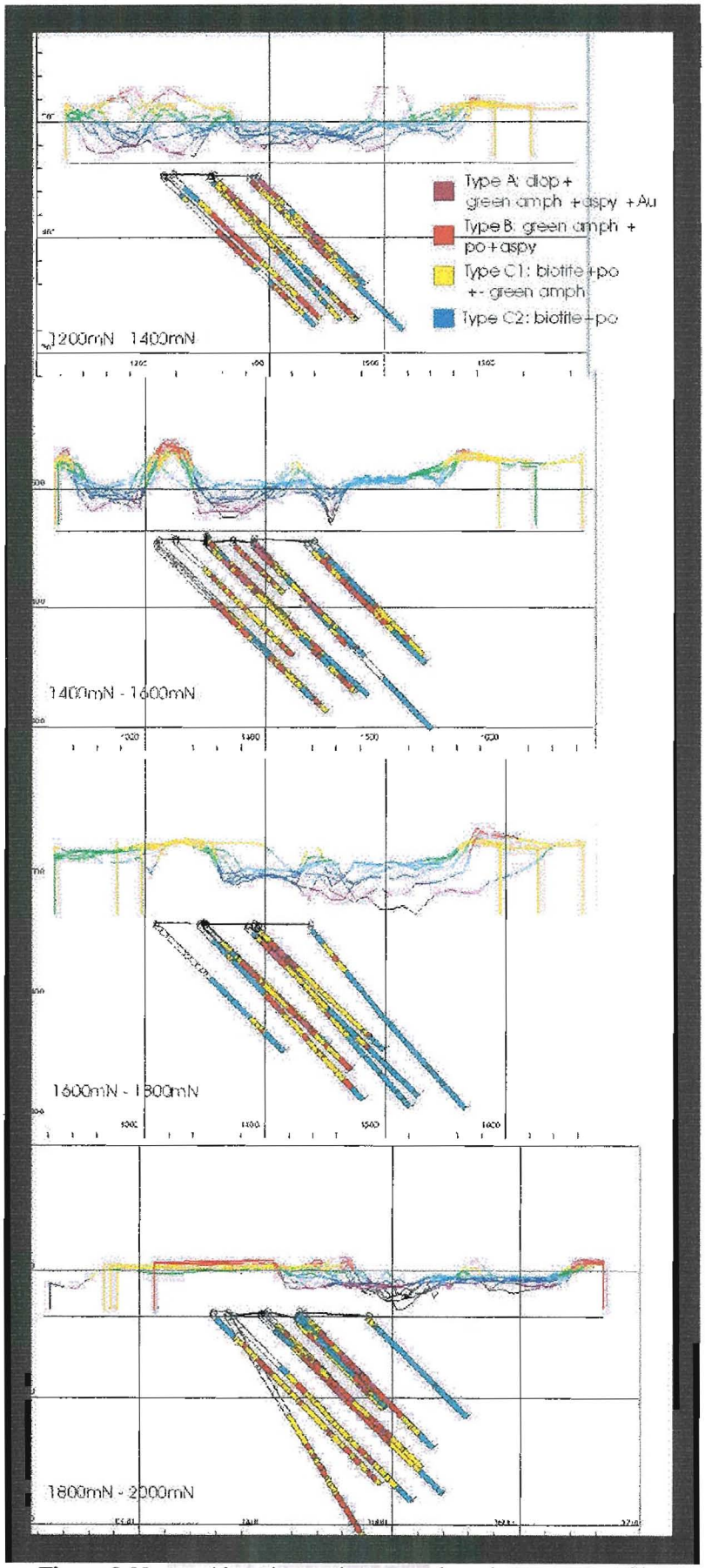

Figure 8.33 Alteration against ground quadrature EM profiles

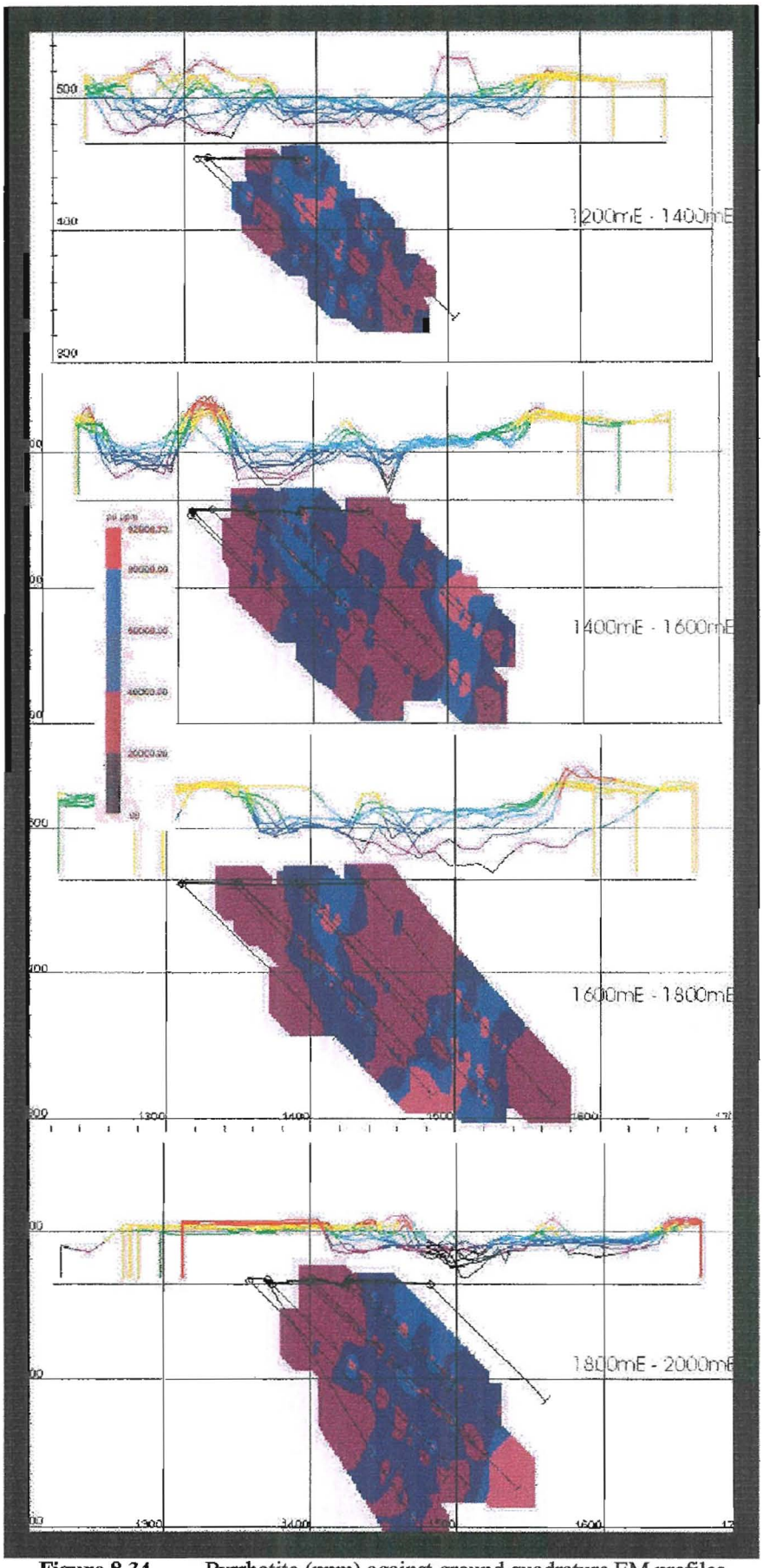

Figure 8.34 Pyrrhotite (ppm) against ground quadrature EM profiles

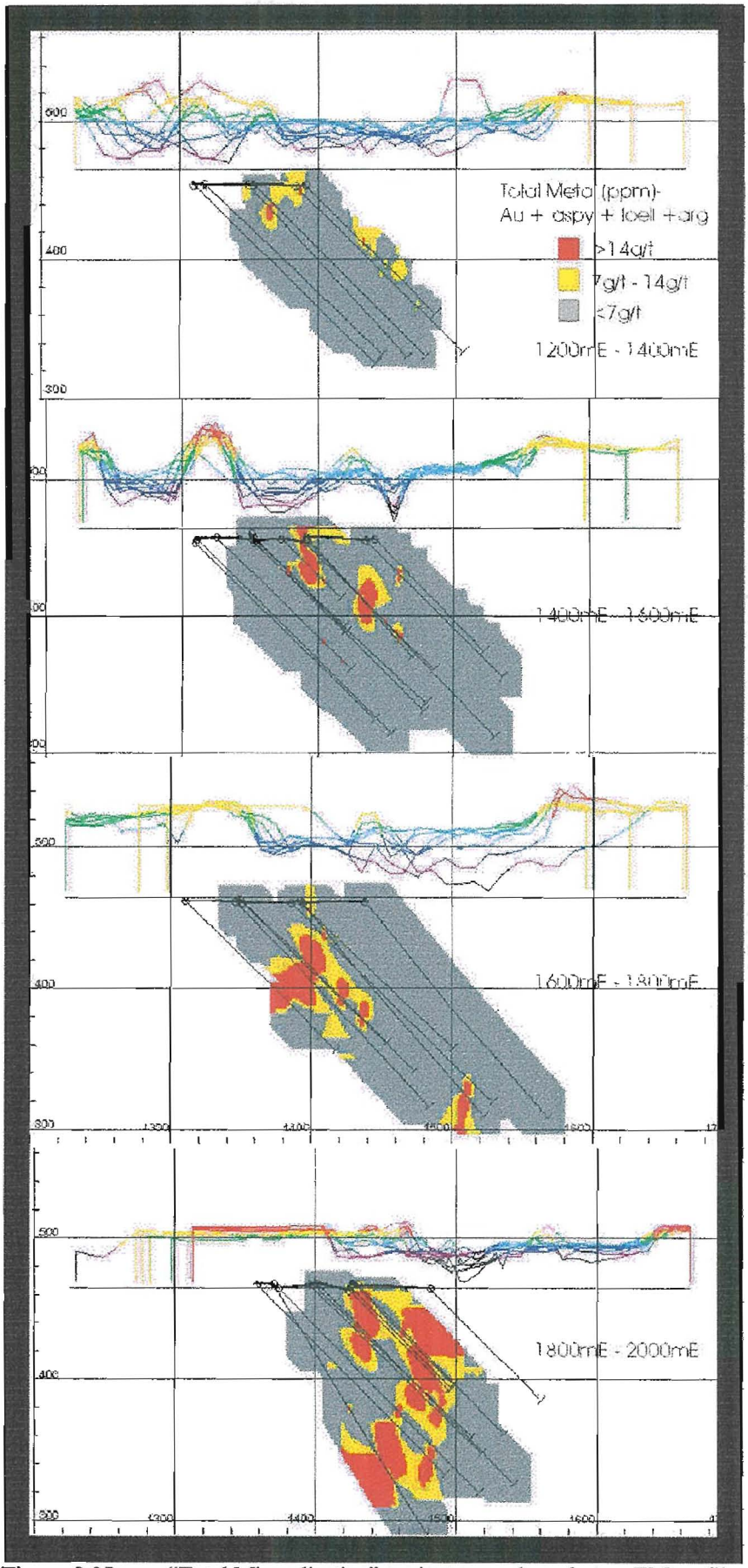

Figure 8.35 "Total Mineralisation" against ground quadrature EM profiles

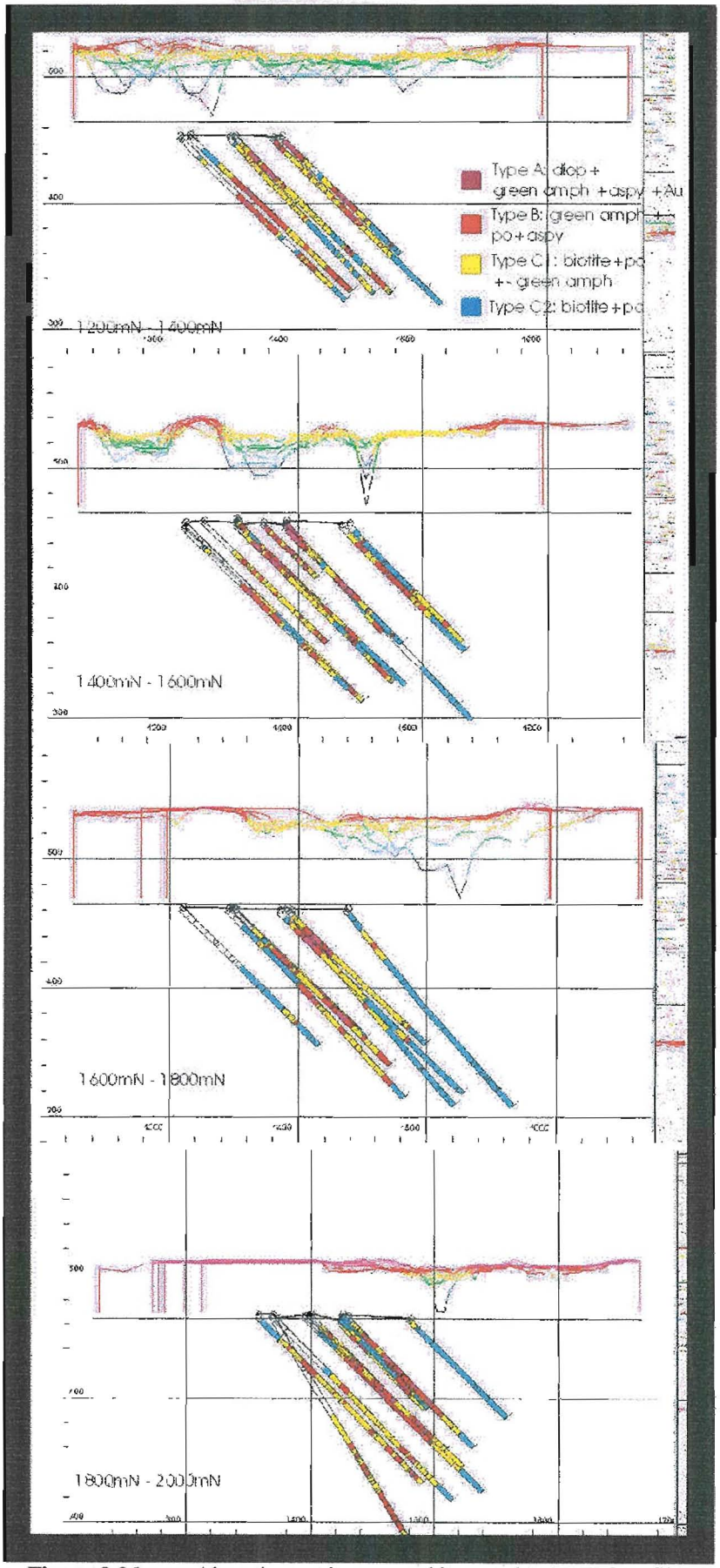

Figure 8.36 Alteration against ground log quadrature EM profiles

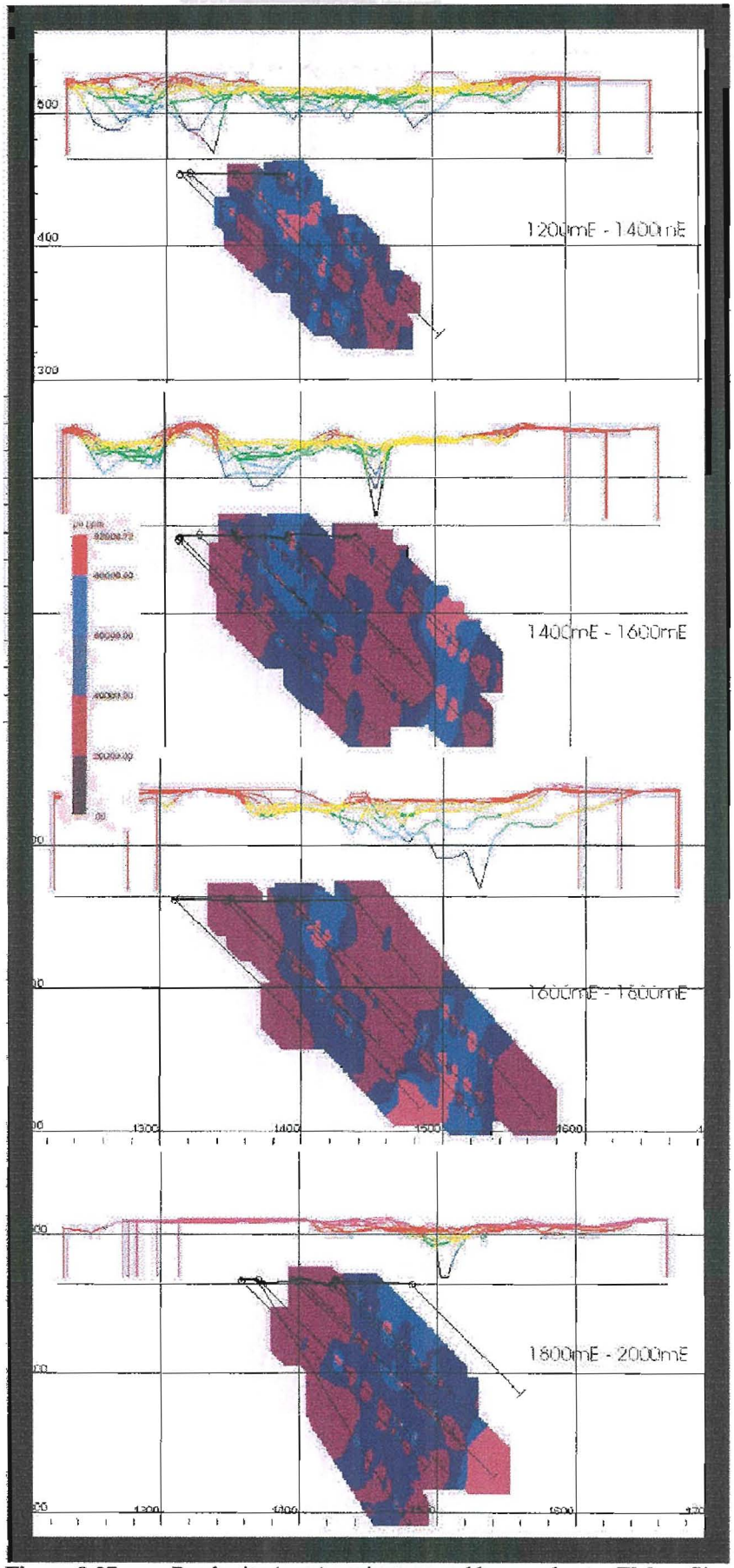

Figure 8.37 Pyrrhotite (ppm) against ground log quadrature EM profiles

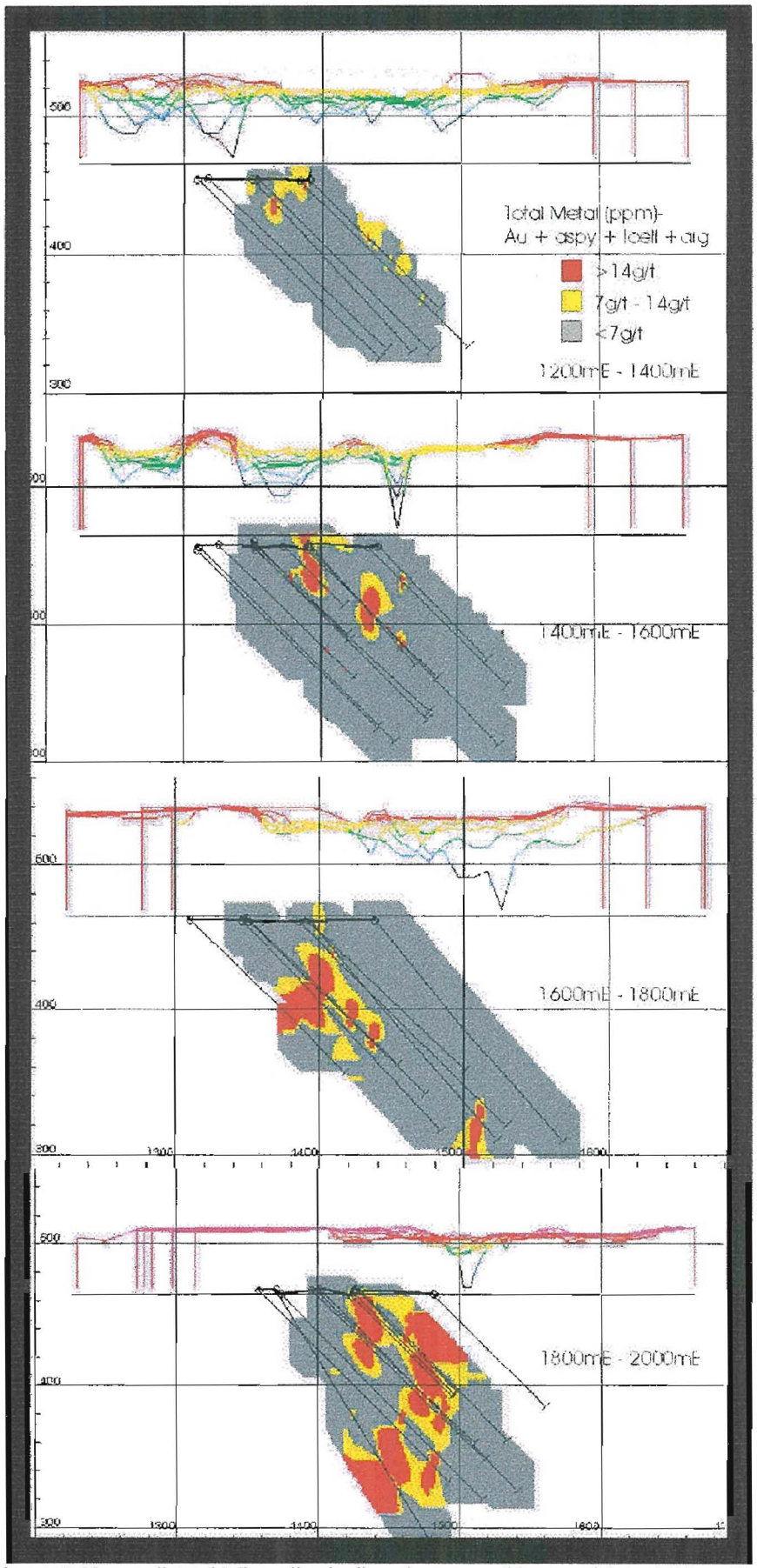

Figure 8.38 "Total Mineralisation" against ground log quadrature EM profiles

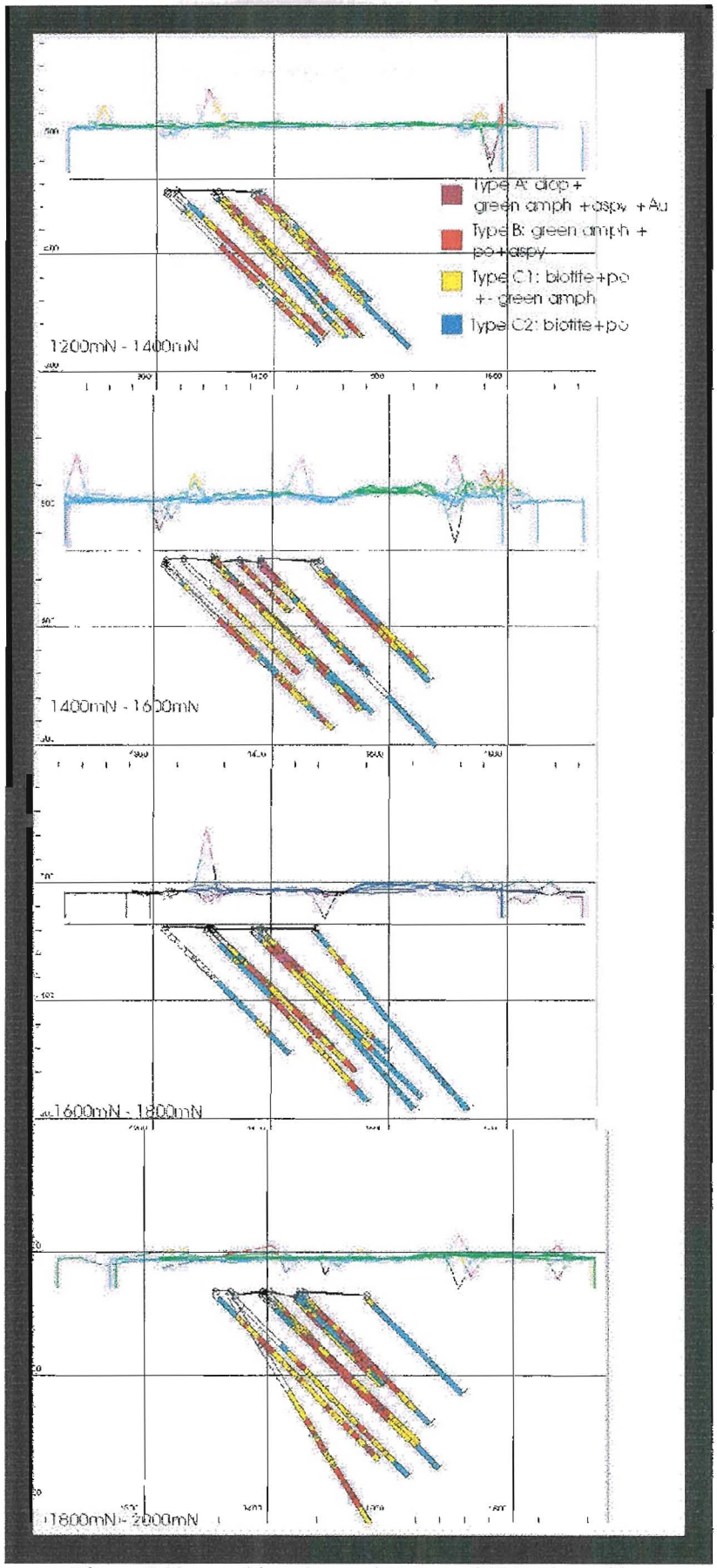

Figure 8.39 Alteration against ground EM ratio profiles

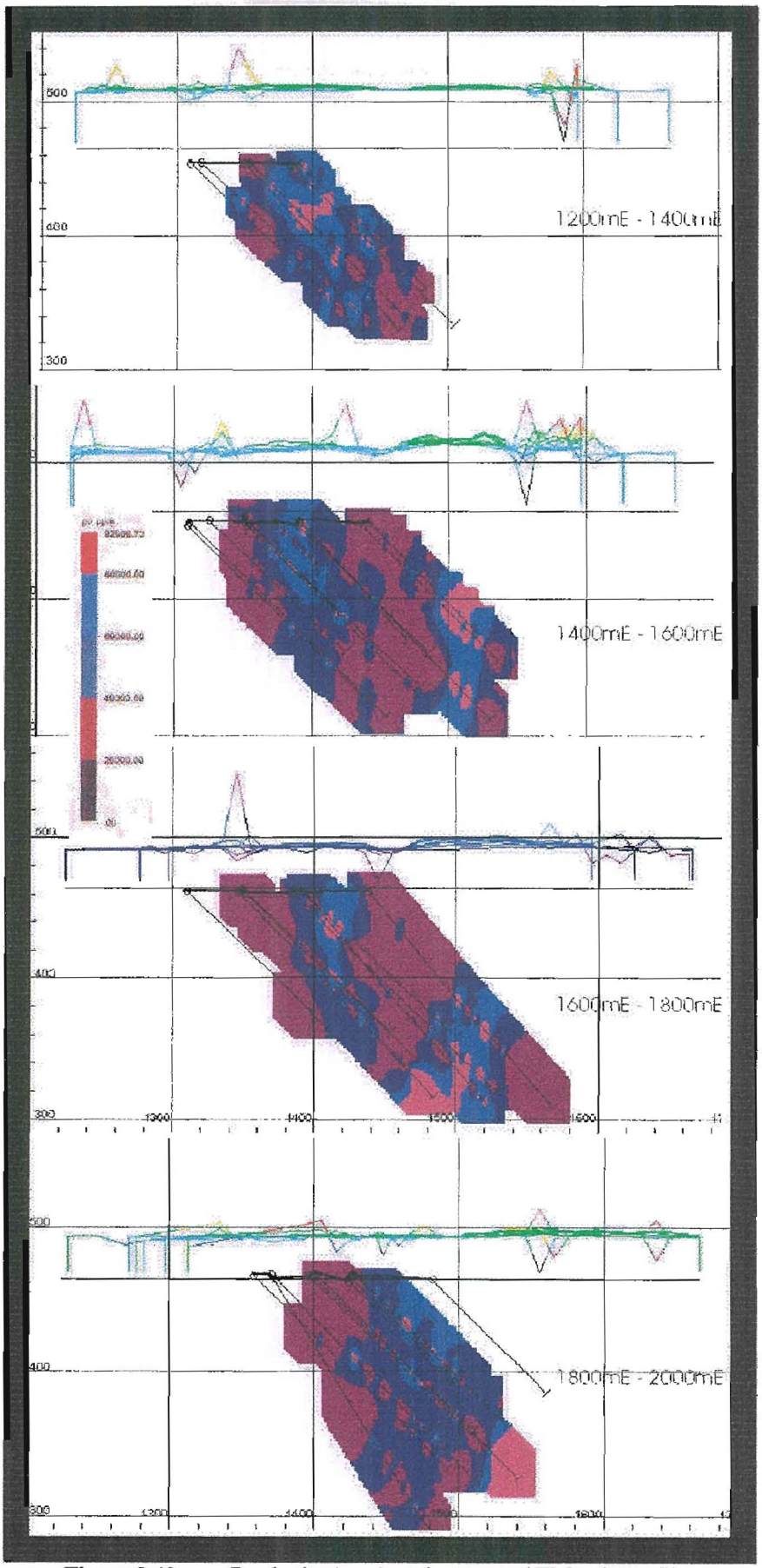

Figure 8.40 Pyrrhotite (ppm) against ground EM ratio profiles

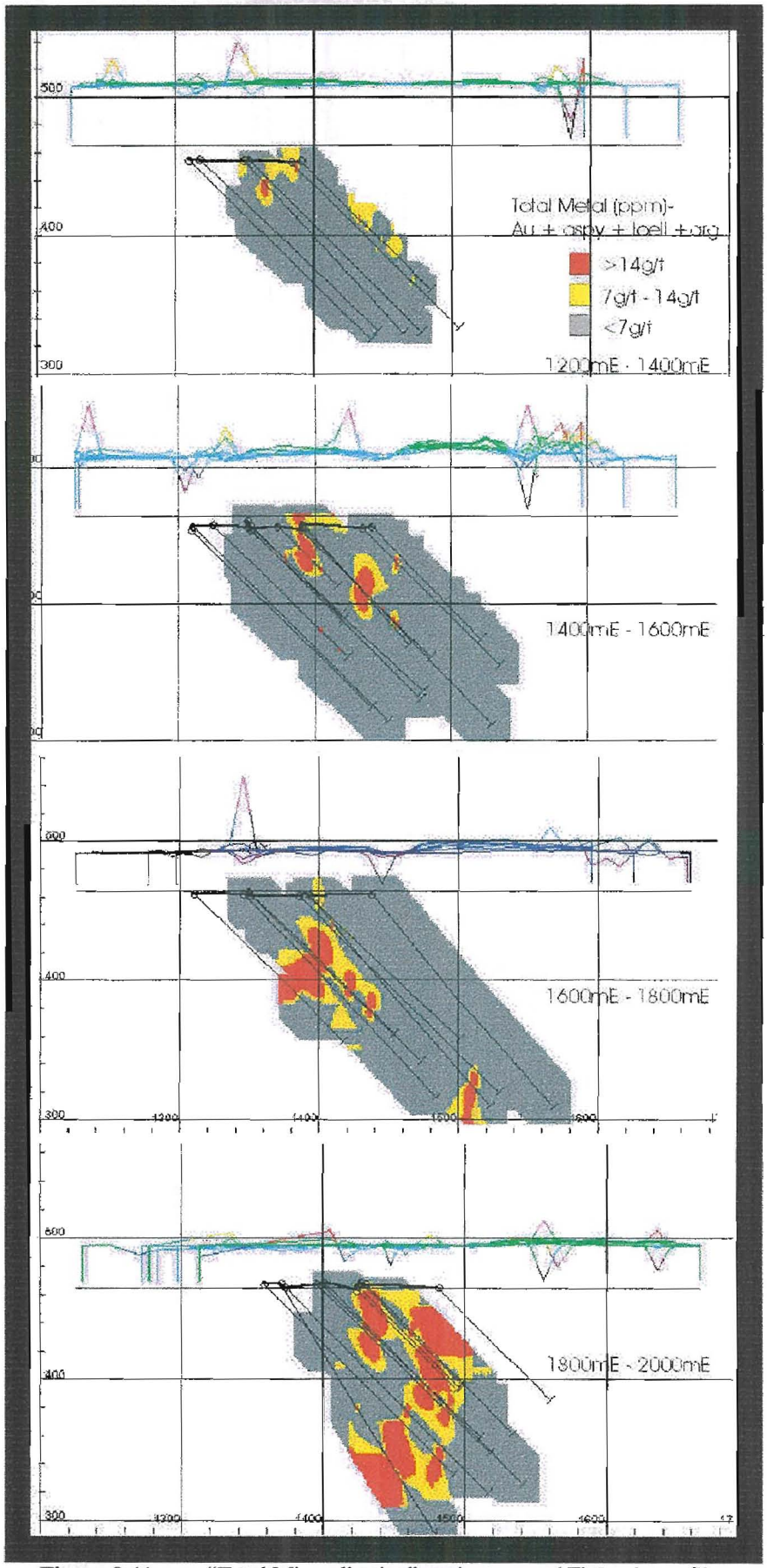

Figure 8.41 "Total Mineralisation" against ground EM ratio profiles

8.2.2 Downhole Geophysics

The downhole geophysical anomalies identified in chapter 7 are overlain on the alteration image (figure 8.42), pyrrhotite image (figure 8.43) and "Total Mineralisation" image (figure 8.44) along Section 1700mN.

The interpreted alteration image along Section 1700mE shows Type A and B alteration coincident with the southern zone (~1400mN) of high chargeability, strong magnetic susceptibility and high conductivity (figure 8.42). The northern zone of high chargeability, high magnetic susceptibility and high conductivity correlates with Type C2 alteration. This alteration type represents the strongly foliated pyrrhotite-bearing carbonaceous sediments along the 1500mN. The zones of low chargeability, low magnetic susceptibility but resistive all lie in Type C2 alteration, which are predominantly thick granitoid and weakly altered volcanic sequences.

The northern zone of high chargeability, high magnetic susceptibility and high conductivity correlates with the pyrrhotite rich zone (figure 8.43), found within the pyrrhotite-bearing carbonaceous sediments. The southern pyrrhotite zone also correlates with the southern zone of high chargeability, high magnetic susceptibility and high conductivity. This zone is due to the presence of pyrrhotite remobilised into the mineralised Type A and B alteration zone. This zone also contains the highest "Total Mineralisation" dominated by arsenopyrite and gold (figure 8.44).

The northern zone of high chargeability, high magnetic susceptibility and high conductivity has barren to trace gold and arsenopyrite mineralisation. All the zones of poor chargeability, poor magnetic susceptibility but low conductivity are also barren in gold and arsenopyrite mineralisation.

To provide a statistical distribution, alteration, pyrrhotite, arsenopyrite and gold mineralisation are plotted against the three, downhole geophysical methods taken from drillholes SV9702, SV9703 and SV9706.

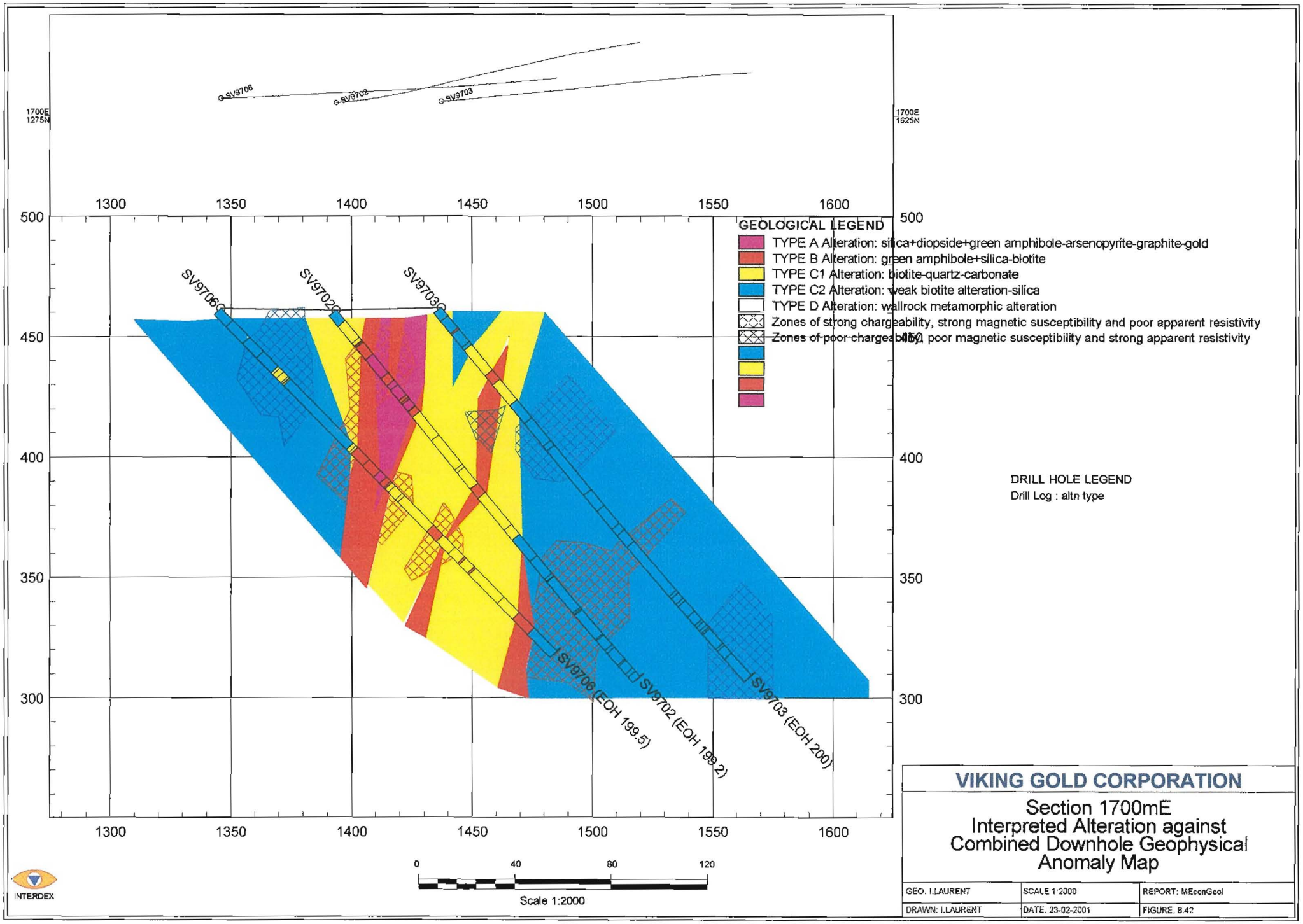
SV9706
SV9702
SV9703
1700E
1275N
1700E
1625N
1300
1350
1400
1450
1500
1550
1600
500
450
400
350
300
GEOLOGICAL LEGEND
TYPE A Alteration: silica+diopside+green amphibole-arsenopyrite-graphite-gold
TYPE B Alteration: green amphibole+silica-biotite
TYPE C1 Alteration: biotite-quartz-carbonate
TYPE C2 Alteration: weak biotite alteration-silica
TYPE D Alteration: wallrock metamorphic alteration
Zones of strong chargeability, strong magnetic susceptibility and poor apparent resistivity
Zones of poor chargeability, poor magnetic susceptibility and strong apparent resistivity
SV9706 (EOH 199.5)
SV9702 (EOH 199.2)
SV9703 (EOH 200)
DRILL HOLE LEGEND
Drill Log : altn type
0
40
80
120
Scale 1:2000
INTERDEX
VIKING GOLD CORPORATION
Section 1700mE
Interpreted Alteration against
Combined Downhole Geophysical
Anomaly Map
GEO. I.LAURENT
SCALE 1:2000
REPORT: MEconGeol
DRAWN: I.LAURENT
DATE. 23-02-2001
FIGURE. 8.42

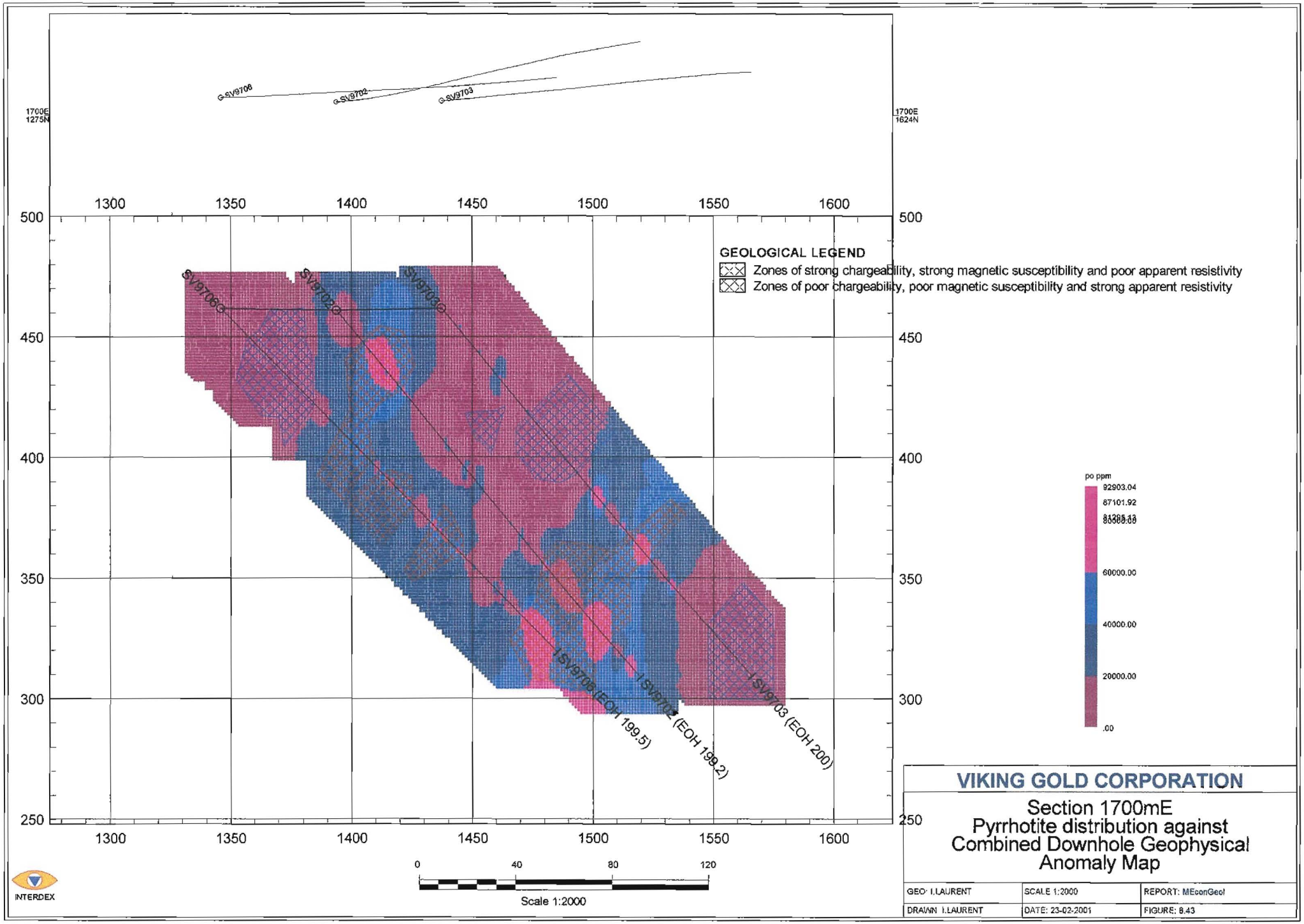
1700E
1275N
1700E
1624N
G-SV9706
G-SV9702
G-SV9703
1300
1350
1400
1450
1500
1550
1600
500
450
400
350
300
250
GEOLOGICAL LEGEND
Zones of strong chargeability, strong magnetic susceptibility and poor apparent resistivity
Zones of poor chargeability, poor magnetic susceptibility and strong apparent resistivity
SV9706G
SV9702G
SV9703G
SV9706 (EOH 199.5)
SV9702 (EOH 199.2)
SV9703 (EOH 200)
po ppm
92903.04
87101.92
60000.00
40000.00
20000.00
.00
0
40
80
120
Scale 1:2000
INTERDEX
VIKING GOLD CORPORATION
Section 1700mE
Pyrrhotite distribution against
Combined Downhole Geophysical
Anomaly Map
GEO: I.LAURENT
SCALE 1:2000
REPORT: MEconGeol
DRAWN: I.LAURENT
DATE: 23-02-2001
FIGURE: 8.43

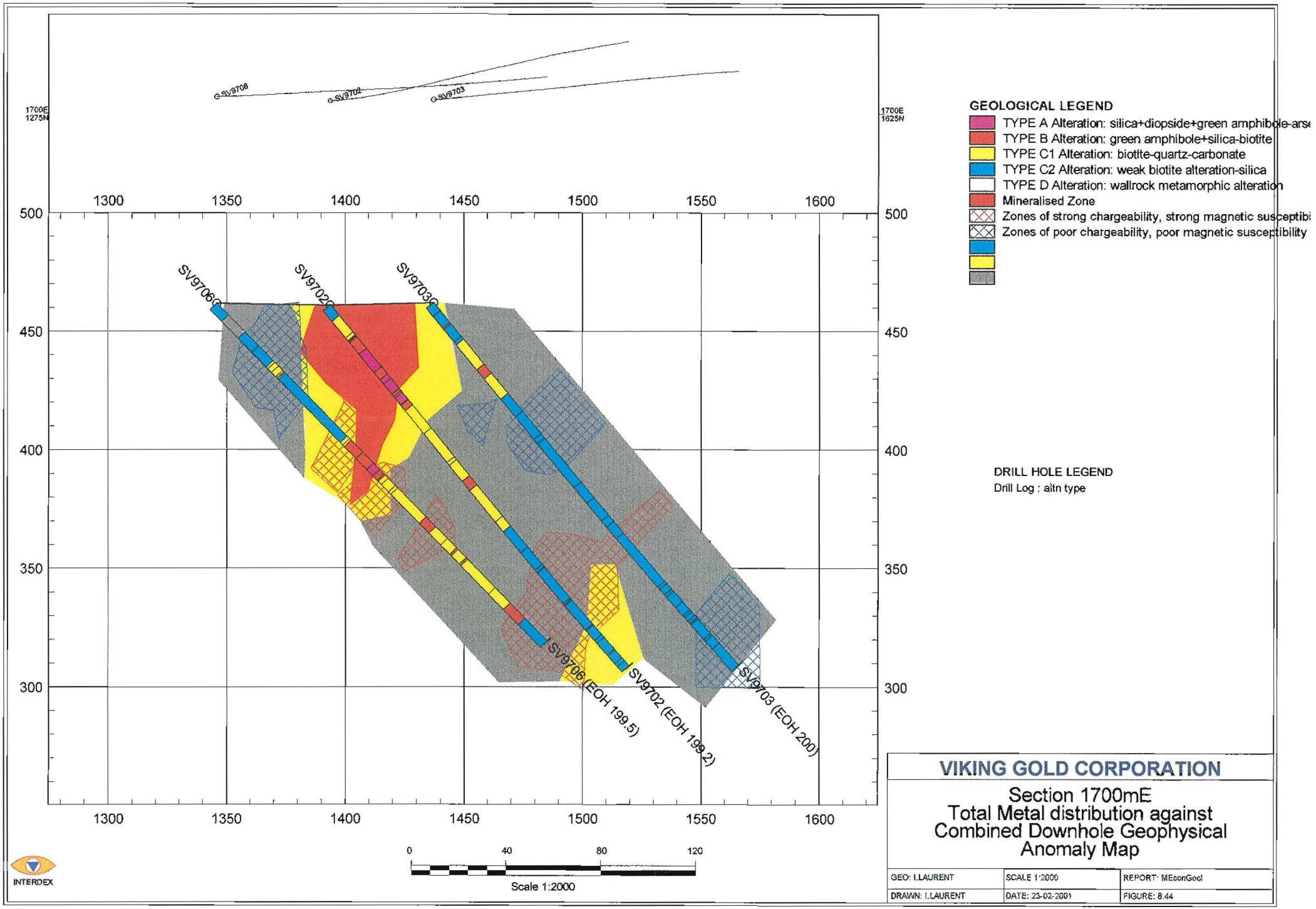
1700E
1275N
1700E
1625N
G-SV9706
G-SV9702
G-SV9703
1300
1350
1400
1450
1500
1550
1600
500
450
400
350
300
SV9706
SV9702
SV9703
SV9706 (EOH 199.5)
SV9702 (EOH 199.2)
SV9703 (EOH 200)
0
40
80
120
Scale 1:2000
INTERDEX
GEOLOGICAL LEGEND
TYPE A Alteration: silica+diopside+green amphibole-ars
TYPE B Alteration: green amphibole+silica-biotite
TYPE C1 Alteration: biotite-quartz-carbonate
TYPE C2 Alteration: weak biotite alteration-silica
TYPE D Alteration: wallrock metamorphic alteration
Mineralised Zone
Zones of strong chargeability, strong magnetic susceptibi
Zones of poor chargeability, poor magnetic susceptibility
DRILL HOLE LEGEND
Drill Log : altn type
VIKING GOLD CORPORATION
Section 1700mE
Total Metal distribution against
Combined Downhole Geophysical
Anomaly Map
GEO: I.LAURENT
SCALE 1:2000
REPORT: MEconGeol
DRAWN: I.LAURENT
DATE: 23-02-2001
FIGURE: 8.44

166

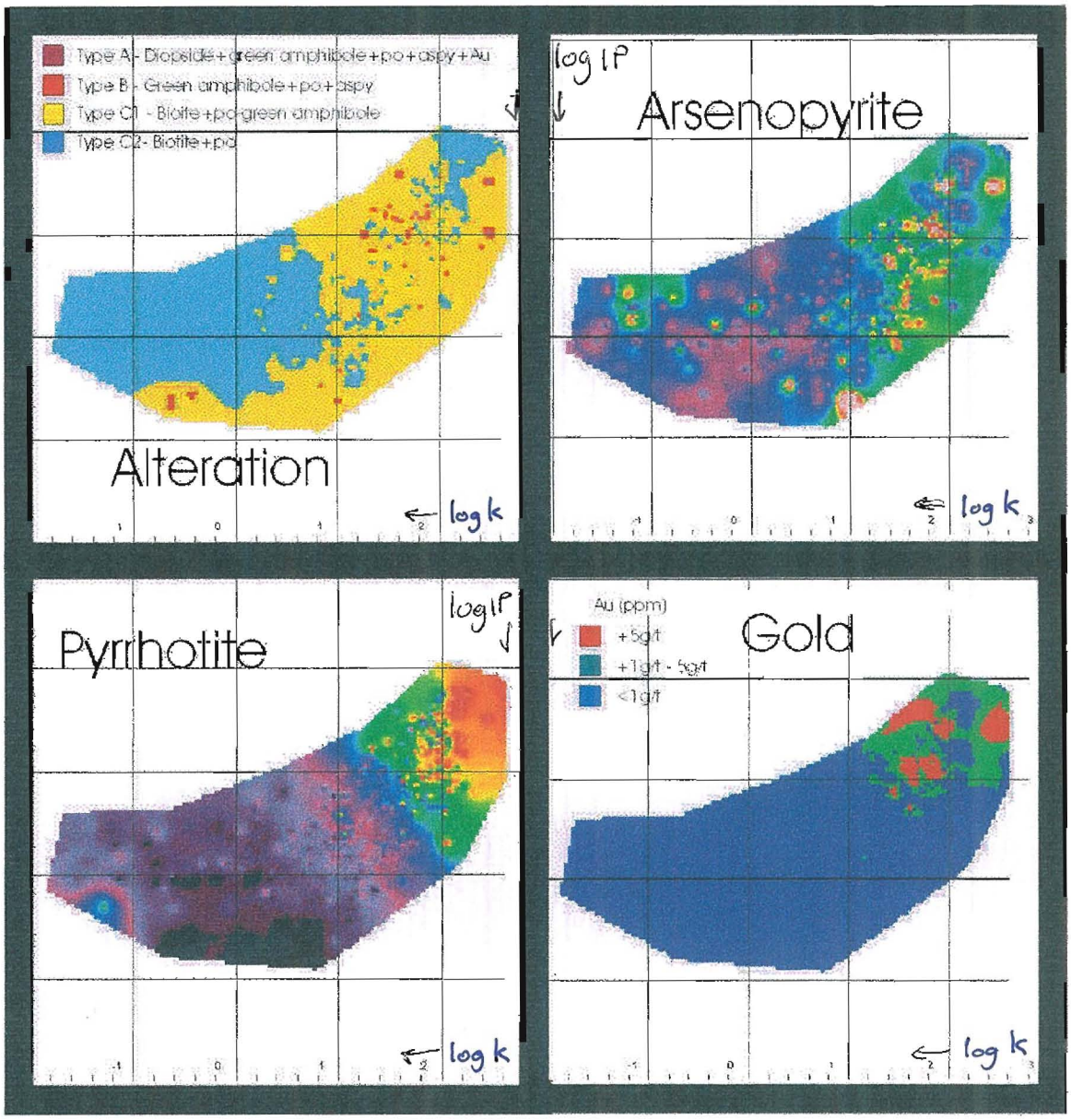

Figure 8.45 Log k – log IP plots for alteration, pyrrhotite, arsenopyrite and gold. $\Sigma_x = 5{,}709$

On the log k – log IP plot (figure 8.45), the core of the alteration zone (Type C1, B and A) is situated predominantly in highly magnetic zones. There is, however, a range in chargeability, which is dependent on the pyrrhotite and graphite content. Arsenopyrite is coincident with Type A and B alteration. Gold occurs with arsenopyrite but only in zones of high magnetic response and moderate chargeability. The greatest concentration of pyrrhotite is located in the zone of highest magnetic susceptibility and highest chargeability. The pyrrhotite overlaps the core of the alteration zone (Type C1, B and A) and Type C2 alteration. The pyrrhotite-rich Type C2 alteration zone is coincident with the pyrrhotite-bearing, carbonaceous sediments.

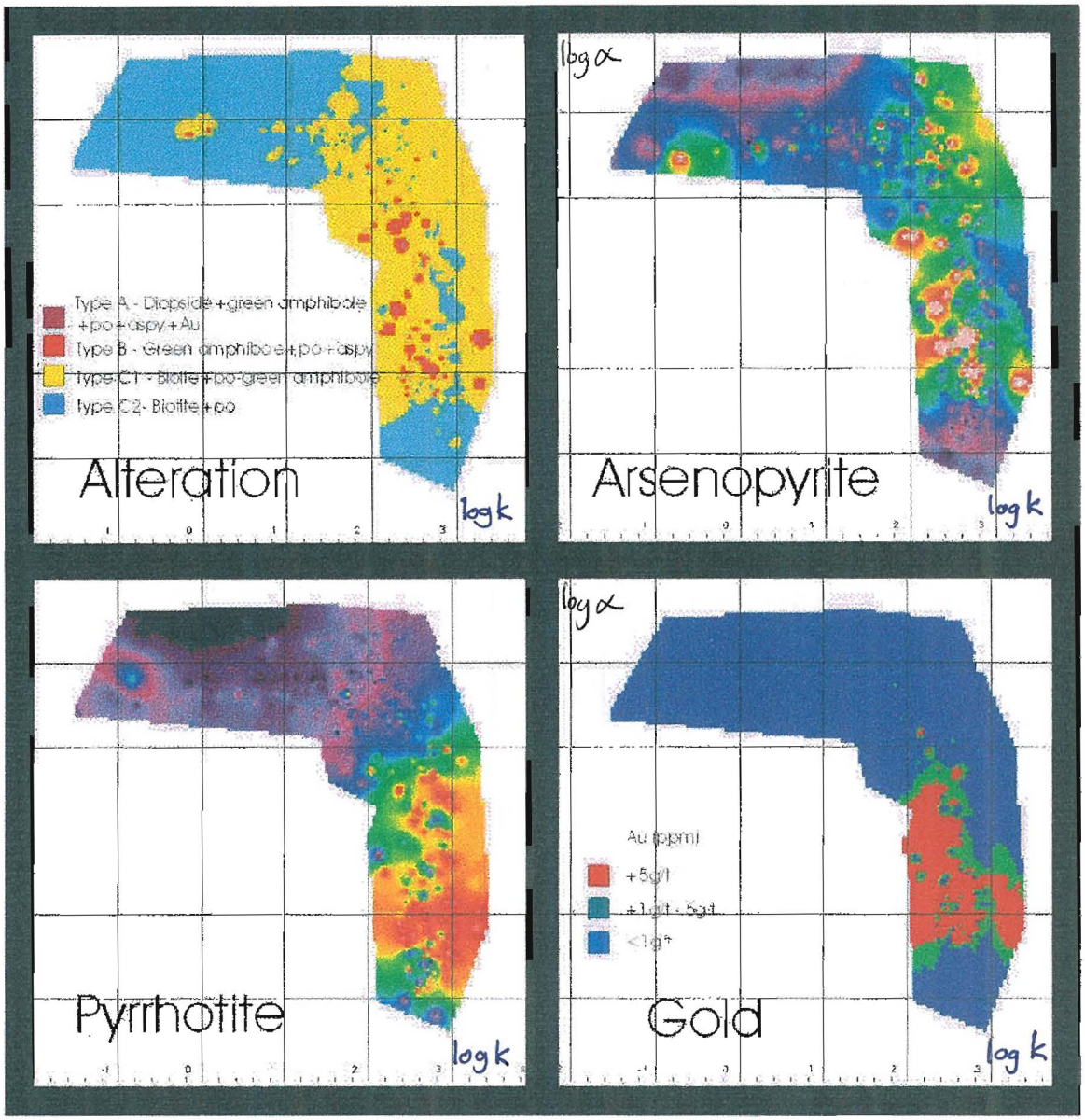

Figure 8.46 log k – log α plots of alteration, pyrrhotite, arsenopyrite and gold. $\Sigma_x = 5{,}709$

On the log k – log α plot (figure 8.46), the core of the alteration zone (Type C1, B and A) is found in more magnetic zones with a wide range in apparent resistivity. The degree of silicification in the "Mineralised Zone" may explain the variable apparent resistivity. Gold mineralisation and arsenopyrite mineralisation are coincident, adding support to the use of arsenopyrite as a primary indicator mineral for gold mineralisation. Pyrrhotite concentrations are in zones of high magnetic susceptibility and high conductivity. There is a 50% overlap between the zones of highest concentration of pyrrhotite and the concentration of gold and arsenopyrite mineralisation.

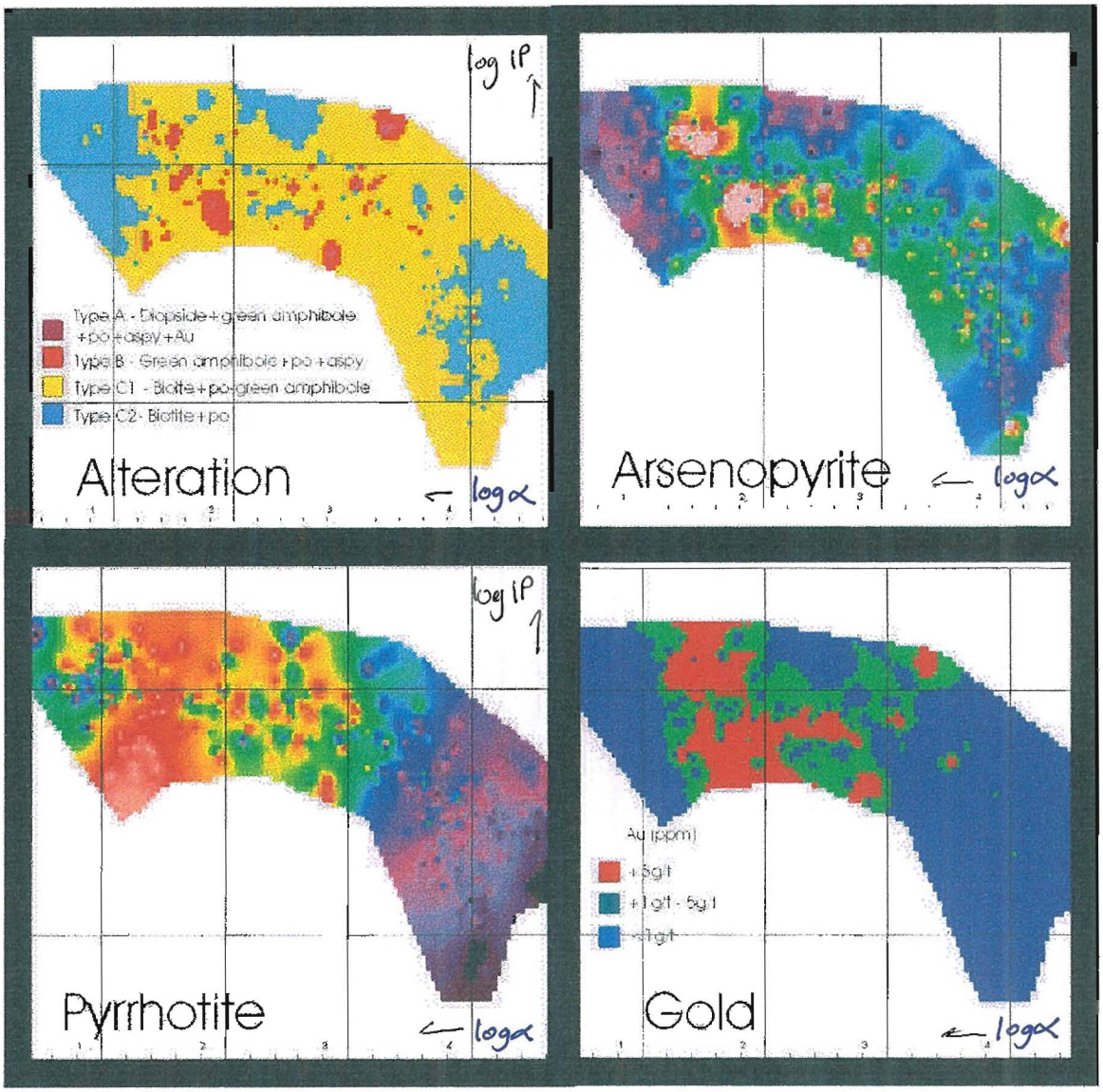

Figure 8.47 Log α– log IP plots for alteration, pyrrhotite, arsenopyrite and gold. $\Sigma_x = 5{,}709$

On the log α – log IP plot (figure 8.47), the core of the alteration zone (Type C1, B and A) ranges from moderately resistive to moderately conductive. In general Type A and B alteration is moderately conductive with elevated chargeability.

Arsenopyrite and gold mineralisation are coincident an are situated in a moderately conductive zone with elevated chargeability. The elevated chargeability correlates with the pyrrhotite and graphite concentrations identified in the "Mineralised Zone". Pyrrhotite is concentrated at the point of highest conductivity and high chargeability.

8.2.3 Synthesis

The alteration and mineralisation exhibit specific geophysical characteristics. The alteration was identified mineralogically and geochemically and did not take into account the necessary presence of any geophysically responsive minerals. The core of the shear zone has Type A, B and C1 alteration and, in general, is situated within zones of elevated conductivity that have high chargeability and are moderately to strongly magnetic.

The distribution and proportion of pyrrhotite directly affects the magnetic and electromagnetic responses. The greatest concentration is found within the northern carbonaceous sedimentary unit (~1500mN). This unit is a marker horizon, which lies on the outer rim of the Svartliden Shear Zone. Despite this unit being strongly foliated due to the primary deformation event, there is little or no hydrothermal alteration. The presence of the pyrrhotite is therefore considered as a primary magmatic or depositional mineral rather than a hydrothermal mineral. The strong foliation formed during deformation has created thin bands of interlocking pyrrhotite resulting in high conductivity and chargeability. This is shown as the first-order log in-phase EM anomalies.

The pyrrhotite within the "Mineralised Zone" is a combination of a secondary remobilised mineral initially exsolved from the northern carbonaceous sedimentary unit, and low temperature sulphide in solution within the hydrothermal fluids. The variance in conductivity and chargeability is due to the irregular distribution of pyrrhotite within the highly silicified "Mineralised Zone".

From the petrographic analyses, in conjunction with the mass balancing calculations, arsenopyrite is a primary indicator mineral for gold. Arsenopyrite is present in small proportions within the "Mineralised Zone" and has low conductivity and magnetism. "Total Mineralisation" (gold+arsenopyrite+loellingite) does not directly produce any unique geophysical responses but is associated with the pyrrhotite in the "Mineralised Zone". The combination of pyrrhotite and "Total Mineralisation" is situated within the second-order log in-phase EM anomalies.

8.3 TARGET DEFINITION

8.3.1 Svartliden Project

From the second-order, log-transformed, ground in-phase EM image (figure 8.20), which is coincident with the "Mineralised Zone" (Type A, B and C1 Alteration), two distinct anomalies to the west were delineated. One anomaly along the 700mE (between 800mN and 1000m), and the other anomaly along the 1500mN (between 500mE and 700mE).

To the southwest of the project area, a traverse along the 900mN was selected across the anomaly along the 700mE. The ground magnetic, electromagnetic and EM ratio profiles between the 800mN and 1000mN are drawn along the 900mN. On each section, the alteration methodology is used in assigning the varying geophysical bodies. Two 'scissor' holes are proposed over the area of highest prospectivity based on the like geophysical properties identified over the "Mineralised Zone" within the Svartliden Project area.

The ground magnetic profiles along the 900mN displays a magnetic anomaly between the 650mE and 750mE (figure 8.48). Based on the observations in the project area, this area hosts Type C1 alteration with potential for having Type B and A. As the ground magnetics do not differentiate the magnetite-bearing volcanic rocks and the pyrrhotite-bearing sedimentary rocks, it is difficult to attribute a lithological unit to this anomaly. The log ground magnetic profiles confirm the presence of a magnetic anomaly between the 650mE and 750mE (figure 8.49).

The ground in-phase EM profiles along the 900mN display a conductive anomaly between the 650mE and 800mE (figure 8.50). The ground log in-phase EM profiles clearly shows a coincident first- and second-order anomaly between the 650mE and 800mE (figure 8.51). The second-order anomaly was identified in figure 8.20. Using the alteration methodology, the first-order log in-phase EM anomaly represents Type C2 alteration (the pyrrhotite-bearing sediments). The second-order log in-phase EM anomaly (situated along the western contact of the first-order anomaly) represents Type C1 alteration and potentially a Type B and Type A alteration.

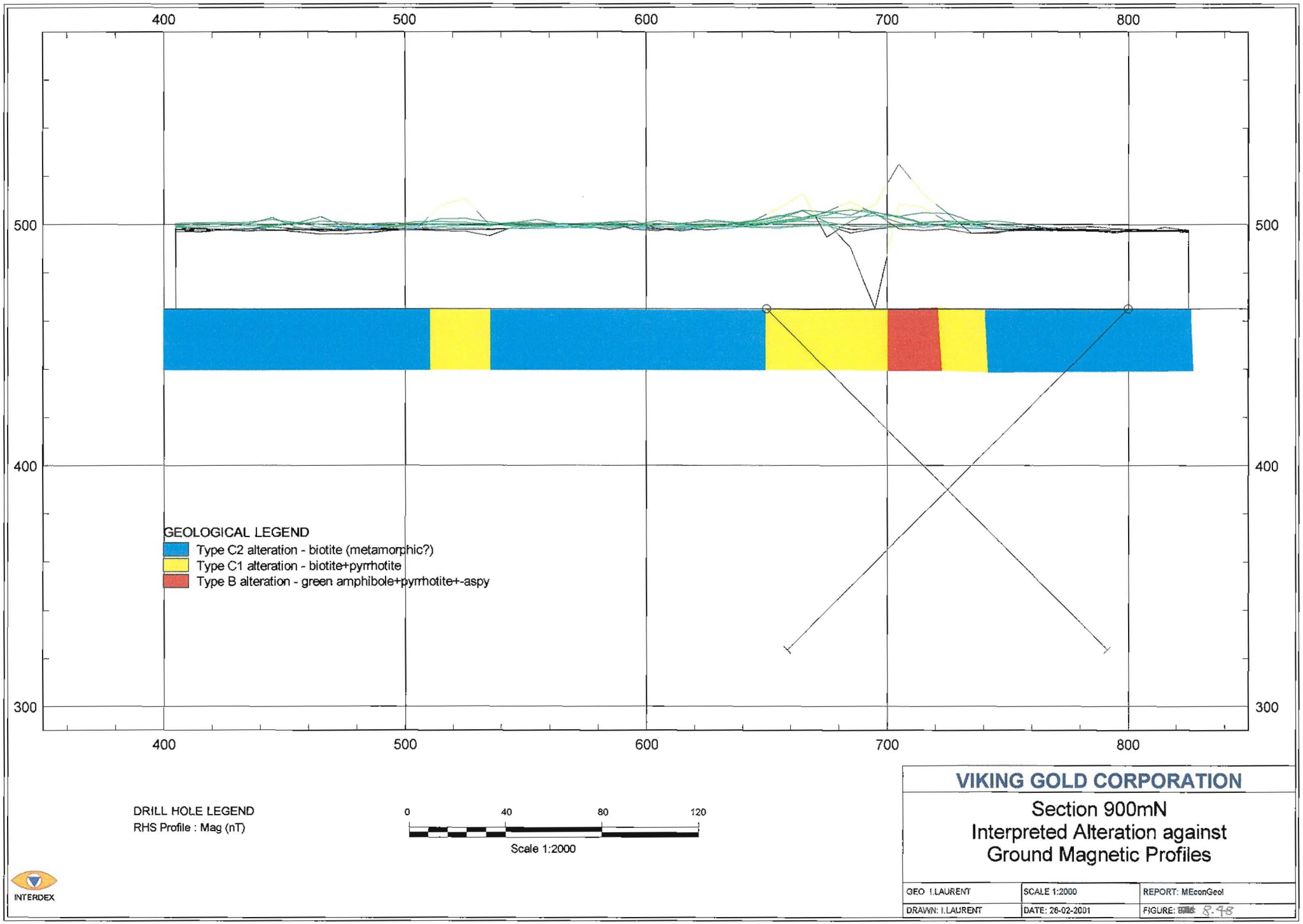

Figure 8.48

172

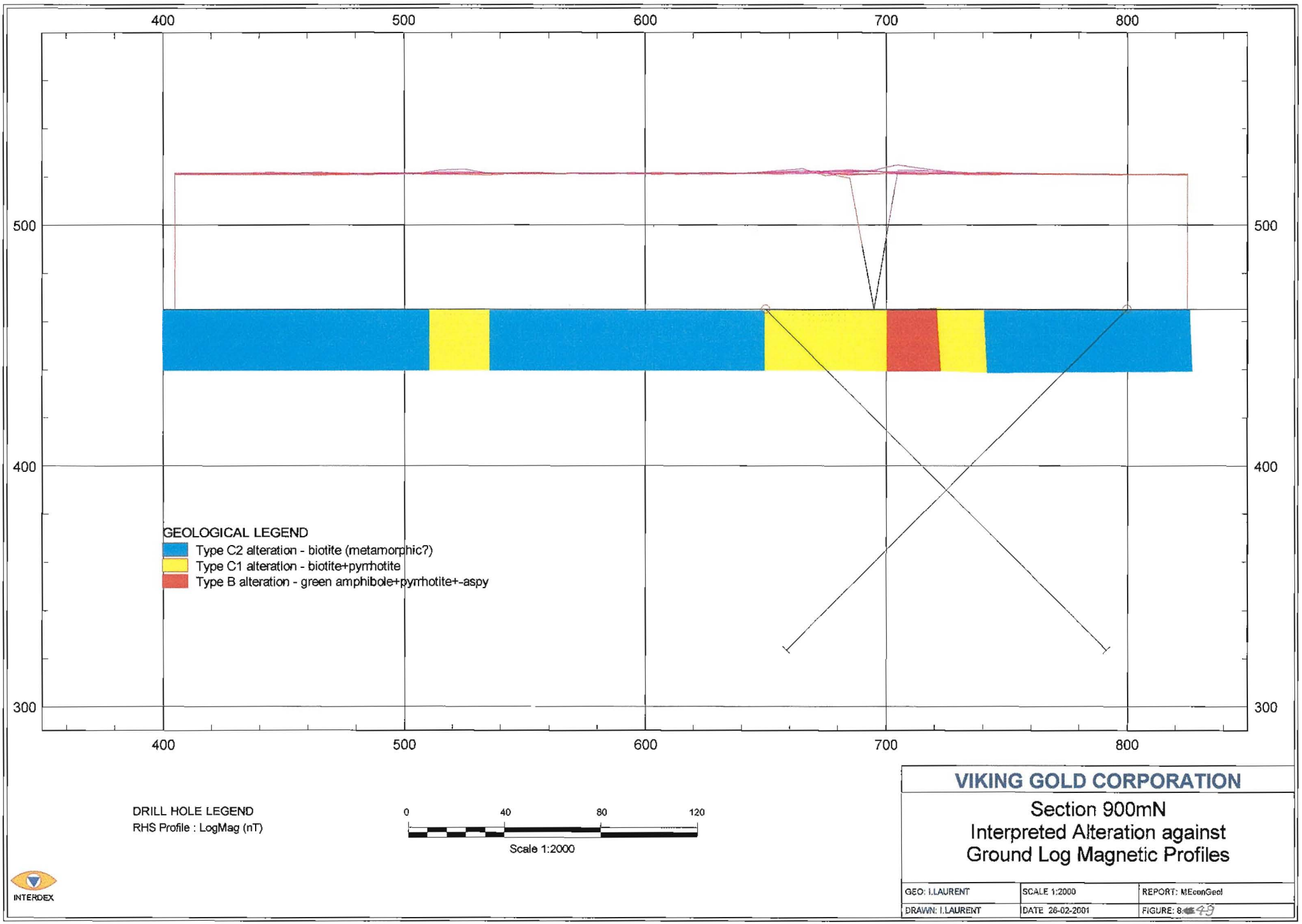
400
500
600
700
800
500
400
300
GEOLOGICAL LEGEND
Type C2 alteration - biotite (metamorphic?)
Type C1 alteration - biotite+pyrrhotite
Type B alteration - green amphibole+pyrrhotite+-aspy
DRILL HOLE LEGEND
RHS Profile : LogMag (nT)
0
40
80
120
Scale 1:2000
INTERDEX
VIKING GOLD CORPORATION
Section 900mN
Interpreted Alteration against
Ground Log Magnetic Profiles
GEO: I.LAURENT
SCALE 1:2000
REPORT: MEconGeol
DRAWN: I.LAURENT
DATE 26-02-2001
FIGURE: 8.49

Figure 8.49

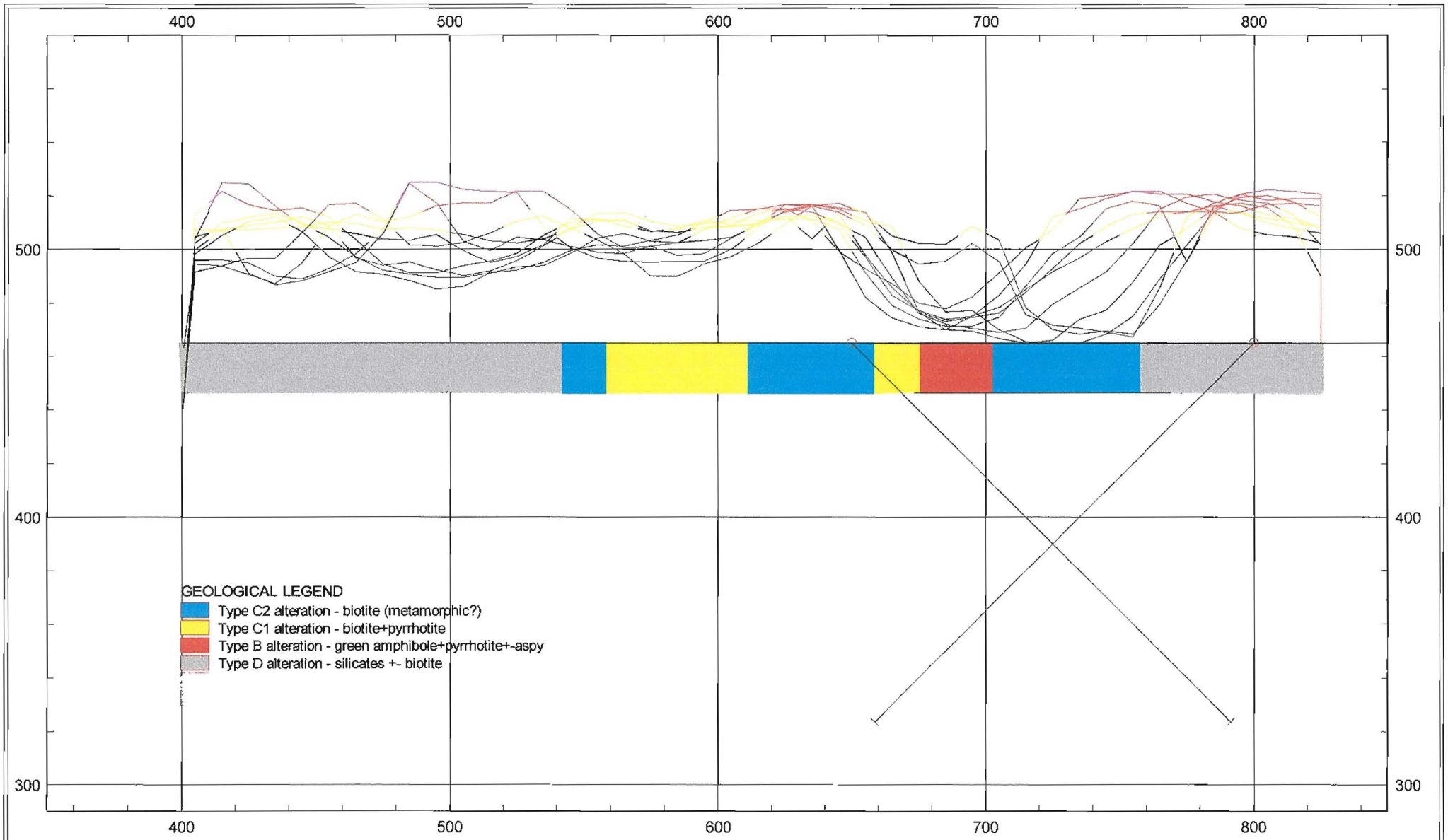

DRILL HOLE LEGEND
RHS Profile : In-phase

0 40 80 120
Scale 1:2000

INTERDEX

VIKING GOLD CORPORATION

Section 900mN
Interpreted Alteration against
Ground In-phase EM Profiles

GEO. I.LAURENT	SCALE 1:2000	REPORT: MEconGeol
DRAWN. I.LAURENT	DATE: 28-02-2001	FIGURE: 8.50

Figure 8.50

174

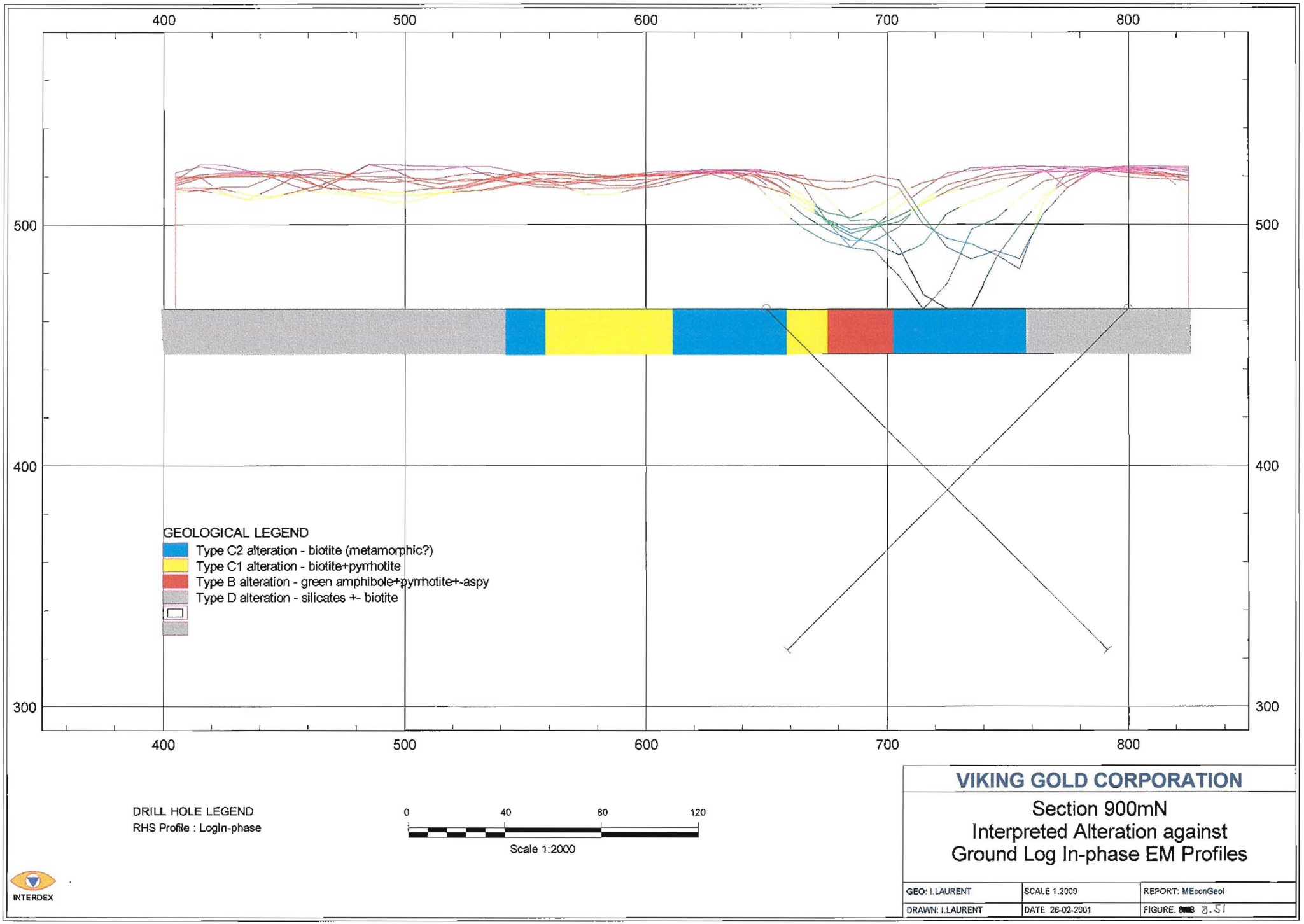
400
500
600
700
800
500
400
300
GEOLOGICAL LEGEND
Type C2 alteration - biotite (metamorphic?)
Type C1 alteration - biotite+pyrrhotite
Type B alteration - green amphibole+pyrrhotite+-aspy
Type D alteration - silicates +- biotite
DRILL HOLE LEGEND
RHS Profile : LogIn-phase
0
40
80
120
Scale 1:2000
INTERDEX
VIKING GOLD CORPORATION
Section 900mN
Interpreted Alteration against
Ground Log In-phase EM Profiles
GEO: I.LAURENT
SCALE 1:2000
REPORT: MEconGeol
DRAWN: I.LAURENT
DATE: 26-02-2001
FIGURE: 8.51

Figure 8.51

The ground quadrature EM profiles (figure 8.52) and ground log quadrature EM profiles (figure 8.53) show highly resistive units west of 650mE. Conductive anomalies, between the 650mE and 750mE, are coincident with the in-phase EM anomalies. The EM ratio profiles (figure 8.54) do not distinguish any significant anomalies along the 900mN traverse.

8.3.2 Regional Targets

The Svartliden Project is situated within a shear zone that shows a magnetic response based on the magnetite content in the volcanic rocks and the pyrrhotite content in the sedimentary rocks and "Mineralised Zone". The regional aeromagnetic image data illustrates similar patterns to that of the Svartliden Project, elsewhere within the 'greenstone' belt. Two such prospects are circled on the regional aeromagnetic image in figure 8.55.

The area to the west (SNG[2] 1575000mE; 7188000mN) lies almost parallel to the Svartliden Project on a parallel 'greenstone' sequence. In common with Svartliden, this greenstone sequence appears to have rotated from north-south to east-west strike. A syn-tectonic granitoid dome is present on the southern contact of this prospect, suggesting that the 'greenstone' sequence is part of a dilational zone and low shear strain.

The area to the north (SNG 1585000mE; 7215000mN) lies along the same 'greenstone' sequence as Svartliden. At this location, the strike of the 'greenstone sequence has also rotated from north-south to east-west. The prospect is known as Barsele and was identified in the 1980's. For historical and economic reasons, the prospect was never fully explored and the full potential for gold mineralisation is unknown. The magnetic intensity is strongest at this prospect as it is situated on the edge of the Skellefteå District, known to have some galena and sphalerite mineralisation (Weihed et al, 1996).

The geological and ground geophysical setting identified at the Svartliden Project suggests that these two regions may be highly prospective as gold exploration targets.

[2] SNG = Swedish National Grid

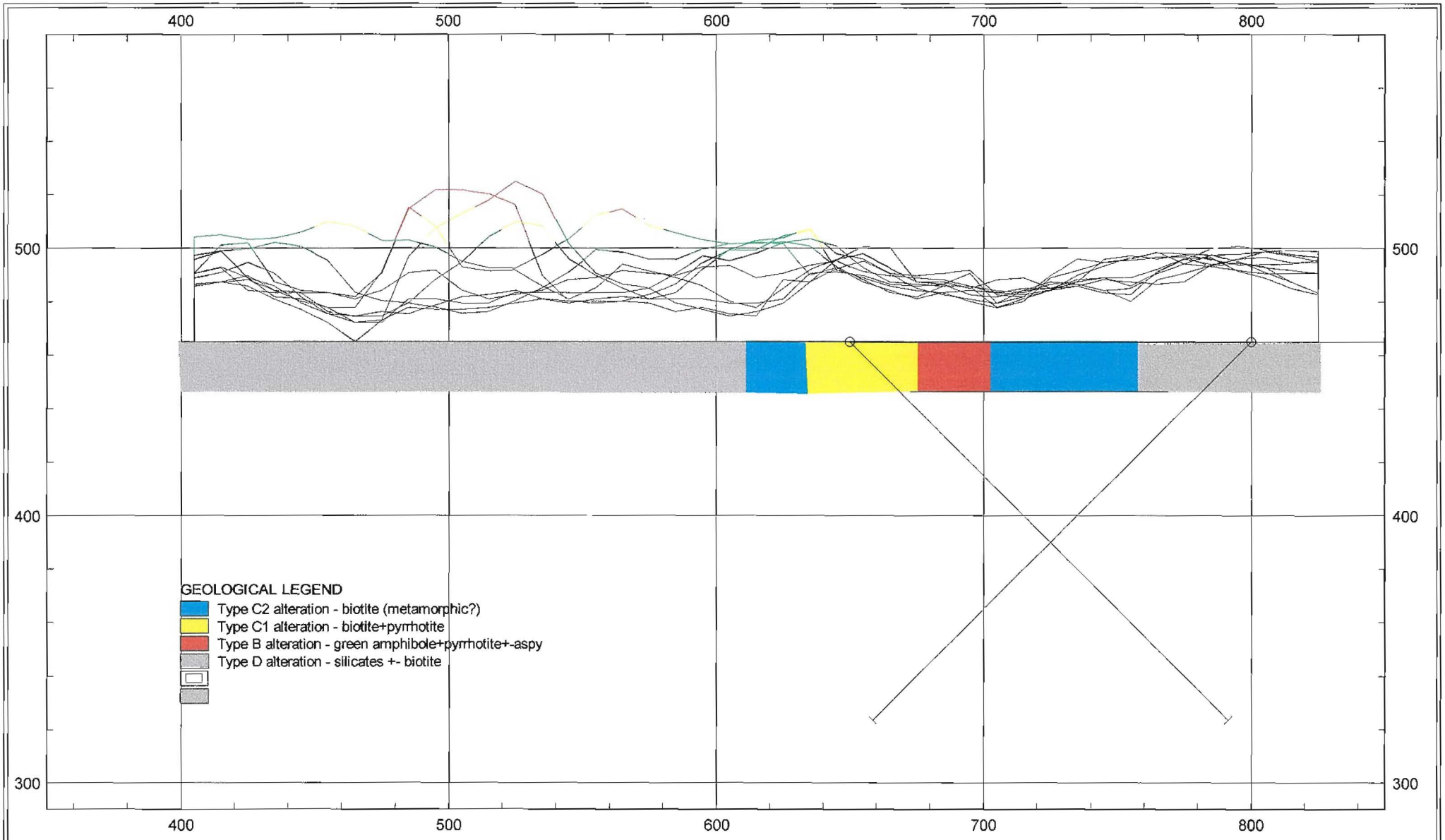

DRILL HOLE LEGEND
RHS Profile : Quadrature

0 40 80 120
Scale 1:2000

INTERDEX

VIKING GOLD CORPORATION

Section 900mN
Interpreted Alteration against
Ground Quadrature EM Profiles

GEO: I.LAURENT	SCALE 1:2000	REPORT: MEconGeol
DRAWN I.LAURENT	DATE 26-02-2001	FIGURE: 8.52

Figure 8.52

400
500
600
700
800
500
400
300
GEOLOGICAL LEGEND
Type C2 alteration - biotite (metamorphic?)
Type C1 alteration - biotite+pyrrhotite
Type B alteration - green amphibole+pyrrhotite+-aspy
Type D alteration - silicates +- biotite
DRILL HOLE LEGEND
RHS Profile : Quadrature
0
40
80
120
Scale 1:2000
VIKING GOLD CORPORATION
Section 900mN
Interpreted Alteration against
Ground Quadrature EM Profiles

Figure 8.52

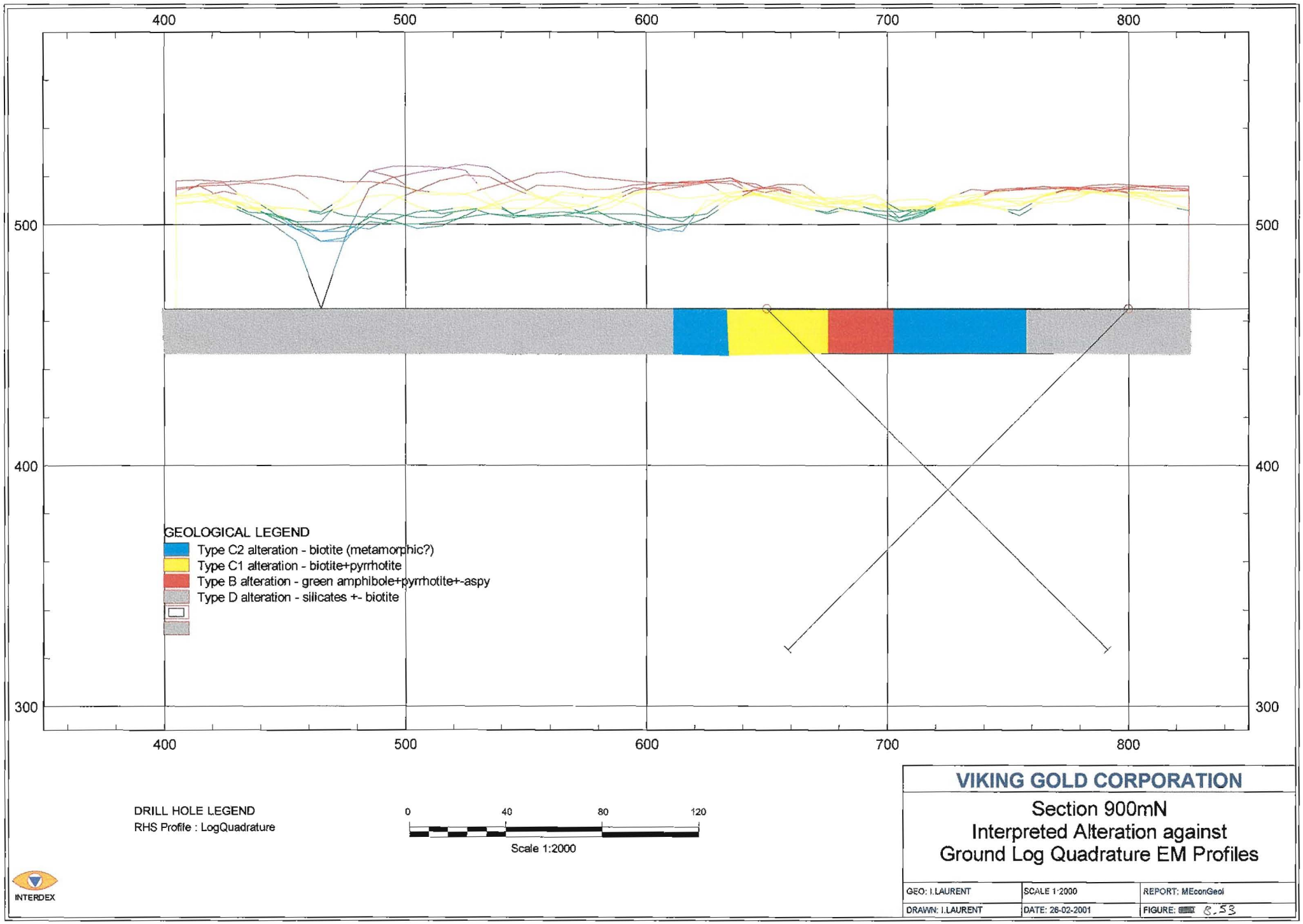
400
500
600
700
800
500
400
300
GEOLOGICAL LEGEND
Type C2 alteration - biotite (metamorphic?)
Type C1 alteration - biotite+pyrrhotite
Type B alteration - green amphibole+pyrrhotite+-aspy
Type D alteration - silicates +- biotite
DRILL HOLE LEGEND
RHS Profile : LogQuadrature
0
40
80
120
Scale 1:2000
INTERDEX
VIKING GOLD CORPORATION
Section 900mN
Interpreted Alteration against
Ground Log Quadrature EM Profiles
GEO: I.LAURENT
SCALE 1:2000
REPORT: MEconGeol
DRAWN: I.LAURENT
DATE: 26-02-2001
FIGURE: 8.53

Figure 8.53

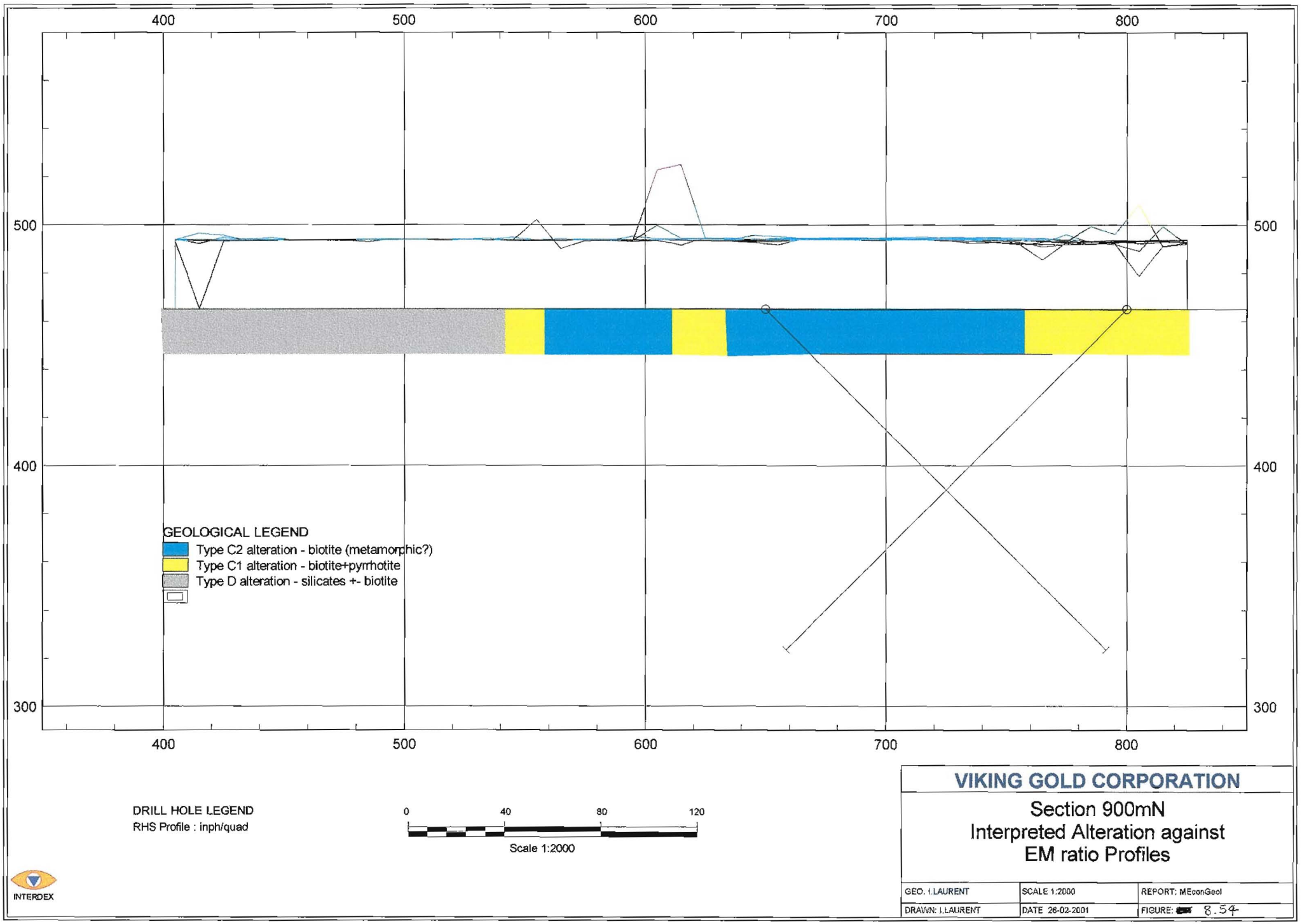
400
500
600
700
800
500
400
300
GEOLOGICAL LEGEND
Type C2 alteration - biotite (metamorphic?)
Type C1 alteration - biotite+pyrrhotite
Type D alteration - silicates +- biotite
DRILL HOLE LEGEND
RHS Profile : inph/quad
0
40
80
120
Scale 1:2000
INTERDEX
VIKING GOLD CORPORATION
Section 900mN
Interpreted Alteration against
EM ratio Profiles
GEO. I.LAURENT
SCALE 1:2000
REPORT: MEconGeol
DRAWN: I.LAURENT
DATE 26-02-2001
FIGURE: 8.54

Figure 8.54

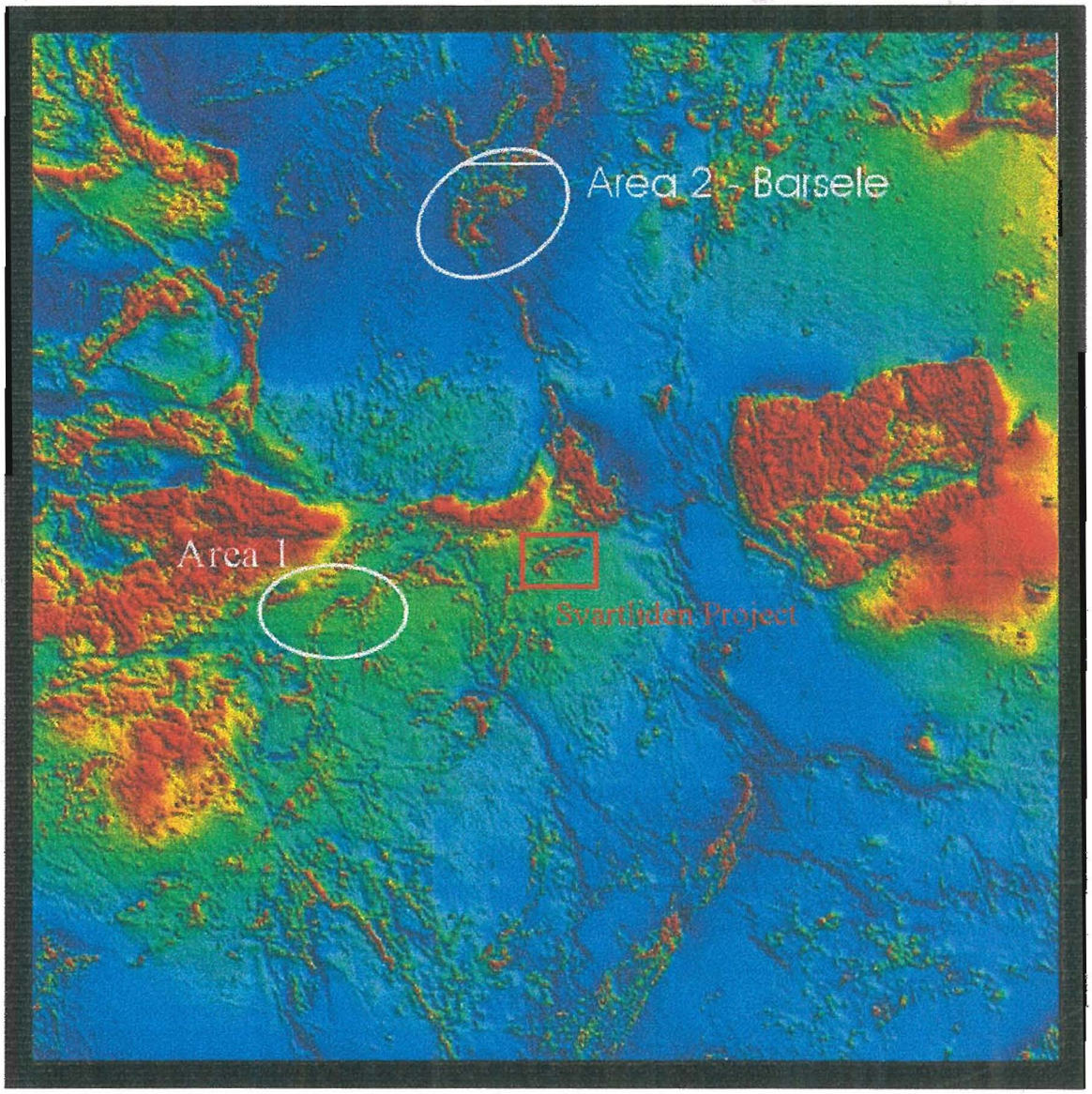

Figure 8.55 Regional gold exploration targets based on the similar geological and geophysical setting as the Svartliden Project. Scale 1cm = 5km. Svartliden Project = Red Square

Area 1 is located to the west of the Svartliden Project on a parallel greenstone belt. The pressure shadow, low shear strain zone in Area 1 has developed on the northwestern rim of the granitoid dome, suggesting a dextral rotation of the granitoid, the same as at Svartliden.

Area 2 is situated in the Barsele Region north of the Svartliden Project along the same greenstone belt. The entire Barsele Region appears to be a large pressure shadow zone created by the large regionally dominant Pauträsk granitoid.

8.4 SUMMARY

The ground magnetic field defines the shear zone, however it overlaps the stratigraphy and is therefore not lithologically constrained. The magnetic field is dependent on the presence of the magnetite-bearing volcanic rocks and pyrrhotite-bearing sedimentary rocks (Type C2 alteration) and the "Mineralised Zone" (Type A and B alteration).

The ground EM profiles distinguish the "Mineralised Zone" and carbonaceous sediments from the remaining lithologies within the shear zone. This is due to the high conductivity associated with the elevated pyrrhotite concentration. From the log in-phase EM profiles, the carbonaceous sedimentary units form first-order anomalies and the "Mineralised Zone" (Type A, B and C1 alteration) forms second-order anomalies. The second-order in-phase EM anomalies can be used to target the "Mineralised Zone"s, throughout the project area.

Downhole magnetic susceptibility correlates with magnetite-bearing volcanics (Type C1 and C2 alteration), the pyrrhotite-bearing carbonaceous sediments (Type C2 alteration) and the pyrrhotite-bearing "Mineralised Zone" (Type A, B and C1 alteration).

The resistive zone in downhole apparent resistivity logs correlate with the granitoid units and weakly altered pyrrhotite-poor volcanic rocks. This response is lithologically constrained. The highest conductivity is found in the pyrrhotite-bearing carbonaceous sedimentary unit. Variable conductivity within the "Mineralised Zone" is based on the irregular distribution of the pyrrhotite and irregular but high degree of silicification.

Downhole IP has an inverse correlation with the downhole apparent resistivity and is, also, lithologically constrained. The chargeability within the "Mineralised Zone" is due to the combined presence of graphite and pyrrhotite. The high chargeability in the carbonaceous sedimentary unit is caused by the high pyrrhotite content.

9. SUMMARY AND DISCUSSION

9.1 GEOLOGICAL SETTING

The proposed geological model and interpreted geological history of the Svartliden Project can be broken up into six (6) stages and is summarised below.

Stage 1 – Deposition of supracrustal rocks (1.95Ga – 1.85Ga)

- The deposition of the turbiditic sedimentary package and basalt in a submarine, reducing environment.

Stage 2 - Burial, diagenesis and intrusion of pre-orogenic granitoids (1.88 – 1.85Ga)

- Pervasive silica+pyrrhotite alteration and quartz veining (V_1).
- Intense silica+pyrrhotite alteration occurring in the sedimentary rocks, particularly the carbonaceous shales.

Stage 3 - First deformation event (D_1) (1.85Ga – 1.83Ga)

- Isoclinal upright folding along ENE subhorizontal fold axes (F_1) and development of a strong, penetrative subvertical cleavage (S_1).
- Folding of V_1 and remobilisation of pyrrhotite into fold hinges, along cleavage planes and into open fractures.
- Pervasive silicification and quartz veining (V_2), particularly in the sedimentary units i.e. carbonaceous shales and mudstones.
- Intrusion of syn-deformational granitoid bodies.

Stage 4 - Gold mineralisation

- Faulting and shearing along F_1 axial planes and influx of gold-bearing hydrothermal fluids within the zones of low shear strain created by the rotating granitoids.
- These zones of low shear strain resulted in dilation along the shallow plunging intersection lineation between S_0 and S_1. These zones are silica-flooded during the hydrothermal event.

- Mineralisation resulting from precipitation of gold, diopside, green amphibole, and arsenopyrite within these silica-rich zones.
- Hydrothermal alteration of the wallrock developed along the axial planar cleavage (S_1) forming an outer alteration halo consisting of an assemblage of remobilised pyrrhotite and high temperature biotite.
- Porous siltstones and sandstones are the most favourable host rocks.
- Within the shear zone, mineralisation can occur in all other rock types.

Stage 5 - Second deformation event (D_2) (1.84Ga – 1.80Ga)

- E-W compression and development of NW to NE-striking, open folds causing warping of the subhorizontal "Mineralised Zone".
- NW-striking faults which displace the stratigraphy. This may be related to this event and represent a conjugate fracture system through the area.

Stage 6 - Dinosaurs and Iceage (post Svecokarelian)

- Cainozoic iceage with the deposition of glacial till over Scandinavia.

9.2 GEOPHYSICAL SETTING

The regional aeromagnetics delineates several greenstone belts through North-central Sweden. The greenstone belts are traceable due to high concentration of magnetite and pyrrhotite found within the volcano-sedimentary sequence. The ground magnetic survey at Svartliden clearly delineates the shear zone due to anomalous magnetite and pyrrhotite.

SGU studies have found that the Bottnian Basin is highly resistive requiring high frequencies for the effective use of electromagnetics. Frequency domain electromagnetic surveys have the advantage in such a highly resistive terrain to delineate discrete conductive and chargeable bodies at a regional and project scale.

Downhole IP assisted in delineating pyrrhotite and graphite bearing units. IP, alone, cannot separate the pyrrhotite-bearing sediments from the pyrrhotite- and graphite-bearing "Mineralised Zone".

9.3 GEOLOGICAL AND GEOPHYSICAL SYNTHESIS

The geological and geophysical synthesis is based on observations and interpretations from the ground magnetic and EM data, and downhole geophysical data in conjunction with the drillhole geological logs.

The structural setting at Svartliden is interpreted from the geological and geophysical synthesis to be an isoclinal anticline, which strikes east-northeast with a fold axis that plunges between 6-18° to the east and west of 1500mE. The axial plane cleavage data indicates the presence of a slightly overturned fold axis to the south with local internal variation to the north. The ground magnetics and EM, also, identified brittle structures (late-stage faults), which crosscut the project area.

Within the Svartliden Shear Zone, gold mineralisation is localised and concentrated, and therefore, very difficult to determine any unambiguous geophysical properties or signatures. The broader hydrothermal alteration zones were used to obtain any signatures or properties from the ground and downhole geophysics.

Although graphite was identified in the ore, the proportion was too insignificant on a project scale to use as a conductive identifier for gold mineralisation. The amount of pyrrhotite was proportionally too high in the "Mineralised Zone" and masked the graphite response.

Type A and B alteration, referred to as the "Mineralised Zone", are coincident with the second-order in-phase EM anomalies. The second-order response is the result of a high content of irregularly distributed conductive pyrrhotite within a strongly silicified, and thus resistive, alteration zone.

The first-order in-phase EM anomalies correlate with the poorly altered, pyrrhotite-bearing carbonaceous sediments, which make up the northern contact of the Svartliden Shear Zone.

9.4 EXPLORATION POTENTIAL

At project scale, the use of detailed ground electromagnetics will help delineate strike extensions of the near surface "Mineralised Zone" (Type A and B alteration). The depth potential is unknown but there is evidence of repetition of the shallow plunging "Mineralised Zone" 100m below surface. Downhole apparent resistivity and IP surveys may help delineate the deeper mineralised lenses.

East of the 2000mE, an infil ground magnetic and EM survey is required to define the limits of the shear zone. Silver mineralisation has been encountered in drilling east of 2200mE suggesting that the alteration system is present. Calculations and interpretations made from the ground in-phase EM may help locate the alteration zone along strike from the 2200mE.

West of the 1200mE, the stratigraphic package flexes to the south. The anomalies formed by the ground geophysics are disjointed and incoherent in this zone. The disjointed aspect is caused by the late-stage west-northwest to north-northwest trending faults, which fan out from the southeast, cross cutting the shear zone. Although this affects continuity of the "Mineralised Zone", there is still the potential for delineating small pockets of highly concentrated gold mineralisation from the ground electromagnetics.

In the western part of the project area, the second-order in-phase EM anomaly (coincident with the "Mineralised Zone" in the project area) found along the 700mE, between the 800mN and 1000mN, remains the most prospective area for Type A and B alteration and subsequent gold mineralisation.

On a regional scale, greenstone belts with similar structural setting to Svartliden should be targeted. Ground electromagnetics (specifically the in-phase EM) should be an effective tool in this environment to delineate alteration systems similar to the Svartliden system, since the host rock and composition of the hydrothermal fluids are similar. The pyrrhotite-bearing carbonaceous shales should be used as a marker horizon as they are potentially associated with alteration zones.

10. CONCLUSIONS

The Svartliden Project is a shear-hosted meso-(kato?)thermal gold deposit. Gold mineralisation is associated with Type A and B alteration. This inner alteration halo consists of silica +diopside +green amphibole +pyrrhotite +graphite ±arsenopyrite ±gold. The outer alteration halo (Type C1) has a pyrrhotite+biotite mineral assemblage.

Pyrrhotite is a pervasive sulphide and has a direct influence on conductivity and chargeability. For this reason, pyrrhotite cannot be used geochemically or geophysically as an indicator mineral. The poorly altered, pyrrhotite-bearing, carbonaceous sedimentary unit can be used a footwall marker horizon across the northern limits of the Svartliden Shear Zone.

The geophysics does not differentiate the different lithologies, however lithology, structure and alteration control certain responses. After processing, modelling and interpreting the ground and downhole geophysical data, the in-phase electromagnetic response proved to be the most useful. The in-phase EM effectively delineated pyrrhotite-bearing conductive units, resistive volcanic and granitoid units within the shear zone.

Following log-transformation of the in-phase EM data, the pyrrhotite-bearing units can be separated into first-order and second-order anomalies. The second-order in-phase EM anomalies are coincident with the graphite- and pyrrhotite-bearing "Mineralised Zone" (Type A and B alteration) and pyrrhotite-bearing wallrock (Type C1 alteration).

Airborne and ground electromagnetic surveys should be conducted for future regional exploration. Second-order in-phase EM anomalies calculated from the log-transformed data should be targeted for potential in hosting Type A and B alteration. At the very least, the zone of alteration within a shear zone should be clearly delineated by the second-order in-phase EM anomalies.

In general, ductile shear-hosted orebodies such as Svartliden, are irregularly shaped, not sheet-like, and have varying conductivity and thickness. This should always be kept in mind when using interpretation schemes from different geophysical methods.